



universität  
wien

# DISSERTATION

Titel der Dissertation

“Warriors versus working men?” – An entheses and  
joint study on the Early Medieval skeletal remains of  
Thunau/Kamp

Verfasserin

Mag. rer. nat. Doris Pany-Kucera

angestrebter akademischer Grad

Doktorin der Naturwissenschaften (Dr.rer.nat.)

Wien, Juni 2015

Studienkennzahl lt. Studienblatt: A 091 442

Dissertationsgebiet lt. Studienblatt: Anthropologie

Betreuerin: Hr. Ao.Univ. Prof. Dr. Maria Teschler-Nicola



## **ABSTRACT**

### **“Warriors versus working men?” – An entheses and joint study on the Early Medieval skeletal remains of Thunau/Kamp**

The combination of two supposed indicators of activity on the skeleton, i.e. frequency of enthesal changes (EC) and osteoarthritis (OA), should give a broader insight into the daily activities of two early medieval (9<sup>th</sup>/10<sup>th</sup> century A.D.) skeletal populations from Thunau/Kamp, Austria. They were recovered at two archaeological sub-sites: one is a fortified settlement at the “Schanzberg”, including a necropolis on a hill plateau within and next to the remains of a fortified manor house. Supposedly it was at least partially reserved for a “social elite” and included burials of “warriors” (“uphill site”). The other site is a large riverine settlement at the foot of this hill, a “suburb”, where burials and a probably craft-production oriented settlement area were discovered (“downhill site”). Social differences between the two sites have been deduced from archaeological analysis (settlement structures and grave goods). The age structure in the two groups is very similar. The skeletons were analysed for selected fibrocartilaginous enthesal changes (EC) and joint alterations (OA), which were finally pooled functionally for comparison. Males and females were compared separately. A covariance of the features was hypothesized. Furthermore, sex and population differences, an increase of EC and OA with increasing age, and a social difference between the archaeological sites (in this case warriors versus working men) between the two groups were hypothesized and tested by the statistical group analyses. Only a weak association could be found for the covariance of EC and OA, a relationship is somewhat more accentuated in both male groups. During analysis, other differences were detected between the two populations. Both sexes in all groups show high frequencies in OA, but high EC frequencies were only found in males, and the increase of changes with higher age can be confirmed for all individuals in both groups. The downhill males and females show more distinct asymmetric changes in entheses and joints than the uphill group, especially in the upper limb, pointing to a stronger involvement in physical work. Additionally, the data of the downhill females show a younger age when the changes first appear compared to the uphill females, and a higher mobility of the former is indicated (significantly higher frequency and scores in the right hip entheses). Overall, these results reflect an earlier entry into worklife of the

downhill females as well as a stronger involvement in physically demanding tasks in their life. Concerning the uphill males, significant enthesal changes are mainly visible between the young and the middle age group, indicating work related changes. In addition, significant results in the hip joints on both body sides between the series were found, where the downhill males showed higher scores, providing an indication of greater mobility of the latter. Moreover, the downhill males display the highest frequencies of enthesal changes in some shoulder and elbow entheses and a distinctly stronger asymmetry in two entheses, especially in the upper extremity, and significant in one upper and one lower extremity entheses. Assuming that the downhill males were traditionally more involved in physical work, these findings probably represent not only higher mobility but also greater specialisation due to their obviously craft production related tasks. Otherwise, when comparing the “uphill warriors” to the “downhill working men”, activity patterns that would be related to “warriors” do not seem to be reflected in the group statistics, but noticeable sex-related group differences between the Schanzberg and the valley samples are apparent. Therefore, these results highly reflect the potential of the methodological combination for group analyses, providing relevant information on the social organisation of activities and occupational behaviour in past societies.

# CONTENTS

ABSTRACT .....	ii
Contents.....	iv
List of Figures .....	ix
List of Tables .....	xxi
Acknowledgements.....	xxiv
1 Introduction .....	1
1.1 Aims.....	1
1.2 Hypotheses.....	3
2 Material.....	5
2.1 Origin of the skeletons.....	5
2.1.1 Archaeology of the Schanzberg site/uphill group .....	7
2.1.2 Archaeology of the valley site/downhill group .....	12
2.2 Demography .....	16
3 Methods .....	18
3.1 Selection of the skeletons .....	18
3.2 Enthesis analysis.....	20
3.3 Joint analysis.....	23
3.4 Statistical analysis.....	26
3.5 Entheses and body height .....	27
3.6 Evaluation of a new methodological 3D approach in quantifying the surface structures of entheses .....	28
3.6.1 An attempt in using a 3D surface scanner for the recording of enthesal changes .....	28
4 Thunau males – Results I – Visual analyses: Frequencies .....	42
4.1 Males – entheses – frequencies, right side .....	42
4.1.1 True prevalence rate of enthesal changes in the males, right side, upper and lower extremities.....	42

4.1.2	Mean frequencies of single muscle groups, males right side .....	43
4.1.3	Description of the tables and figures for entheses frequencies of the right upper and lower extremities in uphill and downhill males .....	46
4.2	Males – joints – frequencies, right side .....	47
4.2.1	True prevalence rate of joint changes in the males, right side, upper and lower extremity .....	47
4.2.2	Mean frequencies of single joint groups, males right side .....	48
4.2.3	Description of the tables and figures for joint frequencies of the right upper and lower extremities in uphill and downhill males .....	51
4.3	Males – entheses – frequencies, left side .....	53
4.3.1	True prevalence rate of enthesal changes in the males, left side, upper and lower extremities.....	53
4.3.2	Mean frequencies of single muscle groups, males left side .....	55
4.3.3	Description of the tables and figures for entheses frequencies of the left upper and lower extremities in uphill and downhill males .....	57
4.4	Males – joints – frequencies, left side .....	58
4.4.1	True prevalence rate of joint changes in the males, left side, upper and lower extremities.....	58
4.4.2	Mean frequencies of single joint groups, males left side .....	60
4.4.3	Description of the tables and figures for joint frequencies of the left upper and lower extremities in uphill and downhill males .....	62
5	Thunau males – Results II – Visual analysis: Asymmetry .....	64
5.1	Males – entheses – asymmetry, upper and lower extremities .....	64
5.1.1	Significant differences in entheses asymmetry (univariate analysis) .....	65
5.2	Males – joints – asymmetry, upper and lower extremities .....	69
6	Thunau Males – Results III – Association between Entheses and Mean Age/Body Height.....	71
6.1	Scatterplots entheses– mean age– males .....	71
6.1.1	Scatterplots entheses – mean age, comparison males uphill-downhill – right side .....	71
6.1.2	Short summary .....	75
6.1.3	Scatterplots joints – mean age, comparison males uphill-downhill – right side .....	76
6.1.4	Short summary .....	82

6.1.5	Scatterplots entheses – mean age, comparison males uphill-downhill – left side .....	83
6.1.6	Short summary .....	87
6.1.7	Scatterplots joints – mean age, comparison males uphill-downhill – left side ..	88
6.1.8	Short summary .....	94
6.2	Scatterplots entheses – body height –males .....	95
6.2.1	Scatterplots entheses – body height, comparison males uphill-downhill – right side .....	95
6.2.2	Short summary .....	100
6.2.3	Scatterplots entheses – body height, comparison males uphill-downhill – left side .....	101
6.2.4	Short summary .....	105
7	Results IV – Age-Dependency of the Features .....	106
7.1	Males and females, uphill series: scores and age, right side .....	106
7.2	Males and females, uphill series: scores and age, left side.....	108
7.3	Males and females, downhill series: scores and age, right side .....	109
7.4	Males and females, downhill series: scores and age, left side.....	110
7.5	Exemplary test of scores and age without osteophyte growth.....	111
7.5.1	Males and females, uphill series: scores and age, right side without osteophyte growth.....	111
7.5.2	Males and females, downhill series: scores and age, left side without osteophyte growth.....	112
8	Thunau Females – Results I – Visual Analyses: Frequencies .....	113
8.1	Females – entheses – frequencies, right side .....	113
8.1.1	True prevalence rate of enthesal changes in the females, right side, upper and lower extremities.....	113
8.1.2	Mean frequencies of single muscle groups, females right side .....	114
8.1.3	Description of tables and figures for entheses frequencies of the right upper and lower extremities in uphill and downhill females .....	117
8.2	Females – joints – frequencies, right side.....	118
8.2.1	True prevalence rate of joint changes in the females, right side, upper and lower extremities.....	118
8.2.2	Mean frequencies of single joint groups, females right side .....	119

8.2.3	Description of tables and figures for joint frequencies of the right upper and lower extremities in uphill and downhill females .....	122
8.3	Females – entheses – frequencies, left side .....	124
8.3.1	True prevalence rate of enthesal changes in the females, left side, upper and lower extremities.....	124
8.3.2	Mean frequencies of single muscle groups, females left side .....	125
8.3.3	Description of tables and figures for entheses frequencies of the left upper and lower extremities in uphill and downhill females .....	128
8.4	Females – joints – frequencies, left side.....	129
8.4.1	True prevalence rate of joint changes in the females, left side, upper and lower extremities.....	129
8.4.2	Mean frequencies of single joint groups, females left side .....	131
8.4.3	Description of tables and figures for joint frequencies of the left upper and lower extremities in uphill and downhill females .....	133
9	Thunau Females – Results II – Visual Analyses: Asymmetry .....	135
9.1	Females – entheses – asymmetry, upper and lower extremities.....	135
9.2	Females – joints – asymmetry, upper and lower extremities .....	137
10	Thunau Females – Results III – Association between Entheses and Mean Age/Body Height.....	139
10.1	Scatterplots entheses – mean age – females .....	139
10.1.1	Scatterplots entheses – mean age, comparison females uphill-downhill – right side.....	139
10.1.2	Short summary .....	147
10.1.3	Scatterplots joints – mean age, comparison females uphill-downhill – right side .....	148
10.1.4	Short summary .....	154
10.1.5	Scatterplots entheses – mean age, comparison females uphill-downhill – left side.....	155
10.1.6	Short summary .....	160
10.1.7	Scatterplots joints – mean age, comparison females uphill-downhill – left side .....	161
10.1.8	Short summary .....	167
10.2	Scatterplots entheses – body height – females.....	168

10.2.1	Scatterplots entheses – body height, comparison females uphill-downhill – right side .....	168
10.2.2	Short summary .....	174
10.2.3	Scatterplots entheses – body height, comparison females uphill-downhill – left side .....	175
10.2.4	Short summary .....	180
10.2.5	Comments on the body height sections for males and females.....	181
11	Discussion.....	183
11.1	General comments .....	183
11.2	Association between enthesal and joint changes in the Thunau samples .....	184
11.3	Differences between the Thunau sub-sites .....	186
11.3.1	Sex differences .....	186
11.3.2	Population differences.....	187
11.4	Age differences in the Thunau sub-sites.....	189
11.4.1	Population differences.....	189
11.4.2	Sex differences and age.....	191
11.5	Social differences in the Thunau sub-sites.....	193
12	Conclusion.....	198
13	References .....	202
	Addendum .....	212
13.1	Scoring sheet entheses .....	212
13.2	Scoring sheet joints .....	215
13.3	List of analysed individuals from Thunau for enthesal changes, right extremities .....	216
13.4	List of analysed individuals from Thunau for joint changes, right extremity.....	218
13.5	List of analysed individuals from Thunau for enthesal changes, left extremities .....	221
13.6	List of analysed individuals from Thunau for joint changes, left extremities .....	223
13.7	ZUSAMMENFASSUNG.....	226
13.8	CURRICULUM VITAE .....	228

## List of Figures

<b>Figure 1.</b>	Location of the place of discovery in Gars/Thunau in north-eastern Austria. ....	5
<b>Figure 2.</b>	Aerial photography of the two sub-sites at Thunau/Kamp, Austria, where the skeletons were found.....	6
<b>Figure 3.</b>	Left side: male skeleton lying in supine position (G 129) from Thunau Schanzberg/ Herrenhof (uphill site). Right side: male skeleton lying in supine position (G 6) from Thunau-valley (downhill site). ....	7
<b>Figure 4.</b>	Archaeological plan of the excavation sites from 1965 to 2003 at the Schanzberg in Thunau/Kamp. ....	8
<b>Figure 5.</b>	Map of the hillfort of Herrenhof/Thunau showing the graveyard, the settlement and the palisade system (Palisadensystem). ....	9
<b>Figure 6.</b>	Map of the cemetery at the hillfort Herrenhof. ....	10
<b>Figure 7.</b>	Examples of drawings of the skeletons in situ in the graves, with grave goods of a male (grave 129, right side) and a female (grave 208, left side) individual, buried in the cemetery of the hillfort (uphill) site. ....	11
<b>Figure 8.</b>	Map of the downhill graveyard and settlement area. ....	12
<b>Figure 9.</b>	Remains of a Grubenhaus with evidence of an oven, loom weights and millstones, discovered in the downhill settlement. ....	13
<b>Figure 10.</b>	Evidence of a baking oven (left side) and loom weights (right side) found in the downhill settlement area.....	14
<b>Figure 11.</b>	Evidence of a blacksmith`s shop discovered in the downhill settlement.....	14
<b>Figure 12.</b>	Examples of drawings of the skeletons in situ in the graves with grave goods of a male (grave 6, left side) and a female (grave 27, right side) buried in the graveyard of the downhill site of Thunau.....	15
<b>Figure 13.</b>	There is considerable variation in the long bones, visible here in 4 humeri from graves (from left to right), 82 (male), 45/1 (male), 20 (female), 101 (female), uphill site. ....	17
<b>Figure 14.</b>	Examples of enthesal changes in the Thunau population. Compare text for details. ....	22
<b>Figure 15.</b>	Examples of joint changes in the Thunau populations. Compare text for details. ....	25

<b>Figure 16.</b> Pictures of two humeri from the Thunau sample, showing normal enthesis surface (left side, grave 102) and strong enthesial change (right side, grave 45/1) of the <i>M. pectoralis major</i> at the proximal humerus .....	29
<b>Figure 17.</b> Breuckmann Opto-Top HE optotopometric surface scanner used for analysis.	29
<b>Figure 18.</b> Femur in scanning position. ....	30
<b>Figure 19.</b> In the surface scan of <i>M. pectoralis major</i> Thunau 45/1, the rugosity of the surface is much better visible than in the photograph (compare Figure 16, right side). ....	30
<b>Figure 20.</b> The area of the enthesis was delimited using a nurbs curve before cropping the surrounding bone.....	31
<b>Figure 21.</b> The area of the enthesis was delimited using a nurbs curve after cropping the surrounding bone. The resulting delimited curve was projected onto a plane fitted to it, thus converting it into two dimensions. ....	33
<b>Figure 22.</b> 3D area is strongly correlated with the composite enthesopathy score.....	33
<b>Figure 23.</b> The points of the surface were exported and treated as if they were the points of a digital elevation model. ....	34
<b>Figure 24.</b> The aspect of the resulting surface, visualizing the directions in which the slopes are facing. ....	35
<b>Figure 25.</b> Majority filter applied to remove small patches.....	35
<b>Figure 26.</b> Neighbourhood pixels are grouped. ....	36
<b>Figure 27.</b> Relative Surface Complexity is negatively correlated with the robusticity score and also the composite enthesopathy score.....	37
<b>Figure 28.</b> Surface compared to the plane fitted to the curve delimiting the enthesis.....	38
<b>Figure 29.</b> The maximum deviation from the plane is correlated to the Composite Enthesopathy Score. ....	39
<b>Figure 30.</b> Individuals with higher Composite Enthesopathy Scores have higher maximum and average distances from the base plane.....	40
<b>Figure 31.</b> Graph showing the true prevalence rate of the enthesial changes of the right side in the uphill (UPM) and downhill males (DOM) of Thunau/Kamp, for upper and lower extremity. ....	43
<b>Figure 32.</b> Graphs of the single muscle groups, right side, comparison of uphill and downhill males, upper and lower extremity. ....	44

<b>Figure 33.</b> Graph showing the true prevalence rate of the joint changes of the right side in the uphill (UPM) and downhill males (DOM) of Thunau/Kamp, for upper and lower extremity. ....	48
<b>Figure 34.</b> Graphs of the joint groups, right side, comparison of uphill and downhill males. . .....	49
<b>Figure 35.</b> Graph showing the true prevalence rate of the enthesal changes of the left side in the uphill (UPM) and downhill males (DOM) of Thunau/Kamp, for upper and lower extremity. ....	54
<b>Figure 36.</b> Graphs of pooled entheses groups, left side, comparison of uphill and downhill males. ....	55
<b>Figure 37.</b> Graph showing the true prevalence rate of the joint changes of the left side in the uphill and downhill males of Thunau/Kamp, for upper and lower extremity.....	59
<b>Figure 38.</b> Graphs of the joint groups, left side, comparison of uphill and downhill males.	60
<b>Figure 39.</b> Asymmetries in enthesal changes calculated from scores in the right and left upper and lower extremities of the uphill and downhill males. ....	65
<b>Figure 40.</b> Graph of the results of the univariate analysis calculated from scores according to the <i>M. triceps brachii</i> (scapula/ulna), where the downhill males show the higher asymmetry. ....	66
<b>Figure 41.</b> Univariate group differences calculated from scores according to the <i>M. quadriceps femoris</i> (Patella/Ligamentum patellae), where the downhill males show higher asymmetry. ....	68
<b>Figure 42.</b> Asymmetries in joint changes calculated from scores in the right and left upper and lower extremities of the uphill and downhill males. ....	70
<b>Figure 43.</b> Scatterplot of the pooled muscle group <i>M. biceps brachii</i> – <i>M. subscapularis</i> (humerus, scapula), uphill (1) and downhill males (2), right side. ....	71
<b>Figure 44.</b> Scatterplot of the pooled muscle group <i>M. supraspinatus</i> - <i>M. infraspinatus</i> – <i>M. teres minor</i> (proximal humerus), uphill (1) and downhill males (2), right side. ....	72
<b>Figure 45.</b> Scatterplot of the pooled muscle group <i>M. triceps brachii</i> (scapula, ulna), uphill (1) and downhill males (2), right side. ....	72
<b>Figure 46.</b> Scatterplot of the pooled muscle group <b>common extensors</b> (distal lateral humerus), uphill (1) and downhill males (2), right side.....	73
<b>Figure 47.</b> Scatterplot of the pooled muscle group <b>common flexors</b> (distal medial humerus), uphill (1) and downhill males (2), right side. ....	73

<b>Figure 48.</b> Scatterplot of the pooled muscle group <i>M. biceps brachii</i> – <i>M. brachialis</i> (proximal radius and proximal ulna - elbow), uphill (1) and downhill males (2), right side. ....	74
<b>Figure 49.</b> Scatterplot of the pooled muscle group <i>M. semimembranosus</i> – <i>M. semitendinosus</i> – <i>M. biceps femoris</i> (tuber ischiadicum), uphill (1) and downhill males (2), right side. ....	74
<b>Figure 50.</b> Scatterplot of the pooled muscle group <i>M. quadriceps femoris</i> (Patella – patellar ligament), uphill (1) and downhill males (2), right side. ....	75
<b>Figure 51.</b> Pooled joint group <i>Caput humeri</i> – <i>Cavitas glenoidalis</i> (shoulder - humerus, scapula), comparison between males of the uphill (1) and downhill (2) site, right side. ....	76
<b>Figure 52.a.</b> Pooled joint group <i>Capitulum humeri</i> – <i>Trochlea</i> (dist. humerus -elbow), males of the uphill (1) and downhill site (2), right side. This pooled joint group is significantly affected by age (see Figure 52b). ....	77
<b>Figure 52.b.</b> Univariate analysis of the pooled joint group <i>Capitulum humeri</i> – <i>Trochlea</i> . ....	77
<b>Figure 53.a.</b> Pooled joint group <i>Caput radii</i> , <i>Circumferentia articularis radii</i> , <i>Incisura trochlearis</i> , <i>Incisura radialis</i> (proximal radius and ulna - elbow), males of the uphill (1) and downhill site (2), right side. ....	78
<b>Figure 53.b.</b> Univariate analysis of the pooled joint group <i>Caput radii</i> , <i>Circumferentia articularis radii</i> , <i>Incisura trochlearis</i> , <i>Incisura radialis</i> . ....	78
<b>Figure 54.</b> Scatterplot of the pooled joint group <i>Incisura ulnaris</i> , <i>Circumferentia articularis ulnae</i> , <i>Caput ulnae</i> , <i>proximal row of wrist bones</i> , <i>Facies articularis carpalis</i> (distal radius and ulna; wrist), males of the uphill (1) and downhill site (2), right side. ....	79
<b>Figure 55.a.</b> Scatterplot of the pooled joint group <i>Fossa acetabuli</i> , <i>Caput femoris</i> , <i>Fovea capitis</i> ( <i>Os ilium (acetabulum)</i> ), <b>femoral head - hip joint</b> , males of the uphill (1) and downhill (2) site, right side. The increase of scores in hip joint changes in the males of both sites is significantly affected by age (see Figure 55b). ....	79
<b>Figure 55.b.</b> Univariate analysis of the pooled joint group <i>Fossa acetabuli</i> , <i>Caput femoris</i> , <i>Fovea capitis</i> . ....	79
<b>Figure 56.a.</b> Scatterplot of the pooled joint group <i>Facies patellaris</i> , <i>Condylus medialis femoris</i> , <i>Condylus lateralis femoris</i> , distal margin of <i>Fossa intercondylaris</i> (distal femur - knee), males of the uphill (1) and downhill site (2), right side. ....	81
<b>Figure 56.b.</b> Univariate analysis of the pooled joint group <i>Facies patellaris</i> , <i>Condylus medialis femoris</i> , <i>Condylus lateralis femoris</i> , distal margin of <i>Fossa intercondylaris</i> . ....	81

<b>Figure 57.</b> Scatterplot of the pooled joint group <i>Facies articularis inferior tibiae, Facies articularis superior talus, Facies articularis talaris posterior calcanei</i> (distal tibia - ankle), males of the uphill (1) and downhill (2) site, right side. ....	82
<b>Figure 58.</b> Scatterplot of the pooled muscle group <i>M. biceps brachii – M. subscapularis</i> (scapula and proximal humerus - shoulder), males of the uphill (1) and downhill site (2), left side. ....	83
<b>Figure 59.</b> Scatterplot of the pooled muscle group <i>M. triceps brachii</i> (scapula – proximal ulna), males of the uphill (1) and downhill site (2), left side. ....	84
<b>Figure 60.</b> Scatterplot of the pooled muscle group <i>M. supraspinatus - M. infraspinatus – M. teres minor</i> (proximal humerus), males of the uphill (1) and downhill site (2), left side. ....	84
<b>Figure 61.</b> Scatterplot of the pooled muscle group <i>M. biceps brachii – M. brachialis</i> (proximal radius and proximal ulna - elbow), males of the uphill (1) and downhill site (2), left side. ....	85
<b>Figure 62.</b> Scatterplot of the pooled <b>common extensors</b> group (distal lateral humerus), males of the uphill (1) and downhill site (2), left side. ....	85
<b>Figure 63.</b> Scatterplot of the pooled <b>common flexors</b> group (distal medial humerus), males of the uphill (1) and downhill site (2), left side. ....	86
<b>Figure 64.</b> Scatterplot of the pooled muscle group <i>M. semimembranosus – M. semitendinosus – M. biceps femoris (tuber ischiadicum)</i> males of the uphill (1) and downhill site (2), left side. ....	86
<b>Figure 65.</b> Scatterplot of the pooled muscle group <i>M. quadriceps femoris</i> (Patella – patellar ligament), males of the uphill (1) and downhill site (2), left side. ....	87
<b>Figure 66.</b> Pooled joint group <i>Caput humeri – Cavitas glenoidalis</i> (shoulder - humerus, scapula), males of the uphill (1) and downhill site (2), left side. ....	88
<b>Figure 67.a.</b> Pooled joint group <i>Capitulum humeri – Trochlea</i> (dist. humerus -elbow), males of the uphill (1) and downhill (2) site, left side. ....	89
<b>Figure 67.b.</b> Univariate analysis of the pooled joint group <i>Capitulum humeri – Trochlea</i> . ...	90
<b>Figure 68.</b> Pooled joint group <i>Caput radii, Circumferentia articularis radii, Incisura trochlearis, Incisura radialis</i> (proximal radius and ulna - elbow), males of the uphill (1) and downhill site (2), left side. ....	90
<b>Figure 69.</b> Pooled joint group <i>Incisura ulnaris, Circumferentia articularis ulnae, Caput ulnae, proximal row of wrist bones, Facies articularis carpalis</i> (distal radius and ulna, - wrist), males of the uphill (1) and downhill site (2), left side. ....	90

<b>Figure 70.a.</b> Scatterplot of the pooled joint group <i>Fossa acetabuli, Caput femoris, Fovea capitis</i> ( <i>Os ilium (acetabulum)</i> ), femoral head - hip joint), males of the uphill (1) and downhill site (2), left side. ....	91
<b>Figure 70.b.</b> Univariate analysis of the pooled joint group <i>Fossa acetabuli, Caput femoris, Fovea capitis</i> . ....	91
<b>Figure 71.</b> Scatterplot of the pooled joint group <i>Facies patellaris, Condylus medialis femoris, Condylus lateralis femoris, distal margin of Fossa intercondylaris</i> (distal femur - knee), males of the uphill (1) and downhill site (2), left side.....	92
<b>Figure 72.</b> Scatterplot of the pooled joint group <i>Condylus medialis tibiae, Condylus lateralis tibiae, Facies medialis patellae, Facies lateralis patellae</i> (proximal tibia, patella - knee joint), males of the uphill (1) and downhill site (2), left side. ....	93
<b>Figure 73.</b> Scatterplot of the pooled joint group <i>Facies articularis inferior tibiae, Facies articularis superior talus, Facies articularis talaris posterior calcanei</i> (distal tibia - ankle), males of the uphill (1) and downhill site (2), left side. ....	93
<b>Figure 74.</b> Scatterplot of the pooled muscle group <i>M. biceps brachii – M. subscapularis</i> (scapula, proximal humerus), males of the uphill (1) and downhill site (2), right side. ....	95
<b>Figure 75.</b> Scatterplot of the pooled muscle group <i>M. triceps brachii</i> (scapula – proximal ulna), males of the uphill (1) and downhill site (2), right side. ....	96
<b>Figure 76.</b> Scatterplot of the pooled muscle group <i>M. supraspinatus - M. infraspinatus – M. teres minor</i> (proximal humerus), males of the uphill (1) and downhill site (2), right side.....	96
<b>Figure 77.</b> Scatterplot of the pooled <b>common extensors</b> muscle group (distal lateral humerus), males of the uphill (1) and downhill site (2), right side. ....	97
<b>Figure 78.a.</b> Scatterplot of the pooled <b>common flexors muscle group</b> (distal medial humerus), males of the uphill (1) and downhill site (2), right side. ....	97
<b>Figure 78.b.</b> Univariate analysis of the pooled common flexors muscle group.....	97
<b>Figure 79.</b> Scatterplot of the pooled muscle group <i>M. biceps brachii – M. brachialis</i> (prox. radius - ulna), males of the uphill (1) and downhill site (2), right side. ....	99
<b>Figure 80.</b> Scatterplot of the pooled muscle group <i>M. semimembranosus – M. semitendinosus – M. biceps femoris</i> (tuber ischiadicum), males of the uphill (1) and downhill site (2), right side. ....	99
<b>Figure 81.</b> Scatterplot of the pooled muscle group <i>M. quadriceps femoris</i> (Patella – patellar ligament), males of the uphill (1) and downhill site (2), right side. ....	100

<b>Figure 82.</b> Scatterplot of the pooled muscle group <i>M. biceps brachii</i> – <i>M. subscapularis</i> (scapula, proximal humerus), males of the uphill (1) and downhill site (2), left side. ....	101
<b>Figure 83.</b> Scatterplot of the pooled muscle group <i>M. triceps brachii</i> (scapula – proximal ulna), males of the uphill (1) and downhill site (2), left side. ....	101
<b>Figure 84.</b> Scatterplot of the pooled muscle group <i>M. supraspinatus</i> - <i>M. infraspinatus</i> – <i>M. teres minor</i> (prox. humerus), males of the uphill (1) and downhill site (2), left side.....	102
<b>Figure 85.</b> Scatterplot of the pooled muscle group <i>M. biceps brachii</i> – <i>M. brachialis</i> (prox. radius and proximal ulna - elbow), males of the uphill (1) and downhill site (2), left side. ..	102
<b>Figure 86.</b> Scatterplot of the pooled <b>common extensors</b> muscle group (distal lateral humerus), males of the uphill (1) and downhill site (2), left side. ....	103
<b>Figure 87.</b> Scatterplot of the pooled <b>common flexors muscle group</b> (distal medial humerus males of the uphill (1) and downhill (2) site, left side. ....	103
<b>Figure 88.</b> Scatterplot of the pooled muscle group <i>M. semimembranosus</i> – <i>M. semitendinosus</i> – <i>M. biceps femoris</i> (tuber ischiadicum), males of the uphill (1) and downhill site (2), left side. ....	104
<b>Figure 89.a.</b> Scatterplot of <i>M. quadriceps femoris</i> (Patella – patellar ligament), males of the uphill (1) and downhill site (2), left side. ....	104
<b>Figure 89.b.</b> Univariate analysis of the right Patella/patellar ligament attachment site in the males. ....	105
<b>Figure 90.</b> True prevalence rate of the enthesal changes of the right side (RS) in the uphill (UPF) and downhill females (DOF) of Thunau/Kamp, for upper and lower extremity. ....	114
<b>Figure 91.</b> Graphs of the entheses groups, right side, comparison of uphill and downhill females. ....	115
<b>Figure 92.</b> True prevalence rate of the joint changes of the right side (RS) in the uphill (UPF) and downhill females (DOF) of Thunau/Kamp, for upper and lower extremity. ....	119
Next page: <b>Figure 93.</b> Graphs of the joint groups, right side, comparison of uphill and downhill females, upper and lower extremity. ....	120
<b>Figure 94.</b> True prevalence rate of the enthesal changes of the left side (LS) in the uphill (UPF) and downhill females (DOF) of Thunau/Kamp, for upper and lower extremity. ....	125
Next page: <b>Figure 95.</b> Graphs of the muscle groups, left side, comparison of uphill and downhill females, upper and lower extremity. ....	126
<b>Figure 96.</b> True prevalence rate of the joint changes of the left side (LS) in the uphill (UPF) and downhill females (DOF) of Thunau/Kamp, for upper and lower extremity. ....	130

<b>Figure 97.</b> Graphs of the muscle groups, left side, comparison of uphill and downhill females, upper and lower extremity. ....	131
<b>Figure 98.</b> Asymmetries in in entheseal changes calculated from scores in the right and left upper and lower extremities of the uphill and downhill females. ....	136
<b>Figure 99.</b> Asymmetries calculated from scores in the right and left upper and lower extremities of the uphill and downhill females. ....	138
<b>Figure 100.a.</b> Pooled muscle group <i>M. biceps brachii</i> – <i>M. subscapularis</i> (humerus, scapula), females of the uphill (1) and downhill site (2), right side. ....	139
<b>Figure 100.b.</b> Univariate analysis of the pooled muscle group <i>M. biceps brachii</i> – <i>M. subscapularis</i> . ....	139
<b>Figure 101.</b> Pooled muscle group <i>M. supraspinatus</i> - <i>M. infraspinatus</i> – <i>M. teres minor</i> (prox. humerus), females of the uphill (1) and downhill site (2), right side. ....	140
<b>Figure 102.a.</b> Pooled <i>M. triceps brachii</i> (scapula–proximal ulna), females of the uphill (1) and downhill site (2), right side. ....	141
<b>Figure 102.b.</b> Result of the univariate analysis of the pooled <i>M. triceps brachii</i> . ....	141
<b>Figure 103.a.</b> Scatterplot of the pooled <b>common extensors</b> muscle group (distal lateral humerus), females of the uphill (1) and downhill site (2), right side. ....	142
<b>Figure 103.b.</b> Results of the univariate analysis for the right common extensors. ....	142
<b>Figure 104.a.</b> Scatterplot of the pooled <b>common flexors muscle group</b> (distal medial humerus), females of the uphill (1) and downhill site (2), right side. ....	143
<b>Figure 104.b.</b> Results of the univariate analysis for the right common flexors. ....	143
<b>Figure 105.a.</b> Scatterplot of the pooled muscle group <i>M. biceps brachii</i> – <i>M. brachialis</i> (proximal radius - ulna), females of the uphill (1) and downhill site (2), right side. ....	144
<b>Figure 105.b.</b> Results of the univariate analysis for the right <i>M. biceps brachii</i> – <i>M. brachialis</i> . ....	144
<b>Figure 106.a.</b> Scatterplot of the pooled muscle group <i>M. semimembranosus</i> – <i>M. semitendinosus</i> – <i>M. biceps femoris</i> (tuber ischiadicum), females of the uphill (1) and downhill site (2), right side. ....	145
<b>Figure 106.b.</b> Results of the univariate analysis for the right <i>M. semimembranosus</i> – <i>M. semitendinosus</i> – <i>M. biceps femoris</i> . ....	146
<b>Figure 107.</b> Scatterplot of the pooled muscle group <i>M. quadriceps femoris</i> (Patella – patellar ligament), females of the uphill (1) and downhill site (2), right side. ....	147

<b>Figure 108.</b> Scatterplot of pooled joint group <i>Caput humeri – Cavitas glenoidalis</i> (humerus, scapula – shoulder), females of the uphill (1) and downhill site (2), right side. ....	148
<b>Figure 109.a.</b> Scatterplot of the pooled joint group <i>Capitulum humeri – Trochlea</i> (distal humerus - elbow), right side, females of the uphill (1) and downhill site (2), right side. ....	149
<b>Figure 109.b.</b> Results of the univariate analysis for the right <i>Capitulum humeri – Trochlea</i> . ....	149
<b>Figure 110.</b> Scatterplot of the pooled joint group <i>Caput radii, Circumferentia articularis radii, Incisura trochlearis, Incisura radialis</i> (distal humerus - elbow), females of the uphill (1) and downhill (2) site, right side. ....	150
<b>Figure 111.</b> Pooled joints <i>Incisura ulnaris, Circumferentia articularis ulnae, Caput ulnae, proximal wrist bones, Facies articularis carpalis</i> (distal radius and ulna, proximal row of wrist bones - wrist), females of the uphill (1) and downhill site (2), right side. ....	151
<b>Figure 112.a.</b> Scatterplot of the pooled joint group <i>Fossa acetabuli, Caput femoris, Fovea capitis (Os ilium (acetabulum))</i> , femoral head - hip joint), females of the uphill (1) and downhill site (2), right side. ....	151
<b>Figure 112.b.</b> Results of the univariate analysis for the right <i>Fossa acetabuli, Caput femoris, Fovea capitis</i> . ....	151
<b>Figure 113.</b> Pooled joint group <i>Facies patellaris, Condylus medialis femoris, Condylus lateralis femoris</i> , distal margin of <i>Fossa intercondylaris</i> (distal femur - knee), females of the uphill (1) and downhill (2) site, right side. ....	152
<b>Figure 114.</b> Scatterplot of the pooled joint group <i>Condylus medialis tibiae, Condylus lateralis tibiae, Facies medialis patellae, Facies lateralis patellae</i> (proximal tibia, patella - knee joint), females of the uphill (1) and downhill site (2), right side. ....	153
<b>Figure 115.</b> Scatterplot of the pooled joint group <i>Facies articularis inferior tibiae, Facies articularis superior talus, Facies articularis talaris posterior calcanei</i> (distal tibia - ankle), females of the uphill (1) and downhill site (2), right side. ....	153
<b>Figure 116.</b> Scatterplot of the pooled muscle group <i>M. triceps brachii</i> (scapula – proximal ulna), females of the uphill (1) and downhill site (2), left side. ....	156
<b>Figure 117.</b> Scatterplot of the pooled muscle group <i>M. supraspinatus - M. infraspinatus – M. teres minor</i> (prox. humerus), females of the uphill (1) and downhill site (2), left side. ..	156
<b>Figure 118.</b> Scatterplot of the pooled muscle group <i>M. biceps brachii – M. brachialis</i> (prox. radius and proximal ulna - elbow), females of the uphill (1) and downhill site (2), left side. ....	157
<b>Figure 119.a.</b> Scatterplot of the pooled <b>common extensors</b> muscle group (distal lateral humerus), females of the uphill (1) and downhill site (2), left side. ....	157

<b>Figure 119.b.</b> Results of the univariate analysis for the left common extensors. ....	158
<b>Figure 120.</b> Scatterplot of the pooled <b>common flexors muscle group</b> (distal medial humerus), females of the uphill (1) and downhill site (2), left side. ....	158
<b>Figure 121.</b> Scatterplot of the pooled muscle group <i>M. semimembranosus – M. semitendinosus – M. biceps femoris</i> (tuber ischiadicum), females of the uphill (1) and downhill site (2), left side. ....	159
<b>Figure 122.</b> Scatterplot of the pooled muscle group <i>M. quadriceps femoris</i> (Patella – patellar ligament), females of the uphill (1) and downhill site (2), left side. ....	159
<b>Figure 123.</b> Scatterplot of the pooled joint group <i>Caput humeri – Cavitas glenoidalis</i> (shoulder - humerus, scapula), females of the uphill (1) and downhill site (2), left side. ....	161
<b>Figure 124.a.</b> Scatterplot of the pooled joint group <i>Capitulum humeri – Trochlea</i> (dist. humerus - elbow), females of the uphill (1) and downhill site (2), left side. ....	162
<b>Figure 124.b.</b> Results of the univariate analysis for the left <i>Capitulum humeri –Trochlea</i> . ....	162
<b>Figure 125.</b> Pooled joint group <i>Caput radii, Circumferentia articularis radii, Incisura trochlearis, Incisura radialis</i> (proximal radius and ulna - elbow), females of the uphill (1) and downhill site (2), left side. ....	163
<b>Figure 126.</b> Pooled joint group <i>Incisura ulnaris, Circumferentia articularis ulnae, Caput ulnae, proximal wrist bones, Facies articularis carpalis</i> (distal radius and ulna, proximal row of wrist bones - wrist), females of the uphill (1) and downhill site (2), left side. ....	164
<b>Figure 127.a.</b> Scatterplot of the pooled joint group <i>Fossa acetabuli, Caput femoris, Fovea capitis</i> ( <i>Os ilium (acetabulum)</i> ), femoral head - hip joint), females of the uphill (1) and downhill site(2), left side. ....	164
<b>Figure 127.b.</b> Results of the univariate analysis for the left <i>Fossa acetabuli, Caput femoris, Fovea capitis</i> . ....	164
<b>Figure 128.a.</b> Scatterplot of the pooled joint group <i>Facies patellaris, Condylus medialis femoris, Condylus lateralis femoris</i> , distal margin of <i>Fossa intercondylaris</i> (distal femur - knee), females of the uphill (1) and downhill site (2), left side. This feature is significantly affected by age in both female sub-sites (see Figure 128b). ....	165
<b>Figure 128.b.</b> Results of the univariate analysis for the left <i>Facies patellaris, Condylus medialis femoris, Condylus lateralis femoris, distal margin of Fossa intercondylaris</i> . ....	165
<b>Figure 129.</b> Scatterplot of the pooled joint group <i>Condylus medialis tibiae, Condylus lateralis tibiae, Facies medialis patellae, Facies lateralis patellae</i> (proximal tibia, patella - knee joint), females of the uphill (1) and downhill site (2), left side. ....	166

<b>Figure 130.</b> Scatterplot of the pooled joint group <i>Facies articularis inferior tibiae</i> , <i>Facies articularis superior talus</i> , <i>Facies articularis talaris posterior calcanei</i> (distal tibia - ankle), females of the uphill (1) and downhill (2) site, left side. ....	167
<b>Figure 131.</b> Scatterplot of the pooled muscle group <i>M.biceps brachii</i> – <i>M. subscapularis</i> (scapula – proximal humerus), females of the uphill (1) and downhill site (2), right side. ...	168
<b>Figure 132.a.</b> Scatterplot of the pooled muscle group <i>M. triceps brachii</i> (scapula – proximal ulna), females of the uphill (1) and downhill site (2), right side. ....	169
<b>Figure 132.b.</b> Results of the univariate analysis for the pooled <i>M. triceps brachii</i> . ....	169
<b>Figure 133.</b> Scatterplot of the pooled muscle group <i>M. supraspinatus</i> - <i>M. infraspinatus</i> – <i>M. teres minor</i> (prox. humerus), females of the uphill (1) and downhill site (2), right side.	170
<b>Figure 134.</b> Scatterplot of the pooled <b>common extensors</b> muscle group (distal lateral humerus), females of the uphill (1) and downhill (2) site, right side. ....	170
<b>Figure 135.</b> Scatterplot of the pooled <b>common flexors muscle group</b> (distal medial humerus), females of the uphill (1) and downhill (2) site, right side. ....	171
<b>Figure 136.a.</b> Scatterplot of the pooled muscle group <i>M. biceps brachii</i> – <i>M. brachialis</i> (prox. radius - ulna), females of the uphill (1) and downhill site (2), right side. T.....	171
<b>Figure 136.b.</b> Results of the univariate analysis for the pooled entheses attachment sites <i>M. biceps brachii</i> – <i>M. brachialis</i> . ....	171
<b>Figure 137.a.</b> Scatterplot of the pooled muscle group <i>M. semimembranosus</i> – <i>M. semitendinosus</i> – <i>M. biceps femoris</i> (tuber ischiadicum), females of the uphill (1) and downhill site (2), right side. ....	172
<b>Figure 137.b.</b> Results of the univariate analysis for the pooled entheses attachment sites <i>M. semimembranosus</i> – <i>M. semitendinosus</i> – <i>M. biceps femoris</i> . ....	173
<b>Figure 138.</b> Scatterplot of the pooled muscle group <i>M. quadriceps femoris</i> (Patella – patellar ligament), females of the uphill (1) and downhill (2) site, right side. ....	174
<b>Figure 139.</b> Scatterplot of the pooled muscle group <i>M.biceps brachii</i> – <i>M. subscapularis</i> (scapula – proximal humerus), females of the uphill (1) and downhill site (2), left side. ....	175
<b>Figure 140.</b> Scatterplot of the pooled muscle group <i>M. triceps brachii</i> (scapula – proximal ulna), females of the uphill (1) and downhill site (2), left side. ....	175
<b>Figure 141.</b> Scatterplot of the pooled muscle group <i>M. supraspinatus</i> - <i>M. infraspinatus</i> – <i>M. teres minor</i> (prox. humerus), females of the uphill (1) and downhill site (2), left side. ..	176
<b>Figure 142.</b> Scatterplot of the pooled <b>common extensors</b> muscle group (distal lateral humerus), females of the uphill (1) and downhill (2) site, left side. ....	176

<b>Figure 143.</b> Scatterplot of the pooled <b>common flexors muscle markings group</b> (distal medial humerus), females of the uphill (1) and downhill (2) site, left side. ....	177
<b>Figure 144.a.</b> Scatterplot of the pooled muscle group <i>M. biceps brachii</i> – <i>M. brachialis</i> (prox. radius - ulna), females of the uphill (1) and downhill site (2), left side. ....	177
<b>Figure 144.b.</b> Results of the univariate analysis of the pooled muscle group <i>M. biceps brachii</i> – <i>M. brachialis</i> . ....	177
<b>Figure 145.</b> Scatterplot of the pooled muscle group <i>M. semimembranosus</i> – <i>M. semitendinosus</i> – <i>M. biceps femoris</i> (tuber ischiadicum), females of the uphill (1) and downhill site (2), left side. ....	178
<b>Figure 146.a.</b> Scatterplot of the pooled muscle markings group <i>M. quadriceps femoris</i> (Patella – patellar ligament), females of the uphill (1) and downhill (2) site, left side. ....	179
<b>Figure 146.b.</b> Results of the univariate analysis of the right <i>M. quadriceps femoris</i> . ....	179

## List of Tables

<b>Table 1.</b> Total numbers of individuals and number of individuals feasible for this study (n adults in bold) from the two analysed sites in Thunau/Kamp*.....	16
<b>Table 2.</b> Mean age of males and females of series 1 (uphill) and series 2 (downhill)*.....	16
<b>Table 3.</b> Mean body height of the uphill and downhill individuals*.....	17
<b>Table 4.</b> Number of individuals used for visual inspection of entheses and joints, right and left side. ....	18
<b>Table 5.</b> Recorded entheses and joint facets on the skeleton. ....	19
<b>Table 6.</b> Table showing attachment sites (region/bone) of the analysed muscles, their exact location, functions and acronyms.....	21
Table 7. Table showing analysed joints, their exact location and acronyms. ....	24
<b>Table 8.</b> Number of individuals and true prevalence rate (TPR) of the enthesal changes of the right side (RS) in the uphill (UPM) and downhill males (DOM) of Thunau/Kamp, for upper and lower extremity.....	42
<b>Table 9.</b> Mean frequencies in percent of the single muscle groups, right side, comparison of uphill and downhill males, upper and lower extremity.....	44
<b>Table 10.</b> Number of individuals and true prevalence rate of the joint changes of the right side in the uphill (UPM) and downhill males (DOM) of Thunau/Kamp, for upper and lower extremity. ....	47
<b>Table 11.</b> Mean frequencies in percent of the single joint groups, right side, comparison of uphill and downhill males, upper and lower extremity.....	49
Next page: <b>Table 12.</b> Pooled entheses and joint frequencies of the right extremity of the uphill/downhill males in comparison. ....	51
<b>Table 13.</b> Number of individuals and true prevalence rate of the enthesal changes of the left side in the uphill (UPM) and downhill males (DOM) of Thunau/Kamp, for upper and lower extremity. ....	53
<b>Table 14.</b> Mean frequencies in percent of the single pooled muscle groups, left side, comparison of uphill and downhill males, upper and lower extremity.....	55
<b>Table 15.</b> Number of individuals and true prevalence rate of the joint changes of the left side in the uphill and downhill males of Thunau/Kamp, for upper and lower extremity. ....	58
<b>Table 16.</b> Mean frequencies in percent of the single joint groups, left side, comparison of uphill and downhill males, upper and lower extremity.....	60

<b>Table 17.</b> Pooled entheses and joint frequencies of the left extremity of the males in comparison. ....	62
<b>Table 18.</b> Comparison of asymmetry in the scores of enthesal changes between right and left extremity for uphill and downhill males. ....	64
<b>Table 19.</b> Results of the univariate analysis calculated from scores according to the <i>M. triceps brachii</i> (scapula/ulna). ....	66
<b>Table 20.</b> Results of the univariate analysis calculated from scores according to the <i>M. quadriceps femoris</i> (Patella/Ligamentum patellae). ....	67
<b>Table 21.</b> Comparison of asymmetry in joint changes between right and left extremity calculated from scores for uphill and downhill males. ....	69
<b>Table 22.</b> Statistically significant results of the one-way ANOVA between the age groups in the uphill series, right side. ....	106
<b>Table 23.</b> Significant results of the one-way ANOVA between the age groups in the uphill series, left side. ....	108
<b>Table 24.</b> Significant results of the one-way ANOVA between the age groups in the downhill series, right side. ....	109
<b>Table 25.</b> Significant results of the one-way ANOVA between the age groups in the downhill series, left side. ....	110
<b>Table 26.</b> Significant results of the one-way ANOVA between the age groups excluding osteophyte growth in the uphill series, right side. ....	111
<b>Table 27.</b> Significant results of the one-way ANOVA between the age groups excluding osteophyte growth in the downhill series, left side. ....	112
<b>Table 28.</b> Number of individuals and true prevalence rate (TPR) of the enthesal changes of the right side (RS) in the uphill (UPM) and downhill males (DOM) of Thunau/Kamp, for upper and lower extremity. ....	113
<b>Table 29. a.</b> Mean frequencies in percent of the single muscle groups, right side, comparison of uphill and downhill males, upper and lower extremity. ....	115
<b>Table 29. b.</b> Significant result in t-test for <i>M. semimembranosus</i> / <i>M. semitendinosus</i> / <i>M. biceps femoris</i> . ....	115
<b>Table 30.</b> Number of individuals and true prevalence rate of the joint changes of the right side (RS) in the uphill (UPF) and downhill females (DOF) of Thunau/Kamp, for upper and lower extremity. ....	118

<b>Table 31 .</b>	Mean frequencies in percent of the single joint groups, right side, comparison of uphill and downhill females, upper and lower extremity. ....	120
<b>Table 32.</b>	Pooled entheses and joint frequencies of the right extremity of the females in comparison. ....	122
<b>Table 33.</b>	Number of individuals and true prevalence rate of the enthesal changes of the left side (LS) in the uphill (UPF) and downhill females (DOF) of Thunau/Kamp, for upper and lower extremity. ....	124
<b>Table 34.</b>	Mean frequencies in percent of the single muscle groups, left side, comparison of uphill and downhill females, upper and lower extremity. ....	126
<b>Table 35.</b>	Number of individuals and true prevalence rate of the joint changes of the left side (LS) in the uphill (UPF) and downhill females (DOF) of Thunau/Kamp, for upper and lower extremity. ....	129
<b>Table 36.</b>	Mean frequencies in percent of the single joint groups, left side, comparison of uphill and downhill females, upper and lower extremity. ....	131
<b>Table 37.</b>	Pooled entheses and joint frequencies of the left extremity of the females in comparison. ....	133
<b>Table 38.</b>	Comparison of asymmetry calculated from scores in enthesal changes between right and left extremity for uphill and downhill females. ....	135
<b>Table 39.</b>	Comparison of asymmetry in joint changes between right and left extremity for uphill and downhill females. ....	137

## **Acknowledgements**

I would like to express my sincere thanks to Maria Teschler-Nicola for supervising this thesis, for her support, patience and belief in me, despite the longevity. Furthermore I want to thank her for allowing me to use the workplace and the infrastructure of the Department of Anthropology at the Natural History Museum over all the years. I would also like to express my gratitude to Margit Berner and Karin Wiltschke-Schrotta for their valuable advice, support and encouragement not only concerning this thesis. The members of the Department of Anthropology at the museum, Ronald Mühl, Wolfgang Reichmann, Bettina Voglsinger and August Walch made my working life a lot easier several times through their supportive (technical) help. Special thanks go to Wolfgang Reichmann for the photographs in this thesis and general help with figures. For financial support, I would like to thank the Austrian Academy of Sciences for funding the data acquisition of this work, and Ernst Lauermann from the Lower Austrian state museum together with the provincial government of Lower Austria, section of culture and science for further funding. Furthermore I want to thank Katharina Rebay-Salisbury for submitting the motherhood project, which was the inducement I needed for finishing this work. For revision of language I want to thank Roderick Salisbury.

In addition, special thanks go to Philipp Mitteröcker, particularly for his valuable help and patience with me in statistical issues concerning this thesis; to Bence Viola, for working with me on the 3D method; to Maria Marschler for her help in formatting this thesis; all of them for their friendship; to Sabi, for being there all along.

Finally, this thesis would never have been finished without the support and help of my family. I would like to thank my mother Marianne especially for taking care of Gabriel, and both my mother and my sister Dagmar for their unrestricted support, encouragement and belief in me. My cordial thanks go to my husband Matthias, for his love, friendship and encouragement in the highs and lows over all the years. Without you and Gabriel, this would not have been worth it.

To my family

# 1 INTRODUCTION

## 1.1 Aims

The main focus of this thesis is to shed light on patterns of work of an Early Medieval society from Thunau/Kamp (Lower Austria, 9<sup>th</sup>/10<sup>th</sup> century A.D.) that is represented by two subpopulations, living in close proximity but seemingly diverse in their form of work organisation. Therefore, an analysis of enthesal- and osteoarthritic changes at the joints (EC and OA) of the skeletons has been performed.

Entheses are the attachment sites of muscles, tendons and ligaments to bone. These markers are recognized as important indicators of workload and activity in osteoarchaeology. The limitations of an association between special tasks and their reflections on the skeleton has been frequently discussed in anthropological and clinical literature since the first standardized method for recording entheses was published by Hawkey & Merbs in 1995 (e.g. Alves Cardoso & Henderson 2010, Bridges 1997, Campanacho & Santos 2013, Cunha & Umbelino 1995, Doying 2010, Henderson *et al.* 2013, Jurmain 1991 & 1999, Jurmain *et al.* 2012, Kennedy 1998, Mariotti *et al.* 2004, 2007, Meyer *et al.* 2011, Robb 1998, Schlecht 2012, Villotte 2006, Villotte & Knüsel 2013, Weiss & Jurmain 2007). Hawkey & Merbs called the different changes at muscle attachment sites “musculoskeletal stress markers” (MSM), a term which became very popular in literature, but the term enthesopathies (Dutour 1986) is also very widespread. However, these terms imply a (pathologic) cause for the changes, which is mostly unclear due to their multifactorial aetiology, and Jurmain & Villotte (2010) recently suggested “enthesal changes” as a neutral term (compare chapter 5.1.). Correspondingly, these markers will from here on be called enthesal changes in this thesis, and the neutral term “muscle markings” (Bridges 1997, Pearson & Buikstra 2006) will also be maintained.

Osteoarthritis is a disease of the synovial joints. It probably results from normal remodelling or a repair process and represents a natural reaction of these joints to joint failure either through injury or activity, but age, systemic and genetic predisposition also play a role (Rogers & Waldron 1995, Carter & Beaupré 2001). The term osteoarthritis (OA) will be used in this thesis because it is widespread, alternating with (the more neutral term) joint changes. It is not the purpose here to ascribe an underlying aetiology of the changes (Carter & Beaupré 2001, for more explanations compare chapter 5.2.). These decisions were drawn because it

was not the purpose of this thesis to find strongly pathological cases (in fact, those were excluded) in the series, but a pattern of work-related changes over the groups, which can give information on the social organisation of activities in a group without ruling out special movements of single individuals (Robb 1998). Hence, the combination of entheses and joint features, as performed in this study, is supposed to yield a broader insight into the distribution of activities in past populations in conjunction with the archaeologically derived data from settlements and the graves. The hypotheses are based on settlement structure and grave goods. The findings of the uphill site imply a social elite, a population residing in a fortified settlement, whereas especially the settlement structure of the downhill site, a suburbium, points to a production oriented population (compare chapter 4). The hypotheses were to be tested through anthropological data derived from a comparison of the skeletons from the two contemporary sub-sites. Statistically recognisable patterns on the skeletons over the groups should be observable in selected pooled entheses and joints, which will be compared in the same anatomical regions of the body, e.g. the entheses and joint alterations in the shoulder.

After the data collection for this thesis was finished in 2006, a new method for the analysis of enthesal changes was published by Villotte (2006). This paper brought new insights into the anatomical understanding of muscular attachment sites; Villotte therefore differentiates between two types of entheses: fibrous entheses, occurring in all regions of the appendicular skeleton with a thick layer of cortical bone, and fibrocartilaginousentheses, occurring at epiphyses and apophyses (Benjamin *et al.* 1986, Benjamin & Ralphs 1998, compare chapter 5.1.). Because of the differences in mechanical properties, the two types of entheses cannot be compared directly, and should therefore not be scored with the same system. This new information led, among other properties (compare chapter 5.3.), to my decision to use only the fibrocartilaginousentheses for the calculation of the final results. Later, in 2009, during the “Workshop in musculoskeletal stress markers (MSM): limitations and achievements in the reconstruction of past activity patterns” (Santos *et al.* 2011) held in Coimbra (Portugal) a Working Group on Methodologies (“MSM working group on methods”) was established to review the various methodologies used to record enthesal changes (EC) and develop a standardized system to facilitate comparisons across studies. This group consists of people who had already worked intensively with enthesal changes on practical and/or methodological aspects (e.g. Henderson 2003, 2009, Henderson & Gallant 2006, 2007; Mariotti 1998, Mariotti *et al.* 2004, 2007; Pany 2003, Pany *et al.* 2007, 2008, 2009; Villotte 2006, Villotte *et al.* 2009;

Wilczak 1998a, b). Therefore, a new qualitative method (the “Coimbra method”) was developed by the working group for fibrocartilaginousentheses. The new method records individual features of enthesal changes at fibrocartilaginousentheses (marginal bone formation and erosion, and surface bone formation, erosion, fine porosity, macroporosity and cavitation) and the results indicate once more the effects of age on the single features and shows differences in single entheses (Henderson *et al.* 2010, 2012, 2013, 2015 forthcoming, Wilczak *et al.* 2014). Several meetings of the group were held in the following years (Geneva (Switzerland) 2010, Vienna (Austria) 2010, Coimbra (Portugal) 2013) and led to a further improvement of the method. The revised “Coimbra method” paper is under peer assessment at the moment (Henderson *et al.* 2015, submitted to IJO).

According to age, several studies predicted and showed that enthesal and joint alterations can be strongly associated with biological ageing (especially the feature marginal osteophyte growth, e.g. Alves Cardoso 2008, Jurmain 1991, Henderson *et al.* 2013, Merbs 1983, Rogers & Waldron 1995, Weiss & Jurmain 2007, Jurmain *et al.* 2012, and Weiss *et al.* 2012). This association will also be tested in the present thesis.

Further, this thesis draws attention to the evaluation of a new methodological approach in quantifying the surface structures of entheses (Pany *et al.* 2007, 2008, 2009, Viola *et al.* 2008). A new, observer independent and reproducible 3D method was tested by using a surface scanner (OptoCAT, Breuckmann GmbH) producing digital images of the muscle insertions. By quantifying 3D/2D surface areas and perimeters, surface complexity measures and planarity statistics, the visual differentiation between the grades of entheses, scored with a standard method, could be confirmed. The results of this exploratory study could help provide a basis for creating new standards for visual scoring of entheses and joint features (chapter 3.6).

## **1.2 Hypotheses**

The following hypotheses have been verbalised at the beginning of the thesis:

1. There is a correlation between the degree of changes of selected musculoskeletal markings and the degree of the joint changes; this would mean that stronger enthesal changes should be associated with more severe osteoarthritic changes in the same skeletal area.

2. It is expected that the degree of changes of musculoskeletal markings and joint changes increases with age; this means that older individuals should show stronger changes in entheses and joints and this will be controlled for.
3. There is a specific pattern of musculoskeletal markings and joint changes visible in both sexes between the populations. A pattern of enthesal and joint changes is expected to become visible over the statistical group analysis due to different activities in the two sub-sites.
4. Presumably, the two archaeologically located sub-sites (fortified settlement/production oriented settlement) had different “functions”. Therefore, we assume a social difference between the two subpopulations: warriors versus working men? It is suspected that social differences should be detected by the statistical group analysis.

The skeletal populations of Thunau/Kamp seemed to be very appropriate to answer these questions, for the skeletons are well preserved and two archaeologically separate groups from the same time horizon could be identified. However, at the time of data acquisition, the valley site group consisted of a low number of individuals, limiting the validity of the results. The hypotheses are tested using different approaches, like calculating frequencies (how many individuals are affected by changes), asymmetries in the upper and lower limbs and tests on the dependency of the features on age. These assumptions also made it possible to test for biological questions frequently discussed in the anthropological literature by means of the Thunau skeletons. The objectives of this work are therefore of theoretical (archaeological) and practical (biological) nature and value.

All in all, this thesis deals primarily with aspects important for the reconstruction of living conditions, in particular forms of work organisation of the Early Medieval society from Thunau/Kamp. The results can be useful for further analyses of enthesal changes. Moreover, a new, observer independent and reproducible 3D method for quantifying the surface structures of entheses was tested and can be recommended for further studies. The history of this work extended my perspective from a rather practically oriented interest in musculoskeletal markings to a theoretically accentuated focus for my scientific future.

## 2 MATERIAL

### 2.1 Origin of the skeletons

The village of Thunau/Kamp, where the skeletons analysed in this thesis were found, is located in the north-western part of Lower Austria (Figure 1). The skeletons were recovered at two Early Medieval archaeological sub-sites, dating from the 9<sup>th</sup> to 10<sup>th</sup> century AD (Nowotny 2011, Obenaus *et al.* 2006, 367). It consists of a hillfort on the “Schanzberg” and a settlement in the valley close to the river Kamp. The Early Medieval central place of Thunau probably served as a “junction” along a trading route (Herold 2008, Obenaus 2011).



**Figure 1.** Location of the place of discovery in (Gars)/Thunau in north-eastern Austria (© NHM, Department of Anthropology, W. Reichmann).



**Figure 2.** Aerial photography of the two sub-sites at Thunau/Kamp, Austria, where the skeletons were found. 1: Fortified hillfort settlement with manor house and outer bailey “Schanze”; 2: Outer bailey of hillfort, settlement with big settlement terraces; 3: Downhill graveyard from 9th-10th century AD; 4: Downhill settlement with residential and industrial area (Obenaus 2013; © Bild Nr. 02000607.168 Luftbildarchiv, Institut für Urgeschichte und Historische Archäologie, Universität Wien).

The two sub-sites at Thunau, the Schanzberg and the valley site, differ archaeologically according to settlement structures and amount and way of setting of the grave goods. More than 300 skeletons, among them about 64% subadults (Teschler-Nicola *et al.* in preparation, compare demography section 2.2.), have been excavated at the Schanzberg site (“uphill site”, series 1) between 1965 and 1990, and between 1993 and 2003 (supervisor H. Friesinger until 1990, from 1993 supervisor E. Szameit until 2003; Breibert & Wiltschke-Schrotta 2010, 128, Obenaus 2013). From the valley sub-site (“downhill site”, series 2), about 60 individuals were excavated since 2004 (Obenaus *et al.* 2006, 347) including about 58% children (Teschler-Nicola *et al.*, in preparation, compare table 1). The Thunau-valley excavation is still ongoing (supervisor M. Obenaus, pers. comm.). The last skeletons included in this analysis are from the excavation campaign of the year 2006.

The skeletons are mostly well preserved (Figure 3), though the bone surface and the joints tend to be eroded. Supine burials were the norm (Nowotny 2011, 37). All the analysed skeletons are currently housed at the Natural History Museum in Vienna, Austria.



**Figure 3.** Left side: male skeleton lying in supine position (G 129) from Thunau Schanzberg/Herrenhof (uphill site). Right side: male skeleton lying in supine position (G 6) from Thunau-valley (downhill site). (left: Fig. 15 in Friesinger & Friesinger 1991, right: photo M. Obenaus, printed with friendly permission).

### 2.1.1 Archaeology of the Schanzberg site/uphill group

This site is located on a hill plateau (“uphill site”, = series 1), about 400m above sea level, extending approximately 600m west-east and 140m north-south (Friesinger & Friesinger 1991). The whole hillfort area at the Schanzberg overlooks the river valley, and the graveyard sector where the most graves were found was presumably reserved, at least partially, for a social elite as identified by a special grave group within the site. The hillfort probably represented a seat of administrative power, and the settlement had a military function and

served as a trading centre in the periphery of the Frankish empire (Nowotny 2011, Obenaus 2011, Teschler-Nicola *et al.* 2015).

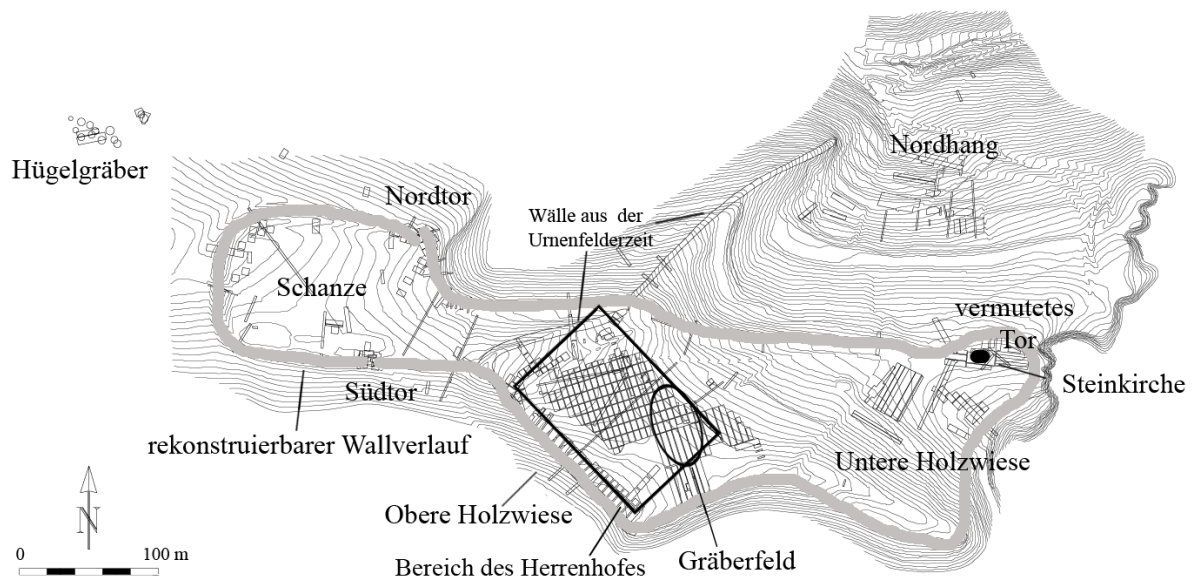


**Figure 4.** Archaeological plan of the excavation sites from 1965 to 2003 at the Schanzberg in Thunau/Kamp. **Legend:** Gräberfeld = graveyard, Untere Holzwiese = area at the Schanzberg, Steinkirche = stone church, vermutetes Tor = supposed gate, Nordhang = northern slope, Wälle aus der Urnenfelderzeit = ramparts from the Urnfield Period, Nordtor = northern gate, Schanze = small earthwork, Hügelgräber = tumuli, rekonstruierbarer Wallverlauf = reconstructable course of the rampart, Obere Holzwiese = area at the Schanzberg, Südtor = southern gate, Bereich des Herrenhofes = Herrenhof area; (Figure 3 in Nowotny 2011, reprinted with friendly permission).

The Schanzberg consists of an outer bailey (Schanze) and a main castle with the hillfort “Herrenhof” (“Holzwiese”, Herold 2008, Szameit 1995). The “Herrenhof”, interpreted as fortified manor house and defined with wooden palisades (Figures 4 & 5), includes the graveyard at the uphill site. Further graves analysed here were excavated at the “Saugrube” and “Schanze” areas (Figure 4). About in the middle of the graveyard, there is an 8 m broad band, interpreted as access to the cemetery and separating it into a north-western and a south-eastern part (Figure 6, Nowotny 2011, Szameit 1995). The amount and quality (but not presence) of grave settings in the south-eastern part of the cemetery is meagre (Nowotny 2011, 163). In the uphill series there is a grave group (graves 129/130) which is interpreted as a special “elite”, males buried with swords (n=2, one of them decapitated, Figures 3 & 7). Further, a grave containing a juvenile buried with an axe (grave 75) and individuals interred with spurs (n=4) are interpreted as socially higher standing. They are mainly buried around a

grave-free area at the western end of the cemetery, where a wooden church is assumed to have stood (Figure 6, Friesinger & Friesinger 1991, Herold 2008). Further, males buried with knives longer than 15cm could be interpreted as belonging to a social elite (n=7; Nowotny 2011, 95). The three burials containing the swords and the axe are the only ones in the graveyard comprising offensive weapons (Nowotny 2013, 441).

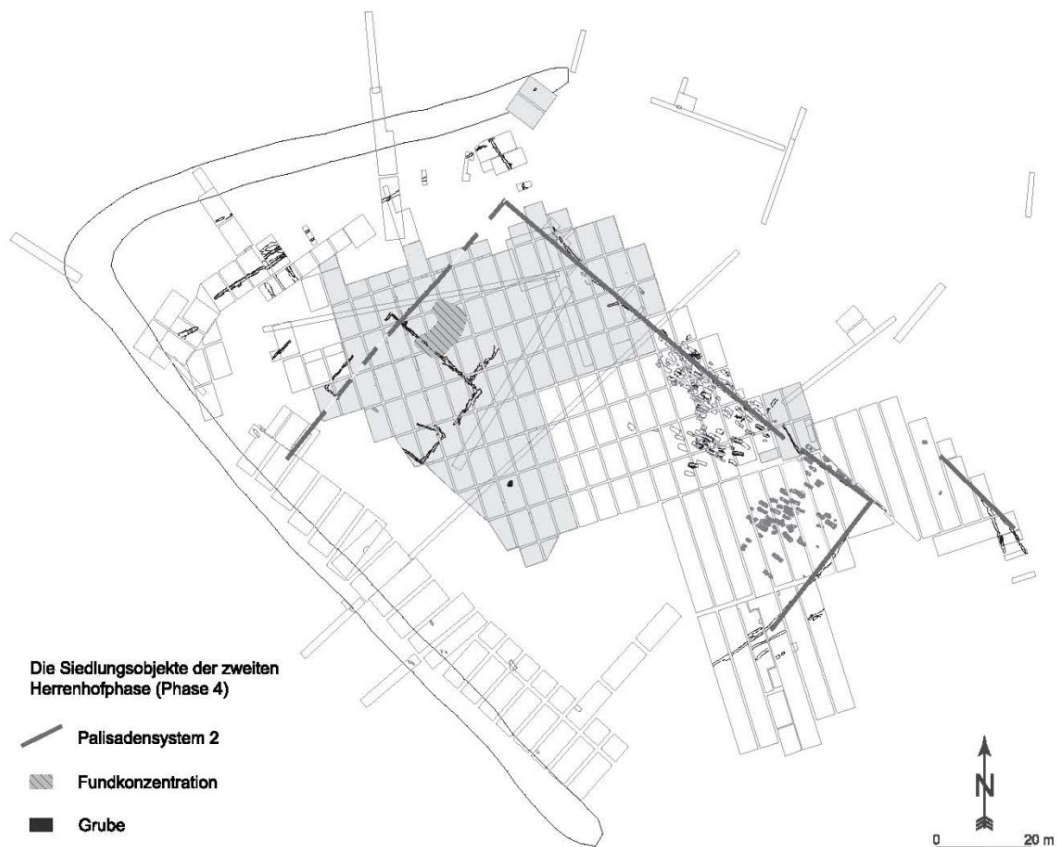


**Figure 5.** Map of the hillfort of Herrenhof/Thunau showing the graveyard, the settlement and the palisade system (Palisadensystem). (Fig. 9 in Herold 2008, reprinted with friendly permission).

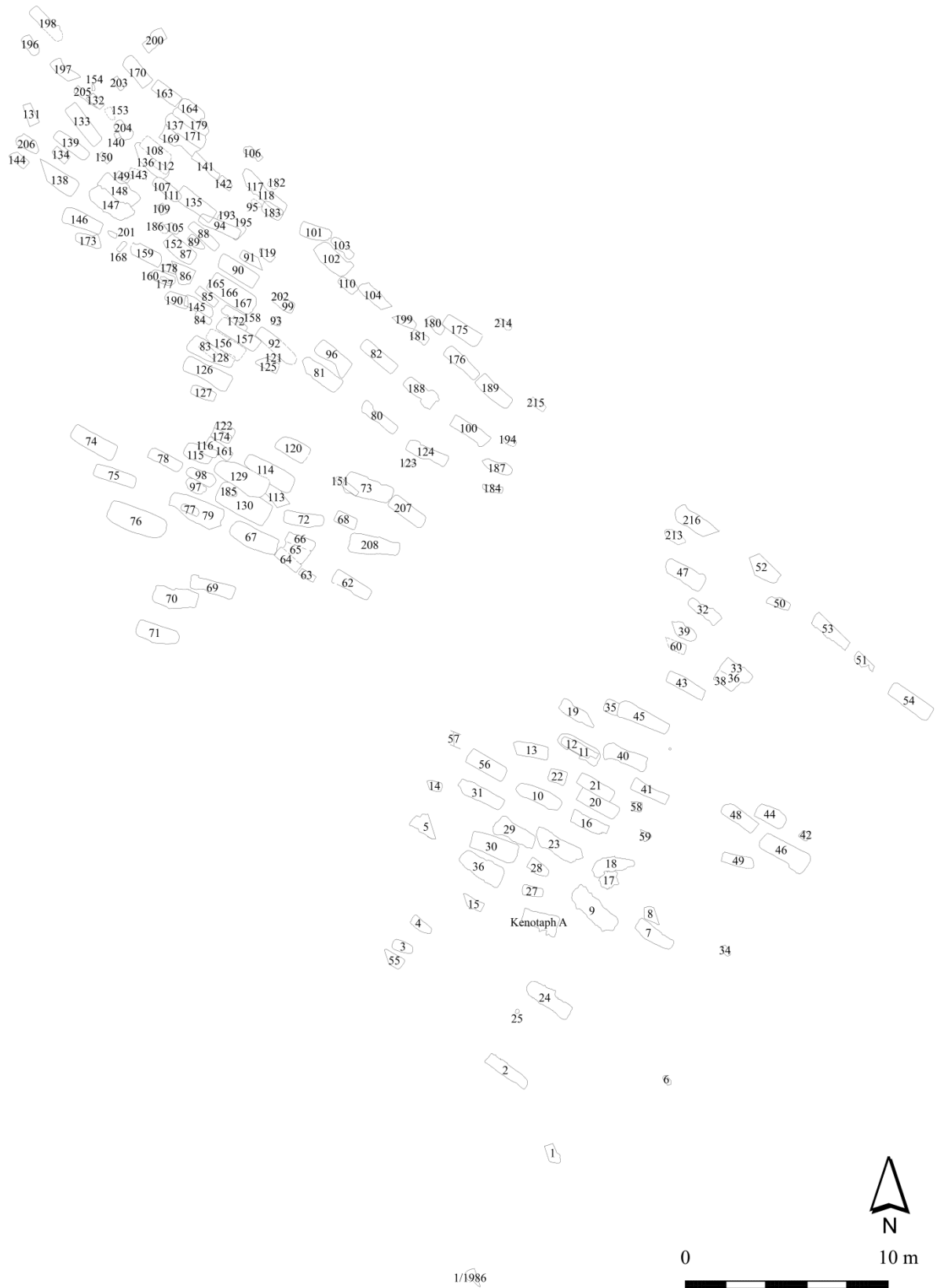


**Figure 6.** Map of the cemetery at the hillfort Herrenhof (Fig. 5 in Nowotny 2011, reprinted with friendly permission).

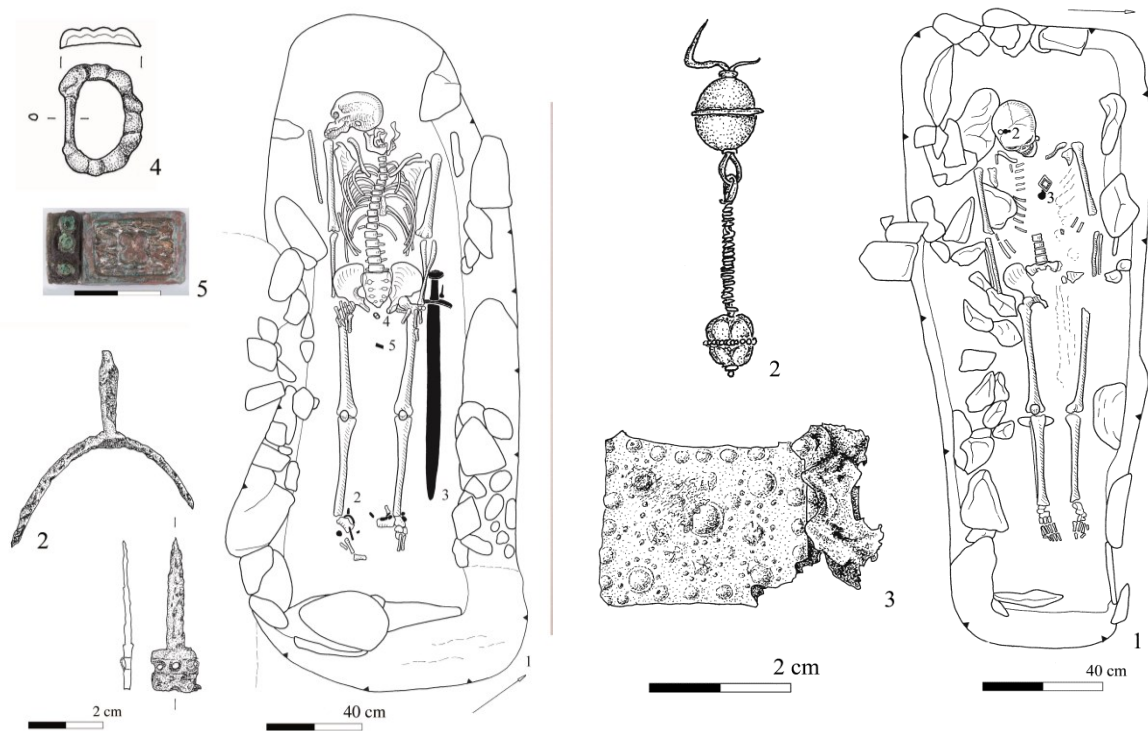


**Figure 7.** Examples of drawings of the skeletons in situ in the graves with grave goods. Left side: male individual (grave 129), right side: female individual (grave 208) buried in the cemetery of the hillfort (uphill) site (panels 28 and 41 in Nowotny 2011, reprinted with friendly permission).

A small group of elite females buried with gilded and silver earrings was identified (Nowotny 2013, Obenaus 2013). The most common grave goods with females are jewellery, rings for headdresses, ear- and finger rings (Figure 7). Findings in the settlement or among the grave goods revealed no indication of any special activity for the females (Nowotny 2011).

## 2.1.2 Archaeology of the valley site/downhill group

The second excavation site where skeletons analysed in this thesis have been found is a large, unfortified settlement situated at the foot of the Schanzberg, near the river Kamp. The altitude difference between the two sites is about 120 m. The below called “downhill site” (=series 2, “Thunau-valley”) has the structure of a “suburb”, and consists of the localities Goldberggasse and Schimmelsprunggasse. The valley site includes a graveyard, a settlement with residential and production function, and an area of “industrial” character at the banks of the river Kamp (Figure 8). The valley settlement supplied the whole centre in cooperation with the hinterland to the east and north of it (Obenaus 2011, 529). It was probably inhabited by craftspeople, farmers and their families (Obenaus 2011).

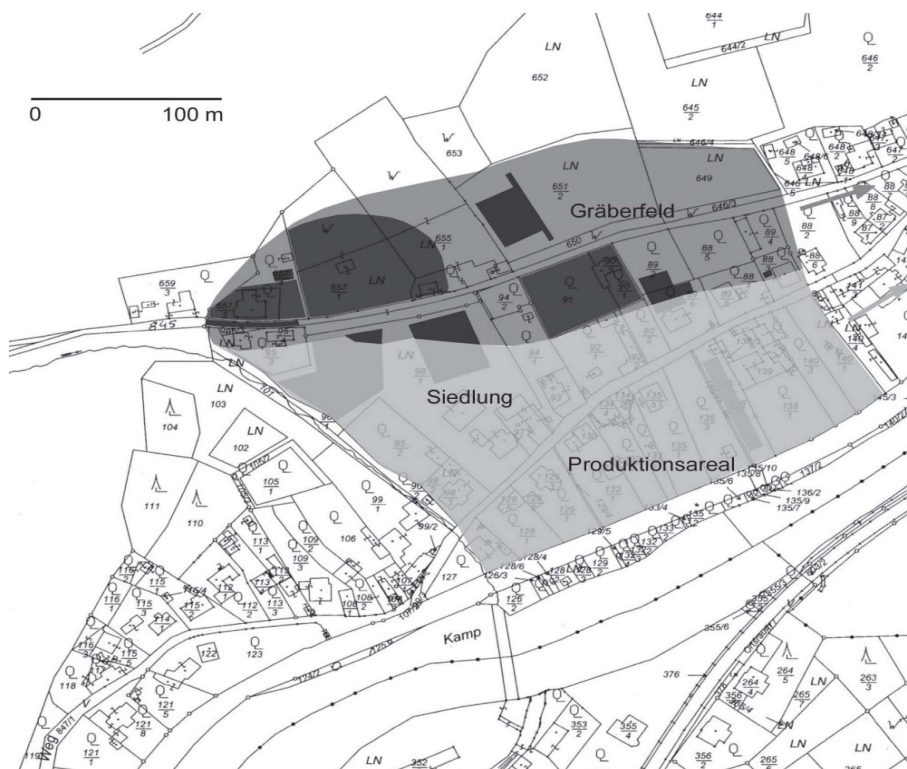


**Figure 8.** Map of the downhill graveyard and settlement area. Legend: Gräberfeld = graveyard, Siedlung = settlement, Produktionsareal = production area. (Figure 3 in Obenaus 2011, reprinted with friendly permission).



**Figure 9.** Remains of a pit-house (Grubenhäus) with evidence of an oven, loom weights and millstones, discovered in the downhill settlement (Photo: M. Obenaus, printed with friendly permission).

About half of the burials contained grave goods, mainly pottery and costume parts (headdresses), but also weapons (the tip of a winged lance) and riding equipment (one pair of spurs). Interestingly, the most comprehensive costume parts were found in girls' graves, as is also known for Dolní Věstonice (Obenaus 2011). Textile production and ironworks seem to have been the main branches of production in the valley settlement. Moreover, semi-subterranean pit-houses with ovens (Figure 9 & 10), mill stones and several hundreds of loom weights (Figures 9 & 11), spindle whorls, a pottery kiln and a blacksmith's shop (Figure 12) have been identified in the industrial area (Obenaus 2011 & 2013, Szameit & Obenaus 2007, 727 & 2009, 462). Due to constricted room, agricultural commodities were very probably mainly purchased from outside the community and only processed in the settlement (Obenaus 2011, 542). Interestingly, as in the hillfort site (male with a sword and spurs), there was also a decapitated male with spurs found in the downhill site (Obenaus 2011, 535). This could point to an affiliation of those men to a military establishment and possible punitive measures (Obenaus 2008, 197).



**Figure 10.** Evidence of a baking oven (left side) and loom weights (right side) found in the downhill settlement area (Photos: M. Obenaus, printed with friendly permission).



**Figure 11.** Evidence of a blacksmith's shop (central part) discovered in the downhill settlement (Figure 18 in Obenaus 2011, reprinted with friendly permission).

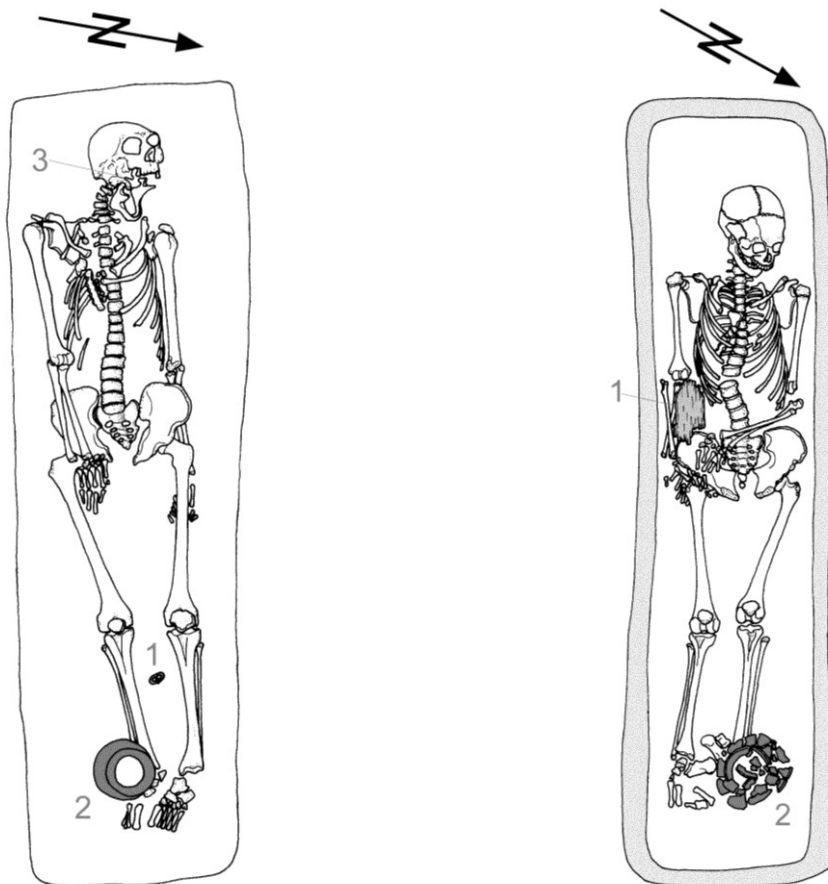


**Figure 12.** Examples of drawings of the skeletons in situ in the graves with grave goods of a male (grave 6, left side) and a female (grave 27, right side) buried in the graveyard of the downhill site of Thunau (left: Figure 5, right: Figure 8 in Obenaus *et al.* 2006, reprinted with friendly permission).

Initially the valley site was supposed to be a simple rural settlement, but meanwhile it is clear that it represents a production-oriented junction between the hillfort at the Schanzberg and the fertile hinterland. Such closely to a central place like the Schanzberg associated localities are called “suburbs” and are well known from contemporary Moravian and Bohemian centers, displaying a similar structural division as seen in Thunau (Obenaus 2013, 330).

## 2.2 Demography

Table 1 shows the total number of individuals from the two sub-sites of Thunau. 309 individuals were recovered from the uphill (Schanzberg) site, and 64 from the downhill (valley) site (until 2006). There are a very high number of children included in both samples, about two thirds in each, but especially in the uphill site individual number. This fact is probably due to the high rate of infectious diseases in these series (e.g. tuberculosis, Teschler-Nicola *et al.* 2015). From the adults, about half were recordable for entheses, and about two thirds for the recording of the joints in the two groups, respectively (compare table 1& chapter 3). The downhill group is comparatively small. Mean age was between 37 and 44 years in the males, and between 39 and 42 years in the females of the two series (Table 2).

**Table 1.** Total numbers of individuals and number of individuals feasible for this study (n adults in bold) from the two analysed sites in Thunau/Kamp\*.

<b>Thunau/Kamp</b>	<b>N total</b>	<b>n adults</b>	<b>% adults</b>	<b>n children</b>	<b>% children</b>
series 1 (uphill)	309	<b>110</b>	35,6	199	64,4
series 2 (downhill)	64	<b>27</b>	42,2	37	57,8

**Table 2.** Mean age of males and females of series 1 (uphill) and series 2 (downhill)\*. SD=standard deviation.

<b>sex/series</b>	<b>mean age/SD [years]</b>
males series 1	37,9 ± 11,1
females series 1	41,6 ± 15,3
males series 2	43,4 ± 19,7
females series 2	39,7 ± 11,7

There is considerable variation in the long bone lengths and shape (Table 3 & Figure 13). Body height differed significantly between males and females in both sub-sites (about 10 cm difference). However, body height was very similar in the males and the females of the two groups, respectively.

**Table 3.** Mean body height of the uphill and downhill individuals\*. SD=standard deviation.  
\*\*including one individual who is noticeably shorter than the others.

<b>sex/series</b>	<b>mean body height/SD [cm]</b>
males series 1	172,5 ± 7
females series 1	160,2 ± 8,5
males series 2**	172,4 ± 11
females series 2	159,5 ± 6,8

\*Many thanks to F. Novotny, M. Spannagl-Steiner, M. Teschler-Nicola & K. Wiltshcke-Schrotta for providing me with the relevant data.



**Figure 13.** There is considerable variation in the long bones, visible here in 4 humeri from the graves (from left to right), 82 (male), 45/1 (male), 20 (female), 101 (female), all from the uphill site (© NHM, Department of Anthropology, W. Reichmann).

### 3 METHODS

#### 3.1 Selection of the skeletons

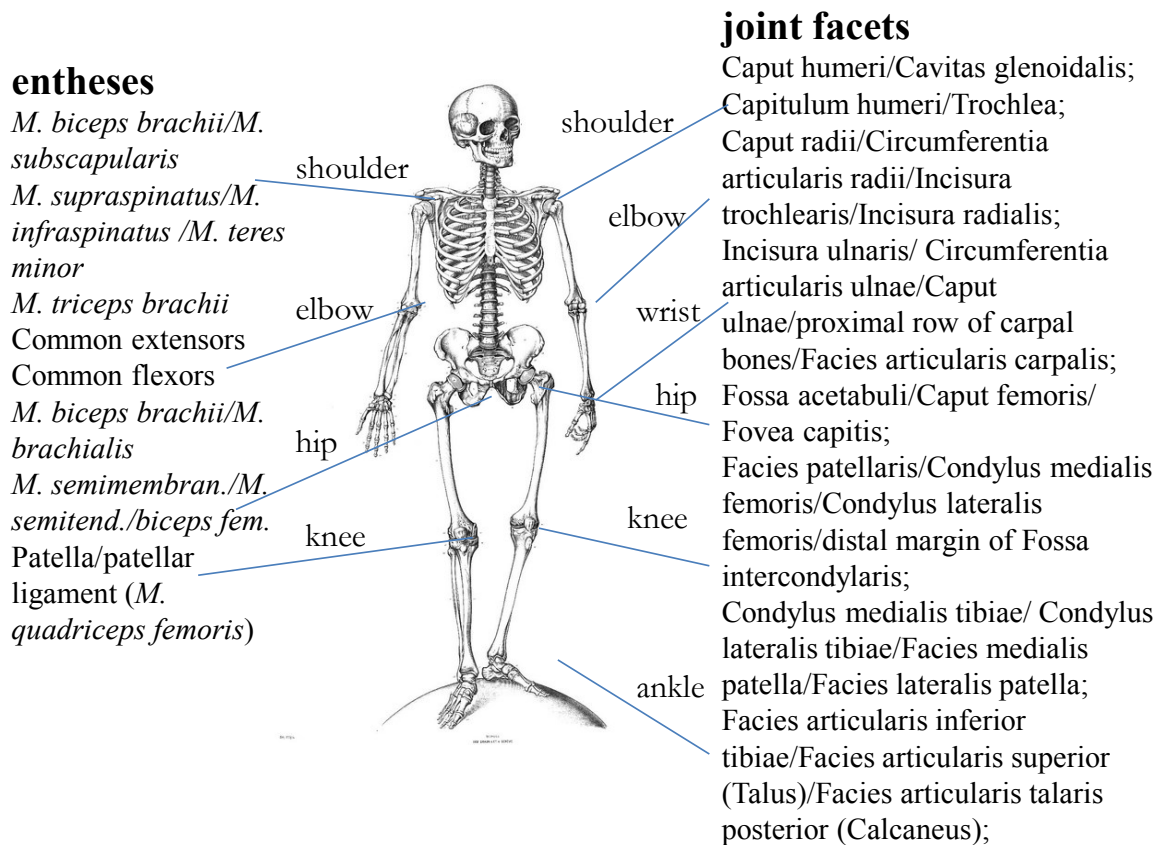
The combination of entheses and joint features, as performed in this study, is a special and innovative approach in order to experience the level of activity and social organization within and between historic populations. The aim was to reconstruct daily activities and maybe identify specialists on group level by means of enthesal and joint changes on the base of archaeological information from the settlements and burial areas. The special entheses and joint investigation on these skeletons is part of a comprehensive study on the Thunau populations. Therefore, data including age, sex and pathologies of the individuals from the different excavation periods have been collected by colleagues (Teschler-Nicola *et al.* 1994, Novotny, Spannagl-Steiner, Teschler-Nicola & Wiltshcke-Schrotta, publication in preparation), using standard anthropological methods. For the special investigation of enthesal and joint changes, growth of the skeleton needs to be completed, and therefore, only adult and reliably aged and sexed individuals were included in the analyses. Obviously, in this population there was a high rate of infectious diseases e.g. tuberculosis (Teschler-Nicola *et al.* 2015), and there is a very high percentage of infant mortality. Further, poorly preserved skeletons, or individuals with evidence of healed fractures or severe pathologies (one case with polyarthritis (2004/6)), or signs of (joint) tuberculosis) were excluded from the final investigation in order to avoid recording of non-work related enthesal and joint changes. Individuals who turned out to have a too few recordable joints and entheses (less than 50%) had to be excluded for the final calculations. Finally, due to the above mentioned causes, it was possible to use the following numbers of individuals for visual inspection of selected upper- and lower extremity entheses and joints (Table 4).

**Table 4.** Number of individuals used for visual inspection of entheses and joints, right and left side.

<b>Thunau/Kamp</b>		<b>n males</b>	<b>n females</b>
<b>right extremities</b>	<b>n entheses/joints</b>	<b>entheses/joints</b>	<b>entheses/joints</b>
series 1 (uphill)	53/70	31/40	22/30
series 2 (downhill)	14/14	7/7	7/7
<b>left extremities</b>	<b>n entheses/joints</b>	<b>n males</b>	<b>n females</b>
series 1 (uphill)	55/70	31/40	24/30
series 2 (downhill)	12/14	6/7	6/7

All big joints and the main fibrocartilaginous entheses on the adequately preserved adult skeletons were recorded in this study. 15 selected fibrocartilaginous entheses and 27 joint facets on right and left sides were pooled into muscle and joint groups functionally for comparison (Table 5).

**Table 5.** Recorded entheses and joint facets on the skeleton.



## 3.2 Enthesis analysis

The term enthesis is defined as “the attachment site (either the origin or the insertion) of muscle, tendon and joint capsule to bone” (Benjamin *et al.* 2002). The visual evaluation of the enthesal changes primarily followed the recording system of Hawkey & Merbs (1995; therein, the changes are called “musculoskeletal stress markers; I chose the recently recommended term (Jurmain & Villotte 2010) “enthesal changes” here for reasons explained in the introduction section 1.1.), i.e. the morphological expression categories robusticity, stress lesion and ossification exostosis. They are represented by the categories robusticity (scores 0-3), stress lesion (scores 4-6) and osteophyte growth (scores 7-9) at muscle attachment sites, which were recoded into 0-3 for calculations. The chosen fibrous and fibrocartilaginous entheses were evaluated macroscopically as well as with the help of a magnifying glass. Medical (Benjamin *et al.* 1986; 2002, Biermann 1957, Knese & Biermann 1958) and anthropological publications of Villotte (2006), Villotte *et al.* (2010), Mariotti *et al.* (2004, 2007) and later the entheses method group (Henderson *et al.* 2010, 2012, 2013), brought new insights into the anatomical understanding of entheses. Being influenced by and following these recommendations, the fibrocartilaginous entheses, which are associated mainly with the region of the epiphyses and apophyses, were finally chosen to be used for the analysis. There are transition zones of tissue at a typical fibrocartilaginous enthesis of an adult tendon: 1. pure dense fibrous connective tissue, 2. uncalcified fibrocartilage; 3. calcified fibrocartilage, and 4. bone (Dolgo-Saburoff 1929/30, 86, Benjamin *et al.* 1986, 89, Benjamin *et al.* 2002, compare also Knese & Biermann, 1958). A “normal” fibrocartilaginous enthesis shows a smooth surface with well-defined margins, and any deviation from this is considered abnormal (Henderson *et al.* 2012, Jurmain *et al.* 2012). Supposedly, a basic function of the fibrocartilage zones is to balance the different modules of elasticity of the bone and the tendon (Benjamin *et al.* 2006, Knese & Biermann, 1958). The other type of muscle insertions on the skeleton, the fibrous entheses, are mainly associated with the diaphysis, and they can be subdivided into periosteal and bony (Benjamin *et al.* 2002, 934). Fibrous entheses show a roughened surface and poorly delimited margins. Here, differentiating between “normal” and “abnormal” entheses is difficult (Henderson *et al.* 2012, Jurmain *et al.* 2012). Fibrocartilaginous entheses are more vulnerable to overuse injuries (Benjamin *et al.* 2002, 934). Because of this and differences in their location at the skeleton, in attachment area size and mechanical properties as well as a multifactorial aetiology, fibrous and fibrocartilaginous entheses cannot be compared directly with the same system, and therefore the fibrous

entheses were discarded from the analysis here (Alves Cardoso & Henderson 2010, Henderson *et al.* 2013, Villotte 2006). For the chosen fibrocartilaginous upper limb entheses in this thesis (Table 6, compare scoring sheet in addendum), mechanically induced changes are known to occur from sports- and/or occupational medicine (compare Villotte *et al.* 2009, 2).

**Table 6.** Table showing attachment sites (region/bone) of the analysed muscles, their exact location, functions and acronyms (\*all taken from Gray’s Anatomy, 1995 & Platzer, 1991)

<b>muscle/region/bone</b>	<b>location</b>	<b>function*</b>	<b>acronym</b>
<i>M. biceps brachii/M. subscapularis</i> (shoulder/scapula/humerus)	supraglenoid tubercle/ lesser tubercle	anteversion of upper arm/internal rotation	SBB_SCC
<i>M. triceps brachii</i> (shoulder/scapula/elbow/ulna)	infraglenoid tubercle/olecranon	extension of elbow (against resistance)	STB_UTB
<i>M. supraspinatus/M. infraspinatus/ M. teres minor</i> (shoulder/humerus)	greater tubercle	abduction, external rotation, adduction	SSP_ISP_HMI
<b>Common extensors</b> (elbow/humerus)	lateral epicondyle of humerus	extension of hand	COM_EXT
<b>Common flexors</b> (elbow/humerus)	medial epicondyle of humerus	flexion of hand, pronation	COM_FLEX
<i>M. biceps brachii/M. brachialis</i> (elbow/radius/ulna)	radial tuberosity	flexion and supination of lower arm/flexion of elbow	BIB_BRA
<i>M. semimembranosus/M. semitendinosus/biceps fem.</i> (os coxae)	ischial tuberosity	retroversion of hip, flexion and internal rotation of knee	SME_STE_BIF
<b>Patella/patellar ligament (<i>M. quadriceps femoris</i>)</b> (lower leg/Patella/tibia)	tibial tuberosity	extension of knee	PAT_TLP

In Figure 14, examples of enthesal changes in the Thunau population can be seen. Porosities, marginal osteophyte growth and new bone formation at the attachments of the *M. subscapularis* at the humeral head, the common flexors at the medial epicondyle of the humerus and the *M. biceps brachii* at the proximal radius are shown. The surfaces should normally be smooth (Henderson *et al.* 2013).

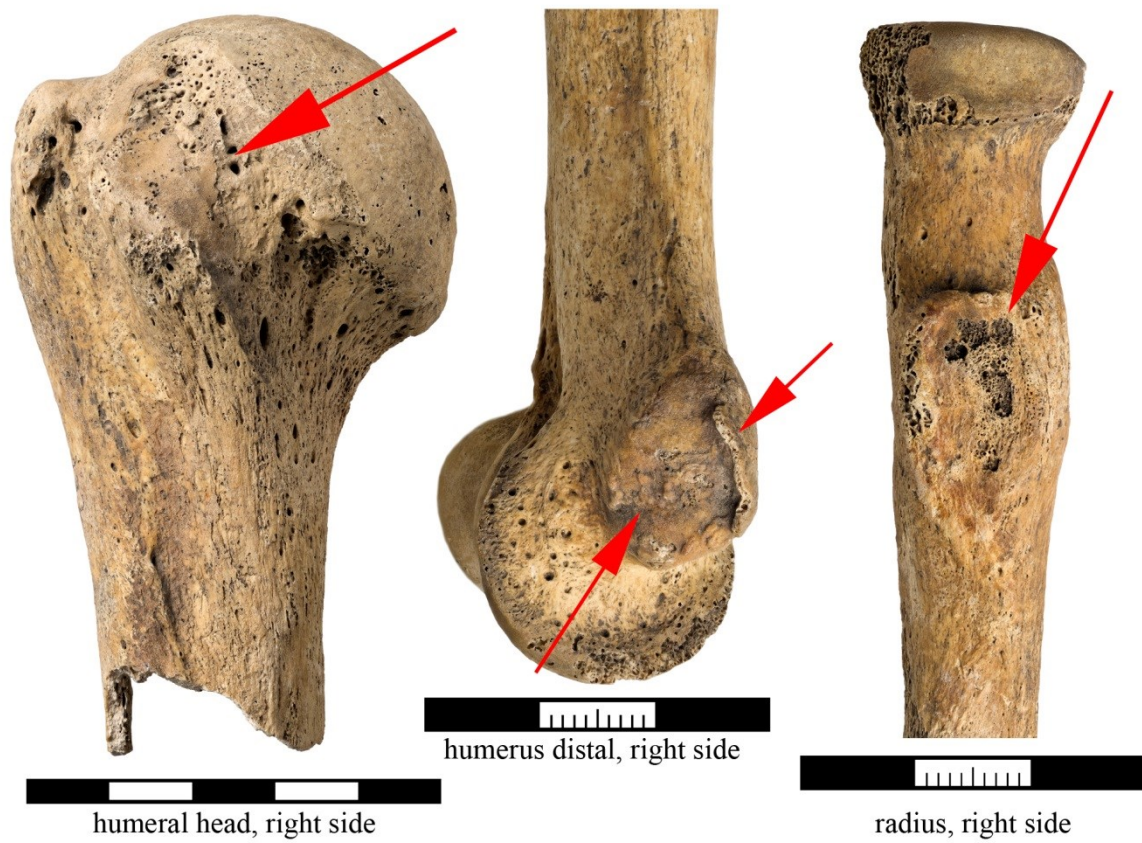


**Figure 14.** Examples of enthesal changes in the Thunau population. Compare text for details. (© Department of Anthropology, NHMW, W. Reichmann).

### 3.3 Joint analysis

Basically, it is possible to discern between degenerative and inflammatory changes at joints (Schultz 1988). The latter, mostly called osteoarthritis (OA), is the most common form of arthritis, and results from idiopathic age-related processes including mechanical factors. The inflammation in OA is probably a secondary response to primary mechanical and/or mechanobiological influences on joint destruction. The term ostoarthrosis is used to distinguish the changes from the primarily inflammatory induced ones. OA is strongly correlated with age, and a systemic and genetic predisposition of the individual play a role (Carter & Beaupré 2001, Rogers & Waldron 1995). OA is probably the product of a normal remodelling or repair process and is the natural reaction of a synovial joint to joint failure (Rogers & Waldron 1995). However, it was not the purpose here to ascribe an underlying aetiology of the changes, and therefore, the term osteoarthritis will be used throughout this thesis because it is widespread, alternating with the more neutral term joint changes/alterations.

From the Thunau samples, 27 joint facets were analysed separately, therefore even only partially preserved joint facets could be included. For the description of osteoarthritic changes at the joints, simplified standards originally defined by Schultz (1988, compare scoring sheet in addendum) were applied. According to the standards of Schultz, osteoarthritic changes are represented by marginal osteophyte growth, new bone formation at joint surfaces, porosities at the joint surface and eburnation at articular surfaces; this is mostly summarized as osteoarthritis (Schultz 1988). The categories were scored separately, where 1 = normal, 2 = pathology visible (OP < 3mm, = II.-III. following Schultz 1988), 3 = strong pathology visible (> half of the joint affected, = IV.-VI. after Schultz 1988); eburnation at articular surfaces, which was analysed as a special form new bone formation (Schultz 1988), was scored separately.

The list of joints was shortened for this analysis compared to the one prepared by Schultz (see table 7). Vertebral joints are analysed in a different study part (Nittmann 2012) and are therefore not included here. Figure 15 shows examples of joint changes like marginal osteophytes at the glenoid cavity and the femoral head, porosities at the distal ulna and new bone formation at the femoral head in the Thunau series. The joint groups shoulder, elbow, wrist/hand, hip, knee and ankle/foot, as also recommended in the Data Collection Codebook

by Steckel *et al.* 2005, were analysed. This was done for the right and left upper and lower extremities. In the upper extremities, both sides were analysed separately in order to find possible side differences or preferences. Comparing statistics were performed for severity of pathological alterations generally between uphill and downhill males and uphill and downhill females, respectively. Further, due to the presumption of a relation between the age of the individuals and higher scores in joint alterations, separate tests were performed according to age differences (compare chapter 7).

Table 7. Table showing analysed joints, their exact location and acronyms.

<b>joint/region</b>	<b>location</b>	<b>acronym</b>
<i>Caput humeri/Cavitas glenoidalis</i> (shoulder)	humerus proximal/scapula lateral	CHU_CGL
<i>Capitulum humeri/Trochlea</i> (elbow/upper arm)	humerus distal	CAH_TRO
<i>Caput radii/Circumferentia art. Rad./Incisura trochlearis/Incisura radialis</i> (elbow/lower arm)	radius proximal/ulna proximal	CRA_CIR_INT_INR
<i>Incisura ulnaris/Circumferentia art. Ulna/Caput ulnae/proximal row of carpal bones/Fac. Art. Carpalis</i> (wrist)	radius distal/ulna distal/carpal bones	INU_CIU_CAU_PHW_FAC
<i>Fossa acetabuli/Caput femoris/Fovea capitis</i> (hip)	os coxae/femur proximal	FOA_CAF_FOC
<i>Facies patellaris/Condylus medialis femoris/Condylus lateralis femoris/distal margin of Fossa intercondylaris</i> (knee)	femur distal/femur medial/lateral condyle	FAP_CMF_CLF_UFO
<i>Condylus medialis tibiae/Condylus lateralis tibiae/Facies med. Patella/Facies lat. Patella</i> (knee)	tibia proximal medial/lateral facet/patella medial/lateral facet	CMT_CLT_FMP_FLP
<i>Fac. Art.inf. Tibiae/Fac. Art. Sup. Talus/Fac. Art.talaris posterior Calcan.</i> (ankle)	tibia distal/talus proximal/calcaneus posterior facet	FIT_FST_FPC

For calculations, scoring categories were changed into absence/presence of degenerative changes (1=normal, >=2=pathology visible). For frequencies, a “true prevalence rate” was calculated from the frequencies to look for differences or similarities between the groups.

Scoring categories (adapted from Schultz 1988):

OP = osteophyte growth, KN = new bone formation at joint surface, P = porosities at the joint surface; / = not present, 0 = not assessable, 1 = normal, 2 = pathology visible (OP < 3mm, = II.-III. following Schultz 1988), 3 = strong pathology visible (> half of the joint affected, = IV.-VI. following Schultz 1988); E = eburnation, a = < less than half of the joint present

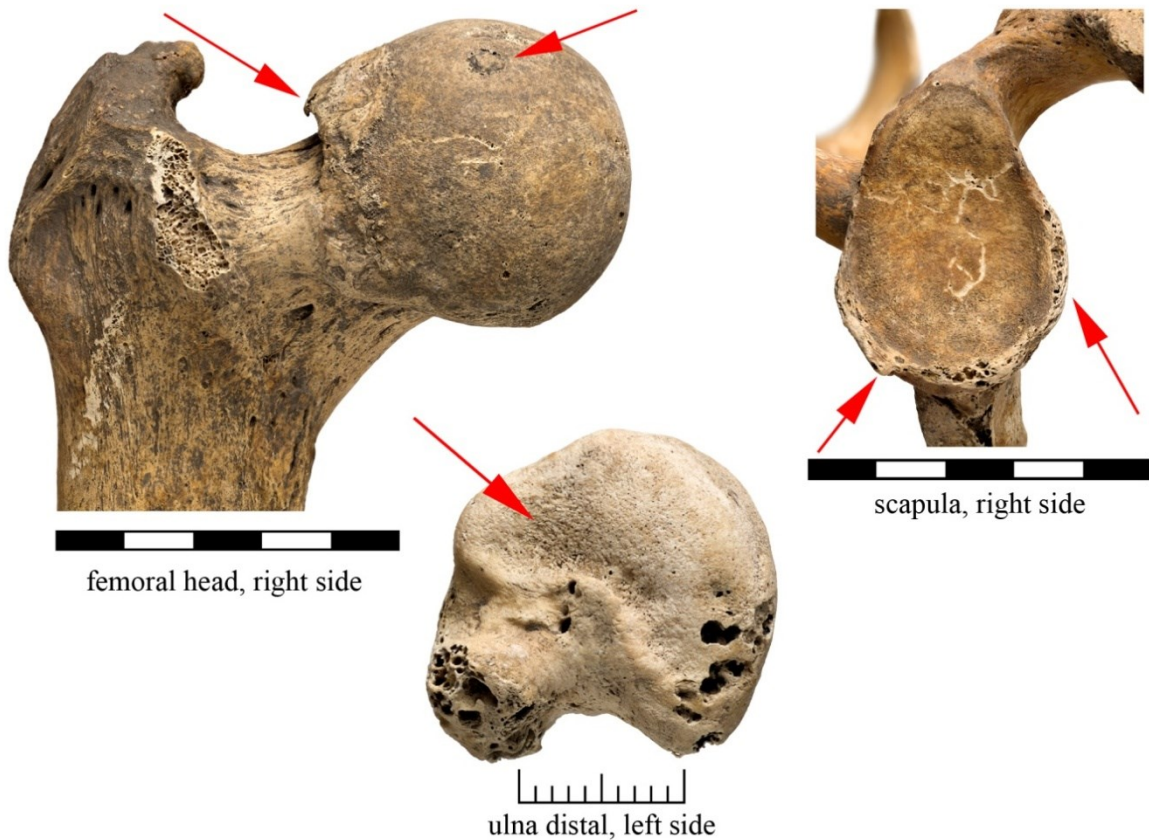


**Figure 15.** Examples of joint changes in the Thunau populations. Compare text for details. (© Department of Anthropology, NHMW, W. Reichmann).

### 3.4 Statistical analysis

For statistical analyses, Microsoft Excel 2007 and SPSS 19.0 were used. Frequencies were calculated in SPSS using descriptive statistics (analyse-descriptive statistics-frequencies) and are shown as histograms. Further, a composite and a mean score of the features was calculated for each analysed muscle in adding the single scores of robusticity, stress lesion and osteophyte growth and dividing them by the number of scores (=mean scores). This combined score should also be less sensitive to anomalies (Niniimäki 2009, 293). The resulting scores were simplified into  $\leq 1$  = normal,  $> 1$  pathology visible, and are represented by robusticity, osteophytic or osteolytic changes at the entheses, being in accordance with an absent/present system (Belcastro *et al.* 2001, Mariotti *et al.* 2004, Alves Cardoso & Henderson 2010).

Further, the muscles were pooled functionally, for they are always working together in special movements (and not singly, Stirland 1998), and the joint facets were pooled per joint. For frequencies, (i.e. how many individuals show pathologic changes) from the absence/presence data, a “true prevalence rate” was calculated, dividing the number of pathological by the number of recordable entheses and joints (Waldron 1994, Rogers & Waldron 1995).

Asymmetry rates were calculated from score differences turned into percent for comparison of the groups (Auerbach & Ruff 2006). Therefore, following the formula of Auerbach & Ruff (2006, 204), the data on asymmetry were converted into percentage directional asymmetries (%DA):

$$\%DA = (\text{right} - \text{left}) / (\text{average of left and right}) \times 100$$

Further, scatterplots were created in order to look at the relationship between mean scores and increasing mean age for right and left sides, entheses and joints and for males and females, respectively. Univariate analysis and corresponding results were added if there was a statistically significant difference visible between the groups (Mariotti *et al.* 2004, Henderson *et al.* 2013, 199).

Sex and population specific group differences between the uphill and the downhill series are expected. Further, a covariance according to the occurrence of enthesal changes (EC) and osteoarthritic changes (OA) is expected. Given the assumption that the changes are caused by physical strain, differences in asymmetry may be expectable in the two samples due to differing subsistence strategies (Weiss & Jurmain 2007). Further, increases in the recorded

features with age are predicted due to other studies showing that these alterations can be strongly correlated with biological ageing (e.g. marginal osteophyte growth, Jurmain 1991, Rogers & Waldron 1995, Weiss & Jurmain 2007).

Muscle and joint data were not recorded contemporaneously in order to avoid any visual interference of the observer. Only adult and reliably sexed and aged individuals were included. Further, individuals displaying (joint) TB or fractured limbs were not recorded. Moreover, only males with males and females with females were compared due to an unknown input of genetic and hormonal changes in enthesopathies, similar body height between males and females, respectively, and a considerable variation in the long bones (compare Figure 13, comparison of humeri).

### **3.5 Enteses and body height**

A possible relationship between body height and higher scores at enteses was tested here because of a significant difference between body height in males and females of the Thunau groups. Scatterplots and univariate analysis were calculated (chapters 7.2 & 10.2).

Total length of the humerus and total and greatest length of the femur (Herrmann 1989), were measured using an osteometric board with 1 mm accuracy, in order to obtain a body size estimate. Normally, right side extremities were used, but if this was missing or broken, the left side bones were used to calculate body height. The calculations were performed using the formulas of Sjøvold (1990). The measurements were partly (downhill sample, selected uphill sample used for 3D) taken by the author and have furthermore been provided by F. Novotny, M. Spannagl and K. Wiltschke-Schrotta (manuscripts in preparation).

## **3.6 Evaluation of a new methodological 3D approach in quantifying the surface structures of entheses**

### **3.6.1 An attempt in using a 3D surface scanner for the recording of enthesal changes**

This method section has an exceptional position in this thesis as it is the self-contained description of an exploratory study that was performed several years ago in collaboration with Th. Bence Viola.

#### **3.6.1.1 Introduction**

Entheses, and especially fibrous entheses, display an enormous variability in size and shape; therefore it remains difficult to assess expression degrees for different stages making meaningful inter-site comparisons difficult. The aim of this exploratory study was to evaluate a new methodological approach to quantifying the surface structures of entheses, i.e. differences in entheses size, surface roughness as well as surface “information content” (see Evans *et al.*, 2007 for an application of similar methods to mammal teeth), using a new, observer independent and reproducible 3D method. We will also discuss technical complexity and expenses in relation to scientific value.

#### **3.6.1.2 Material & methods**

We chose the insertion of the fibrous enthesis of the *M. pectoralis major* on the right humerus for this trial. We used a Breuckmann Opto-Top HE optotopometric surface scanner (Figures 17 & 18, Breuckmann GmbH, Meersburg, Germany), with a field of view of 60 mm to scan the enthesis on a subsample of nine individuals from the Thunau population that span the variability of enthesis development (expression degrees from faint to strong, Hawkey & Merbs 1995; Figure 16). Entheses were first recorded visually using Hawkey & Merbs’ (1995) categories by DP., and a “Composite Enthysis Score” was calculated by BV., recoding the visual scores into the three categories for further calculation. For this, the scores of the single categories robusticity, stress lesion and osteophyte growth were added together, resulting in composite enthesopathy score degrees 1-7 (1-faint, 7-strong). The results are compared to the ones obtained by visual scoring on the same skeletons.



**Figure 16.** Two humeri from the Thunau sample, showing normal enthesis surface (left side, grave 102) and strong enthesial change (right side, grave 45/1) of the *M. pectoralis major* at the proximal humerus (© Department of Anthropology, NHMW, W. Reichmann).



**Figure 17.** Breuckmann Opto-Top HE optotopometric surface scanner used for analysis (picture: [openi.nlm.nih.gov](https://openi.nlm.nih.gov)).

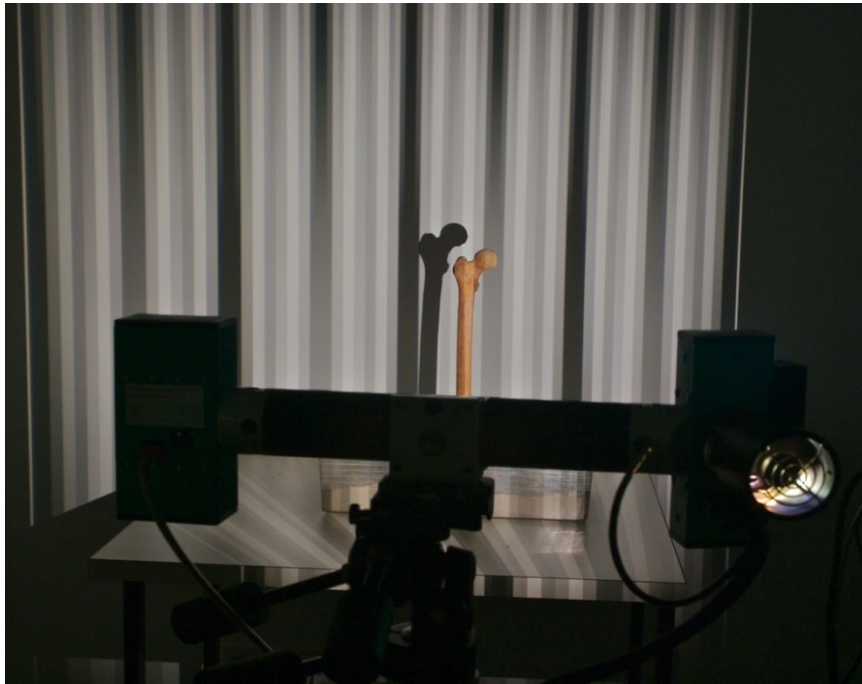


**Figure 18.** Femur in scanning position.

### **3.6.1.3 New methodological approach using surface scanning**

First, different views of the *M. pectoralis major* enthesis were scanned with the 3D surface scanner and aligned (Figure 19) using the least squares algorithm in the software package Optocat 4.0.1 (Breuckmann Inc. 2005).

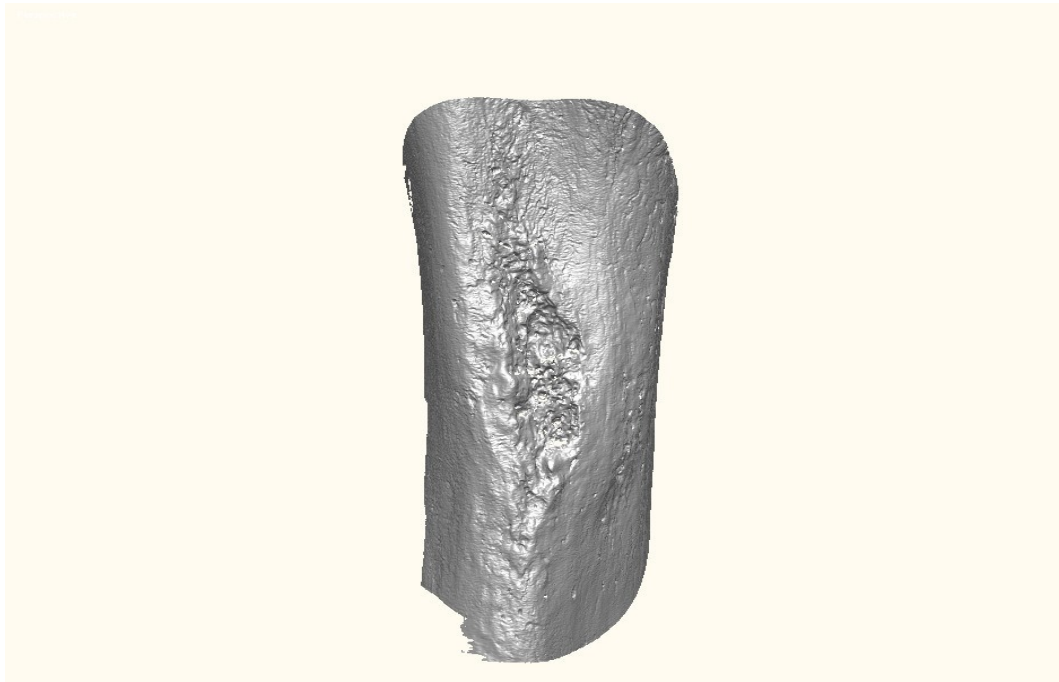


**Figure 19.** In the surface scan of *M. pectoralis major* Thunau 45/1, the rugosity of the surface is much better visible than in the photograph (compare Figure 16, right side).

This took about an hour for the *pectoralis major* site in each bone. The final model is a composite of the different views, fitted together with a least-squares fitting algorithm in the software package Opto- CAT 4.0.1 (Breuckmann Inc., 2005). The resolution of the composite model is better than 20 $\mu$ , and it consists of between 1.5 and 3 million points, depending on the size of the humerus. Then the models were exported as .stl files, losing the texture which was not needed for the analysis. The data were then imported into Rapidform 2006 (Inus Technology Inc., 2006), where the remaining small holes in the scan were filled and abnormal, non-manifold, crossing and self-intersecting faces were removed, thus cleaning up the surface. We delimited the area of the insertion of the *M. pectoralis major* using a NURBS curve (Figure 20, parametrized representation of a three dimensional curve), and then selected all surface points along the curve fitted to a plane (from now on “base plane”) using a least squares algorithm. We then also created a second, two dimensional curve, by projecting the NURBS curve onto the base plane. We measured the 2D (projected) and 3D area of the insertion, the 2D and 3D perimeters (lengths of the curves) and the complexity and information content of the surface. Finally, the planarity of the enthesis was measured (Viola *et al.* 2008).

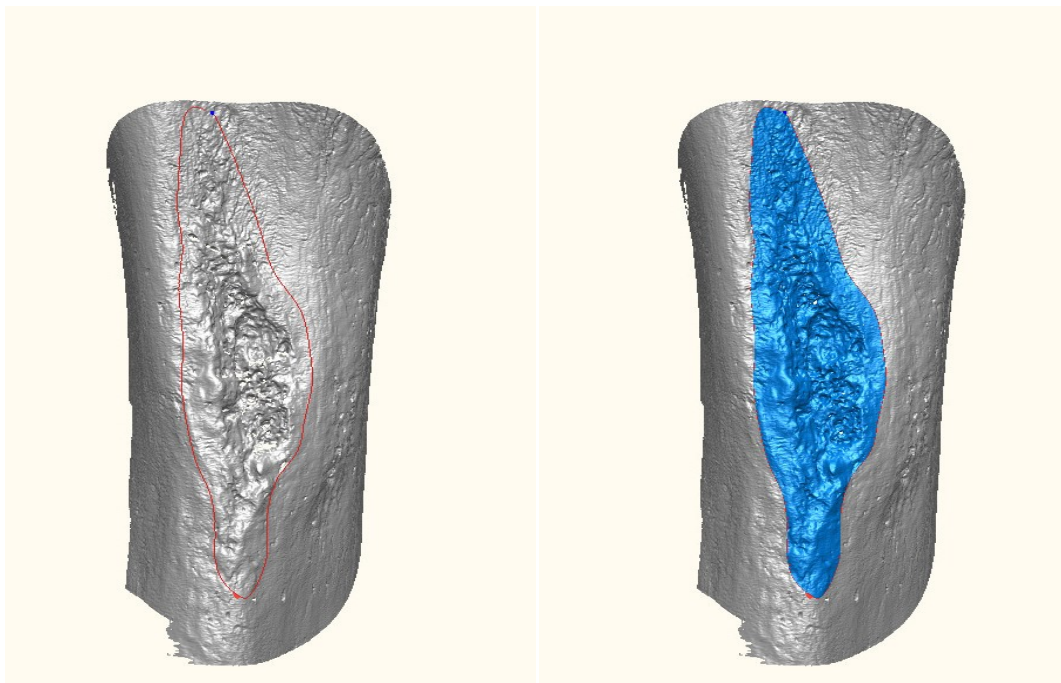


**Figure 20.** The area of the enthesis was delimited using a nurbs curve before cropping the surrounding bone.

We performed the whole procedure repeatedly on several specimens to test for inter- and intra-observer error. We used three different approaches to analyse the surface structure:

- \*3D/2D Surface areas and perimeters (large scale changes)

- \*Surface complexity measures (small scale changes)

- \*Planarity statistics

### **3.6.1.4 Description of the procedures and results**

#### *Surface areas*

In the surface scan of *M. pectoralis major* Thunau 102, the rugosity of the surface is much more visible than in the photograph above (compare Figures 16 & 19). A least squares best fit plane is fit to all points on the surface near the curve delimiting the entheses. A second, 2D curve is created by projecting the delimiting curve onto the base plane (Figure 21). The following variables were used for statistical analysis:

- \*Three dimensional surface area of the entheses, two dimensional area of the entheses (area enclosed on the base plane by the projected curve)

- \*Length of the 3D nurbs curve enclosing the entheses (3D perimeter)

- \*Length of the projected curve (2D perimeter)

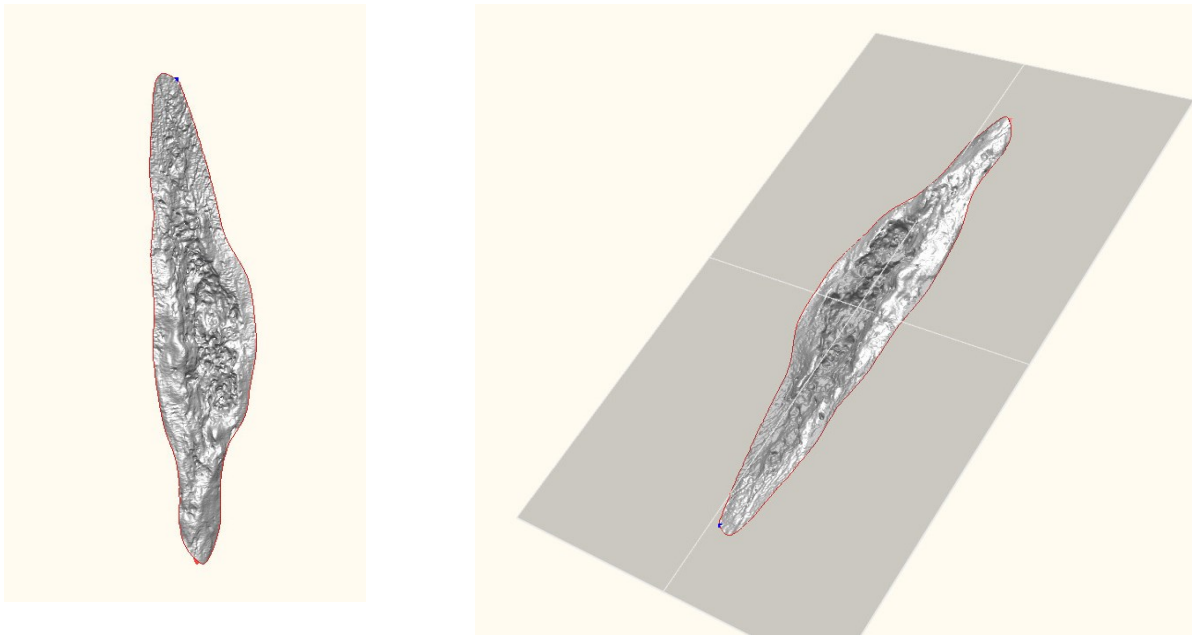


**Figure 21.** The area of the entheses was delimited using a nurbs curve after cropping the surrounding bone. The resulting delimited curve was projected onto a plane fitted to it, thus converting it into two dimensions.

In general, more expressed entheses have a higher surface area, both in 2D and 3D. 3D area is strongly correlated with the composite enthesopathy score (Kendall's Tau 0,833,  $p=0.002$ , Figure 22 left). This is also true when the 3D area is normalized using the 3D perimeter (Figure 22 right).

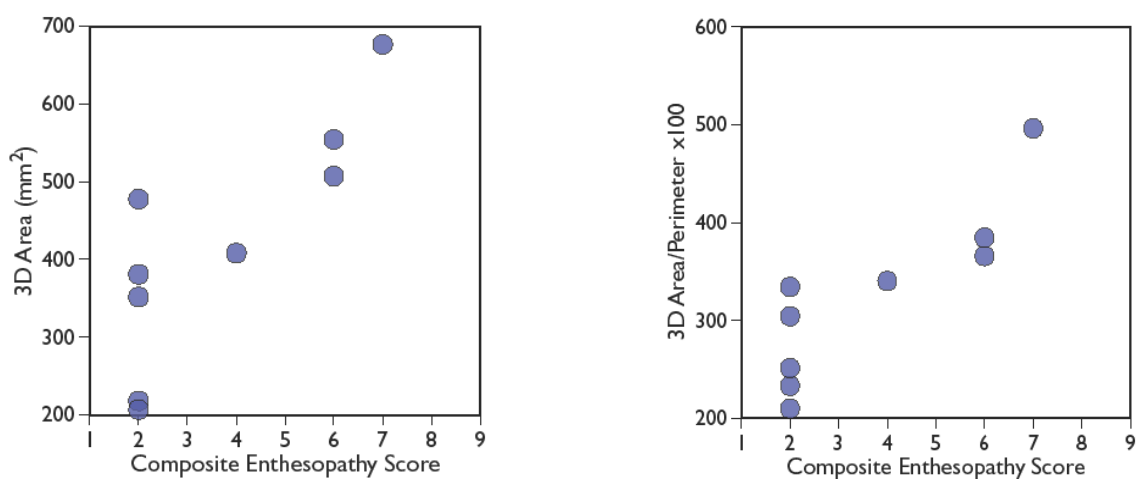


**Figure 22.** 3D area is strongly correlated with the composite enthesopathy score (plots BV.).

### *Surface complexity measures*

This approach tries to measure the complexity and information content of the surface and is based on the method used by Evans *et al.* (2007) to quantify occlusal complexity of rodent and carnivore teeth. As this method operates on digital elevation models, we had to convert the 3D surface into a matrix of elevation values. As a first step we created a new coordinate system using the base plane, with the Z axis as the normal vector of the plane and the X axis is the direction of the maximum diameter of the enthesis. The origin of the system is the centroid of the curve. The points of the surface were exported using this new coordinate system, and imported into ArcGIS 9.2 (ESRI Inc.). We treated the points as if they were the points of a digital elevation model, and interpolated the surface using the Inverse Distance Weighted method (Figure 23). The resulting raster had a resolution of about 35 $\mu$  (again depending slightly on the size of the humerus). In this, and following figures, Gars 1 (Composite Enthesis Score=6) is the specimen depicted on top and Gars 102 (CES=2) on the bottom.

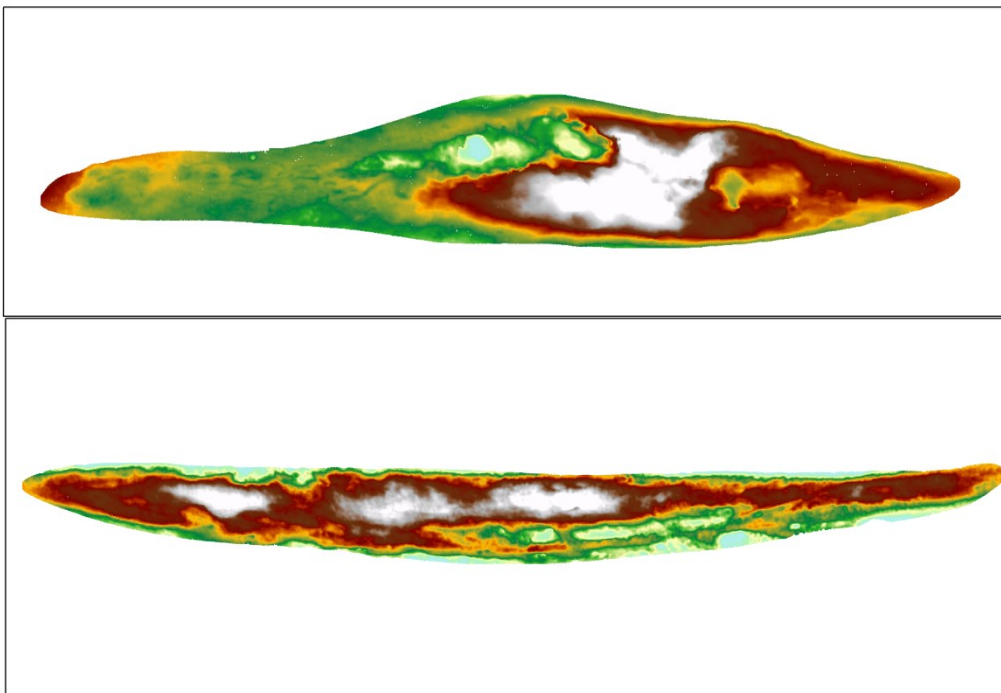


**Figure 23.** The points of the surface were exported and treated as if they were the points of a digital elevation model (graph BV).

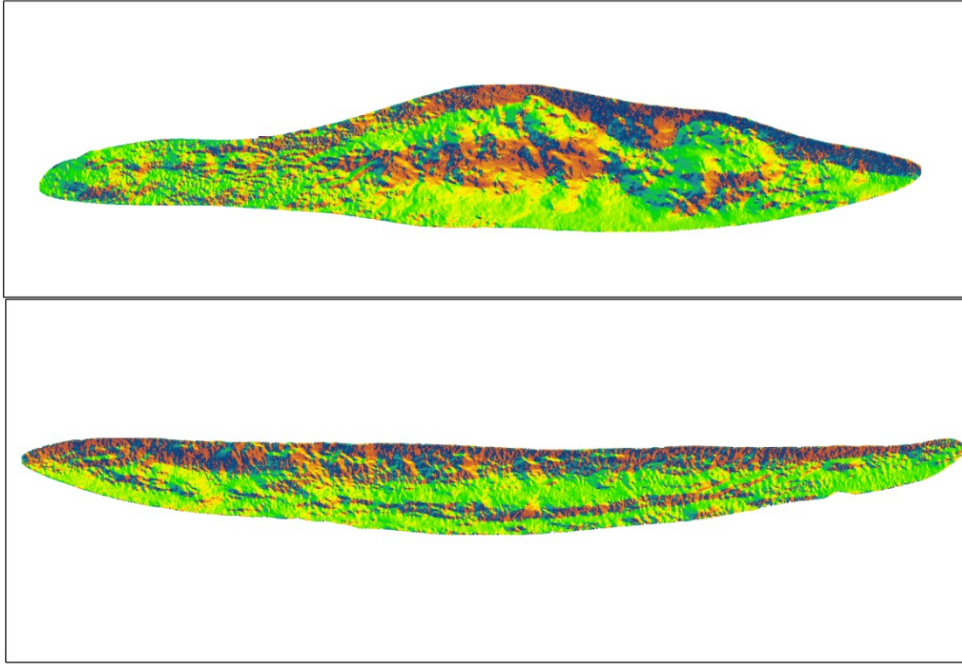


**Figure 24.** The aspect of the resulting surface, visualizing the directions in which the slopes are facing (graph BV).

After this, we calculated the aspect of the DEM, visualizing the directions in which the “slopes” are facing (Figure 24). We recoded the aspect into eight groups, representing  $45^\circ$  categories and we used a majority filter to remove small patches. This filter replaces the value of a cell based upon the value of the majority of its contiguous neighbouring cells (Figure 25).

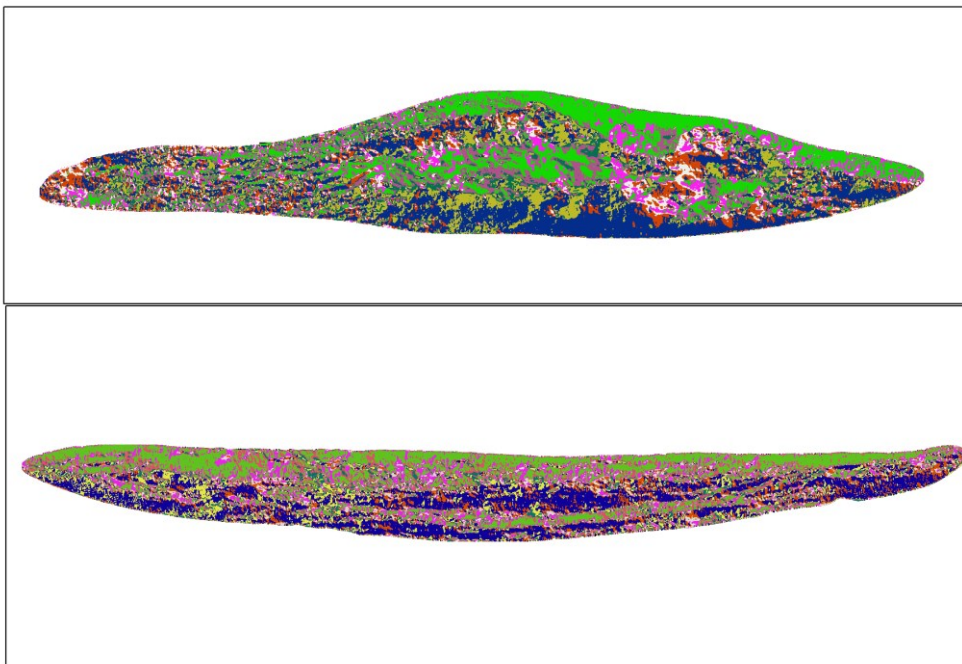


**Figure 25.** Majority filter applied to remove small patches (graph BV.)

Using the Region Group function of ArcGIS we grouped pixels that were neighbouring and had the same value into patches, each receiving a unique ID. After this, we counted the patches with a size of either over 100 cells (Orientation Patch Count 100) or over 10 cells (OPC 10, Figure 26). For analysis we used Relative Surface Complexity, calculated by dividing OPC by the 3D surface area of the enthesis. Relative Surface Complexity is negatively correlated with the robusticity score and also the composite enthesopathy score. The reason for this is that OPC and RSC are measures of small scale changes in surface orientation, while the robusticity category as defined by Hawkey and Merbs (1995) describes the amount of crest and ridge formation on the enthesis surface. Large ridges and crests result in large, interconnected areas having the same orientation, thus decreasing OPC and RSC (Figure 27).

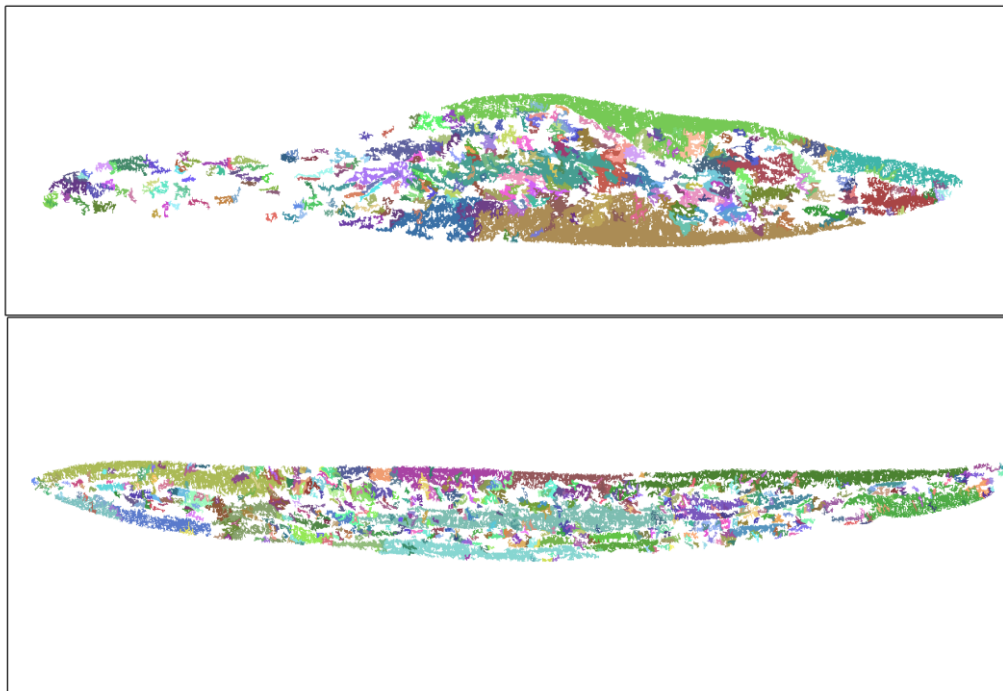


**Figure 26.** Neighbourhood pixels are grouped (graph BV.).

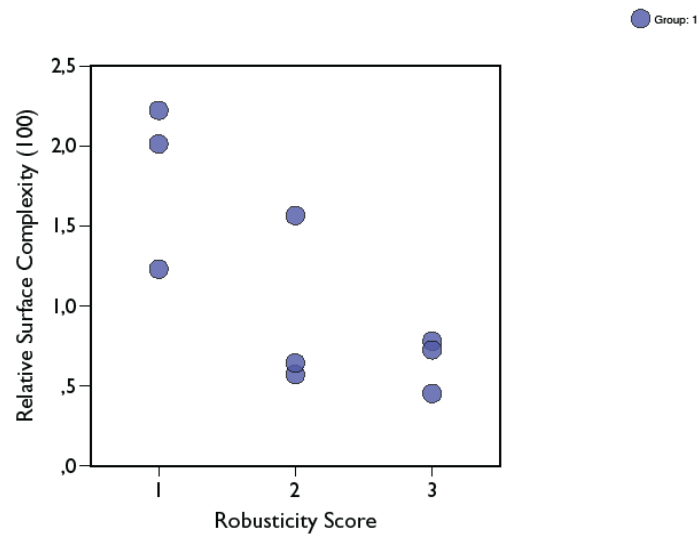


**Figure 27.** Relative Surface Complexity is negatively correlated with the robusticity score and also the composite enthesopathy score (graph BV.).

### *Planarity statistics*

Another possibility to quantify surfaces is to compare them to geometric primitives. In this case, we compared the surface to the base plane fitted to the curve delimiting the entheses, thus measuring its planarity. In Rapidform 2006, we measured the deviation (absolute distance, normal to the plane) of every point of the entheses surface from the base plane. The deviation from the plane can also be visualized; in this illustration cold colours are closer to the plane while warmer colours are more distant. In this case, the direction of the point from the plane (i.e. whether it is above or below the plane) is not relevant (Figure 28).

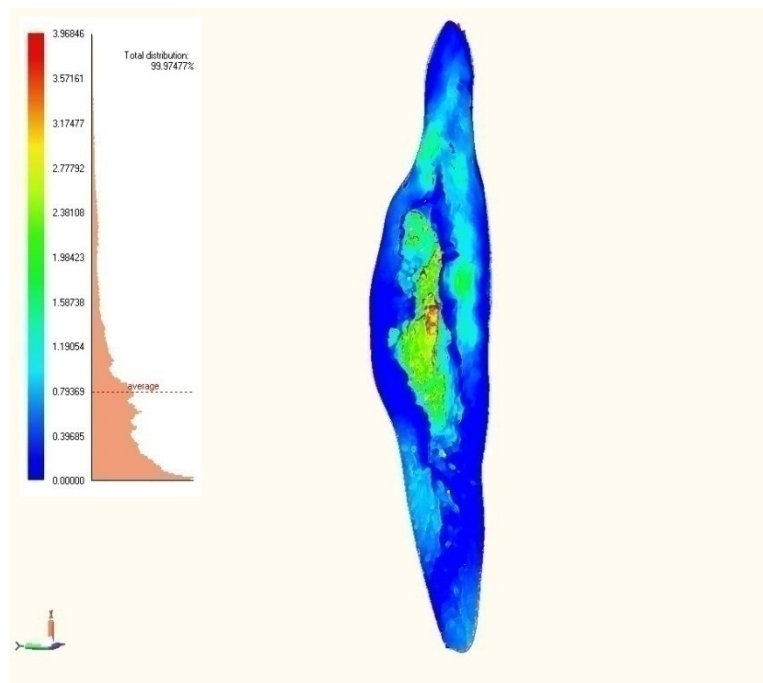


**Figure 28.** Surface compared to the plane fitted to the curve delimiting the entheses (graph BV.).

The maximum deviation from the plane seems to be correlated to the Composite Enthesopathy Score, with the maximum distance increasing with more marked entheses (Figure 29).

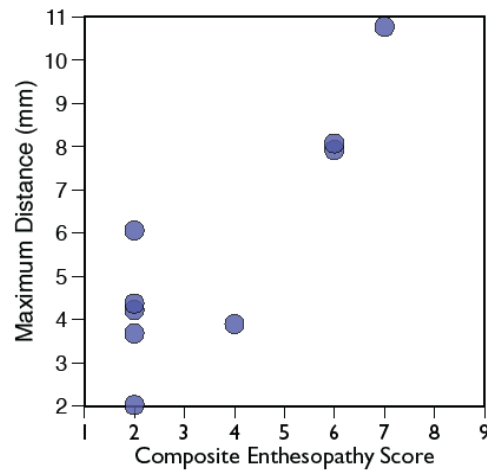


**Figure 29.** The maximum deviation from the plane is correlated to the Composite Enthesopathy Score (graph BV.).

Besides the maximum distance, the average of the distances of all points to the plane, and the standard deviation of all distances was also recorded. As visible in the 3D-plot (Figure 30), individuals with higher Composite Enthesopathy Scores have higher maximum and average distances from the base plane, and also a higher standard deviation of distances. These parameters seem to be related to large scale changes in surface structure. Large differences in distance, as in the case of strong crests and ridges result both in high maximum distances and standard deviations. Flatter surfaces with less relief have lower distances and standard deviations.

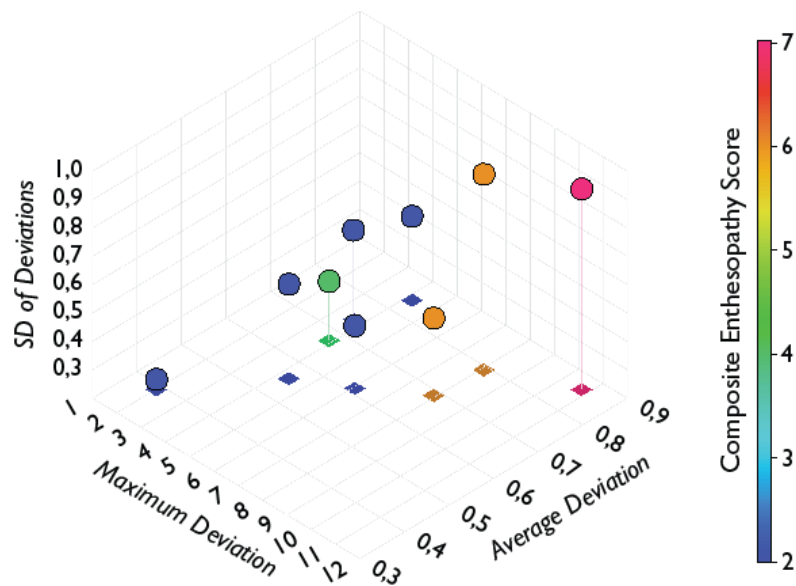


**Figure 30.** Individuals with higher Composite Enthesopathy Scores have higher maximum and average distances from the base plane (plot BV.).

### 3.6.1.5 Discussion & Conclusion

These 3D approaches to quantify the surface and structure of entheses have proven to be successful despite the small sample size. We could demonstrate at the *M. pectoralis major* site that strongly expressed entheses and enthesal changes have large 3D areas and non-planar surfaces. Their surface is not very complex though, when quantifying small scale structures, in contrast to less marked entheses displaying a more complex and more planar surface. A big advantage of using surface scans with resolution of more than  $20\mu$  for muscle marking analyses is that visibility of the surface features of the muscle insertions is greatly enhanced compared to the original specimen. As the texture is discarded, misleading visual clues are minimized. We found that the delimitation of the *M. pectoralis major* insertion does not differ much between observers, even compared to the results of inexperienced people. However, this has to be tested with a higher number of individuals. The results yield a high reproducibility and inter- and intra-observer errors seem to be minimal. This technique allows archival of 3D data and their virtual use in cases of repatriation, reburial or non-disposability of the skeletons due to any other cause.

These new methodological approaches (quantification of 3D/2D surface areas and perimeters, surface complexity measures and planarity statistics), confirmed the visual differentiation between the grades of entheses. Another application could be the creation of new standards for visual scoring using the better visibility of surface structures in the 3D scans. These advances in the 3D quantification of entheses and enthesopathies are promising, and could offer a broader spectrum of applications in various fields and objects.

For future investigations, quantification of the surface complexity of entheses might replace the classification of entheses expression into scores, but further work on the development of these methods is needed, in particular to allow application to fibrocartilaginous entheses.

## 4 THUNAU MALES – RESULTS I – VISUAL ANALYSES: FREQUENCIES

### 4.1 Males – entheses – frequencies, right side

In this chapter, the frequencies of occurrence of enthesal and joint changes in the males of the hillfort and the valley site are calculated and the results are described.

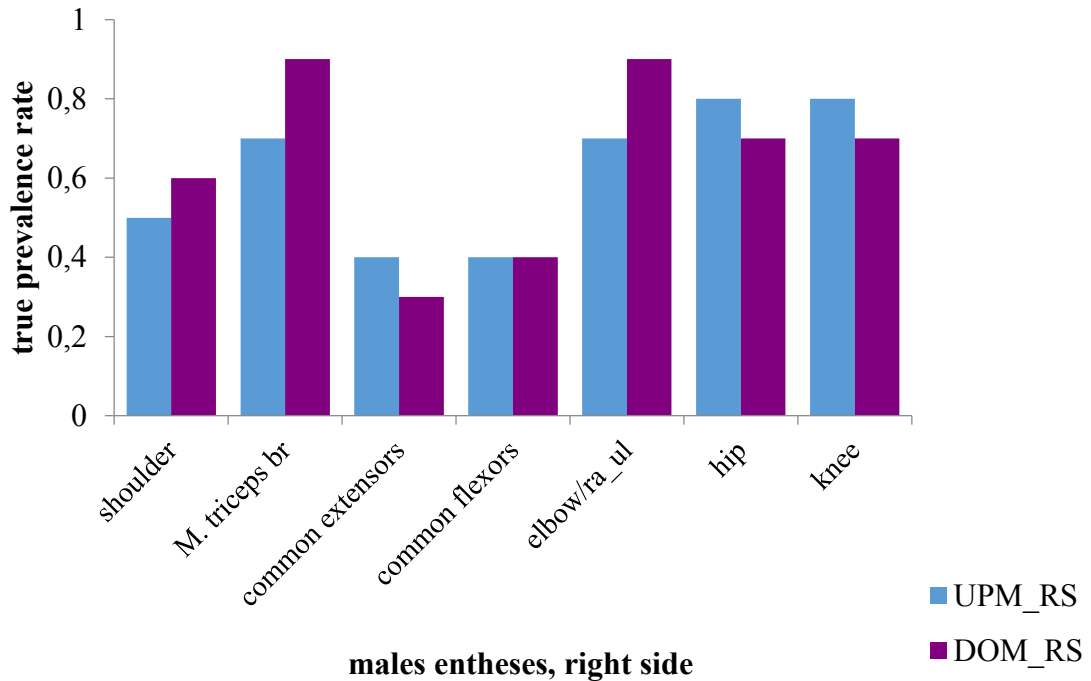
#### 4.1.1 True prevalence rate of enthesal changes in the males, right side, upper and lower extremities

Table 8 and Figure 31 show the differences in the true prevalence rates (TPR, dividing the number of pathological by the number of recordable entheses and joints, compare chapter 3.4., Statistical analysis) of the enthesal changes for the different pooled muscle groups of the uphill and downhill males in comparison. The rates are mainly similar; only in the *M. triceps brachii* and the pooled *M. biceps brachii*/*M. brachialis*, do the downhill males show a somewhat more elevated TPR close to one (TPR=0.9; meaning that nearly 100% of the males show slight enthesal changes here). The rates are similarly rather low in the common extensors and the common flexors of the two sub-sites (TPR=0.3-0.4; see Table 8).

**Table 8.** Number of individuals and true prevalence rate (TPR) of the enthesal changes of the right side (RS) in the uphill (UPM) and downhill males (DOM) of Thunau/Kamp, for upper and lower extremities.

uphill/downhill males, right side, entheses	UPM_RS		DOM_RS	
	n/N	TPR	n/N	TPR
SBB_SCC (shoulder)	17/31	<b>0.5</b>	3/7	<b>0.4</b>
SSP_ISP_HMI (shoulder)	14/29	<b>0.5</b>	5/7	<b>0.7</b>
STB_UTB ( <i>M. triceps br.</i> )	21/31	<b>0.7</b>	7/8	<b>0.9</b>
COM_EXT	10/26	<b>0.4</b>	2/7	<b>0.3</b>
COM_FLEX	9/26	<b>0.4</b>	3/8	<b>0.4</b>
BIB_BRA (elbow-ra/ul)	21/30	<b>0.7</b>	7/8	<b>0.9</b>
SME_STE_BIF (hip)	19/25	<b>0.8</b>	4/6	<b>0.7</b>
PAT_TLP (knee)	21/27	<b>0.8</b>	4/6	<b>0.7</b>

Legend: **sbb\_scc**: *M. biceps brachii*/*M. subscapularis*; **ssp\_isp\_hmi**: *M. supraspinatus*, *M. infraspinatus*, *M. teres minor*; **stb\_utb**: *M. triceps brachii*; **com\_ext**: common extensors; **com flex**: common flexors; **bib\_bra**: *M. biceps brachii*/*M. brachialis*; **sme\_ste\_bif**: *M. semimembranosus*/*M. semitendinosus*/*M. biceps femoris*; **pat\_tlp**: Patella/patellar ligament: *M. quadriceps femoris*;



**Figure 31.** Graph showing the true prevalence rate of the enthesal changes of the right side in the uphill (UPM) and downhill males (DOM) of Thunau/Kamp, for upper and lower extremities.

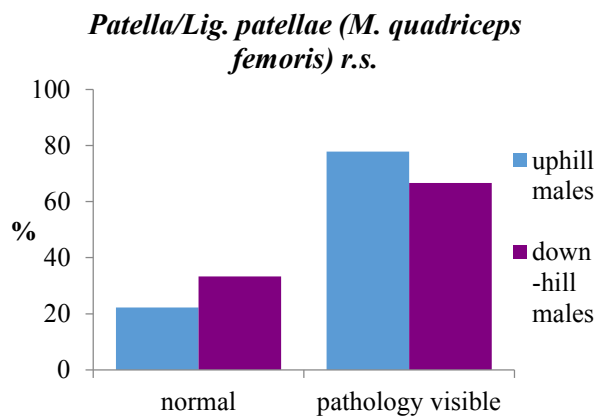
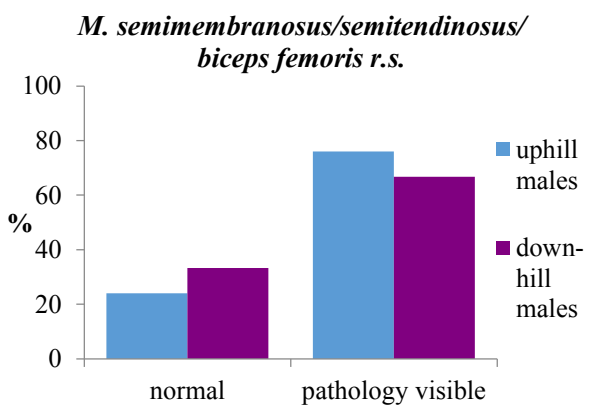
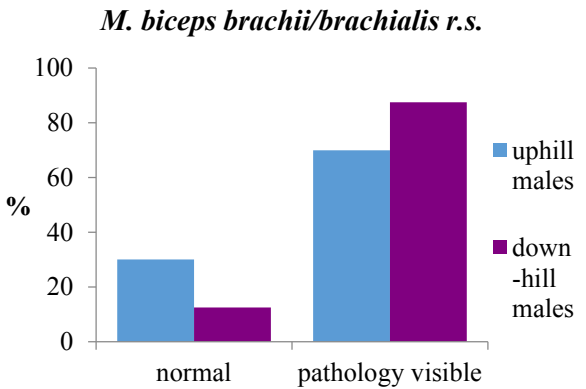
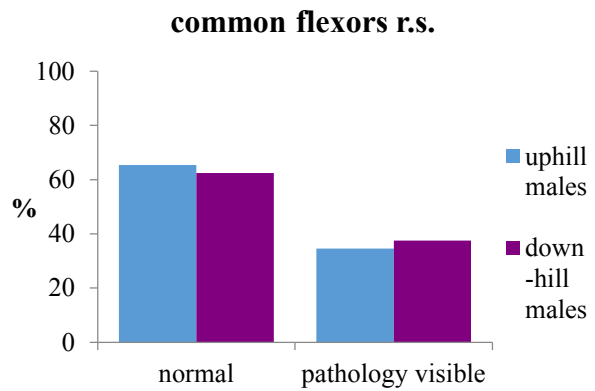
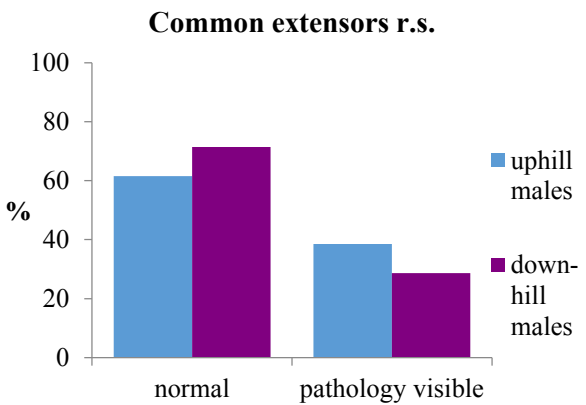
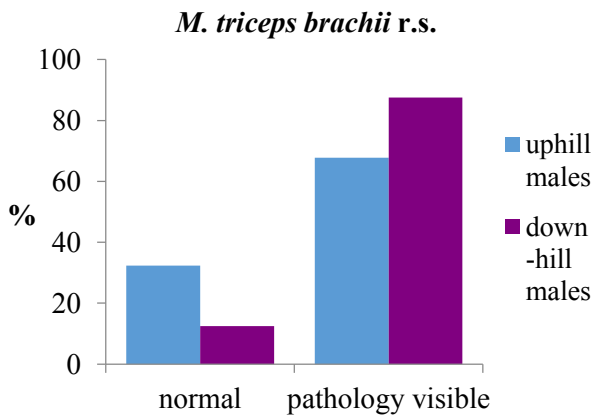
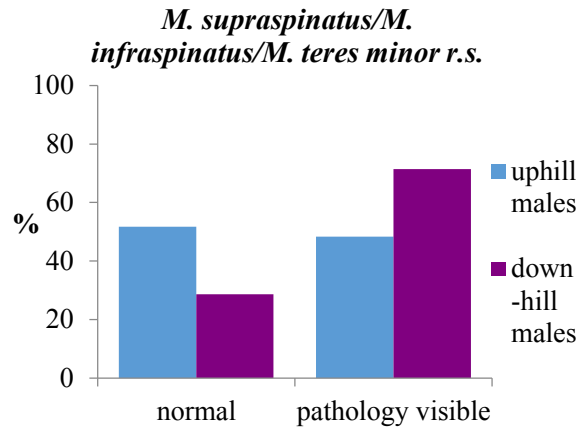
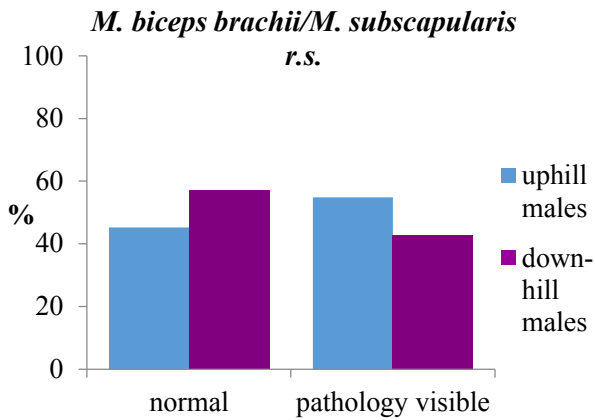
#### 4.1.2 Mean frequencies of single muscle groups, males right side

Here, the differences of the frequencies of the single muscle groups between the uphill and downhill males, normal entheses compared to enthesal changes frequencies (in percent) of the upper and lower extremities, are shown in Table 9 and Figure 32. In many cases, e.g. in the *M. triceps brachii* and the pooled *M. biceps brachii*/*M. brachialis* muscles at the proximal lower arm, the downhill males show higher frequencies of enthesal changes than the uphill males. The percentages in the lower extremities are very similar in the two sub-sites. However, nothing significant was detected.

**Table 9.** Mean frequencies in percent of the single muscle groups, right side, comparison of uphill and downhill males, upper and lower extremities.

<b>entheses, right side</b>	<b>group of males</b>	<b>% normal</b>	<b>% pathology visible</b>
<b>M. biceps brachii/M. subscapularis</b>	uphill	45.2	54.8
	downhill	57.1	42.9
<b>M. supraspinatus/M. infraspinatus/M. teres minor</b>	uphill	51.7	48.3
	downhill	28.6	71.4
<b>M. triceps brachii</b>	uphill	32.3	67.8
	downhill	12.5	87.5
<b>common extensors</b>	uphill	61.5	38.5
	downhill	71.4	28.6
<b>common flexors</b>	uphill	65.4	34.6
	downhill	62.5	37.5
<b>M. biceps brachii/M. brachialis</b>	uphill	30.0	70.0
	downhill	12.5	87.5
<b>M. semimembranosus/M. semitendinosus/M. biceps femoris</b>	uphill	24.0	76.0
	downhill	33.3	66.7
<b>Patella/Lig. patellae (M. quadriceps femoris)</b>	uphill	22.2	77.8
	downhill	33.3	66.7

Next page: **Figure 32.** Graphs of the single muscle groups, right side, comparison of uphill and downhill males, upper and lower extremities.



### **4.1.3 Description of the tables and figures for entheses frequencies of the right upper and lower extremities in uphill and downhill males**

The percentage of enthesal changes (compare Table 9 & Figure 32) at the *M. biceps brachii* and the *M. subscapularis* muscle markings on the right extremities is between about 55% (uphill) and 43% (downhill). About half of the males in the uphill group show normal expression at the supraspinatus/infraspinatus/teres minor muscle marker site, the other half shows enthesal changes. Concerning the downhill males, a little more than 70% display enthesal changes in the latter pooled muscle markings group.

In the *M. triceps brachii*, about two thirds of the uphill and nearly 90% of the downhill males display enthesal changes. More than half of the males in both groups show no pathologies at the common extensor muscle markers. A relatively similar, smaller percentage in both groups shows slight pathologies. As at the extensors, more than half of the males in both groups show no pathologies at the common flexor muscle markings, and a relatively similar number of individuals show alterations at the common flexors origins in the right extremity. The downhill males show a close to 20% higher frequency of enthesal changes at the right biceps brachii/brachialis muscle markings (nearly 90%).

Regarding the lower extremities, between about 67% (downhill) and 76% (uphill) of the males display enthesal changes in the pelvic region, the semimembranosus/ semitendinosus/ biceps femoris muscle attachment at the ischium. Nearly 80% of the uphill, and close to 70% in the downhill males, exhibit alterations at the *M. quadriceps femoris*/patellar ligament attachment at the tibial tuberosity.

## 4.2 Males – joints – frequencies, right side

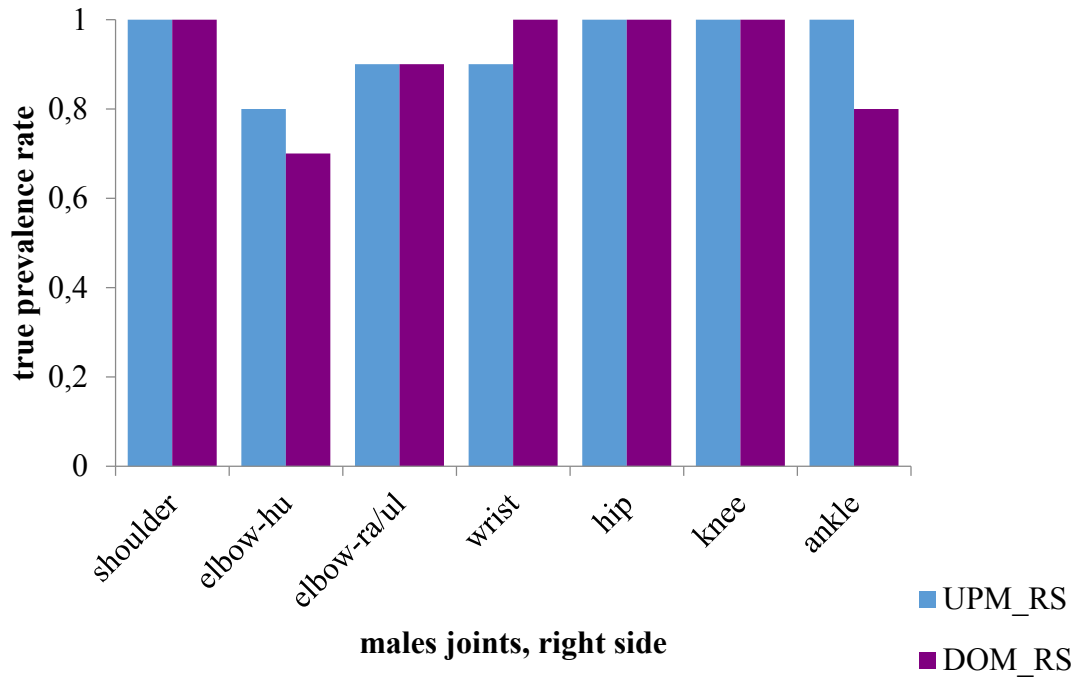
### 4.2.1 True prevalence rate of joint changes in the males, right side, upper and lower extremity

Table 10 and Figure 33 show the differences in the true prevalence rates (TPR, compare chapter 3.4., Statistical analysis) of the joint changes on the right side for the different pooled joint groups of the uphill and downhill males in comparison. The rates are similarly very high in both groups, the TPR rates are frequently close to one (corresponding to 100% affected individuals), and not only in the downhill, but also in the uphill group, and in the upper and lower extremity.

**Table 10.** Number of individuals and true prevalence rate of the joint changes of the right side in the uphill (UPM) and downhill males (DOM) of Thunau/Kamp, for upper and lower extremity.

uphill/downhill males, right side, joints	UPM_RS		DOM_RS	
	n/N	TPR	n/N	TPR
CHU_CGL (shoulder)	38/39	<b>1</b>	8/8	<b>1</b>
CAH_TRO (elbow_hu)	28/36	<b>0.8</b>	5/7	<b>0.7</b>
CRA_CIR_INT_INR (elbow-ra/ul)	33/38	<b>0.9</b>	6/7	<b>0.9</b>
INU_CIU_CAU_PHW_FAC (wrist)	27/31	<b>0.9</b>	7/7	<b>1</b>
FOA_CAF_FOC (hip)	38/40	<b>1</b>	8/8	<b>1</b>
FAP_CMF_CLF_UFO (knee/Fe)	34/35	<b>1</b>	6/6	<b>1</b>
CMT_CLT_FMP_FLP (knee/Ti)	35/35	<b>1</b>	6/6	<b>1</b>
FIT_FST_FPC (ankle)	35/36	<b>1</b>	5/6	<b>0.8</b>

Legend: **chu\_cgl**: *Caput humeri/Cavitas glenoidalis*; **cah\_tro**: *Capitulum humeri/Trochlea*; **cra\_cir\_int\_inr**: *Caput radii/Circumferentia articularis radii/Incisura trochlearis/Incisura radialis*; **inu\_ciu\_cau\_phw\_fac**: *Incisura ulnaris/Circumferentia articularis ulna/Caput ulnae/proximal row of carpal bones/Facies articularis carpalis*; **foa\_caf\_foc**: *Fossa acetabuli/Caput femoris/Fovea capitis*; **fap\_cmf\_clf\_ufo**: *Facies patellaris/Condylus medialis femoris/Condylus lateralis femoris/distal margin of Fossa intercondylaris*; **cmt\_clt\_fmp\_flp**: *Condylus medialis tibiae/Condylus lateralis tibiae/Facies medialis patellae/Facies lateralis patellae*; **fit\_fst\_fpc**: *Facies articularis inferior tibiae/Facies articularis superior (Talus)/Facies articularis talaris posterior (Calcaneus)*;



**Figure 33.** Graph showing the true prevalence rate of the joint changes of the right side in the uphill (UPM) and downhill males (DOM) of Thunau/Kamp, for upper and lower extremity.

#### 4.2.2 Mean frequencies of single joint groups, males right side

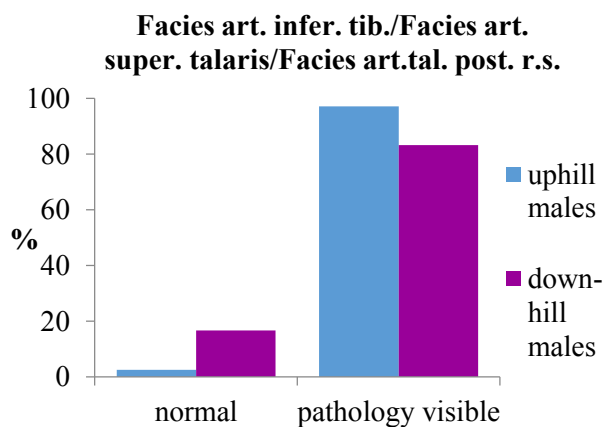
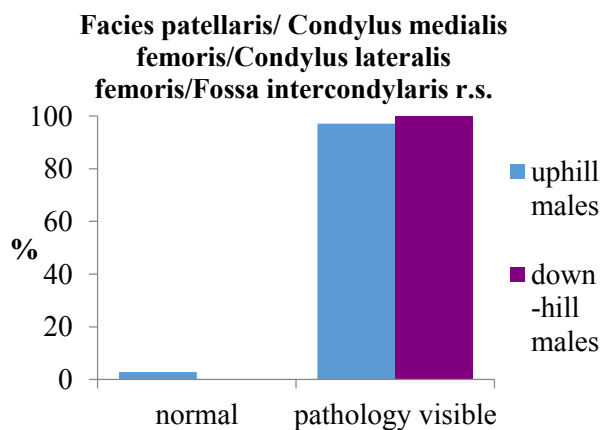
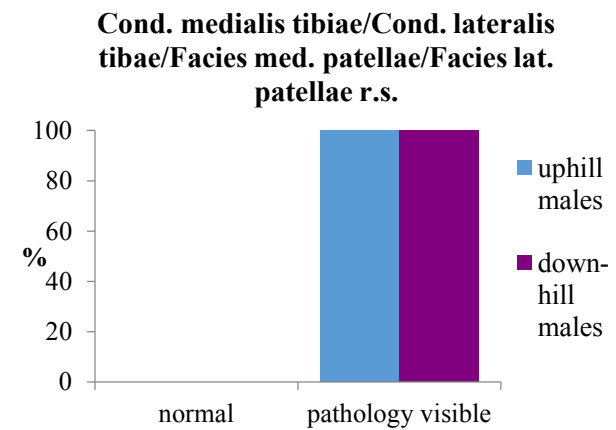
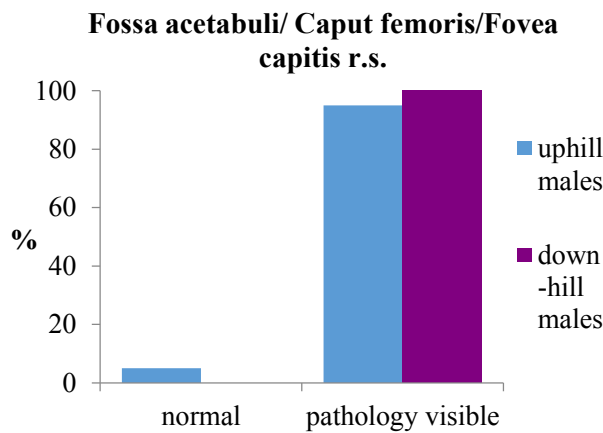
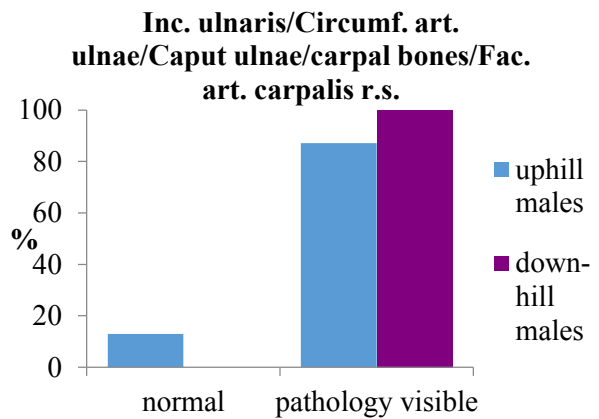
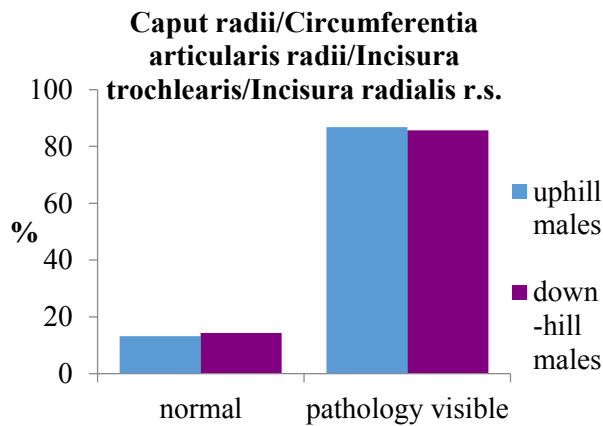
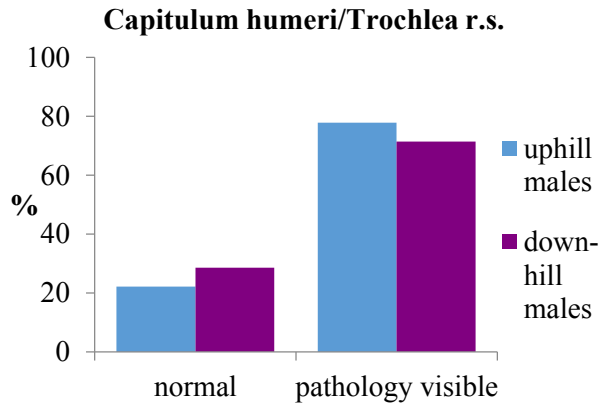
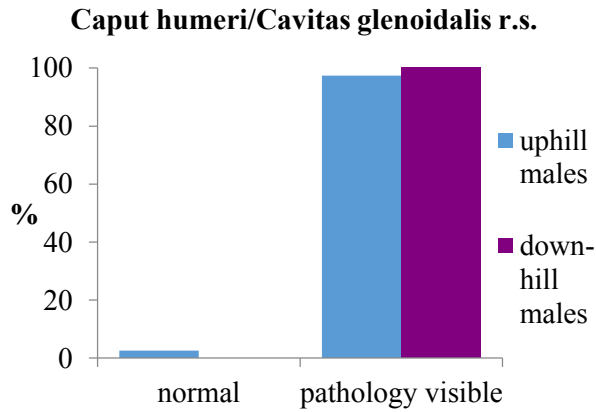
Here, the differences of the frequencies of the single joint groups between the uphill and downhill males of Thunau, normal entheses compared to enthesal changes frequencies (in percent) of the upper and lower extremities, are shown in Table 11 and Figure 34.

**Table 11.** Mean frequencies in percent of the single joint groups, right side, comparison of uphill and downhill males, upper and lower extremity.

<b>joints, right side</b>	<b>group of males</b>	<b>% normal</b>	<b>% pathology visible</b>
<b>Caput humeri/Cavitas glenoidalis</b>	uphill	2.6	97.4
	downhill	0.0	100.0
<b>Capitulum humeri/Trochlea</b>	uphill	22.2	77.8
	downhill	28.6	71.4
<b>Caput radii/Circumferentia articularis radii/Incisura trochlearis/Incisura radialis</b>	uphill	13.2	86.8
	downhill	14.3	85.7
<b>Incis. ulnaris/Circumfer. art. ulnae/Caput ulnae/prox. row carp. bones/F. artic. carp.</b>	uphill	12.9	87.1
	downhill	0.0	100.0
<b>Fossa acetabuli/ Caput femoris/Fovea capitis</b>	uphill	5.0	95.0
	downhill	0.0	100.0
<b>Facies patellaris/Cond. medialis fem/Cond. lateralis fem./Fossa intercondylaris</b>	uphill	2.9	97.1
	downhill	0.0	100.0
<b>Cond. medialis tib./Cond. lateralis tib./F. medialis patellae/Fac. lateralis patellae</b>	uphill	0.0	100.0
	downhill	0.0	100.0
<b>Fac. articularis inferior tibiae/F. articular. superior tali/F. artic. talaris post. calc.</b>	uphill	2.5	97.2
	downhill	16.7	83.3

In the downhill group, the slight joint changes in the shoulder (*Caput humeri/Cavitas glenoidalis*), the wrist (*Incisura ulnaris/Circumferentia articularis ulnae/Caput ulnae/proximal row carpal bones/Facies articularis carpalis*), the hip joint (*Fossa acetabuli/Caput femoris/Fovea capitis*) and the knee joint (distal femur and proximal tibia) reach 100%. The percentage rates in the uphill males are similarly high. No significant results occurred.

Next page: **Figure 34.** Graphs of the joint groups, right side, comparison of uphill and downhill males.



### 4.2.3 Description of the tables and figures for joint frequencies of the right upper and lower extremities in uphill and downhill males

The percentage ratio is very similar for the pathologies visible category at the shoulder joint between the two groups. All individuals of the male valley group, and almost all (97.5%) of the uphill group show slight pathologies at the right shoulder. The bulk of the males in both groups show slight pathologies at the distal humeral pooled joints (*Capitulum humeri/Trochlea*). Most of the individuals in both groups show slight pathologies at the elbow joint bones of the lower arm, the pooled *Caput radii/Circumferentia articularis radii/Incisura trochlearis/Incisura radialis*. An about 12% higher rate of enthesal changes is visible in the downhill males group concerning the wrist joints (*Incisura ulnaris/Circumferentia articularis ulnae/Caput ulnae/proximal row of carpal bones/Facies articularis carpalis*) of the right side. Chi<sup>2</sup> tests displayed no significant differences.

In the lower extremities, the percentage rate of pathologies visible at the hip joint (*Fossa acetabuli/Caput femoris/Fovea capitis*) reaches nearly 100% in both groups. The downhill males display 100% frequency of joint changes in the knee (distal femur and proximal tibia). A percentage rate of about two thirds of the males in both groups exhibits alterations at the distal femur joints of the knee region (*Facies patellaris/Condylus medialis femoris/Condylus lateralis femoris/Fossa intercondylaris*), similar to the uphill males (close to 100% in the distal femur, 100% in the proximal tibia). A 15% higher frequency is visible in the ankle region of the hillfort males, compared to the downhill males. Chi<sup>2</sup> tests displayed no significant results.

The table on the next page recapitulates details on individual numbers and percentage rates of the pooled entheses and joint frequencies of the right extremity of the uphill/downhill males in comparison.

Next page: **Table 12.** Pooled entheses and joint frequencies of the right extremities of the uphill/downhill males in comparison.

<b>pooled entheses frequencies, uphill males, right side</b>	<b>uphill males n</b>				<b>n path. visible</b>	<b>%</b>
	<b>total</b>	<b>recordable</b>	<b>normal</b>	<b>%</b>		
M. biceps bra./subscap.	31	31	14	45.2	17	54.8
M. suprasp./infrasp./teres min.	31	29	15	51.7	14	48.3
M. triceps brachii	31	31	10	32.3	21	67.7
Common extensors	31	26	16	61.5	10	38.5
Common flexors	31	26	17	65.4	9	34.6
M. biceps brachii/brachialis	31	30	9	30.0	21	70.0
M. semim./semit./biceps fem.	31	25	6	24.0	19	76.0
Patella/pat. lig. (M. quadriceps fem.)	31	27	6	22.2	21	77.8
<b>pooled entheses frequencies, downhill males, right side</b>	<b>downhill males n</b>				<b>n path. visible</b>	<b>%</b>
<b>total</b>	<b>recordable</b>	<b>normal</b>	<b>%</b>			
M. biceps bra./subscap.	8	7	4	57.1	3	42.9
M. suprasp./infrasp./teres min.	8	7	2	28.6	5	71.4
M. triceps brachii	8	8	1	12.5	7	87.5
Common extensors	8	7	5	71.4	2	28.6
Common flexors	8	8	5	62.5	3	37.5
M. biceps brachii/brachialis	8	8	1	12.5	7	87.5
M. semim./semit./biceps fem.	8	6	2	33.3	4	66.7
Patella/pat. lig. (M. quadriceps fem.)	8	6	2	33.3	4	66.7
<b>pooled joints frequencies, uphill males, right side</b>	<b>uphill males n</b>				<b>n path. visible</b>	<b>%</b>
<b>total</b>	<b>recordable</b>	<b>normal</b>	<b>%</b>			
Cap. hum./cav. glen.	40	39	1	2.6	38	97.4
Capit. humeri/Trochlea	40	36	8	22.2	28	77.8
Cap. rad./Circ. art. rad./I. trochl./I. rad.	40	38	5	13.2	33	86.8
Inc. ul./Circumf. art. Ulna/Cap. ul./prox. row carp. bones/F. art. carp.	40	31	4	12.9	27	87.1
F. acetabuli/Cap. fem./Fov. Capitis	40	40	2	5.0	38	95.0
Fac. patellaris/Cond. medialis fem./Cond. lateralis fem./F. incercond.	40	35	1	2.9	34	97.1
Cond. medialis tib./Cond. lateralis tib./Fac. med. Patella/Fac. lat. Patella	40	35	0	0.0	35	100.0
Fac. Art.inf. Tibiae/Fac. Art. Sup. Talus/Fac. Art.talaris posterior Calcan.	40	36	1	2.8	35	97.2
<b>pooled joints frequencies, downhill males, right side</b>	<b>downhill males n</b>				<b>n path. visible</b>	<b>%</b>
<b>total</b>	<b>recordable</b>	<b>normal</b>	<b>%</b>			
Caput humeri/cavitas glenoidalis	8	8	0	0.0	8	100.0
Capitulum humeri/Trochlea	8	7	2	28.6	5	71.4
Cap. radii/Circ. art. rad./Inc. trochl./Incis. rad.	6	7	1	14.3	6	85.7
Inc. ulnaris/Circumf. art. uln/C. ul./prox. row carp. bones/Fac. art. carp.	8	7	0	0.0	7	100.0
F. acetabuli/Cap. femoris/Fovea capitis	8	8	0	0.0	8	100.0
F. pat./Cond. medialis fem./Cond. lateralis fem./Fac. incercond.	8	6	0	0.0	6	100.0
Cond. medialis tib./Cond. lateralis tib./Fac. med. Patella/Fac. lat. Patella	8	6	0	0.0	6	100.0
Fac. Art.inf. tib./Fac. Art. sup. tal/Fac. art.talaris post. posterior Calcan.	8	6	1	16.7	5	83.3

### 4.3 Males – entheses – frequencies, left side

#### 4.3.1 True prevalence rate of enthesal changes in the males, left side, upper and lower extremities

Here, the differences of the in the true prevalence rates (TPR) of the single muscle groups between the uphill and downhill males, normal entheses compared to enthesal changes frequencies (in percent) of the upper and lower left extremities, are shown in Table 13 and Figure 35. The differences between the two groups are marginal; the true prevalence rates are very similar in upper and lower extremities. No significant results were detected in t-test analysis.

**Table 13.** Number of individuals and true prevalence rate of the enthesal changes of the left side in the uphill (UPM) and downhill males (DOM) of Thunau/Kamp, for upper and lower extremities.

uphill/downhill males, left side, entheses	UPM_LS		DOM_LS	
	n/N	TPR	n/N	TPR
SBB_SCC (shoulder)	14/26	<b>0.5</b>	2/7	<b>0.3</b>
SSP_ISP_HMI (shoulder)	9/23	<b>0.4</b>	4/6	<b>0.7</b>
STB_UTB (M. triceps br.)	19/27	<b>0.7</b>	5/7	<b>0.7</b>
COM_EXT	7/20	<b>0.4</b>	2/7	<b>0.3</b>
COM_FLEX	8/23	<b>0.3</b>	2/7	<b>0.3</b>
BIB_BRA (elbow-ra/ul)	17/26	<b>0.7</b>	5/7	<b>0.7</b>
SME_STE_BIF (hip)	16/24	<b>0.7</b>	3/4	<b>0.8</b>
PAT_TLP (knee)	17/23	<b>0.7</b>	4/6	<b>0.7</b>

Legend: **sbb\_scc**: *M. biceps brachii*/*M. subscapularis*; **ssp\_isp\_hmi**: *M. supraspinatus*, *M. infraspinatus*, *M. teres minor*; **stb\_utb**: *M. triceps brachii*; **com\_ext**: common extensors; **com flex**: common flexors; **bib\_bra**: *M. biceps brachii*/*M. brachialis*; **sme\_ste\_bif**: *M. semimembranosus*/*M. semitendinosus*/*M. biceps femoris*; **pat\_tlp**: Patella/patellar ligament: *M. quadriceps femoris*;

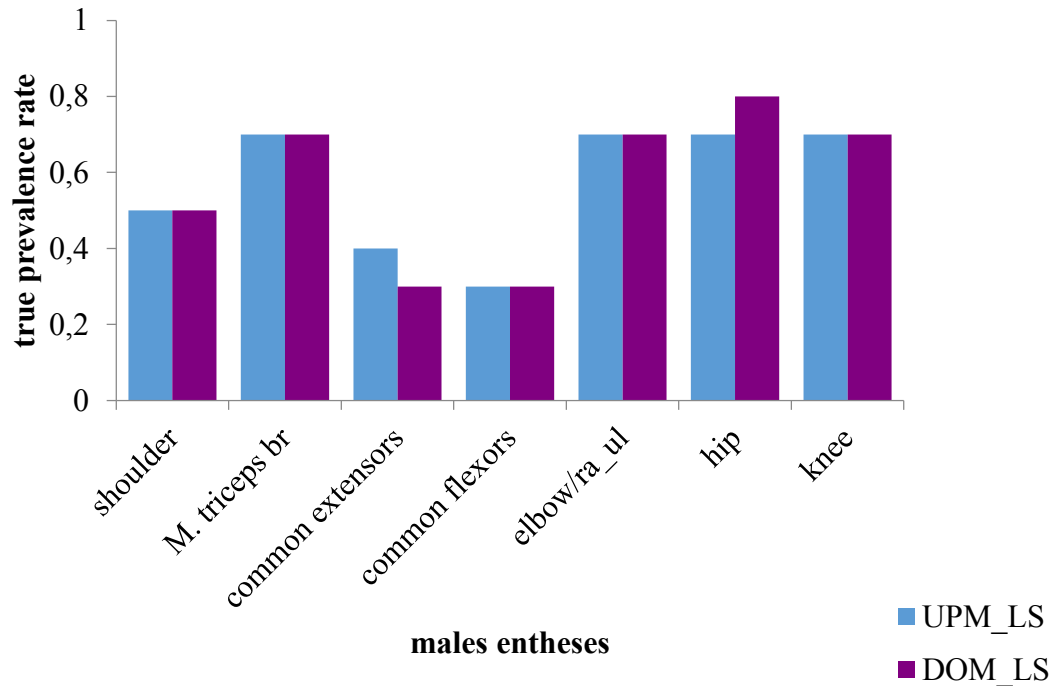


**Figure 35.** Graph showing the true prevalence rate of the enthesal changes of the left side in the uphill (UPM) and downhill males (DOM) of Thunau/Kamp, for upper and lower extremities.

Table 13 and Figure 35 show the differences in the true prevalence rates of the enthesal changes of the uphill and downhill males in comparison. The rates are generally very similar in the two groups (highest in *M. triceps brachii*, *M. biceps/brachialis* and *M. quadriceps femoris*), interestingly quite low in both groups in the common extensor and common flexor entheses.

### 4.3.2 Mean frequencies of single muscle groups, males left side

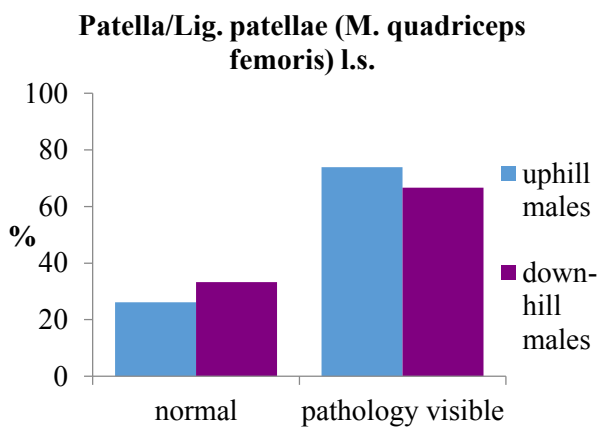
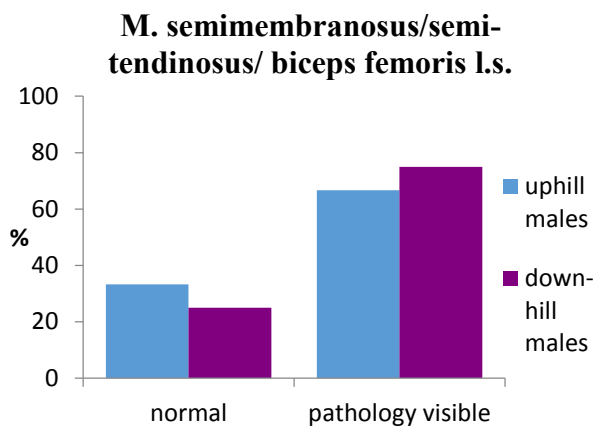
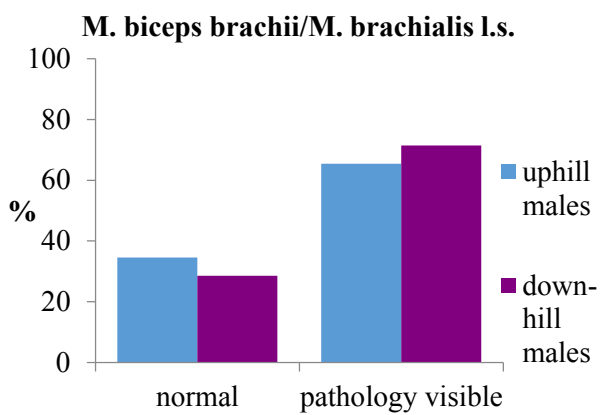
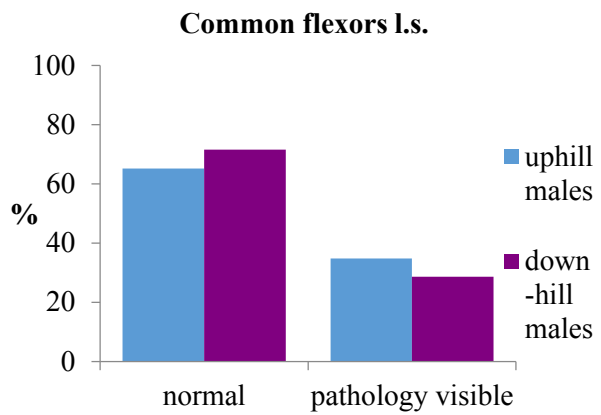
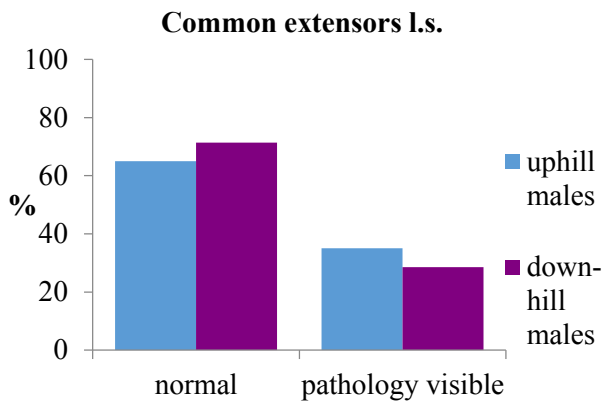
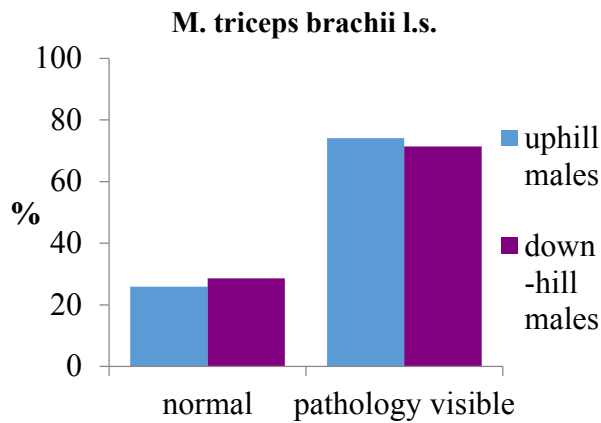
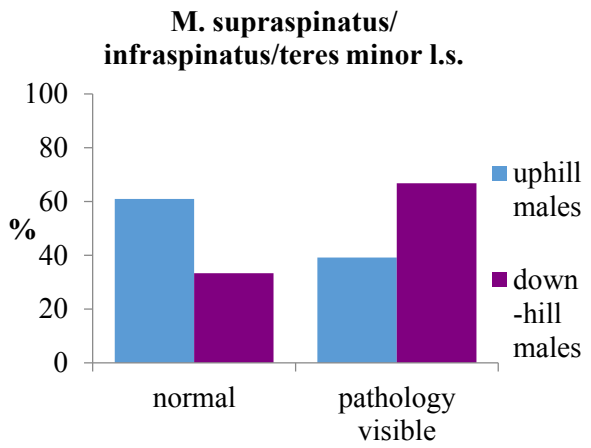
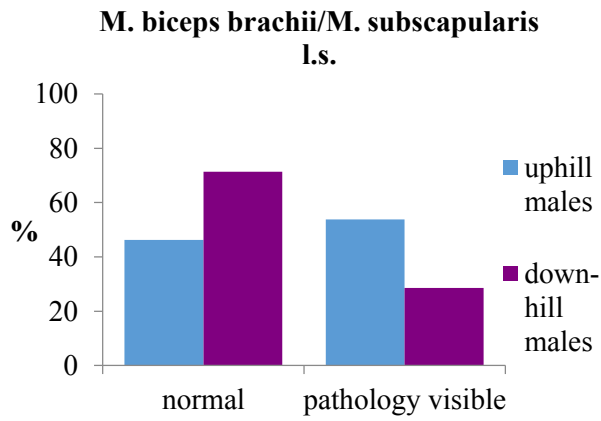
The differences of the frequencies of the single muscle groups between the uphill and downhill males, normal entheses compared to enthesal changes frequencies (in percent) of the upper and lower extremities, left side, are shown in Table 14 and Figure 36. In many cases, e.g. in the *M. triceps brachii* and the pooled *M. biceps brachii/M. brachialis* muscles at the proximal lower arm, the downhill males show higher frequencies of enthesal changes than the uphill males. The percentages in the lower extremities are very similar in the two sub-sites. However, no significant results were found.

**Table 14.** Mean frequencies in percent of the single pooled muscle groups, left side, comparison of uphill and downhill males, upper and lower extremities.

<b>entheses, left side</b>	<b>group of males</b>	<b>% normal</b>	<b>% pathology visible</b>
<b>M. biceps brachii/M. subscapularis</b>	uphill	46.2	53.8
	downhill	71.4	28.6
<b>M. supraspinatus/M. infraspinatus/M. teres minor</b>	uphill	60.9	39.1
	downhill	33.3	66.7
<b>M. triceps brachii</b>	uphill	25.9	74.1
	downhill	28.6	71.4
<b>common extensors</b>	uphill	65	35
	downhill	71.4	28.6
<b>common flexors</b>	uphill	65.2	34.8
	downhill	71.5	28.6
<b>M. biceps brachii/M. brachialis</b>	uphill	35	65.4
	downhill	28.6	71.4
<b>M. semimembranosus/M. semitendinosus/M. biceps femoris</b>	uphill	33.3	66.7
	downhill	25	75
<b>Patella/Lig. patellae (M. quadriceps femoris)</b>	uphill	26.1	73.9
	downhill	33.3	66.7

The downhill males show the highest frequencies of enthesal changes in the left extremity in the *M. triceps brachii* and the pooled *M. biceps brachii* and *M. brachialis* (71.4%). This result is similar to the right extremity, although the frequencies are somewhat higher there (compare section 4.1.2).

Next page: **Figure 36.** Graphs of pooled entheses groups, left side, comparison of uphill and downhill males.



### 4.3.3 Description of the tables and figures for entheses frequencies of the left upper and lower extremities in uphill and downhill males

Nearly two thirds of the downhill males display normal expression at the biceps/subscapularis muscle marking site at the left shoulder. More than half of the uphill males display enthesal changes here, which is an about 25% higher frequency than in the downhill males. In the hillfort male group, there is a higher percentage rate (about 70%) displaying normal shape in the rotator cuff muscles (*M. supraspinatus/M. infraspinatus/M. teres minor*), whereas in the downhill group, close to 70% show slight pathologies in this muscle group. About two thirds of the males in both groups show slight pathologies at the *M. triceps brachii* sites. At the common extensors, there is only a small percentage rate of the males with slight pathologies (28% downhills to 35% uphills). Most of the males are within the normal range of shape in the common flexors. A small percentage of the males show slight pathology here, similar to the common extensors. About a third of the males show a normal development in the proximal lower arm muscles (*M. biceps brachii/M. brachialis*).

The enthesal changes in the left ischial tuberosity (*M. semimembranosus/M. semitendinosus/M. biceps femoris*) reach between about 67% (uphill) and 75% (downhill) Between 66% (downhill) - 74% (uphill) of the males show slight pathologies in the analysed knee muscle markings (Patella/Lig. patellae (*M. quadriceps femoris*)).

## 4.4 Males – joints – frequencies, left side

### 4.4.1 True prevalence rate of joint changes in the males, left side, upper and lower extremities

Table 15 and Figure 37 show the differences in the true prevalence rates (TPR, compare chapter 3.4, Statistical analysis) of the joint changes on the right side for the different pooled joint groups of the uphill and downhill males in comparison. The rates are similarly very high in both groups, as on the right side, the TPR rates are frequently close to one, meaning that 100% or close to this are affected by slight joint changes. The uphill and the downhill males are nearly equally affected.

**Table 15.** Number of individuals and true prevalence rate of the joint changes of the left side in the uphill and downhill males of Thunau/Kamp, for upper and lower extremities.

uphill/downhill males, left side, joints	UPM_LS		DOM_LS	
	n/N	TPR	n/N	TPR
CHU_CGL (shoulder)	39/39	1	7/7	1
CAH_TRO (elbow_hu)	27/33	0.8	5/6	0.8
CRA_CIR_INT_INR (elbow-ra/ul)	31/34	0.9	5/7	0.7
INU_CIU_CAU_PHW_FAC (wrist)	31/32	1	6/6	1
FOA_CAF_FOC (hip)	35/36	1	6/6	1
FAP_CMF_CLF_UFO (knee/Fe)	33/33	1	7/7	1
CMT_CLT_FMP_FLP (knee/Ti)	33/33	1	6/6	1
FIT_FST_FPC (ankle)	36/36	1	5/5	1

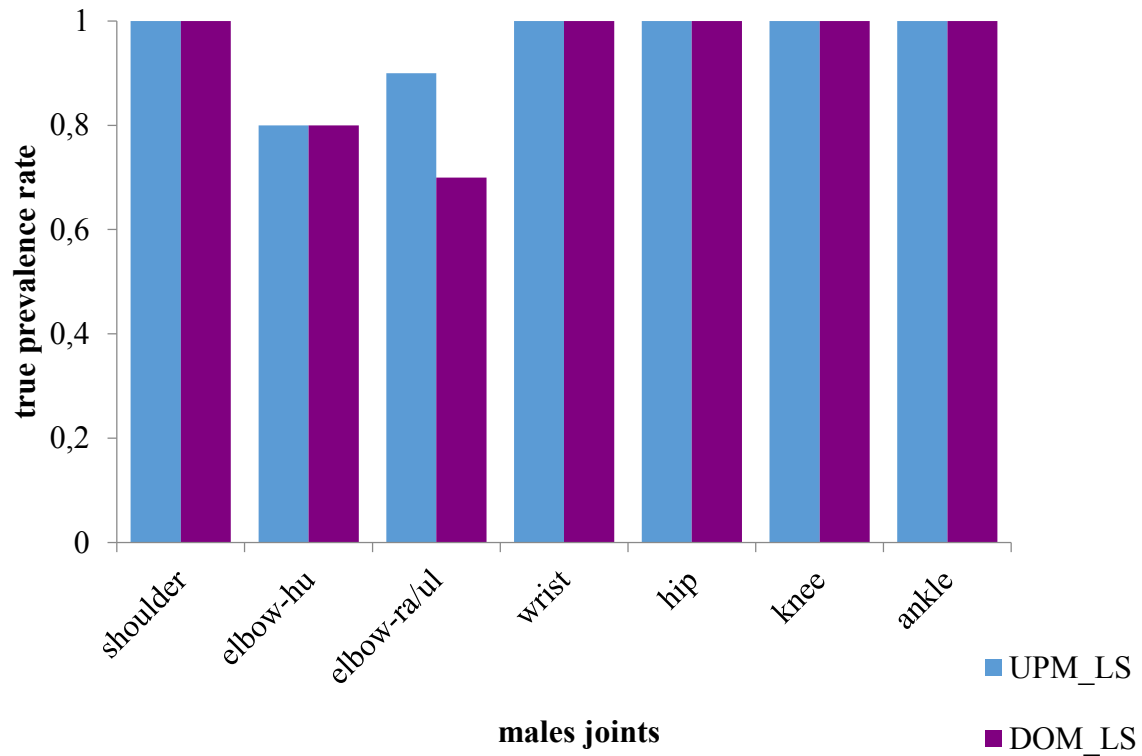


**Figure 37.** Graph showing the true prevalence rate of the joint changes of the left side in the uphill and downhill males of Thunau/Kamp, for upper and lower extremities.

Legend: **chu\_cgl**: *Caput humeri/Cavitas glenoidalis*; **cah\_tro**: *Capitulum humeri/Trochlea*; **cra\_cir\_int\_inr**: *Caput radii/Circumferentia articularis radii/Incisura trochlearis/Incisura radialis*; **inu\_ciu\_cau\_phw\_fac**: *Incisura ulnaris/Circumferentia articularis ulna/Caput ulnae/proximal row of carpal bones/Facies articularis carpalis*; **foa\_caf\_foc**: *Fossa acetabuli/Caput femoris/Fovea capitis*; **fap\_cmf\_clf\_ufo**: *Facies patellaris/Condylus medialis femoris/Condylus lateralis femoris/distal margin of Fossa intercondylaris*; **cmt\_clt\_fmp\_flg**: *Condylus medialis tibiae/Condylus lateralis tibiae/Facies medialis patellae/Facies lateralis patellae*; **fitfst\_fpc**: *Facies articularis inferior tibiae/Facies articularis superior (Talus)/Facies articularis talaris posterior (Calcaneus)*;

The true prevalence rates of the joint changes of the uphill and downhill males are generally similarly high in the two groups (TPR=1 or close to 1), only somewhat lower in the distal humerus (*Capitulum humeri/Trochlea*) and the proximal lower arm joints (*Caput radii/Circumferentia articularis radii/Incisura trochlearis/Incisura radialis*).

#### 4.4.2 Mean frequencies of single joint groups, males left side

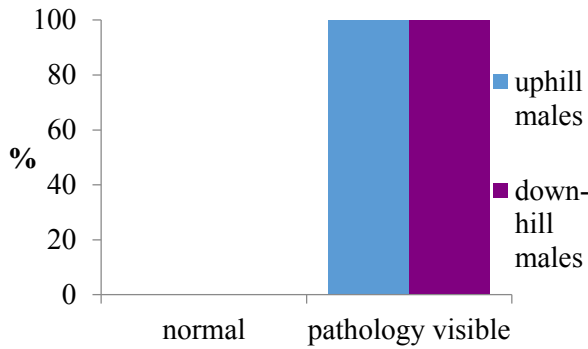
The differences of the frequencies of the single joint groups between the uphill and downhill males, normal entheses compared to enthesal changes frequencies (in percent) of the upper and lower extremities, left side, are shown in Table 16 and Figure 38. Most of the males in both groups show a high frequency of slight joint changes in the joints of the left side.

**Table 16.** Mean frequencies in percent of the single joint groups, left side, comparison of uphill and downhill males, upper and lower extremities.

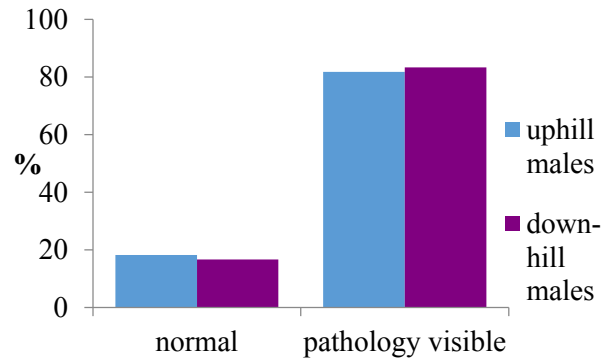
<b>joints, left side</b>	<b>group of males</b>	<b>% normal</b>	<b>% pathology visible</b>
<b>Caput humeri/Cavitas glenoidalis</b>	uphill	0.0	100.0
	downhill	0.0	100.0
<b>Capitulum humeri/Trochlea</b>	uphill	18.2	81.8
	downhill	16.7	83.3
<b>Caput radii/Circumferentia articularis radii/Incisura trochlearis/Incisura radialis</b>	uphill	8.8	91.2
	downhill	28.6	71.4
<b>Incis. ulnaris/Circumfer. art. ulnae/Cap. ul./prox. row carp. bones/F. articul. carp.</b>	uphill	3.1	96.9
	downhill	0.0	100.0
<b>Fossa acetabuli/ Caput femoris/Fovea capitis</b>	uphill	2.8	97.2
	downhill	0.0	100.0
<b>Fac. patellaris/ Cond. medialis femoris/Cond. lateralis fem./F. intercond.</b>	uphill	0.0	100.0
	downhill	0.0	100.0
<b>Cond. medialis tibiae/Cond. lateralis tib./Fac. medialis pat./Fac. lateralis pat.</b>	uphill	0.0	100.0
	downhill	0.0	100.0
<b>Fac. articul. inferior tib./Fac. articularis sup.tali/Fac. articularis tal. posterior calc.</b>	uphill	0.0	100.0
	downhill	0.0	100.0

Next page: **Figure 38.** Graphs of the joint groups, left side, comparison of uphill and downhill males.

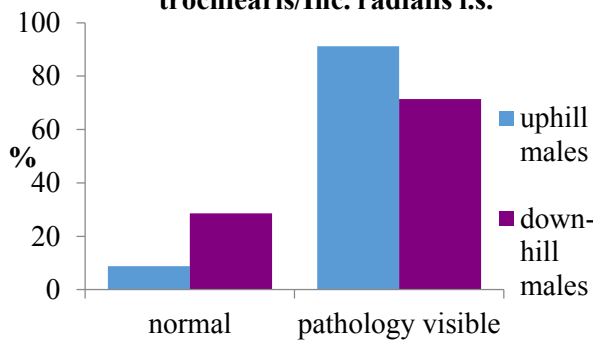
**Caput humeri/Cavitas glenoidalis l.s.**



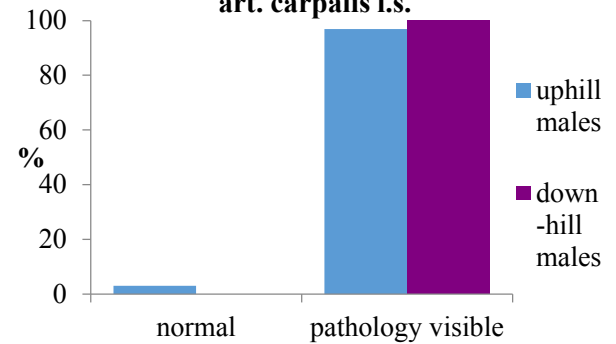
**Capitulum humeri/Trochlea l.s.**



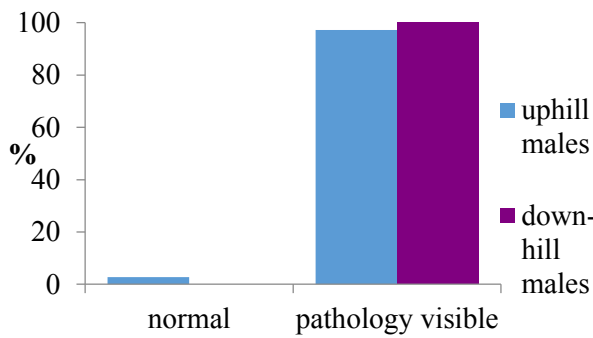
**Caput radii/Circumf. art. radii/Inc. trochlearis/Inc. radialis l.s.**



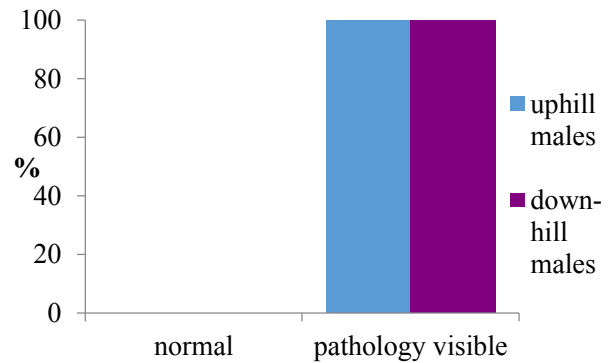
**Inc. ulnae/Circumf. art. ulnae/Caput ulnae/prox. wrist/Fac. art. carpalis l.s.**



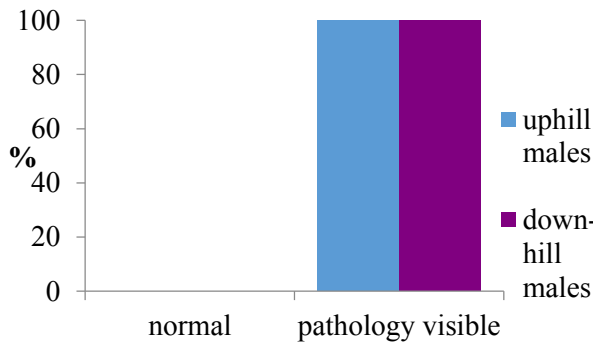
**Fossa acetabuli/ Caput femoris/Fovea capitis l.s.**



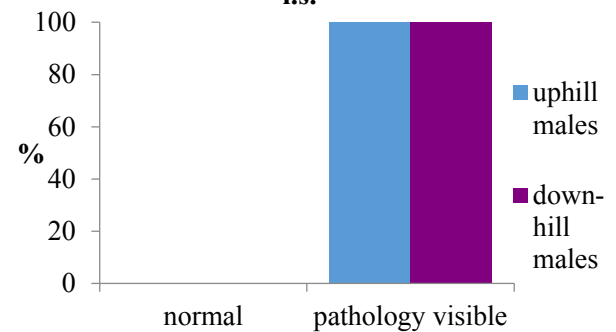
**Facies patellaris/ Cond. med. fem./Cond. lat.fem./F. intercond. l.s.**



**Cond. med. tibiae/Cond.lat. tibiae/Fac. med. patella/Fac.lat. patella l.s.**



**Fac. art. inf. tibiae/Fac. art. inf. Talus/Fac. art. talaris post. Calc. l.s.**



#### 4.4.3 Description of the tables and figures for joint frequencies of the left upper and lower extremities in uphill and downhill males

All analysable males in both groups show slight changes in the left shoulder joint (*Caput humeri/Cavitas glenoidalis*). More than 80% of the males of both groups show slight pathologies in the distal humeral elbow joint (*Capitulum humeri/Trochlea*). About 20% more of the males in the hillfort group show slight changes in the proximal lower arm elbow joint (*Caput radii/Circumferentia articularis radii/Incisura trochlearis/Incisura radialis*) than in the downhill males. Nearly all of the males in both groups display slight joint changes in the wrist bones (*Incisura ulnaris/Circumferentia articularis ulnae/Caput ulnae/proximal row of carpal bones/Facies articularis carpalis*).

In the lower extremity, the distribution of slight pathologies in the hip joint (*Fossa acetabuli/Caput femoris/Fovea capitis*) in the two groups is close to (uphill) or 100% (downhill). All analysed individuals show slight pathology in the knee joint (pooled *Facies patellaris/Condylus medialis femoris/Condylus lateralis femoris/Fossa intercondylaris* and pooled *Condylus medialis tibiae/Condylus lateralis tibiae/Facies medialis patellae/Facies lateralis patellae*). All analysed male skeletons exhibit slight pathologies at the left ankle bone joints (*Facies articularis inferior tibiae/Facies articularis superior tali/Facies articularis talaris posterior*).

Table 17 on the next page recapitulates details on individual numbers and percentage rates of the pooled entheses and joint frequencies of the left extremity of the uphill/downhill males in comparison.

**Table 17.** Pooled entheses and joint frequencies of the left extremity of the males in comparison.

<b>pooled entheses frequencies, uphill males, left side</b>		<b>uphill males n</b>			<b>n path. visible</b>	
	Total	recordable	normal	%	visible	%
M. biceps bra./subscap.	31	26	12	46,2	14	53,8
M. suprasp./infrasp./teres min.	31	23	14	60,9	9	39,1
M. triceps brachii	31	27	7	25,9	20	74,1
Common extensors	31	20	13	65,0	7	35,0
Common flexors	31	23	15	65,2	8	34,8
M. biceps brachii/brachialis	31	26	9	34,6	17	65,4
M. semim./semit./biceps fem.	31	24	8	33,3	16	66,7
Patella/pat. lig. (M. quadr. fem.)	31	23	6	26,1	17	73,9
<b>pooled entheses frequencies, downhill males, left side</b>		<b>downhill males n</b>			<b>n path. visible</b>	
	Total	recordable	normal	%	visible	%
M. biceps bra./subscap.	7	7	5	71,4	2	28,6
M. suprasp./infrasp./teres min.	8	6	2	33,3	4	66,7
M. triceps brachii	7	7	2	28,6	5	71,4
Common extensors	8	7	5	71,4	2	28,6
Common flexors	7	7	5	71,4	2	28,6
M. biceps brachii/brachialis	7	7	2	28,6	5	71,4
M. semim./semit./biceps fem.	7	4	1	25,0	3	75,0
Patella/pat. lig. (M. quadr. fem.)	7	6	2	33,3	4	66,7
<b>pooled joints frequencies, uphill males, left side</b>		<b>uphill males n</b>			<b>n path. visible</b>	
	Total	recordable	normal	%	visible	%
Cap. hum./cav. glen.	40	39	0	0,0	39	100,0
Capit. humeri/Trochlea	40	33	6	18,2	27	81,8
Cap. rad./Circ. art. rad./I. trochl./I. rad.	40	34	3	8,8	31	91,2
Inc. ul./Circ. art. ul./Cap. ul./prox. row of carp. bones/Fac. Art. Carp.	40	32	1	3,1	31	96,9
Fossa acetabuli/Caput femoris/Fovea capitis	40	36	1	2,8	35	97,2
Fac. patellaris/Cond. med. fem./Cond. lat. fem./F. incercodylaris	40	33	0	0,0	33	100,0
Cond. med. tib./Cond. lat. tib./Facies med.	40	33	0	0,0	33	100,0
Patella/Facies lat. Patella	40	33	0	0,0	33	100,0
Fac. Art. inf. tib./Fac. Art. Sup. Tal./Fac. Art.tal.posterior Calcan.	40	36	0	0,0	36	100,0
<b>pooled joints frequencies, downhill males, left side</b>		<b>downhill males n</b>			<b>n path. visible</b>	
	Total	recordable	normal	%	visible	%
Cap. hum./cav. glen.	8	7	0	0,0	7	100,0
Capit. humeri/Trochlea	8	6	1	16,7	5	83,3
Cap. rad./Circ. art. rad./I. trochl./I. rad.	8	7	2	28,6	5	71,4
Inc. ul./Circ. art. ul./Cap. ul./prox. row of carp. bones/Fac. Art. Carp.	8	6	0	0,0	6	100,0
Fossa acetabuli/Caput femoris/Fovea capitis	8	6	0	0,0	6	100,0
Fac. patellaris/ Cond. med. fem./Cond. lat. fem./F. incercodylaris	8	7	0	0,0	7	100,0
Cond. med. tib./Cond. lat. tib./Facies med.	8	6	0	0,0	6	100,0
Patella/Facies lat. Patella	8	6	0	0,0	6	100,0
Fac. Art.inf. tib./Fac. Art. Sup. Tal./Fac. Art.tal.posterior Calcan.	8	5	0	0,0	5	100,0

## 5 THUNAU MALES – RESULTS II – VISUAL ANALYSIS: ASYMMETRY

### 5.1 Males – entheses – asymmetry, upper and lower extremities

Asymmetry was calculated from the scores between the extremities following the recommendations of Auerbach & Ruff (2006, compare chapter 3.4., statistical analysis). In Table 18 and Figure 39), the differences are well visible and asymmetries seem to be more distinct generally in the downhill males (e.g. *M. triceps brachii* right side, common extensors on the left side, *M. biceps/brachialis* on the right side).

**Table 18.** Comparison of asymmetry in the scores of enthesal changes between right and left extremities for uphill and downhill males.

males	uphill, right side	uphill, left side	% asymmetry	downhill, right side	downhill, left side	% asymmetry
sbb_ssc (shoulder)	1.11	1.17	-5.20	1.02	0.96	6.61
ssp_isp_hmi (shoulder)	1.15	1.13	2.18	1.28	1.30	-1.94
<i>M. triceps brachii</i>	1.33	1.35	-1.62	1.45	1.12	<b>25.69</b>
common extensors	1.16	1.18	-1.97	0.86	1.10	-24.39
common flexors	1.21	1.15	4.49	1.54	1.33	14.49
bib_bra (elbow/ra_ul)	1.31	1.25	4.77	1.46	1.18	21.34
sme_ste_bif (hip)	1.48	1.39	5.95	1.47	1.58	-7.12
pat_tlp (knee)	1.48	1.49	-0.72	1.40	1.21	<b>14.40</b>

Legend: **sbb\_scc**: *M. biceps brachii*/*M. subscapularis*; **ssp\_isp\_hmi**: *M. supraspinatus*, *M. infraspinatus*, *M. teres minor*; **stb\_utb**: *M. triceps brachii*; **com\_ext**: common extensors; **com flex**: common flexors; **bib\_bra**: *M. biceps brachii*/*M. brachialis*; **sme\_ste\_bif**: *M. semimembranosus*/*M. semitendinosus*/*M. biceps femoris*; **pat\_tlp**: Patella/patellar ligament: *M. quadriceps femoris*;

Statistically significant differences according to asymmetry between the uphill and the downhill males became visible between the series in the upper extremity for the *M. triceps brachii* and *M. quadriceps femoris* (compare below). No significant results were apparent in

the common extensors and the elbow (radius – ulna), although the differences seemed to be big in the graph.

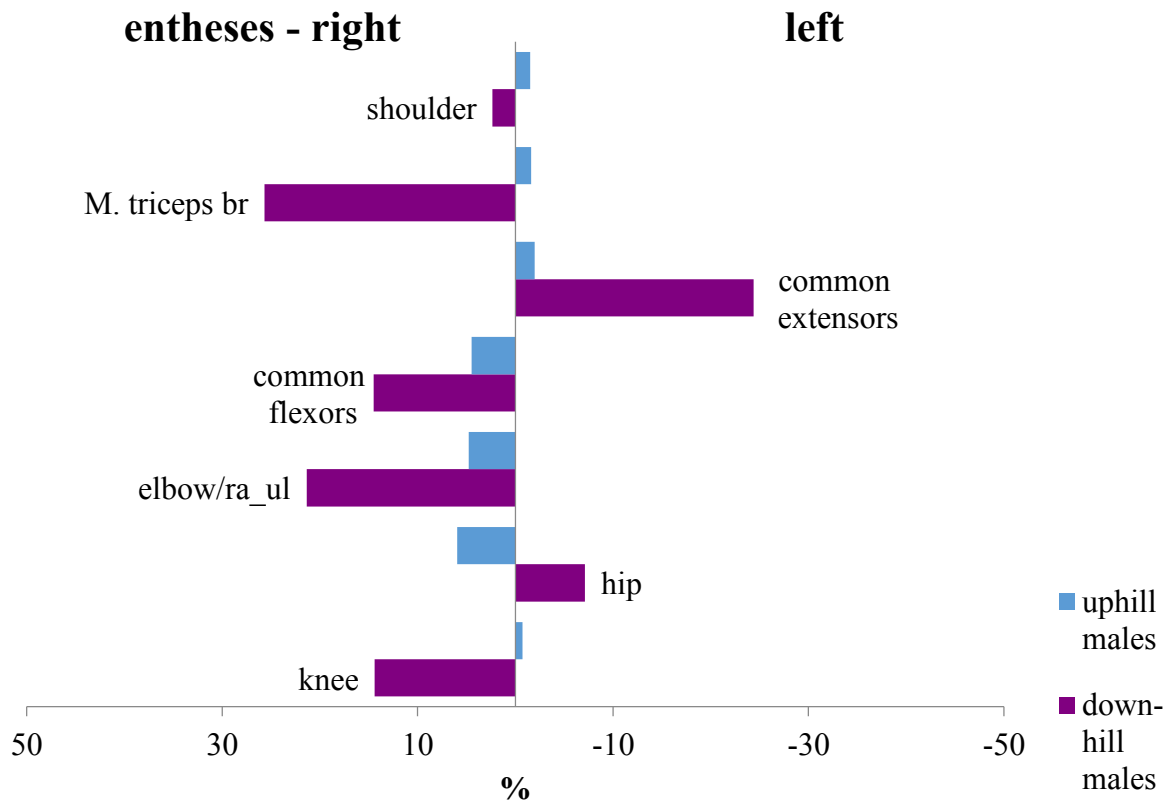


**Figure 39.** Asymmetries in enthesal changes calculated from scores in the right and left upper and lower extremities of the uphill and downhill males.

### 5.1.1 Significant differences in entheses asymmetry (univariate analysis)

According to differences in asymmetry between the males of the two groups, univariate analysis revealed statistically significant results in two muscle pools. In the upper extremities, the *M. triceps brachii*, right side, shows a significant difference between the two series ( $p=.023$ , Table 19), where the downhill males are more asymmetric (Figure 40). In the lower extremities, the differences are clearly significant in the right knee (*Patella/Ligamentum patellae*; *M. quadriceps femoris*; compare univariate analysis below).

**Table 19.** Results of the univariate analysis calculated from scores according to the *M. triceps brachii* (scapula/ulna).

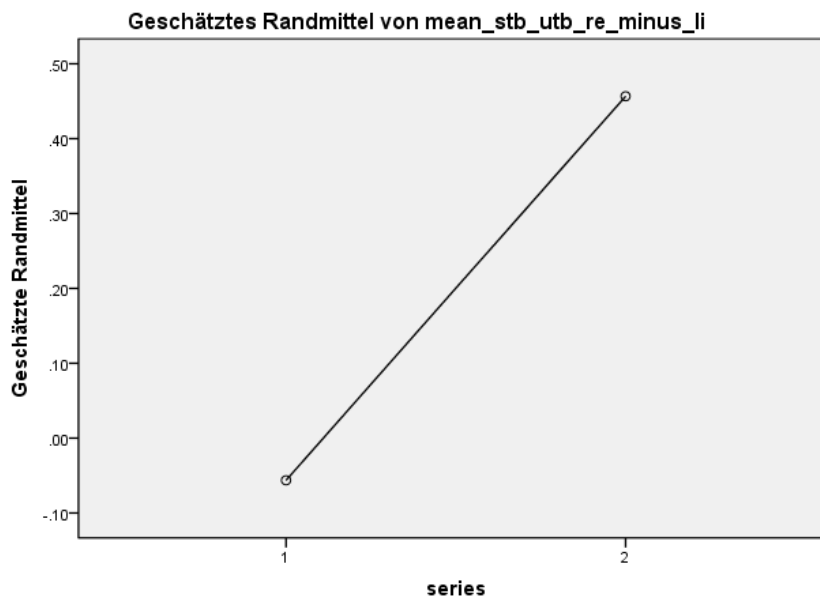
univariate analysis

		N
series	1	25
	2	6

dependent variable: mean\_stb\_utb\_re\_minus\_li

Quelle	Quadratsumme vom Typ III	df	Mittel der Quadrate	F	Sig.
Korrigiertes Modell	1.837 <sup>a</sup>	3	.612	3.094	.044
Konstanter Term	.685	1	.685	3.464	.074
mean_age	.114	1	.114	.575	.455
body height	.559	1	.559	2.827	.104
series	1.156	1	1.156	5.844	<b>.023</b>
Fehler	5.343	27	.198		
Gesamt	7.237	31			
Korrigierte Gesamtvariation	7.180	30			

a. R-Quadrat = .256 (korrigiertes R-Quadrat = .173)



Die Kovariaten im Modell werden anhand der folgenden Werte berechnet: mean age = 38.1452, body height = 172.887

**Figure 40.** Graph of the results of the univariate analysis calculated from scores according to the *M. triceps brachii* (scapula/ulna), where the downhill males show the higher asymmetry.

Differences in the lower extremities between the uphill and downhill males in the *M. quadriceps femoris* was statistically significant (Patella/Ligamentum patellae, right side, Table 20). Significant differences are apparent here between the two series, where the downhill males seem to be more asymmetric ( $p=.021$ , Figure 41). Further, there seems to be a significant result according to body height with this feature ( $p=.016$ ). Although it is a very small number of individuals in the downhill males group, this result is interesting.

**Table 20.** Results of the univariate analysis calculated from scores according to the *M. quadriceps femoris* (Patella/Ligamentum patellae).

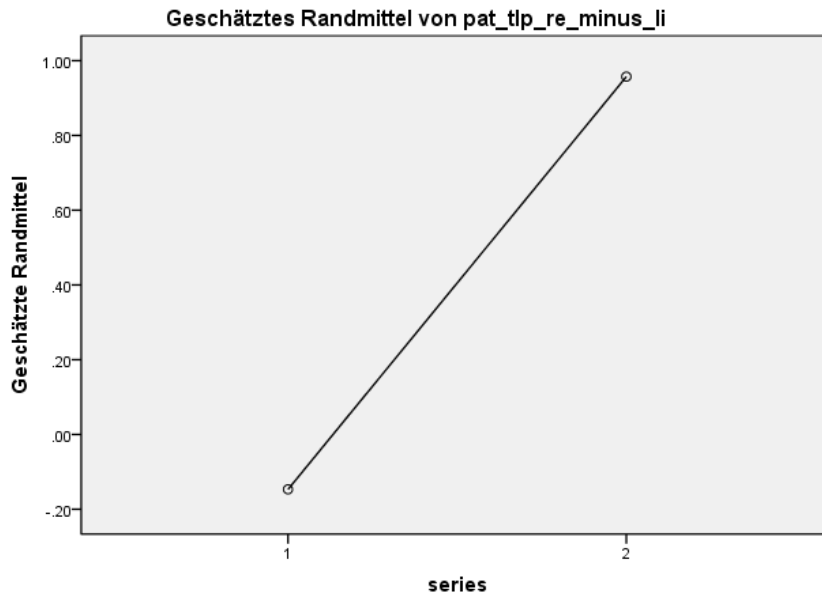
univariate analysis

		N
series	1	19
	2	3

dependent variable: pat tlp re minus li

Quelle	Quadratsumme vom Typ III	df	Mittel der Quadrate	F	Sig.
Korrigiertes Modell	4.508 <sup>a</sup>	3	1.503	3.554	.035
Konstanter Term	2.897	1	2.897	6.853	.017
mean_age	.257	1	.257	.607	.446
body height	2.993	1	2.993	7.079	<b>.016</b>
series	2.692	1	2.692	6.368	<b>.021</b>
Fehler	7.610	18	.423		
Gesamt	12.118	22			
Korrigierte Gesamtvariation	12.118	21			

a. R-Quadrat = .372 (korrigiertes R-Quadrat = .267)



Die Kovariaten im Modell werden anhand der folgenden Werte berechnet: mean age = 41.1364, body height = 173.295

**Figure 41.** Univariate group differences calculated from scores according to the *M. quadriceps femoris* (Patella/Ligamentum patellae), where the downhill males show higher asymmetry.

## 5.2 Males – joints – asymmetry, upper and lower extremities

Asymmetries were also calculated for the joints following the recommendations of Auerbach & Ruff (2006). The results show a slightly higher percentage rate in the distal humeral joint (*Capitulum humeri/trochlea*) on the left side in the downhill males (Table 21 & Figure 42), but the differences were not statistically significant. There were no considerable differences in the joint changes between the males of the two sub-sites for the other analysed joints.

**Table 21.** Comparison of asymmetry in joint changes between right and left extremities calculated from scores for uphill and downhill males.

males	uphill, right side	uphill, left side	% asymmetry	downhill, right side	downhill, left side	% asymmetry
chu_cgl (shoulder)	1.58	1.40	12.23	1.73	1.40	20.70
cah_tro (elbow_hu)	1.32	1.62	-20.32	1.31	1.79	-30.77
cra_cir_int_inr (elbow-ra/ul)	1.37	1.36	0.44	1.41	1.39	1.30
inu_ciu_cau_phw_fac (wrist)	1.41	1.46	-4.02	1.49	1.53	-2.46
foa_caf_foc (hip)	1.61	1.65	-2.17	1.86	1.88	-1.19
fap_cmf_clf_ufo (knee/Fe)	1.59	1.57	1.36	1.67	1.64	1.92
cmt_clt_fmp_flp (knee/Ti)	1.55	1.60	-3.34	1.64	1.69	-3.18
fit_fst_fpc (ankle)	1.53	1.58	-3.41	1.50	1.53	-2.20

Legend: **chu\_cgl**: *Caput humeri/Cavitas glenoidalis*; **cah\_tro**: *Capitulum humeri/Trochlea*; **cra\_cir\_int\_inr**: *Caput radii/Circumferentia articularis radii/Incisura trochlearis/Incisura radialis*; **inu\_ciu\_cau\_phw\_fac**: *Incisura ulnaris/Circumferentia articularis ulna/Caput ulnae/proximal row of carpal bones/Facies articularis carpalis*; **foa\_caf\_foc**: *Fossa acetabuli/Caput femoris/Fovea capitis*; **fap\_cmf\_clf\_ufo**: *Facies patellaris/Condylus medialis femoris/Condylus lateralis femoris/distal margin of Fossa intercondylaris*; **cmt\_clt\_fmp\_flp**: *Condylus medialis tibiae/Condylus lateralis tibiae/Facies medialis patellae/Facies lateralis patellae*; **fit\_fst\_fpc**: *Facies articularis inferior tibiae/Facies articularis superior (Talus)/Facies articularis talaris posterior (Calcaneus)*;

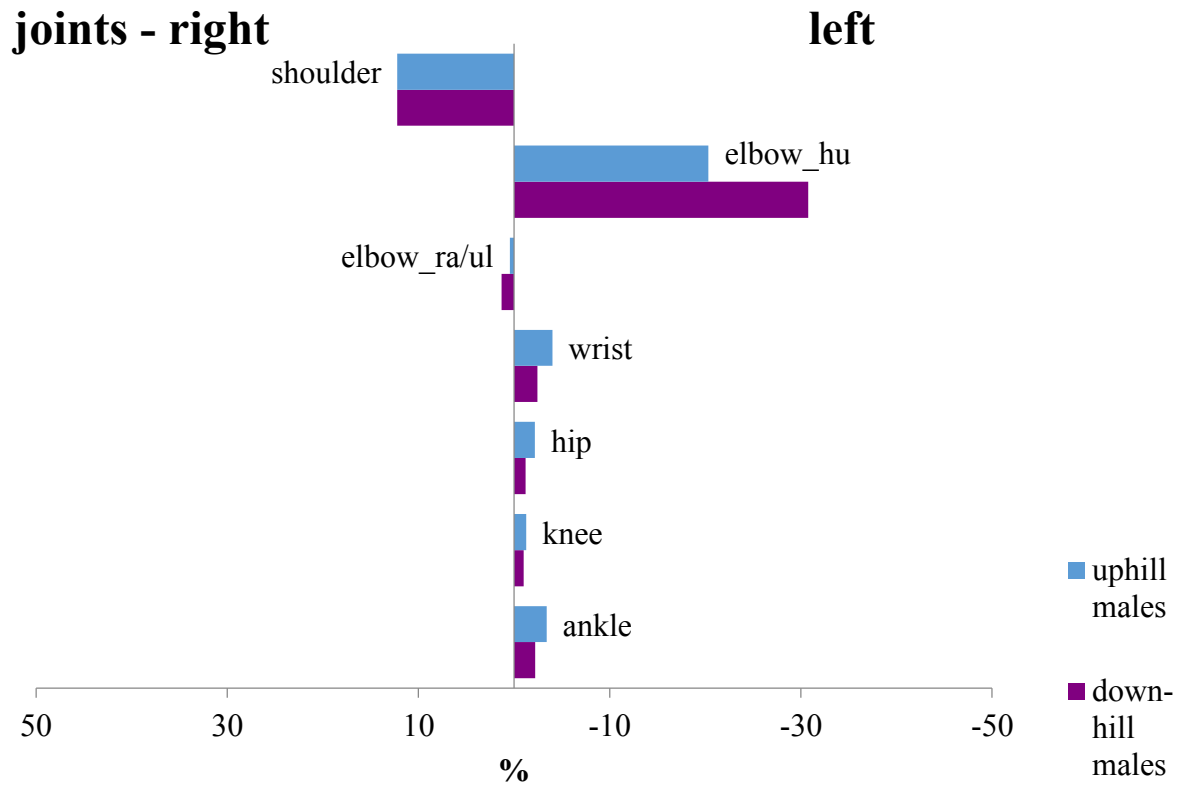


**Figure 42.** Asymmetries in joint changes calculated from scores in the right and left upper and lower extremities of the uphill and downhill males.

## 6 THUNAU MALES – RESULTS III – ASSOCIATION BETWEEN ENTHESES AND MEAN AGE/BODY HEIGHT

### 6.1 Scatterplots entheses– mean age– males

#### 6.1.1 Scatterplots entheses – mean age, comparison males uphill-downhill – right side

Differences between the two archaeological sub-sites from Thunau (series 1 = uphill site, series 2 = downhill site), according to mean scores and mean age are shown here in the scatterplots (Figures 43 – 50) between the uphill males and the downhill males, respectively. The scores of the muscle markings of the males are plotted against increasing age of both groups, along with the least squares regression line and the 95% confidence regions. Univariate analyses were added if the difference between the groups was significant; graphs are added in cases of clear average differences between the sub-sites.

Legend for the graphs: **triangle**: males: entheses – mean age, **square**: males: joints – mean age

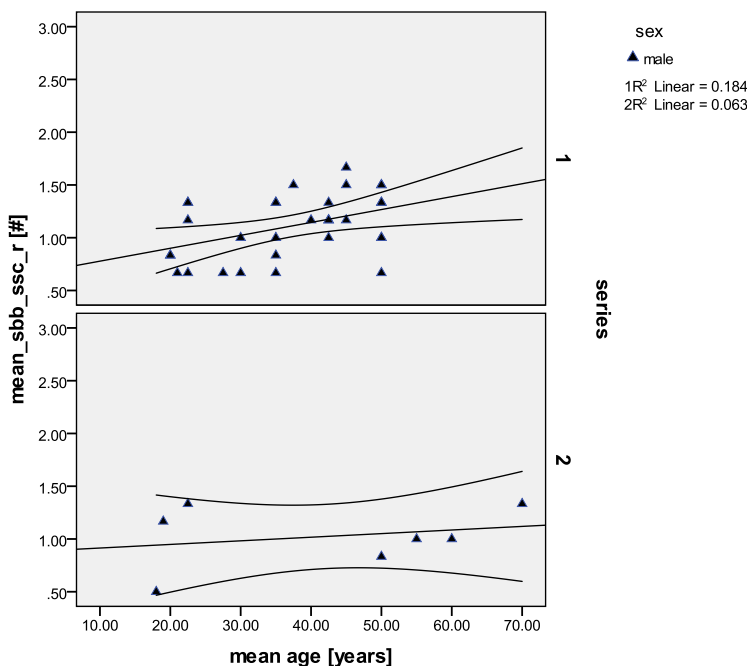


**Figure 43.** Scatterplot of the pooled muscle group *M. biceps brachii* – *M. subscapularis* (humerus, scapula), uphill (1) and downhill males (2), right side. There is a slight increase of entheses scores with higher age in both groups.

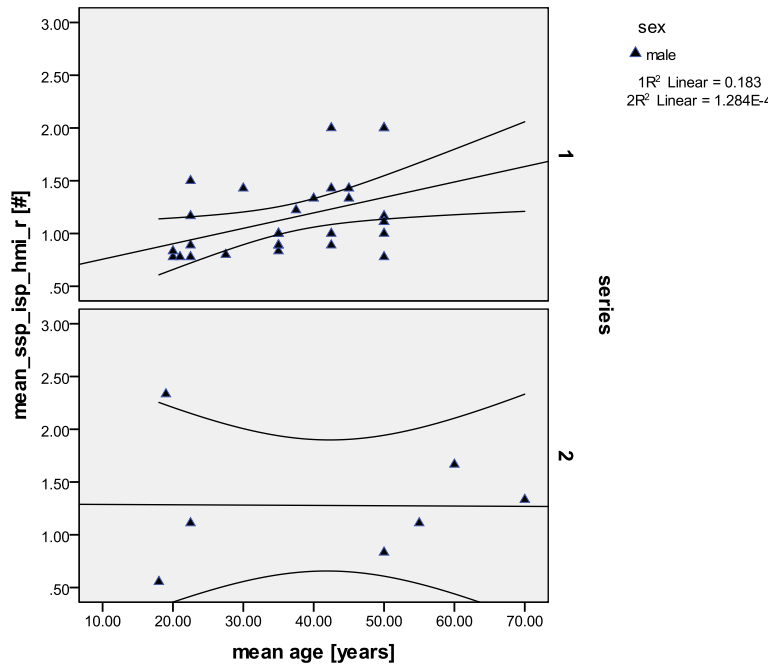


**Figure 44.** Scatterplot of the pooled muscle group *M. supraspinatus - M. infraspinatus - M. teres minor* (proximal humerus), uphill (1) and downhill males (2), right side. There is a slight increase of entheses scores with higher age in the hillfort males, but no significant difference is apparent.

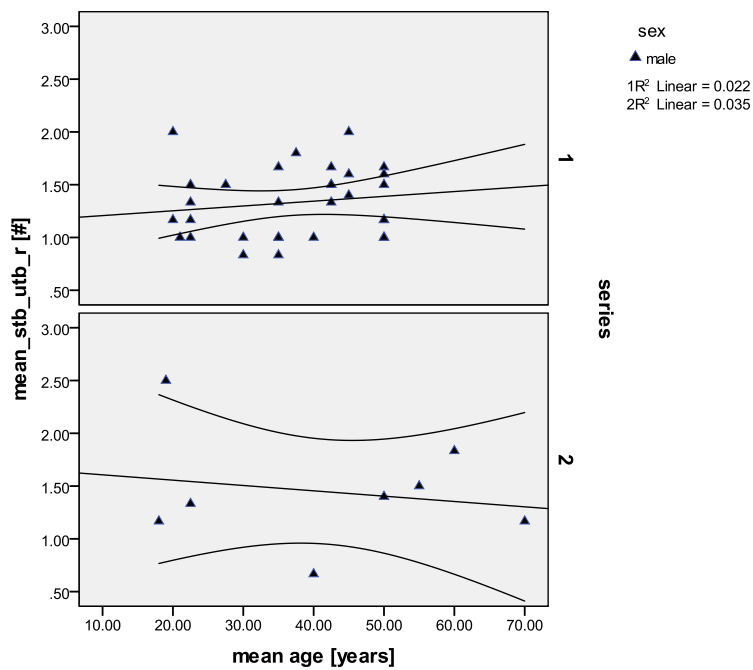


**Figure 45.** Scatterplot of the pooled muscle group *M. triceps brachii* (scapula, ulna), uphill (1) and downhill males (2), right side. There is no noticeable increase in the scores of this feature with higher age in the two groups.

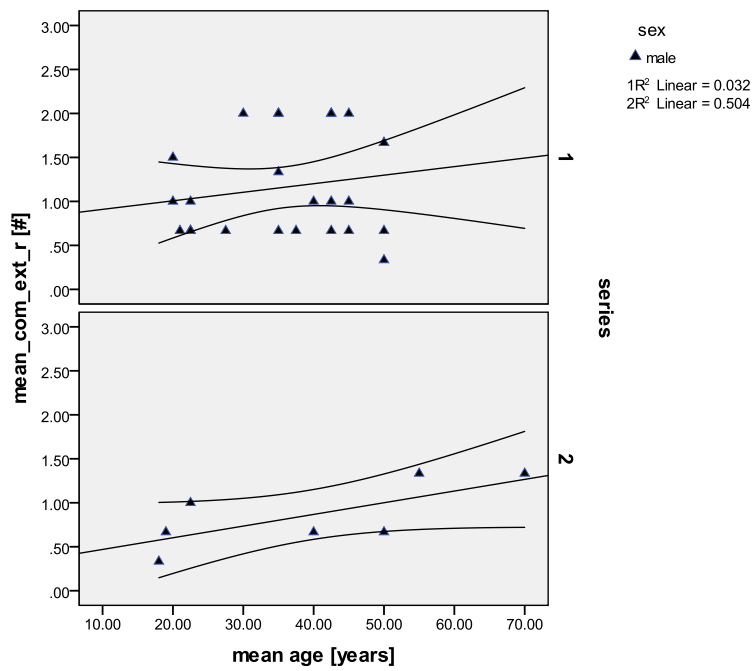


**Figure 46.** Scatterplot of the pooled muscle group **common extensors** (distal lateral humerus), uphill (1) and downhill males (2), right side. There is a slight increase of common extensors entheses scores with increasing age in the males of both sites.

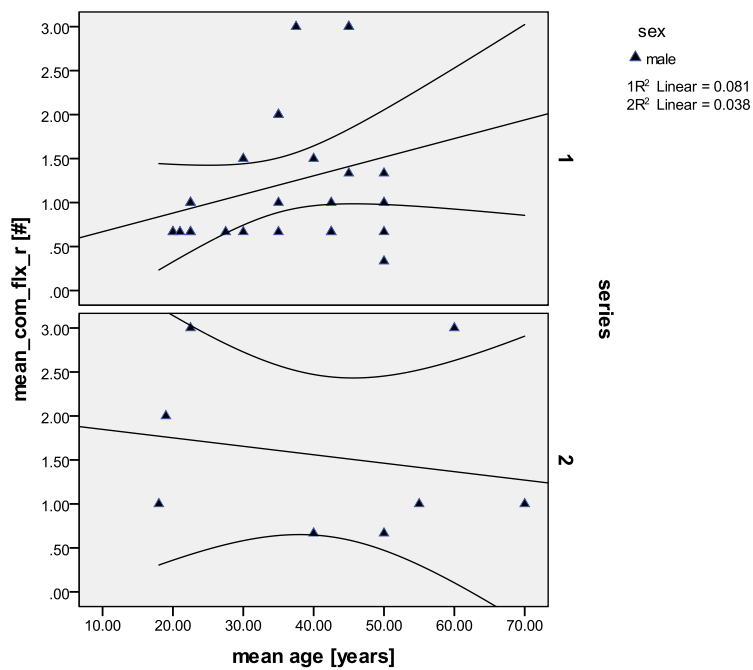


**Figure 47.** Scatterplot of the pooled muscle group **common flexors** (distal medial humerus), uphill (1) and downhill males (2), right side. There is a distinct increase of the common flexors entheses scores with higher age in the males of the uphill site. The downhill males show higher scores already at a younger age.

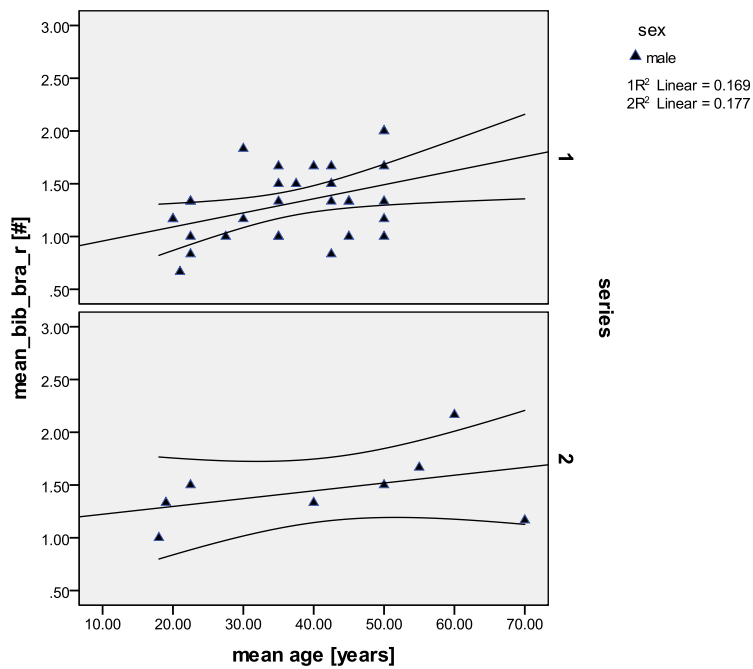


**Figure 48.** Scatterplot of the pooled muscle group *M. biceps brachii* – *M. brachialis* (proximal radius and proximal ulna - elbow), uphill (1) and downhill males (2), right side. There is a slight increase of entheses scores with increasing age in both groups, but there are no significant differences.

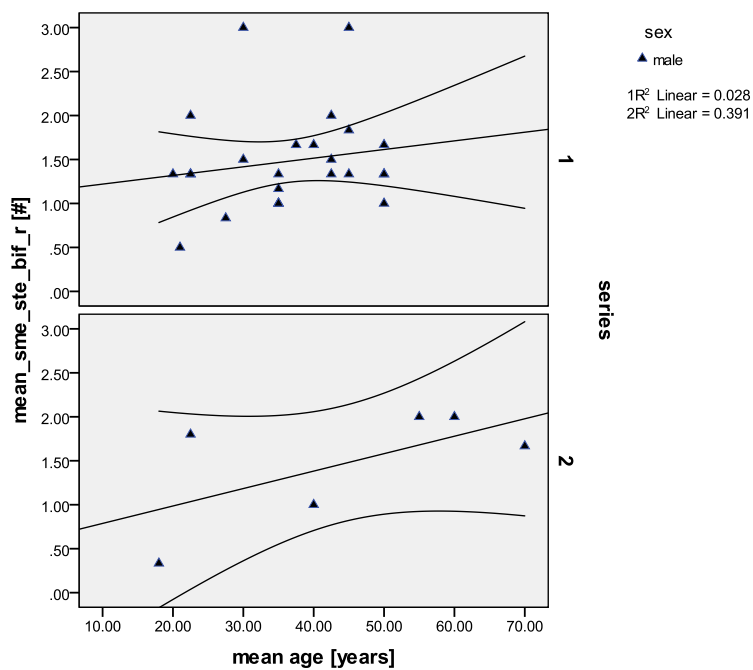


**Figure 49.** Scatterplot of the pooled muscle group *M. semimembranosus* – *M. semitendinosus* – *M. biceps femoris* (tuber ischiadicum), uphill (1) and downhill males (2), right side. There is a slight increase of entheses scores with higher age, more marked in the downhill males; however, half of the individuals in the latter are over the age of fifty years.

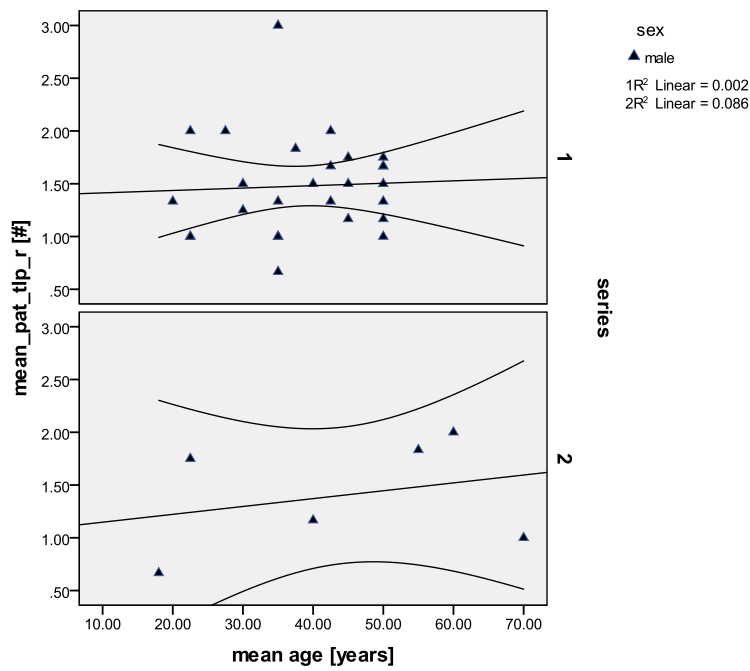


**Figure 50.** Scatterplot of the pooled muscle group *M. quadriceps femoris* (Patella – patellar ligament), uphill (1) and downhill males (2), right side. There is no notable increase of entheses scores with higher age in neither group.

### 6.1.2 Short summary

There is a slight association with higher age in some right side entheses of the males in both groups (common extensors, *M. biceps/M. brachialis*, hip muscles), but no statistically significant results were found.

### 6.1.3 Scatterplots joints – mean age, comparison males uphill-downhill – right side

The scores of the pooled male joints are plotted against age for both groups, along with the least squares regression line =mean scores line and the 95% confidence regions (Figures 51 – 60). Univariate analyses were added if the difference between the groups was significant; graphs are added in cases of clear average differences between the sub-sites.

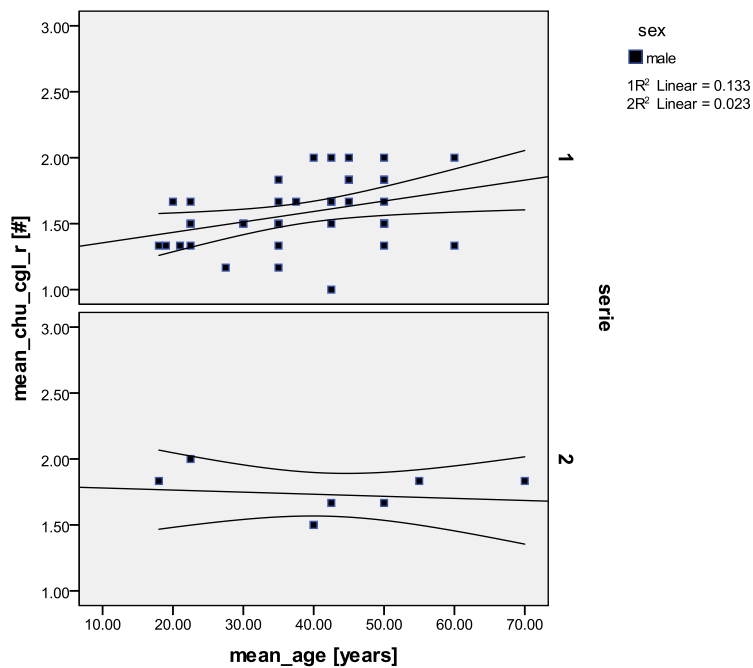


**Figure 51.** Pooled joint group *Caput humeri – Cavitas glenoidalis* (shoulder - humerus, scapula), comparison between males of the uphill (1) and downhill (2) site, right side. There is a slight increase in the shoulder joint scores with increasing age in the males of series 1, contrary to series 2.

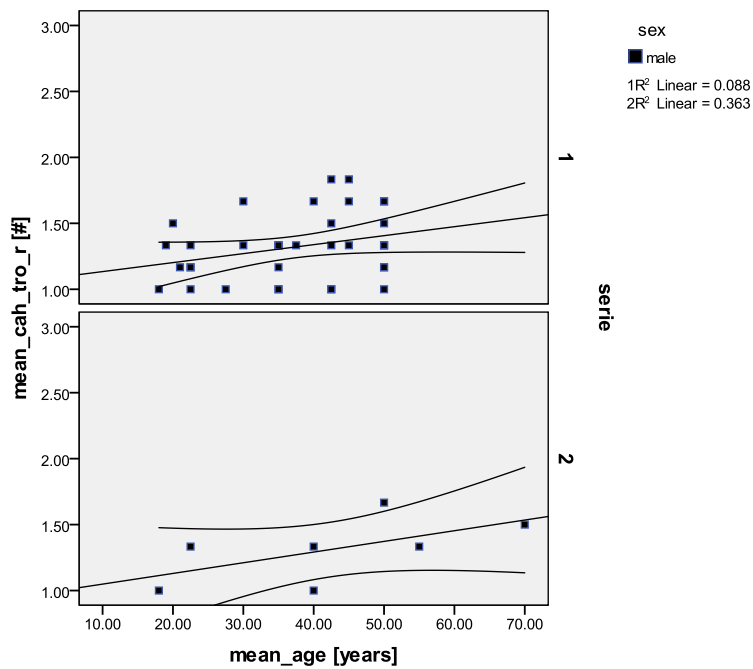


**Figure 52.a.** Pooled joint group *Capitulum humeri* – *Trochlea* (dist. humerus - elbow), males of the uphill (1) and downhill site (2), right side. This pooled joint group is significantly affected by age (see Figure 52b).

**Figure 52. b.** Univariate analysis of the pooled joint group *Capitulum humeri* – *Trochlea*.

		N
series	1	36
	2	7

dependent variable:mean\_cah\_tro\_r

Quelle	Quadratsumme vom Typ III	df	Mittel der Quadrate	F	Sig.
Korrigiertes Modell	.321 <sup>a</sup>	2	.160	2.884	.068
Konstanter Term	3.521	1	3.521	63.315	.000
mean_age	.320	1	.320	5.757	<b>.021</b>
series	.012	1	.012	.217	.644
Fehler	2.224	40	.056		
Gesamt	77.222	43			
Korrigierte Gesamtvariation	2.545	42			

a. R-Quadrat = .126 (korrigiertes R-Quadrat = .082)

The pooled joint group *Capitulum humeri/Trochlea* at the elbow joint is significantly affected by age ( $p=.021$ ) but not by sub-sites.

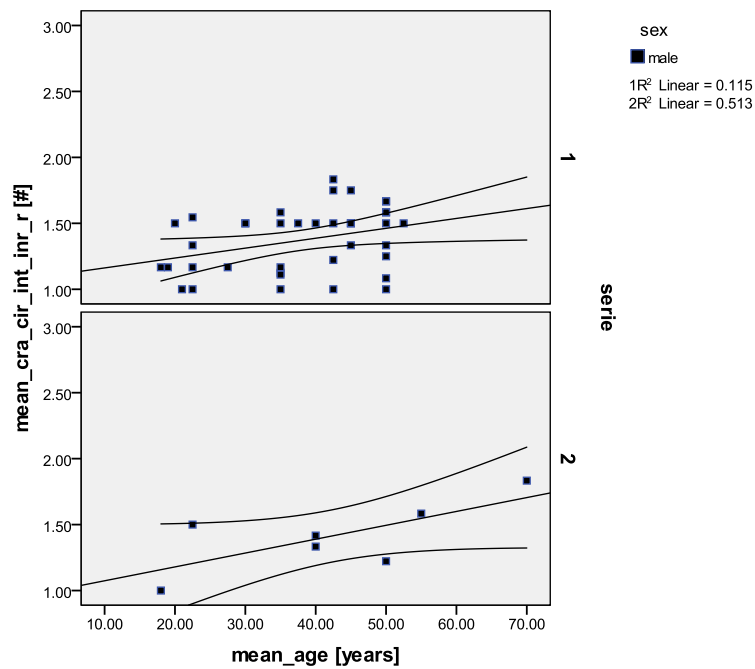


**Figure 53.a.** Pooled joint group *Caput radii*, *Circumferentia articularis radii*, *Incisura trochlearis*, *Incisura radialis* (proximal radius and ulna - elbow), males of the uphill (1) and downhill site (2), right side. There is an increase of scores at the elbow in the males of both sites, which is significantly affected by age (see Figure 53.b).

**Figure 53. b.** Univariate analysis of the pooled joint group *Caput radii*, *Circumferentia articularis radii*, *Incisura trochlearis*, *Incisura radialis*.

		N
serie	1	38
	2	7

dependent variable: mean\_cra\_cir\_int\_inr\_r

Quelle	Quadratsumme vom Typ III	df	Mittel der Quadrate	F	Sig.
Korrigiertes Modell	.467 <sup>a</sup>	2	.233	4.570	.016
Konstanter Term	3.805	1	3.805	74.542	.000
mean_age	.456	1	.456	8.937	<b>.005</b>
serie	.000	1	.000	.003	.957
Fehler	2.144	42	.051		
Gesamt	87.967	45			
Korrigierte Gesamtvariation	2.610	44			

a. R-Quadrat = .179 (korrigiertes R-Quadrat = .140)

The pooled joint features *Caput radii*, *Circumferentia articularis radii*, *Incisura trochlearis*, *Incisura radialis* at the right proximal radius and ulna (elbow) are significantly affected by age in the males.

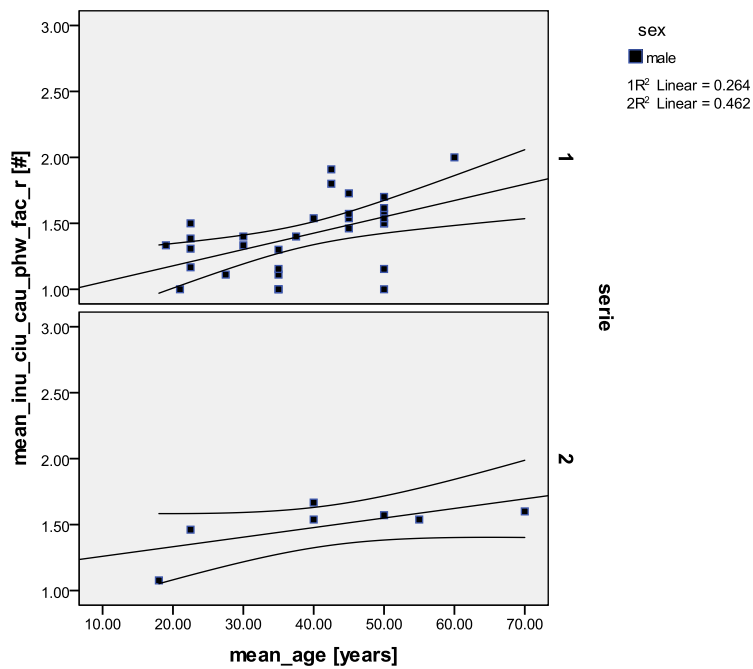


**Figure 54.** Scatterplot of the pooled joint group *Incisura ulnaris, Circumferentia articularis ulnae, Caput ulnae, proximal row of wrist bones, Facies articularis carpalis* (distal radius and ulna; wrist), males of the uphill (1) and downhill site (2), right side. There is an increase of scores with higher age in joint changes in the males of both sites.

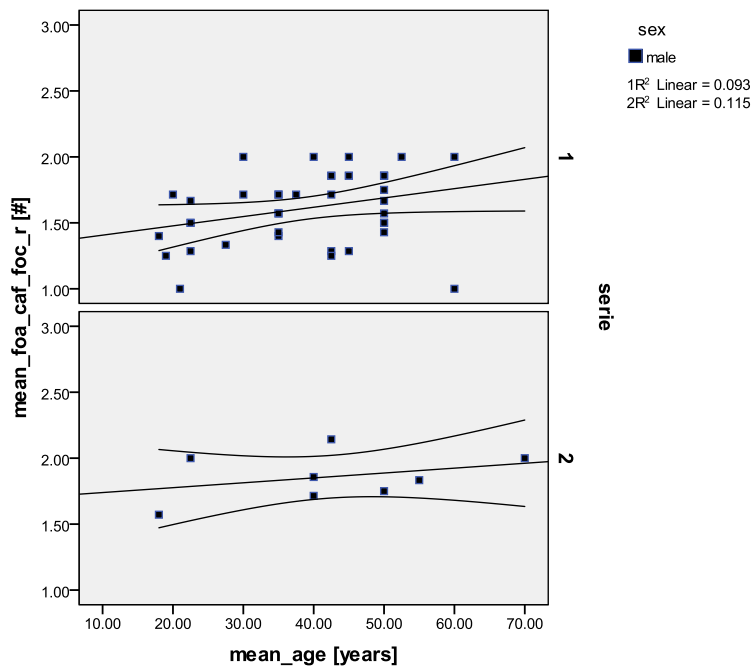


**Figure 55.a.** Scatterplot of the pooled joint group *Fossa acetabuli, Caput femoris, Fovea capitis (Os ilium (acetabulum), femoral head - hip joint)*, males of the uphill (1) and downhill (2) site, right side. The increase of scores in hip joint changes in the males of both sites is significantly affected by age (see Figure 55b).

**Figure 55. b.** Univariate analysis of the pooled joint group *Fossa acetabuli, Caput femoris, Fovea capitis*.

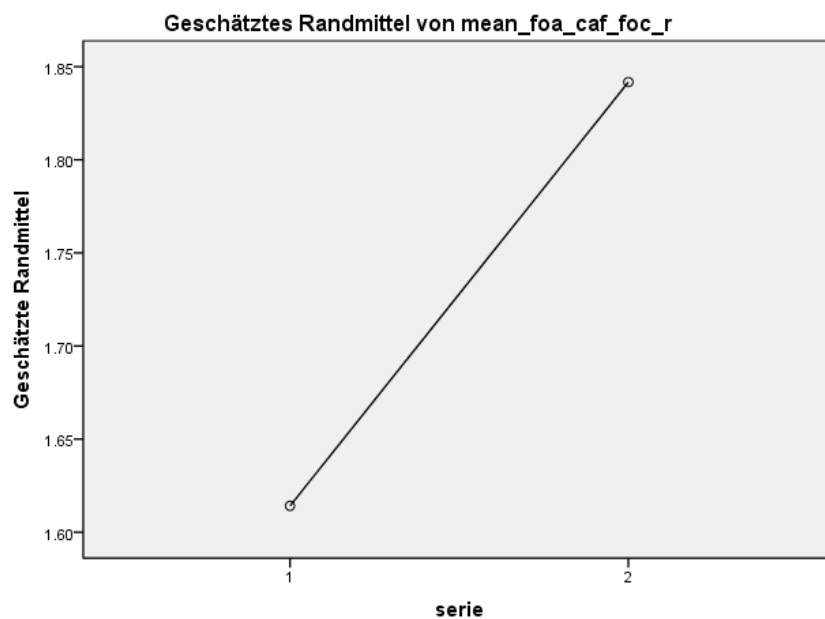
		N
serie	1	40
	2	8

dependent variable:mean foa caf foc r

Quelle	Quadratsumme vom Typ III	df	Mittel der Quadrate	F	Sig.
Korrigiertes Modell	.687 <sup>a</sup>	2	.344	5.445	.008
Konstanter Term	8.423	1	8.423	133.449	.000
mean_age	.278	1	.278	4.401	<b>.042</b>
serie	.342	1	.342	5.416	<b>.025</b>
Fehler	2.840	45	.063		
Gesamt	134.538	48			
Korrigierte Gesamtvariation	3.528	47			

a. R-Quadrat = .195 (korrigiertes R-Quadrat = .159)

The pooled hip joint group in the males show is significantly affected by age ( $p=.042$ ) and there is a significant difference between the series ( $p=.025$ ).



Die Kovariaten im Modell werden anhand der folgenden Werte berechnet: mean\_age = 39.5000

The downhill males display apparently higher scores in hip joint changes on the right side.

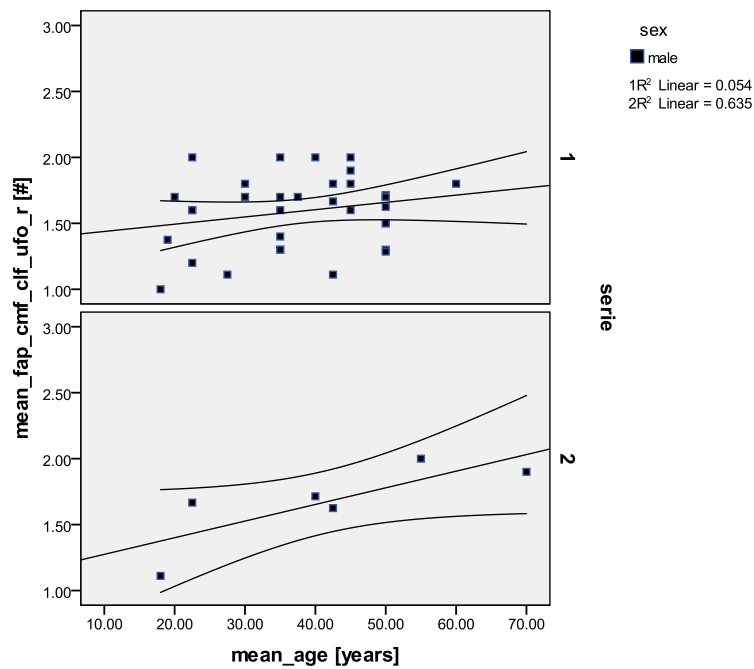


**Figure 56.a.** Scatterplot of the pooled joint group *Facies patellaris, Condylus medialis femoris, Condylus lateralis femoris*, distal margin of *Fossa intercondylaris* (distal femur - knee), males of the uphill (1) and downhill site (2), right side. The increase of scores in joint changes in both male groups is associated with higher age (see Figure 56b).

**Figure 56. b.** Univariate analysis of the pooled joint group *Facies patellaris, Condylus medialis femoris, Condylus lateralis femoris*, distal margin of *Fossa intercondylaris*.

		N
series	1	35
	2	6

dependent variable: mean\_fap\_cmf\_clf\_ufo\_r

Quelle	Quadratsumme vom		Mittel der Quadrate	F	Sig.
	Typ III	df			
Korrigiertes Modell	.399 <sup>a</sup>	2	.199	2.957	.064
Konstanter Term	5.851	1	5.851	86.752	.000
mean_age	.370	1	.370	5.481	<b>.025</b>
series	.014	1	.014	.204	.654
Fehler	2.563	38	.067		
Gesamt	108.582	41			
Korrigierte Gesamtvariation	2.962	40			

a. R-Quadrat = .135 (korrigiertes R-Quadrat = .089)

The pooled right joint group at the distal femur is significantly affected by age in the male sub-sites of Thunau.

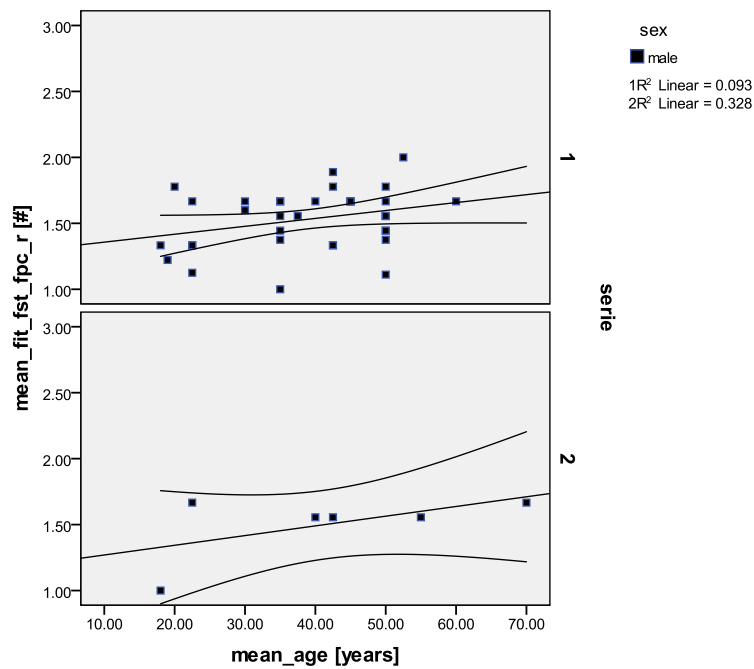


**Figure 57.** Scatterplot of the pooled joint group *Facies articularis inferior tibiae*, *Facies articularis superior talus*, *Facies articularis talaris posterior calcanei* (distal tibia - ankle), males of the uphill (1) and downhill (2) site, right side. There is a slight increase of scores in joint changes in the ankle in the males of both sites, but no significant relationship.

#### 6.1.4 Short summary

A statistically significant association with age was found in the pooled right joint group *Capitulum humeri/Trochlea* (elbow - humerus) and the distal femoral joint. A significant association with both age and series was found in the *Caput radii/Circumferentia articularis radii/Incisura trochlearis* (elbow – radius/ulna) and for the hip joint facets (*Fossa acetabuli*, *Caput femoris* and *Fovea capitis*). The age effect in the wrist and ankle was not significant.

### 6.1.5 Scatterplots entheses – mean age, comparison males uphill-downhill – left side

The scores of the muscle markings of the males of the two sub-sites are plotted against increasing age (Figures 58 - 65), along with the least squares regression line and the 95% confidence regions. Univariate analyses were added if the difference between the groups was significant; graphs are added in cases of clear average differences between the sub-sites.

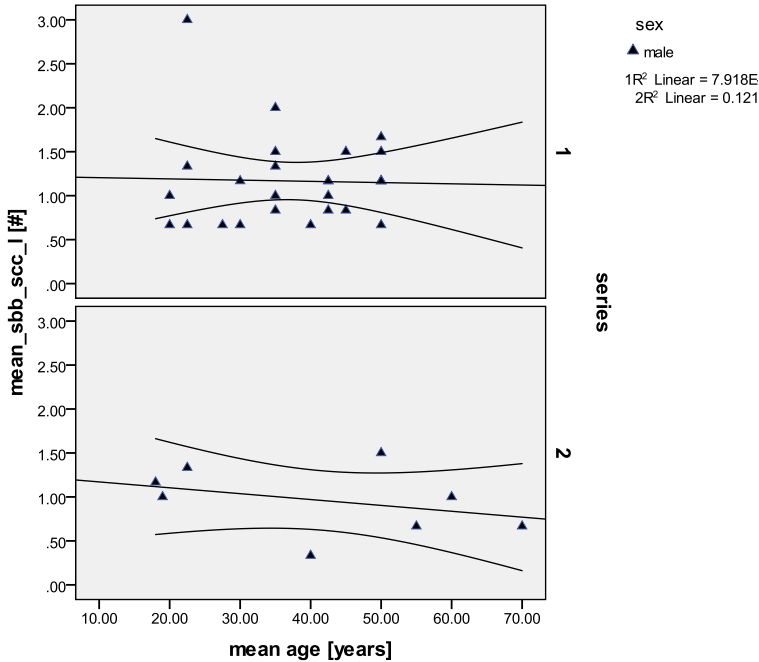


**Figure 58.** Scatterplot of the pooled muscle group *M. biceps brachii* – *M. subscapularis* (scapula and proximal humerus - shoulder), males of the uphill (1) and downhill site (2), left side. There is no clear association between increasing enthesal scores and higher age in neither group.

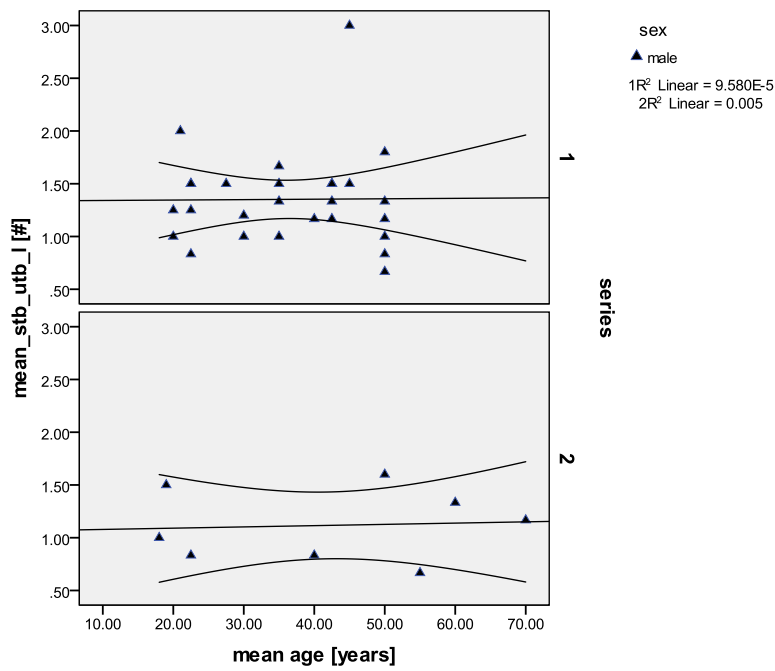


**Figure 59.** Scatterplot of the pooled muscle group *M. triceps brachii* (scapula – proximal ulna), males of the uphill (1) and downhill site (2), left side. There is no association in the *M. triceps brachii* between higher entheses scores and increasing age in neither group.

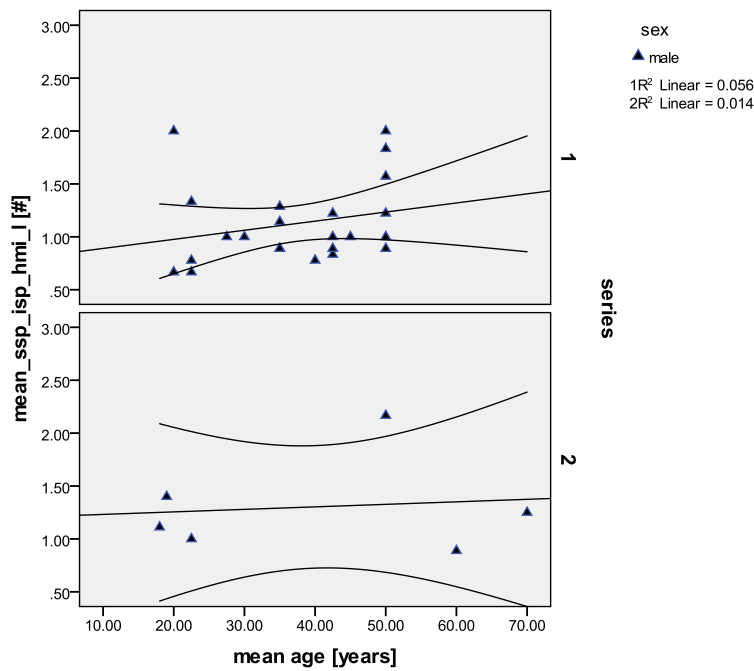


**Figure 60.** Scatterplot of the pooled muscle group *M. supraspinatus - M. infraspinatus - M. teres minor* (proximal humerus), males of the uphill (1) and downhill site (2), left side. There is a slight increase of entheses scores with higher age apparent in group 1, but not in group 2.

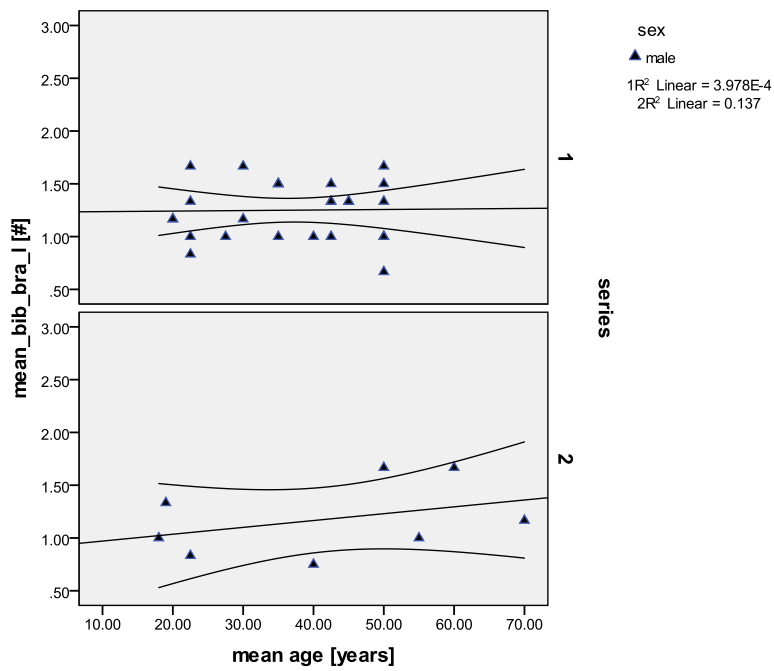


**Figure 61.** Scatterplot of the pooled muscle group *M. brachialis* (proximal radius and proximal ulna - elbow), males of the uphill (1) and downhill site (2), left side. There is no clear relationship of scores with higher age in neither group.

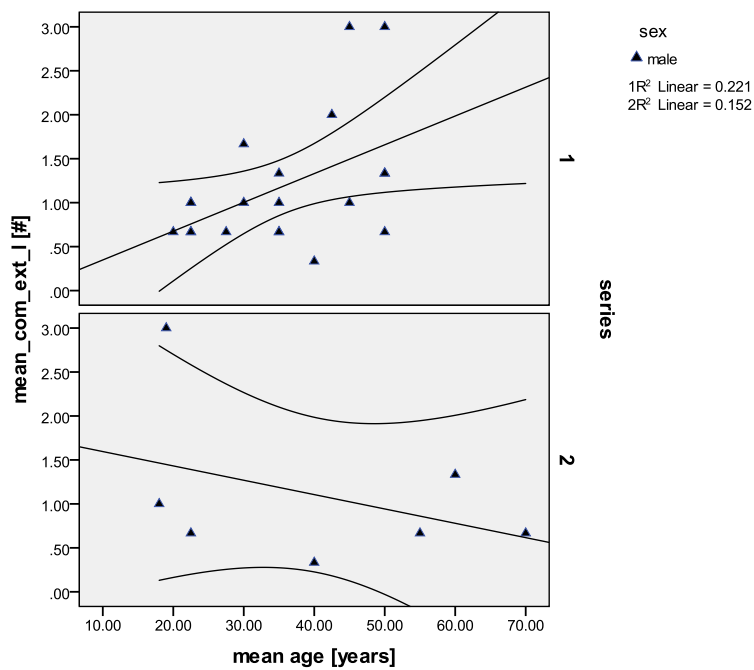


**Figure 62.** Scatterplot of the pooled **common extensors** group (distal lateral humerus), males of the uphill (1) and downhill site (2), left side. There is a marked increase of scores with higher age in series 1, but no clear association in group 2 with higher age.

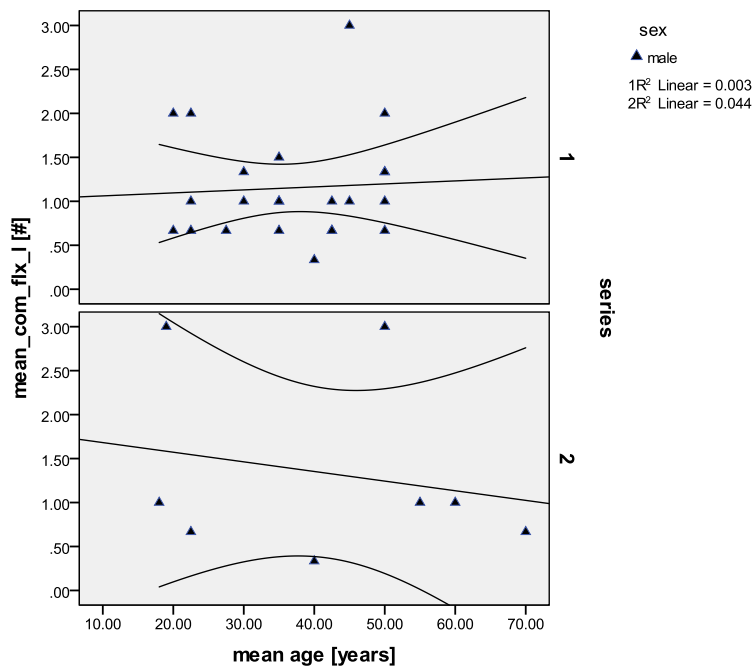


**Figure 63.** Scatterplot of the pooled **common flexors** group (distal medial humerus), males of the uphill (1) and downhill site (2), left side. There is no clear relationship of scores with higher age in neither group.

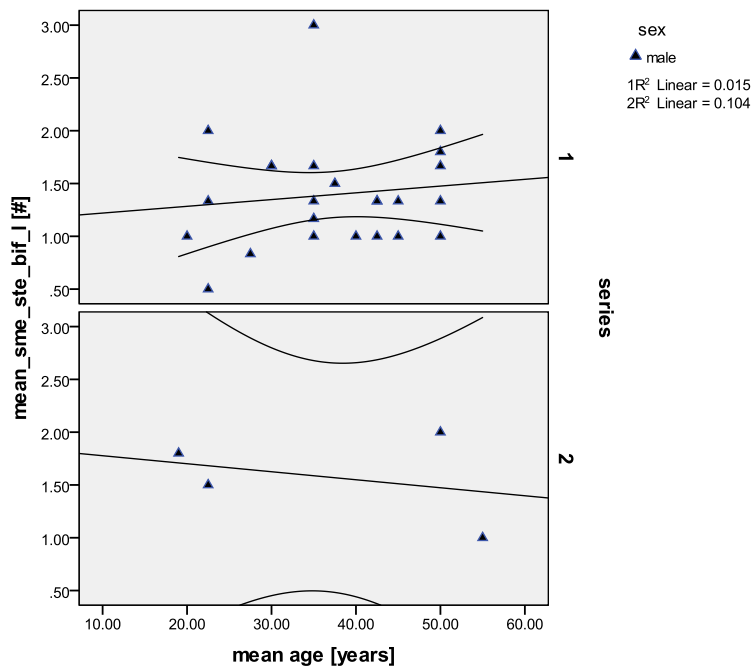


**Figure 64.** Scatterplot of the pooled muscle group *M. semimembranosus* – *M. semitendinosus* – *M. biceps femoris* (*tuber ischiadicum*) males of the uphill (1) and downhill site (2), left side. There is no distinct association between higher scores and increasing age in neither group.

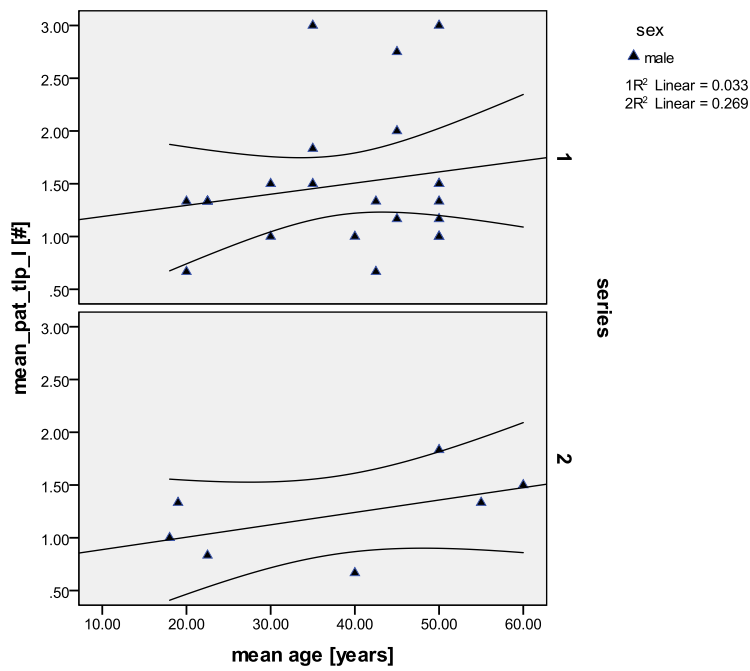


**Figure 65.** Scatterplot of the pooled muscle group *M. quadriceps femoris* (Patella – patellar ligament), males of the uphill (1) and downhill site (2), left side. There are slightly higher entheses scores with increasing age in both groups. In group 1, there are 3 individuals displaying very high scores.

### 6.1.6 Short summary

There was no statistically significant association apparent in the left side entheses of the male sub-sites. There are “outliers” (based on robusticity), according to very high scores in some scatterplots: *M. biceps/subscapularis*, *M. triceps brachii*, common extensors, common flexors, pooled hip and knee muscle markings group.

### 6.1.7 Scatterplots joints – mean age, comparison males uphill-downhill – left side

The scores of the pooled joints of the males of the two groups are plotted against increasing age (Figures 66 - 73), along with the least squares regression line and the 95% confidence regions. Univariate analysis results were added if there was a significant difference between the groups; graphs are added in cases of clear average differences between the sub-sites.

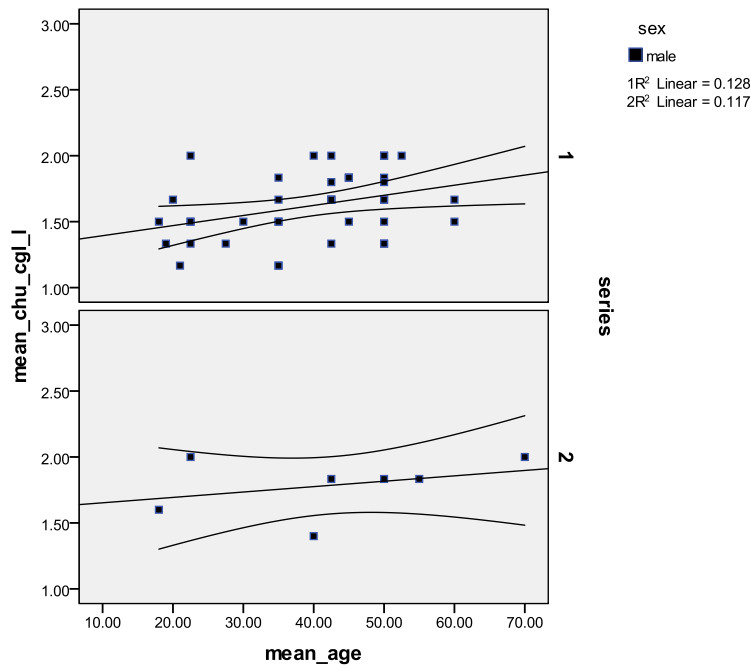


**Figure 66.** Pooled joint group *Caput humeri* – *Cavitas glenoidalis* (shoulder - humerus, scapula), males of the uphill (1) and downhill site (2), left side. There is a slight association between higher scores and higher age, but not statistically significant.

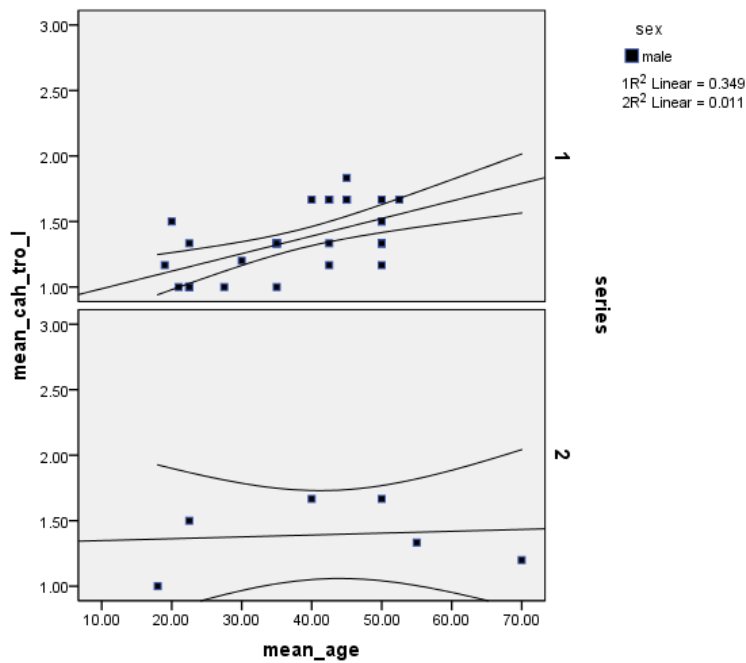


**Figure 67.a.** Pooled joint group *Capitulum humeri – Trochlea* (dist. humerus - elbow), males of the uphill (1) and downhill (2) site, left side. There is a marked increase of joint scores at the distal humerus with higher age in the males of series 1, but not in series 2. This was found to be statistically significant (see below).

**Figure 67.b.** Univariate analysis of the pooled joint group *Capitulum humeri – Trochlea*.

	N
Series 1	33
Series 2	6

dependent variable: mean\_cah\_tro\_l

Quelle	Quadratsumme vom Typ III	df	Mittel der Quadrate	F	Sig.
Korrigiertes Modell	.505 <sup>a</sup>	2	.252	5.007	.012
Konstanter Term	3.042	1	3.042	60.366	.000
mean_age	.500	1	.500	9.924	<b>.003</b>
Series	.001	1	.001	.012	.912
Fehler	1.814	36	.050		
Gesamt	75.436	39			
Korrigierte Gesamtvariation	2.319	38			

a. R-Quadrat = .218 (korrigiertes R-Quadrat = .174)

This pooled muscle markings group in the left distal elbow is significantly affected by age in univariate analysis ( $p=.003$ ) in the males of the two sub-sites.

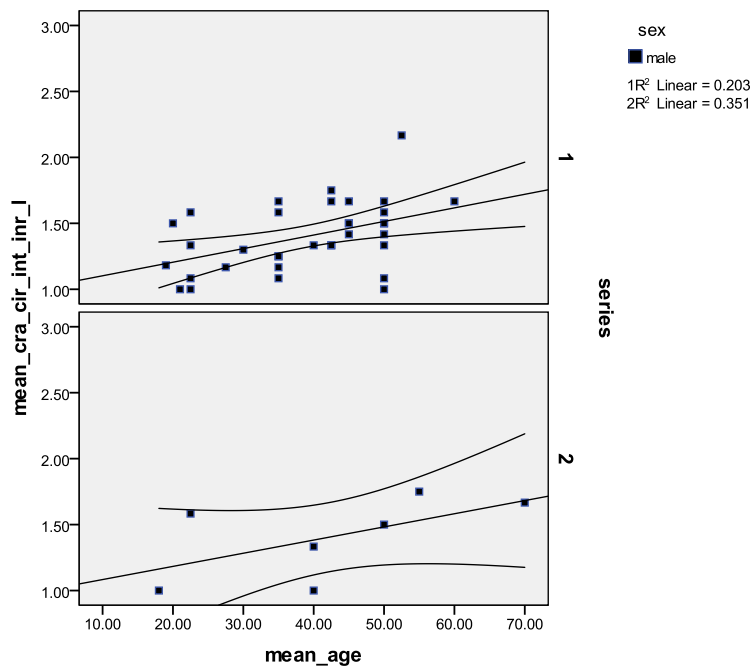


**Figure 68.** Pooled joint group *Caput radii*, *Circumferentia articularis radii*, *Incisura trochlearis*, *Incisura radialis* (proximal radius and ulna - elbow), males of the uphill (1) and downhill site (2), left side. There is an increase of scores with age, but not statistically significant.

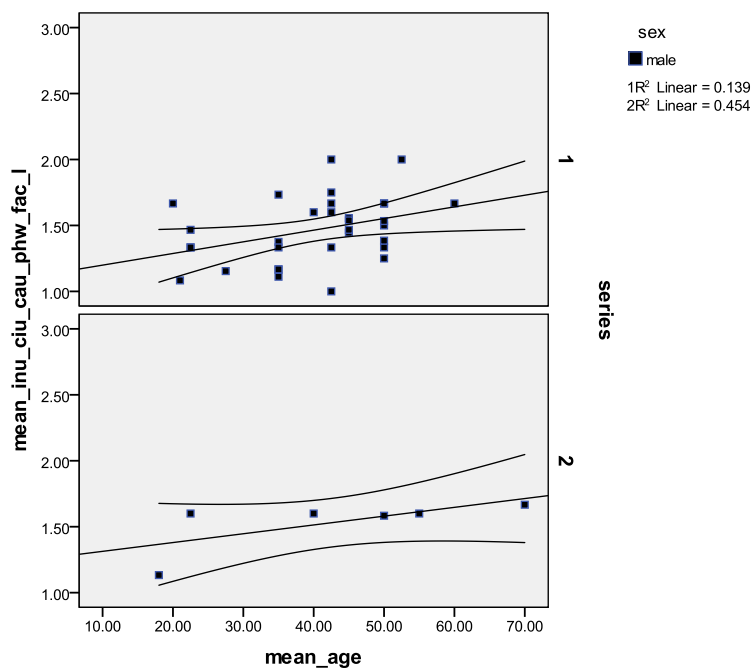


**Figure 69.** Pooled joint group *Incisura ulnaris*, *Circumferentia articularis ulnae*, *Caput ulnae*, proximal row of wrist bones, *Facies articularis carpalis* (distal radius and ulna, - wrist), males of the uphill (1) and downhill site (2), left side. A slight increase of joint changes is apparent in both groups with higher age.

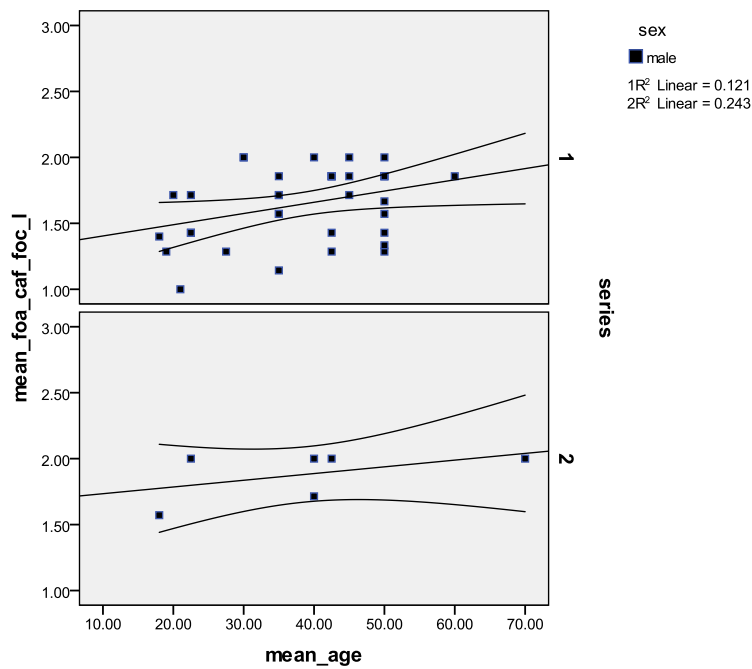


**Figure 70. a.** Scatterplot of the pooled joint group *Fossa acetabuli, Caput femoris, Fovea capitis (Os ilium (acetabulum))*, femoral head - hip joint), males of the uphill (1) and downhill site (2), left side. There is a slight increase of joint changes with higher age in the hip joint of both groups (see Figure 70.b.).

**Figure 70. b.** Scatterplot of the pooled joint group *Fossa acetabuli, Caput femoris, Fovea capitis*.

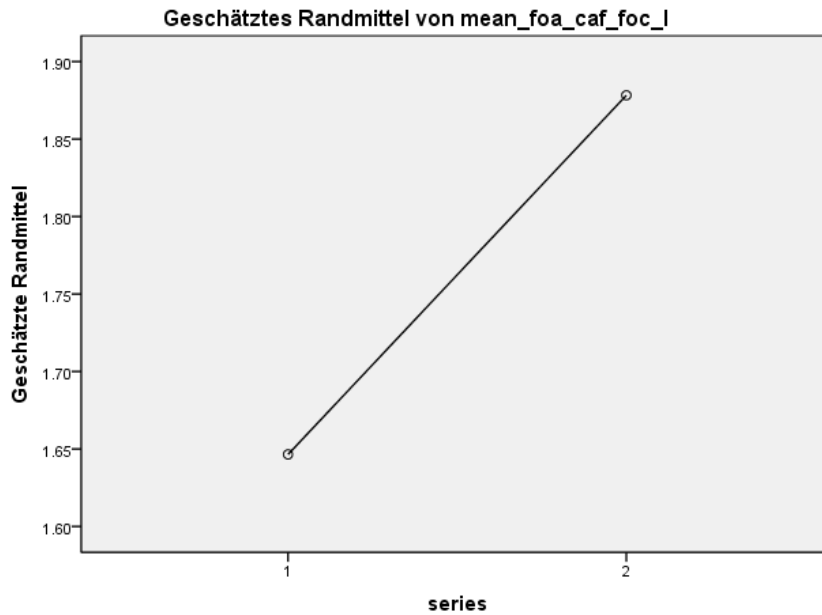
		N
Series	1	36
	2	6

dependent variable: mean\_foa\_caf\_foc\_l

Quelle	Quadratsumme vom Typ III	df	Mittel der Quadrate	F	Sig.
Korrigiertes Modell	.635 <sup>a</sup>	2	.317	4.990	.012
Konstanter Term	7.404	1	7.404	116.455	.000
mean_age	.351	1	.351	5.516	<b>.024</b>
Series	.276	1	.276	4.345	<b>.044</b>
Fehler	2.479	39	.064		
Gesamt	121.597	42			
Korrigierte Gesamtvariation	3.114	41			

a. R-Quadrat = .204 (korrigiertes R-Quadrat = .163)

The pooled features at the hip joint are significantly affected by age ( $p=.024$ ) and by sub-site ( $p=.044$ ) in the males of the hillfort and the downhill site.



Die Kovariaten im Modell werden anhand der folgenden Werte berechnet: mean\_age = 38.4762

The downhill males display higher mean scores in the joint changes at the hip of the left side (as on the right side, compare section 6.1.3).

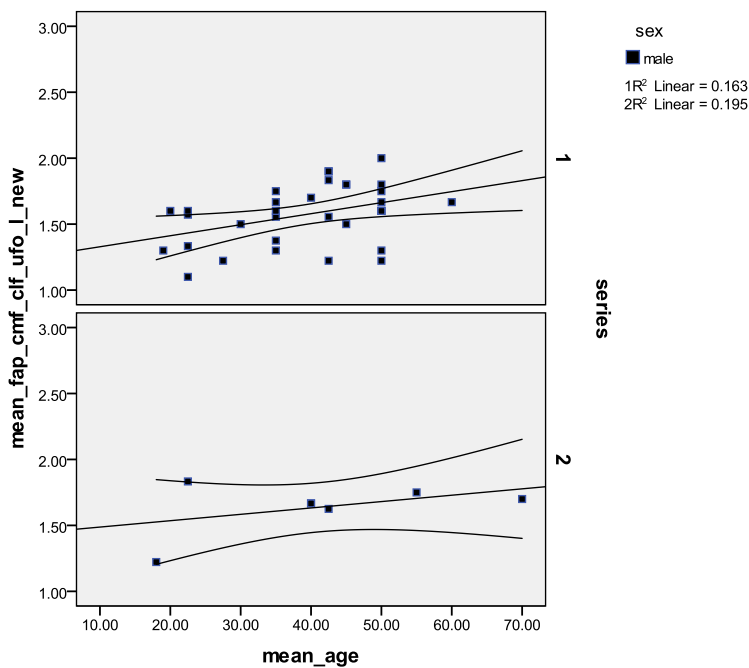


**Figure 71.** Scatterplot of the pooled joint group *Facies patellaris, Condylus medialis femoris, Condylus lateralis femoris, distal margin of Fossa intercondylaris* (distal femur - knee), males of the uphill (1) and downhill site (2), left side. There is a slight increase of joint changes with higher age in both groups.

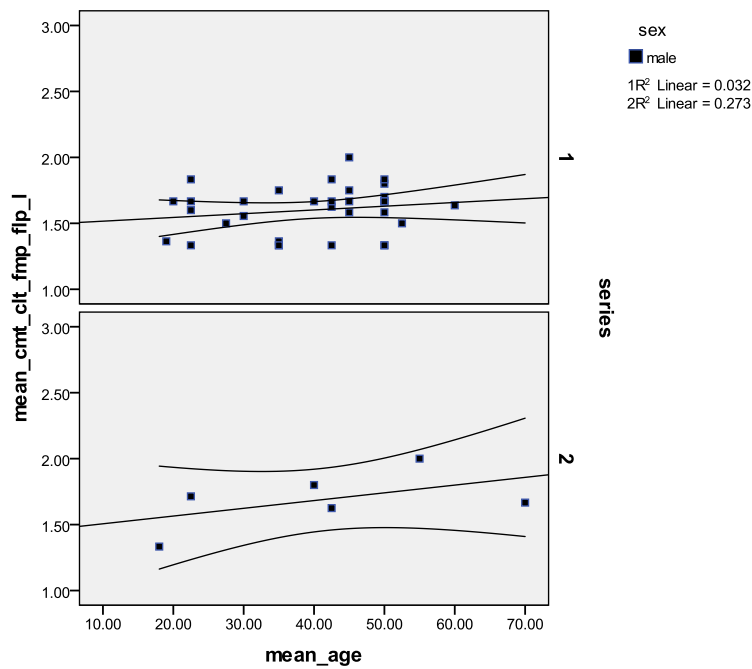


**Figure 72.** Scatterplot of the pooled joint group *Condylus medialis tibiae, Condylus lateralis tibiae, Facies medialis patellae, Facies lateralis patellae* (proximal tibia, patella - knee joint), males of the uphill (1) and downhill site (2), left side. There is a slight increase of joint changes with higher age in the knee joint in both groups.

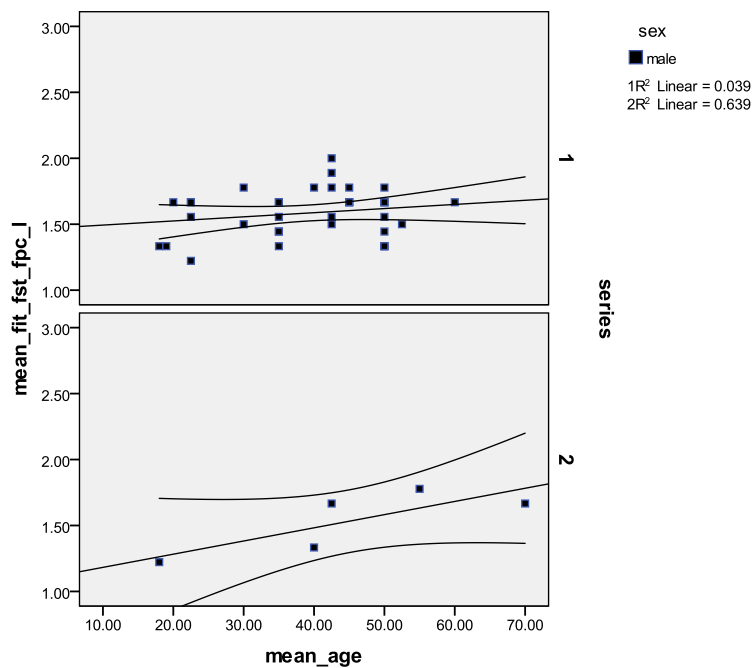


**Figure 73.** Scatterplot of the pooled joint group *Facies articularis inferior tibiae, Facies articularis superior talus, Facies aricularis talaris posterior calcanei* (distal tibia - ankle), males of the uphill (1) and downhill site (2), left side. There is a slight increase of joint changes with higher age in both groups.

### 6.1.8 Short summary

Significant results are apparent on the left side in the males at the *Capitulum humeri/Trochlea* with age, with age and between the series at the *Fossa acetabuli/Caput femoris*. A non-significant age trend was observed in the left *Capitulum humeri/Cavitas glenoidalis*, *Caput radii/Circumferentia articularis ulna/Incisura trochlearis*, *Incisura ulnaris/Circumferentia articularis ulnae*, *Caput ulnae*, *proximal row of wrist bones*, *Facies articularis carpalis*, *Facies patellaris*, *Condylus medialis femoris*, *Condylus lateralis femoris*, distal margin of *Fossa intercondylaris*, *Facies patellaris*, *Condylus medialis femoris*, *Condylus lateralis femoris*, distal margin of *Fossa intercondylaris*.

## 6.2 Scatterplots entheses – body height –males

### 6.2.1 Scatterplots entheses – body height, comparison males

#### uphill-downhill – right side

Differences between the male groups of the two archaeological sub-sites of Thunau (series 1 = uphill site, series 2 = downhill site), according to mean scores of entheses and body height, are shown in scatterplots (Figures 74–81, right side, and section 6.2.3. Figures 82–89, left side). The scores of the muscle markings of the males of the two groups are plotted against increasing body height, along with the least squares regression line and the 95% confidence regions. Univariate analyses were added if the difference between the groups was significant; in cases of clear average differences between the sub-sites, graphs are added accessorially.

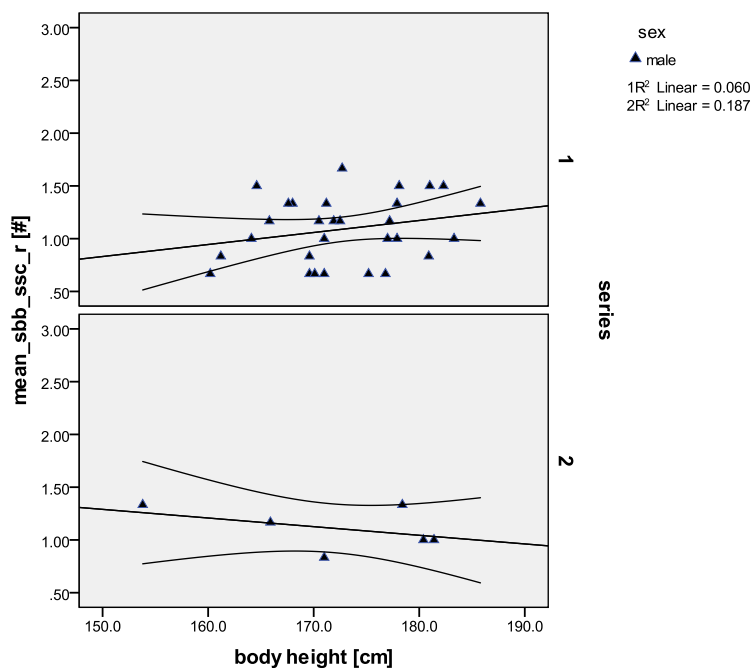


**Figure 74.** Scatterplot of the pooled muscle group *M. biceps brachii* – *M. subscapularis* (scapula, proximal humerus), males of the uphill (1) and downhill site (2), right side. There is no clear association between increasing scores and body size in this feature.

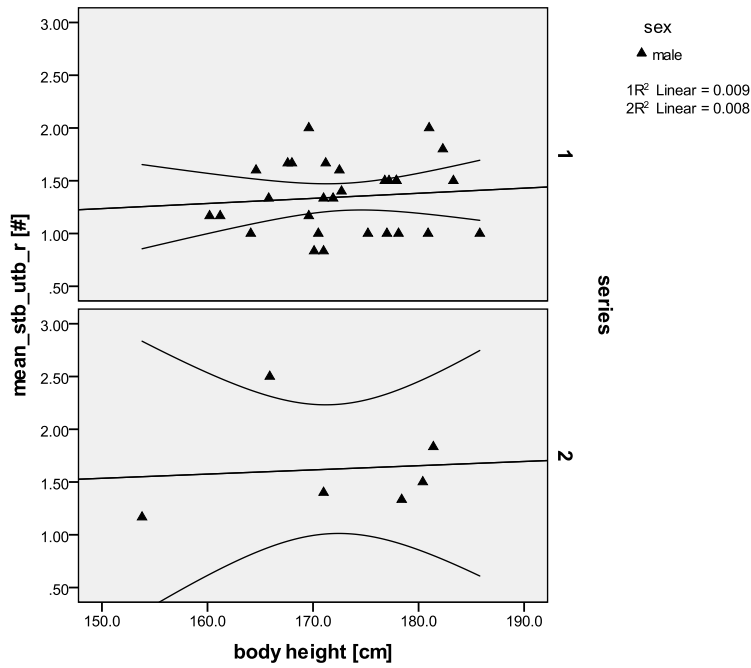


**Figure 75.** Scatterplot of the pooled muscle group *M. triceps brachii* (scapula – proximal ulna), males of the uphill (1) and downhill site (2), right side. There is no clear association between increasing scores and body size in this feature.

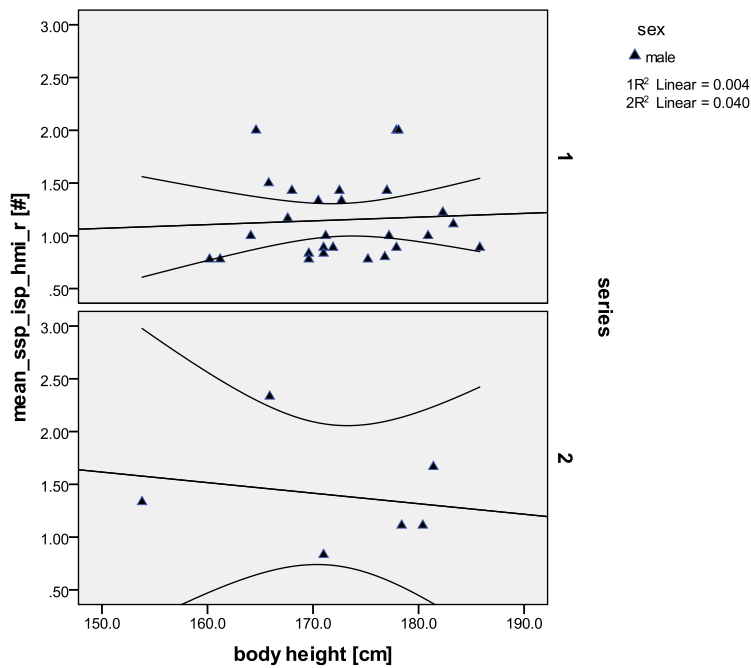


**Figure 76.** Scatterplot of the pooled muscle group *M. supraspinatus - M. teres minor* (proximal humerus), males of the uphill (1) and downhill site (2), right side. No association is apparent between scores and body height in this feature.

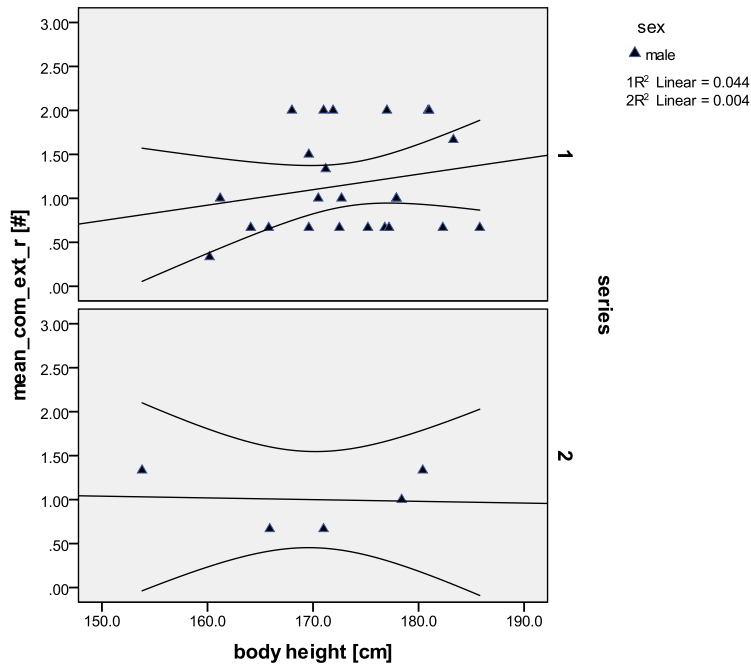


**Figure 77.** Scatterplot of the pooled **common extensors** muscle group (distal lateral humerus), males of the uphill (1) and downhill site (2), right side. In this feature, there is no clear association between scores and body height.

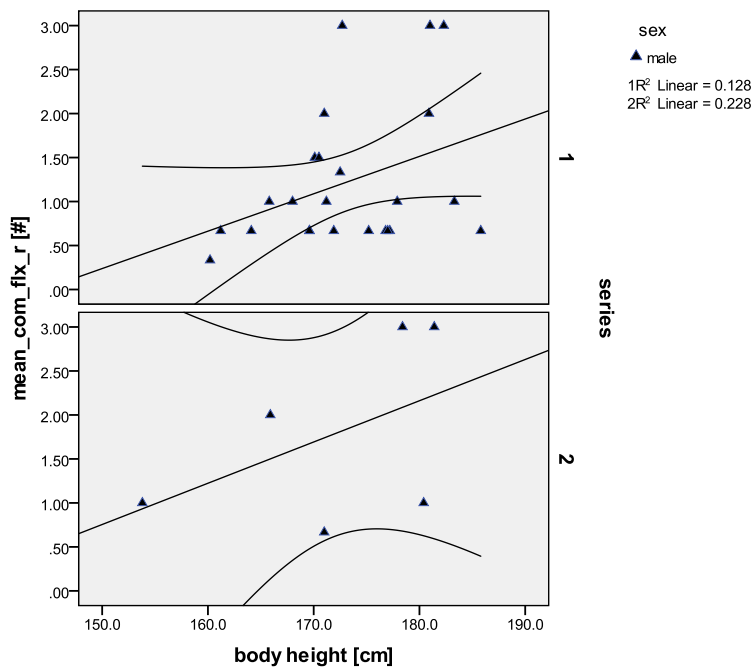


**Figure 78.a.** Scatterplot of the pooled **common flexors** muscle group (distal medial humerus), males of the uphill (1) and downhill site (2), right side. This feature is significantly affected by body height in both groups (see Figure 78b).

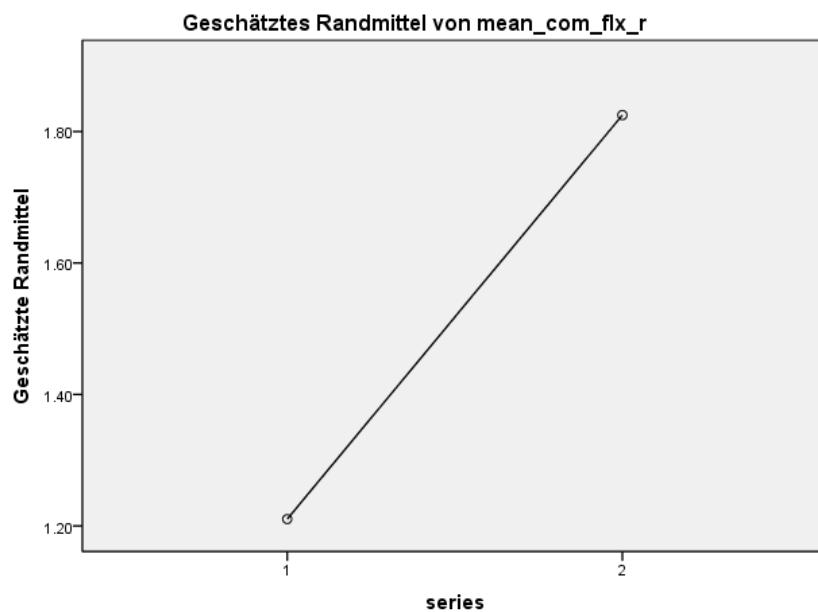
**Figure 78. b.** Univariate analysis in the common flexors muscle attachment group for the males on the right side.

		N
Series	1	24
	2	6

dependent variable: mean\_com\_flx\_r

Quelle	Quadratsumme vom Typ III	df	Mittel der Quadrate	F	Sig.
Korrigiertes Modell	4.649 <sup>a</sup>	2	2.325	3.629	.040
Konstanter Term	2.034	1	2.034	3.176	.086
body height	3.168	1	3.168	4.945	<b>.035</b>
Series	1.804	1	1.804	2.816	.105
Fehler	17.295	27	.641		
Gesamt	75.278	30			
Korrigierte Gesamtvariation	21.944	29			

a. R-Quadrat = .212 (korrigiertes R-Quadrat = .153)



Die Kovariaten im Modell werden anhand der folgenden Werte berechnet: body height = 172.890

The downhill males show higher mean body height with higher entheses scores in the right common flexors.

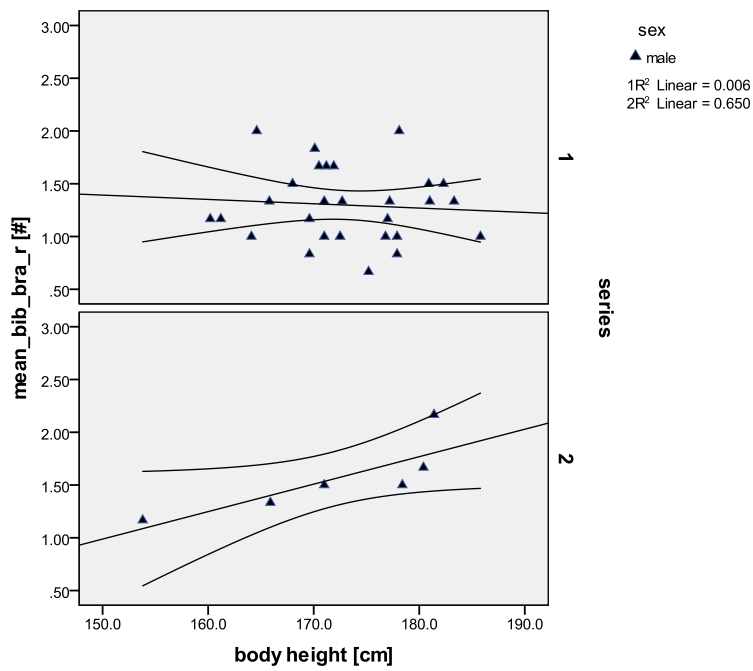


**Figure 79.** Scatterplot of the pooled muscle group *M. biceps brachii* – *M. brachialis* (prox. radius - ulna), males of the uphill (1) and downhill site (2), right side. There is a marked increase of scores with body height in the downhill males, but not in the hillfort males.

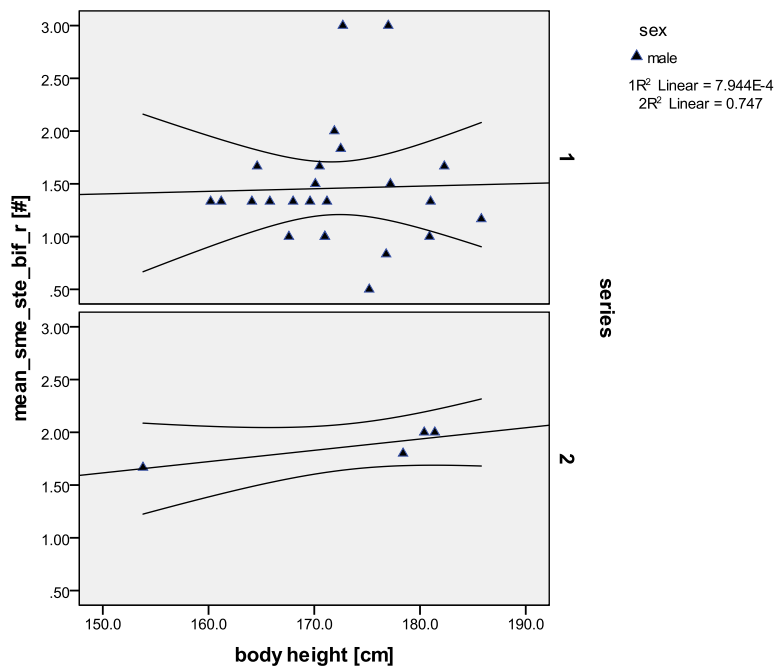


**Figure 80.** Scatterplot of the pooled muscle group *M. semimembranosus* – *M. semitendinosus* – *M. biceps femoris* (tuber ischiadicum), males of the uphill (1) and downhill site (2), right side. There is no clear association between scores and body height in the pooled hip muscle markings group.

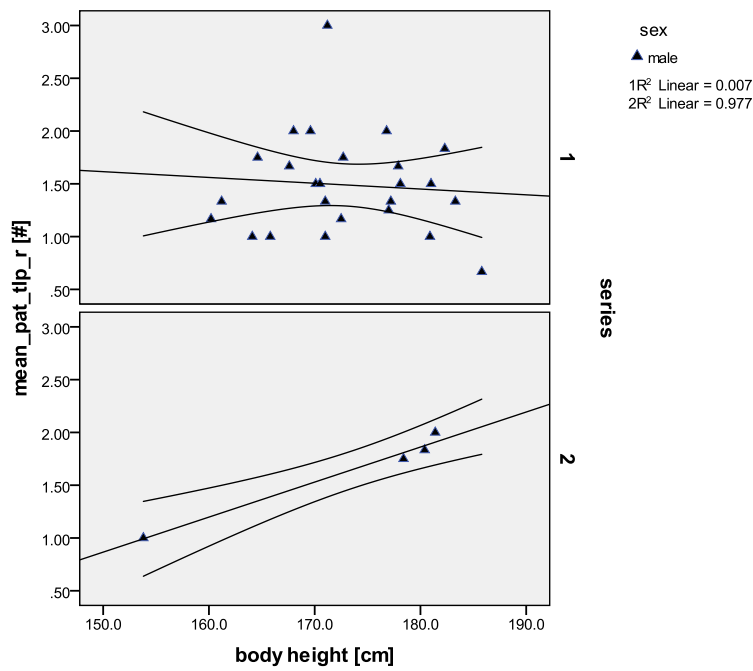


**Figure 81.** Scatterplot of the pooled muscle group *M. quadriceps femoris* (Patella – patellar ligament), males of the uphill (1) and downhill site (2), right side. In the downhill males, there seems to be an association between increasing scores and body height, but the sample size is comparably small.

### 6.2.2 Short summary

A significant result for muscle marking scores and body height was found in the right common flexors of the males.

### 6.2.3 Scatterplots entheses – body height, comparison males uphill-downhill – left side

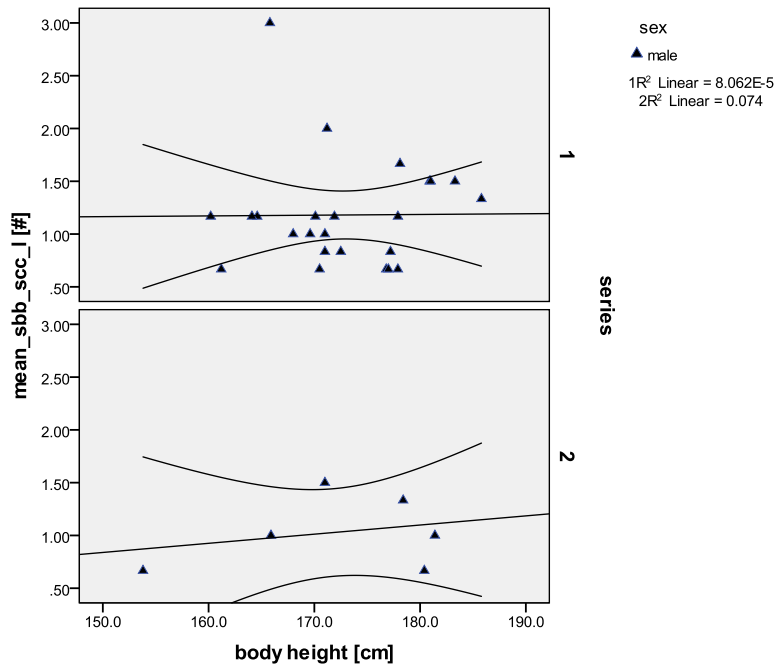


**Figure 82.** Scatterplot of the pooled muscle group *M. biceps brachii* – *M. subscapularis* (scapula, proximal humerus), males of the uphill (1) and downhill site (2), left side. There is no clear association between scores and body height in the shoulder muscle markings.

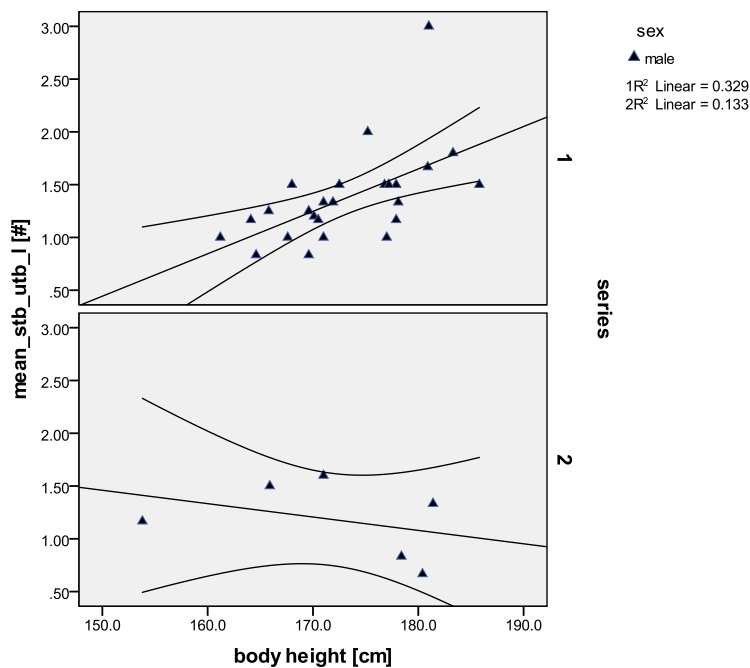


**Figure 83.** Scatterplot of the pooled muscle group *M. triceps brachii* (scapula – proximal ulna), males of the uphill (1) and downhill site (2), left side. A marked increase of scores in the triceps in taller individuals is apparent in the males of sub-site 1, but not in the valley site males.

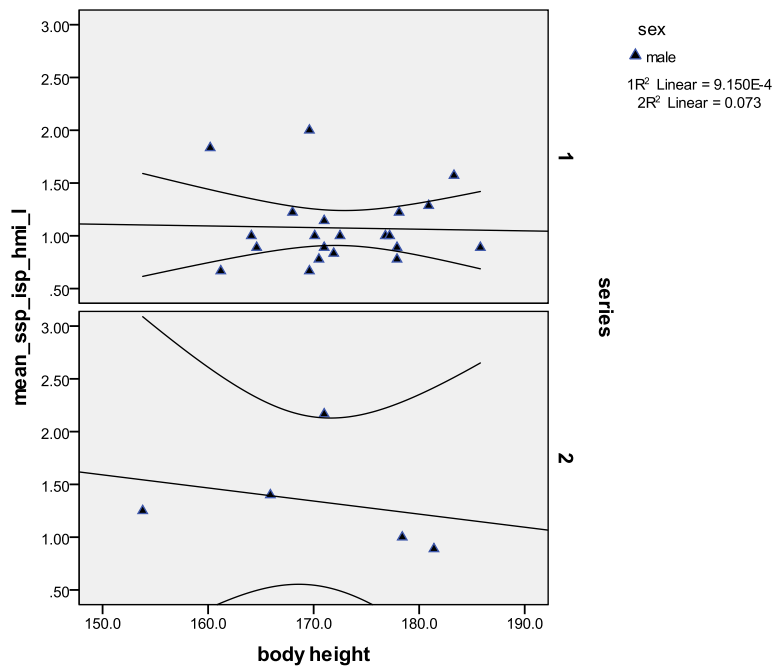


**Figure 84.** Scatterplot of the pooled muscle group *M. supraspinatus - M. infraspinatus - M. teres minor* (prox. humerus), males of the uphill (1) and downhill site (2), left side. There is no clear association between higher scores and body height for the muscle markings at the rotator cuff.

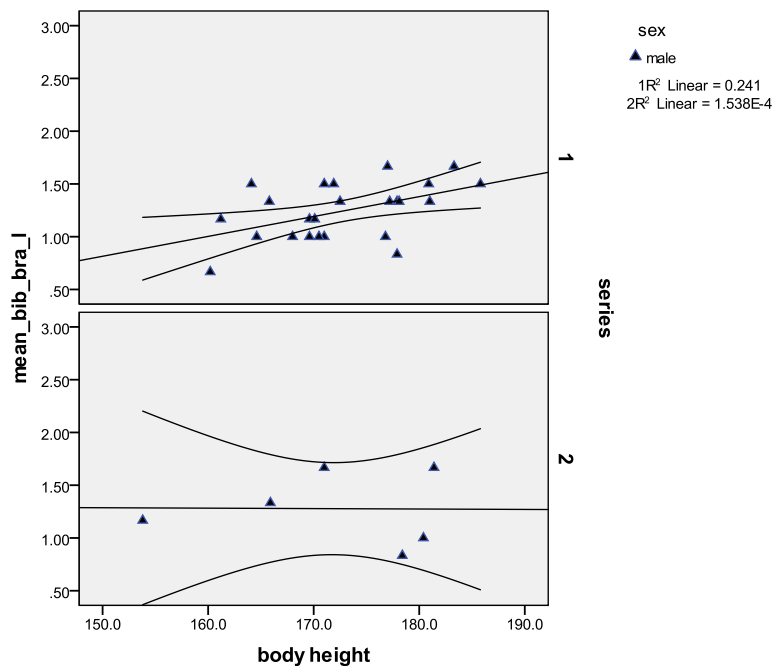


**Figure 85.** Scatterplot of the pooled muscle group *M. biceps brachii - M. brachialis* (prox. radius and proximal ulna - elbow), males of the uphill (1) and downhill site (2), left side. There is a slight increase in the scores in taller individuals in the males of sub-site 1, but not in series 2.

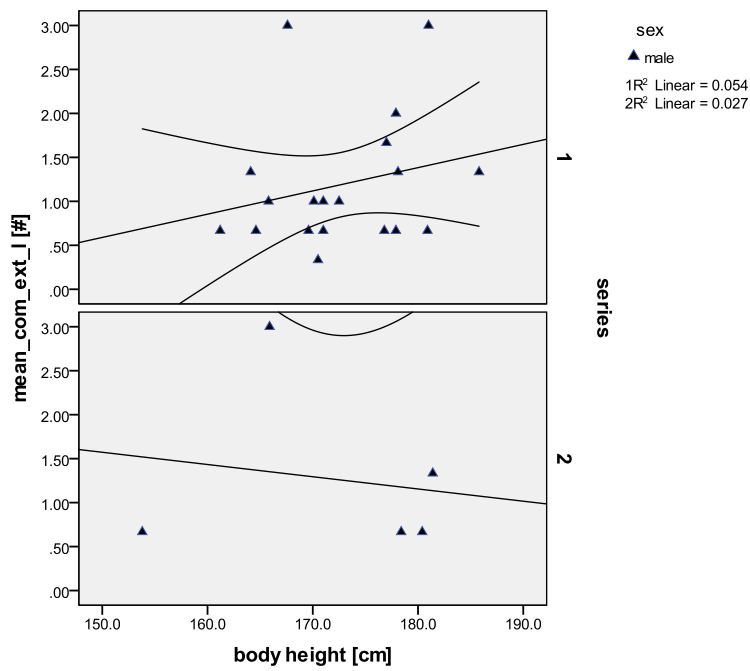


**Figure 86.** Scatterplot of the pooled **common extensors** muscle group (distal lateral humerus), males of the uphill (1) and downhill site (2), left side. A slight increase of the scores in taller individuals is apparent in the males of sub-site 1. Two individuals in the uphill group and one in the downhill group show highest scores.

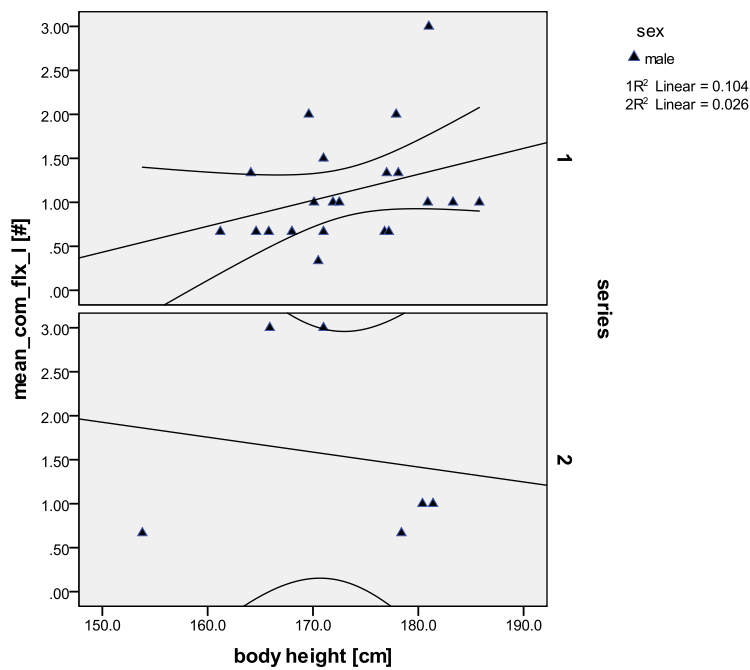


**Figure 87.** Scatterplot of the pooled **common flexors** muscle group (distal medial humerus) males of the uphill (1) and downhill (2) site, left side. A marked increase of scores in taller individuals is apparent in the males of sub-site 1. One individual in the uphill group and two in the downhill group show highest scores.

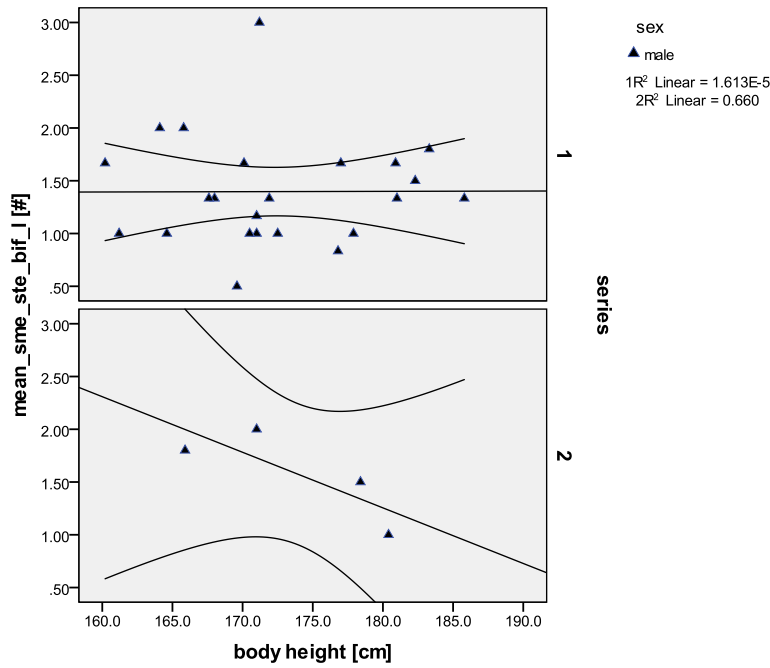


**Figure 88.** Scatterplot of the pooled muscle group *M. semimembranosus* – *M. semitendinosus* – *M. biceps femoris* (tuber ischiadicum), males of the uphill (1) and downhill site (2), left side. There is no clear association between higher scores and body height in neither group.

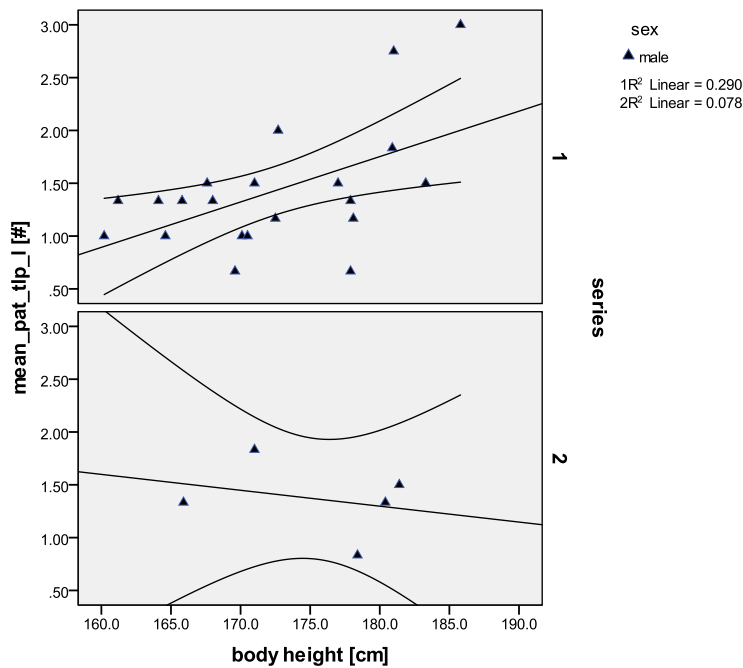


**Figure 89.a.** Scatterplot of *M. quadriceps femoris* (Patella – patellar ligament), males of the uphill (1) and downhill site (2), left side. There is a significant difference in the increase of scores between series 1 and 2 (see Figure 89b).

**Figure 89. b.** Univariate analysis of the right Patella/patellar ligament attachment site in the males.

		N
Series	1	21
	2	5

dependent variable: mean\_pat\_tlp\_1

Quelle	Quadratsumme vom Typ III	df	Mittel der Quadrate	F	Sig.
Korrigiertes Modell	1.508 <sup>a</sup>	2	.754	2.973	.071
Konstanter Term	.879	1	.879	3.468	.075
body height	1.494	1	1.494	5.893	<b>.023</b>
Series	.105	1	.105	.413	.527
Fehler	5.832	23	.254		
Gesamt	59.285	26			
Korrigierte Gesamtvariation	7.340	25			

a. R-Quadrat = .205 (korrigiertes R-Quadrat = .136)

A significant association between higher body size and increasing entheses scores is apparent in the left Patella/patellar ligament attachment site in the males.

#### 6.2.4 Short summary

A significant result for entheses scores with higher body size was found in the Thunau males for the *M. quadriceps femoris* of the left side.

For comments on this section see chapter 10.2.5.

## 7 RESULTS IV – AGE-DEPENDENCY OF THE FEATURES

### 7.1 Males and females, uphill series: scores and age, right side

One-way ANOVA revealed a linear association with age in about half of the features in joints and entheses, mainly in the uphill series. To get a group-relevant result, males and females were tested together here exceptionally. A least significance difference test (LSD) and a post-hoc test (Bonferroni) displayed several inter-age group associations. The significant results frequently include the shoulder and the elbow features, and nearly always the hip (Table 22).

**Table 22.** Statistically significant results of the one-way ANOVA between the age groups in the uphill series, right side.

uphill, males & females entheses, right side	one-way ANOVA			
	F	<i>p</i> -value	LSD	Bonferroni
SBB_SCC	5.875	<b>.005</b>	1/2; 1/3	1/2; 1/3
SSP_ISP_HMI	4.763	<b>.013</b>	1/2; 1/3	1/3
STB_UTB	1.104	.339		
BIB_BRA	3.834	<b>.028</b>	1/2; 1/3	1/2
COM_EXT	2.573	.089	1/2	
COM_FLEX	4.375	<b>.019</b>	1/2	1/2
SME_STE_BIF	3.580	<b>.036</b>	1/2	1/2
PAT_TLP	.921	.405		
joints, right side	F	<i>p</i> -value	LSD	Bonferroni
CHU_CGL	3.024	.056	1/2; 1/3	
CAH_TRO	3.286	<b>.045</b>	1/2; 1/3	(1/3)
CRA_CIR_INT_INR	3.065	.054	1/2; 1/3	(1/2)
INU_CIU_CAU_PHW_FAC	1.963	.150	(1/3)	
FOA_CAF_FOC	8.954	<b>.000</b>	1/2; 1/3	1/2; 1/3
FAP_CMF_CLF_UFO	1.715	.188		
CMT_CLT_FMP_FLP	0.855	.430		
FIT_FST_FPC	2.209	.118	1/3	

LEGEND: series 1 (uphill) males and females, age groups: 1 (young) = 18-29 years, 2 (middle) = 30-49 years, 3 (old) = 50-70 years,  $p=0.05$ ; 1/2 = significance between age group 1 and 2; 1/3 = significance between age group 1 and 3; numbers in brackets: marginal significance

Many significant results according to age can be seen in the uphill group on the right side. Especially enthesal shoulder features, elbow and hip show significant differences between (all) the age groups. A similar picture is observable in the joints, especially in the hip joint. Marginal osteophyte growth is known to be linked with age (compare discussion), and a later test excluding it displayed a noteworthy dependency of several features with age, but the results did not differ so much (compare chapter 7.5).

## 7.2 Males and females, uphill series: scores and age, left side

On the left side in the uphill series, interestingly the common flexors show statistically significant results with age, especially between age groups 1 and 3 (in LSD and Bonferroni test), and also in the hip enthesal changes. Concerning the joints, significant results are visible in the shoulder and a highly significant result was obtained in the distal humeral joint facets. Further, the hip joint and the distal femoral joint are affected here (Table 23).

**Table 23.** Significant results of the one-way ANOVA between the age groups in the uphill series, left side.

uphill, males & females entheses, left side	one-way ANOVA			
	F	<i>p</i> -value	LSD	Bonferroni
SBB_SCC	.241	.787		
SSP_ISP_HMI	3271	<b>.050</b>	1/3	
STB_UTB	2.861	.068	2/3	
BIB_BRA	2.145	.130	1/2	
COM_EXT	4.253	<b>.023</b>	1/2; 2/3	1/3
COM_FLEX	.631	.538		
SME_STE_BIF	3.534	<b>.038</b>	1/2; 2/3	
PAT_TLP	.486	.618		
joints, left side	F	<i>p</i> -value	LSD	Bonferroni
CHU_CGL	4.153	<b>.020</b>	1/2; 1/3	1/3
CAH_TRO	7.854	<b>.001</b>	1/2; 1/3	1/2; 1/3
CRA_CIR_INT_INR	3.170	<b>.049</b>	1/3	1/3
INU_CIU_CAU_PHW_FAC	1.490	.234		
FOA_CAF_FOC	5.009	<b>.010</b>	1/2; 1/3	1/2; 1/3
FAP_CMF_CLF_UFO	4.769	<b>.012</b>	1/2; 1/3	1/2; 1/3
CMT_CLT_FMP_FLP	1.481	.236		
FIT_FST_FPC	3.058	.054	1/2	1/2

LEGEND: series 1 (uphill) males and females, age groups: 1 = 18-29 years, 2 = 30-49 years, 3 = 50-70 years, *p*=0.05; 1/2 = significance between age group 1 and 2; 1/3 = significance between age group 1 and 3; numbers in brackets: marginal significance

### 7.3 Males and females, downhill series: scores and age, right side

A possible association with age was also calculated for the downhill series. One-way ANOVA revealed statistically significant results in the common extensors at the entheses, and in the shoulder joints (Table 24).

**Table 24.** Significant results of the one-way ANOVA between the age groups in the downhill series, right side.

downhill, males & females entheses, right side	one-way ANOVA			
	F	<i>p</i> -value	LSD	Bonferroni
SBB_SCC	.122	.886		
SSP_ISP_HMI	.007	.993		
STB_UTB	.381	.691		
BIB_BRA	1.370	.291		
COM_EXT	4.564	.054	1/2; 2/3	
COM_FLEX	1.187	.345		
SME_STE_BIF	2.403	.141		
PAT_TLP	0.378	.697		
joints, right side	F	<i>p</i> -value	LSD	Bonferroni
CHU_CGL	6.336	<b>.015</b>	1/2; 2/3	(1/3); 2/3
CAH_TRO	1.019	.393		
CRA_CIR_INT_INR	0.152	.861		
INU_CIU_CAU_PHW_FAC	1.397	.288		
FOA_CAF_FOC	1.494	.260		
FAP_CMF_CLF_UFO	0.855	.244		
CMT_CLT_FMP_FLP	0.454	.454		
FIT_FST_FPC	0.350	.350		

LEGEND: series 1 (uphill) males and females, age groups: 1 (young) = 18-29 years, 2 (middle) = 30-49 years, 3 (old) = 50-70 years,  $p=0.05$ ; 1/2 = significance between age group 1 and 2; 1/3 = significance between age group 1 and 3; numbers in brackets: marginal significance

## 7.4 Males and females, downhill series: scores and age, left side

On the left side of the downhill series, the only statistically significant result became apparent in the rotator cuff entheses, especially visible with a high significance in the LSD test between the age group 1 and 3, and in Bonferroni test between age groups 2 and 3. No statistically significant results were found for the joint changes on the left side (Table 25).

**Table 25.** Significant results of the one-way ANOVA between the age groups in the downhill series, left side.

downhill, males & females entheses, left side	one-way ANOVA			
	F	<i>p</i> -value	LSD	Bonferroni
SBB_SCC	2.345	.138		
SSP_ISP_HMI	7.199	<b>.014</b>	1/2; 2/3	2/3
STB_UTB	.092	.913		
BIB_BRA	1.704	.227		
COM_EXT	2.184	.183		
COM_FLEX	.929	.424		
SME_STE_BIF	3.590	.085	1/2	
PAT_TLP	.275	.765		
joints, left side	F	<i>p</i> -value	LSD	Bonferroni
CHU_CGL	1.109	.361		
CAH_TRO	.289	.755		
CRA_CIR_INT_INR	.940	.420		
INU_CIU_CAU_PHW_FAC	1.329	.308		
FOA_CAF_FOC	1.483	.269		
FAP_CMF_CLF_UFO	.705	.515		
CMT_CLT_FMP_FLP	1.578	.250		
FIT_FST_FPC	.661	.542		

LEGEND: series 1 (uphill) males and females, age groups: 1 (young) = 18-29 years, 2 (middle) = 30-49 years, 3 (old) = 50-70 years,  $p=0.05$ ; 1/2 = significance between age group 1 and 2; 1/3 = significance between age group 1 and 3; numbers in brackets: marginal significance

## 7.5 Exemplary test of scores and age without osteophyte growth

### 7.5.1 Males and females, uphill series: scores and age, right side without osteophyte growth

Because osteophyte growth is supposed to be linked with age (compare introduction and discussion), an exemplary test excluding osteophyte growth was performed here for entheses and joint features on the right extremity for both sub-sites. The (highly) significant results of the one-way ANOVA in the hip entheses and joint features remain, and in the enthesesal shoulder changes, but especially in the joints, are less significant without including marginal osteophyte growth (Table 26).

**Table 26.** Significant results of the one-way ANOVA between the age groups excluding osteophyte growth in the uphill series, right side.

uphill, males and females, entheses, right side	one-way ANOVA			
	F	<i>p</i> -value	LSD	Bonferroni
SBB_SCC	3787	<b>.030</b>	1/2;1/3	1/3
SSP_ISP_HMI	4.783	<b>.013</b>	1/3	1/3
STB_UTB	2.626	.082	1/2	
BIB_BRA	2.265	.115	1/2	
COM_EXT	2.603	.087	1/2	
COM_FLEX	2.959	.063	1/2	(1/2)
SME_STE_BIF	6.413	<b>.004</b>	1/2	1/2
PAT_TLP	.994	.378		
joints, right side	F	<i>p</i> -value	LSD	Bonferroni
CHU_CGL	.815	.447		
CAH_TRO	1.428	.248		
CRA_CIR_INT_INR	.736	.483		
INU_CIU_CAU_PHW_FAC	.863	.429		
FOA_CAF_FOC	3.337	<b>.042</b>	1/2;1/3	1/3
FAP_CMF_CLF_UFO	2.079	.134	1/2	
CMT_CLT_FMP_FLP	1.530	.225		
FIT_FST_FPC	.172	.842		

LEGEND: series 1 (uphill) males and females, age groups: 1 = 18-29 years, 2 = 30-49 years, 3 = 50-70 years,  $p=0.05$ ; 1/2 = significance between age group 1 and 2; 1/3 = significance between age group 1 and 3; numbers in brackets: marginal significance

## 7.5.2 Males and females, downhill series: scores and age, left side without osteophyte growth

A statistical significance between the age groups 1 and 3 became apparent in the distal femoral joint features, as well as a marginal significance observed for the age groups 2 and 3 in the ankle joint changes when excluding osteophyte growth from one-way ANOVA (Table 27).

**Table 27.** Significant results of the one-way ANOVA between the age groups excluding osteophyte growth in the downhill series, left side.

downhill, males & females entheses, right side	one-way ANOVA			
	F	<i>p</i> -value	LSD	Bonferroni
SBB_SCC	.173	.843		
SSP_ISP_HMI	.216	.809		
STB_UTB	.328	.727		
BIB_BRA	1.329	.301		
COM_EXT	2.538	.148		
COM_FLEX	.665	.536		
SME_STE_BIF	2.333	.147		
PAT_TLP	.133	.878		
joints, right side	F	<i>p</i> -value	LSD	Bonferroni
CHU_CGL	2.412	.135		
CAH_TRO	.911	.430		
CRA_CIR_INT_INR	.910	.431		
INU_CIU_CAU_PHW_FAC	.560	.590		
FOA_CAF_FOC	1.052	.377		
FAP_CMF_CLF_UFO	3.128	.088	1/3	
CMT_CLT_FMP_FLP	1.595	.250		
FIT_FST_FPC	2.297	.156	(2/3)	

LEGEND: series 1 (uphill) males and females, age groups: 1 (young) = 18-29 years, 2 (middle) = 30-49 years, 3 (old) = 50-70 years,  $p=0.05$ ; 1/2 = significance between age group 1 and 2; 1/3 = significance between age group 1 and 3; numbers in brackets: marginal significance

## 8 THUNAU FEMALES – RESULTS I – VISUAL ANALYSES: FREQUENCIES

### 8.1 Females – entheses – frequencies, right side

#### 8.1.1 True prevalence rate of enthesal changes in the females, right side, upper and lower extremities

Table 28 and Figure 95 show the differences in the true prevalence rates (compare chapter 5.3., statistical analysis) of enthesal changes of the uphill and downhill females on the right extremities in comparison. The rates are generally similarly low in both groups, the only exception is the pooled entheses group at the tuber ischiadicum (*M. semimembranosus/M. semitendinosus/M. biceps femoris*) in the downhill females, reaching a true prevalence rate of 0.9 (corresponding to nearly 100% of slight enthesal changes).

**Table 28.** Number of individuals and true prevalence rate (TPR) of the enthesal changes of the right side (RS) in the uphill (UPM) and downhill males (DOM) of Thunau/Kamp, for upper and lower extremities.

uphill/downhill females, right side, entheses	UPF_RS		DOF_RS	
	n/N	TPR	n/N	TPR
SBB_SCC (shoulder)	7/20	<b>0.4</b>	2/7	<b>0.3</b>
SSP_ISP_HMI (shoulder)	7/18	<b>0.4</b>	2/7	<b>0.3</b>
STB_UTB (M. triceps br.)	9/22	<b>0.4</b>	2/7	<b>0.3</b>
COM_EXT	3/16	<b>0.2</b>	0/3	<b>0.3*</b>
COM_FLEX	6/20	<b>0.3</b>	0/5	<b>0.2*</b>
BIB_BRA (elbow-ra/ul)	8/22	<b>0.4</b>	2/7	<b>0.3</b>
SME_STE_BIF (hip)	7/21	<b>0.3</b>	6/7	<b>0.9</b>
PAT_TLP (knee)	6/22	<b>0.3</b>	1/6	<b>0.2</b>

\*consists only of 3 individuals

Legend: **sbb\_scc**: *M. biceps brachii/M. subscapularis*; **ssp\_isp\_hmi**: *M. supraspinatus, M. infraspinatus, M. teres minor*; **stb\_utb**: *M. triceps brachii*; **com\_ext**: common extensors; **com flex**: common flexors; **bib\_bra**: *M. biceps brachii/M. brachialis*; **sme\_ste\_bif**: *M. semimembranosus/M. semitendinosus/M. biceps femoris*; **pat\_tlp**: Patella/patellar ligament: *M. quadriceps femoris*;

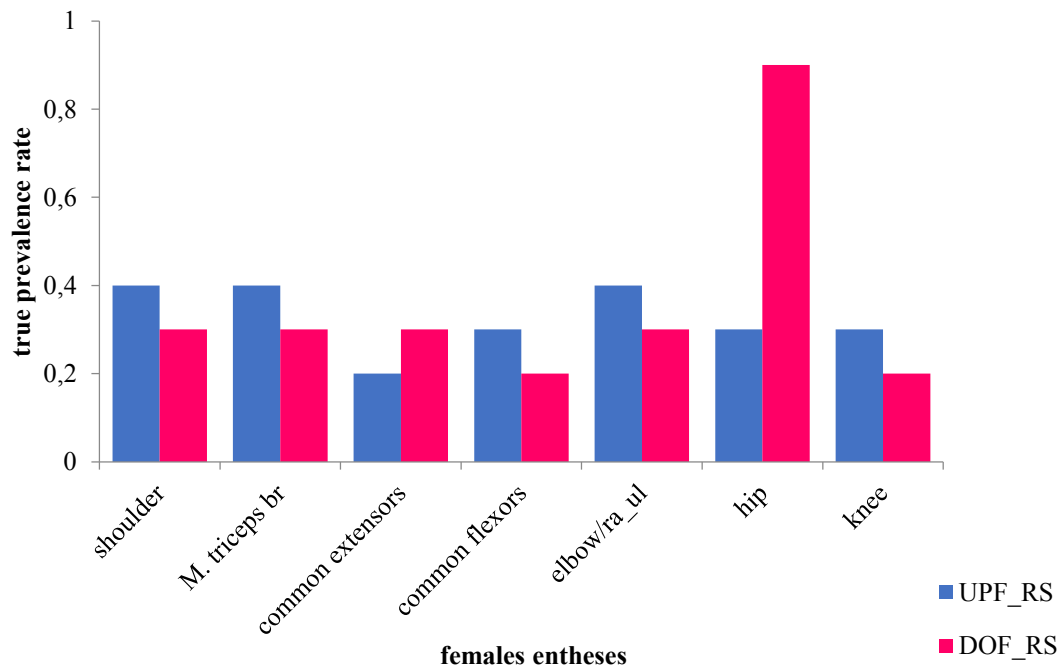


**Figure 90.** True prevalence rate of the enthesal changes of the right side (RS) in the uphill (UPF) and downhill females (DOF) of Thunau/Kamp, for upper and lower extremities.

### 8.1.2 Mean frequencies of single muscle groups, females right side

The mean frequencies of enthesal changes in percent of the single muscle groups, right side, comparison of uphill and downhill females, upper and lower extremities, are shown in Table 29 a and b, and Figure 96. The downhill females show a conspicuously high frequency (which was found to be significant in t-test, see Table 29b) in the pooled *M. semimembranosus/ semitendinosus/biceps femoris*, which is not seen in the hillfort females. The remaining frequencies at the other entheses are comparably low, in the most cases fewer than 50% of the females are affected by enthesal changes.

**Table 29. a.** Mean frequencies in percent of the single muscle groups, right side, comparison of uphill and downhill males, upper and lower extremities.

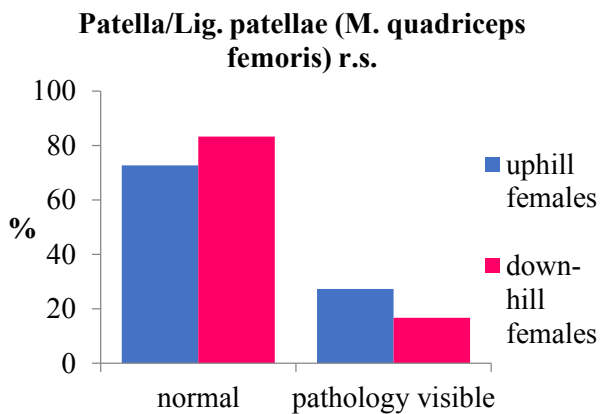
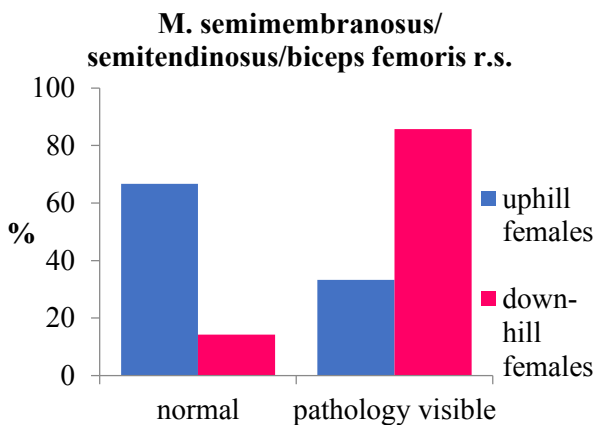
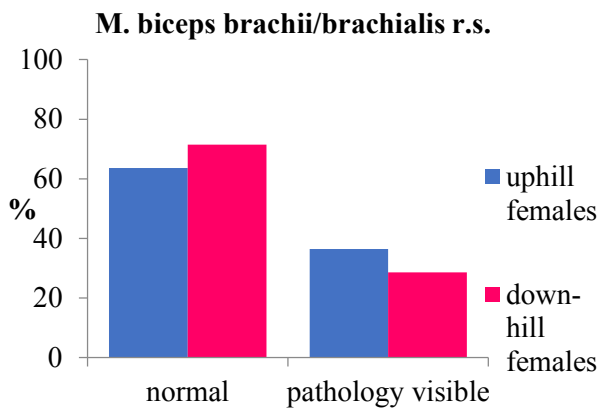
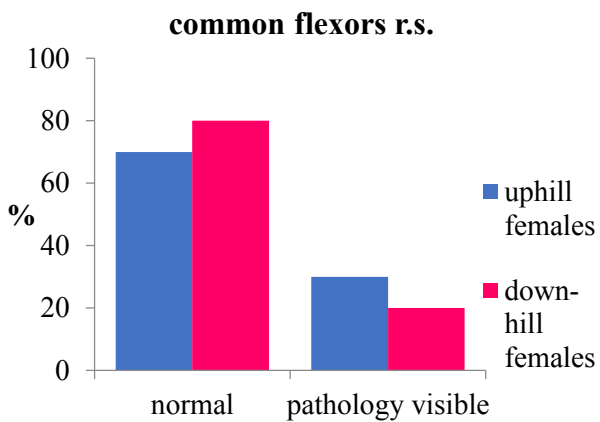
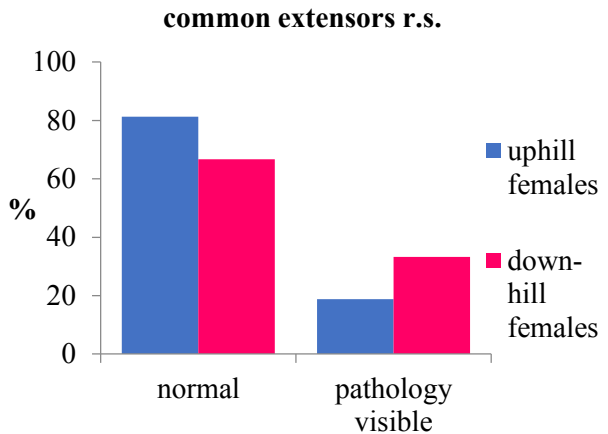
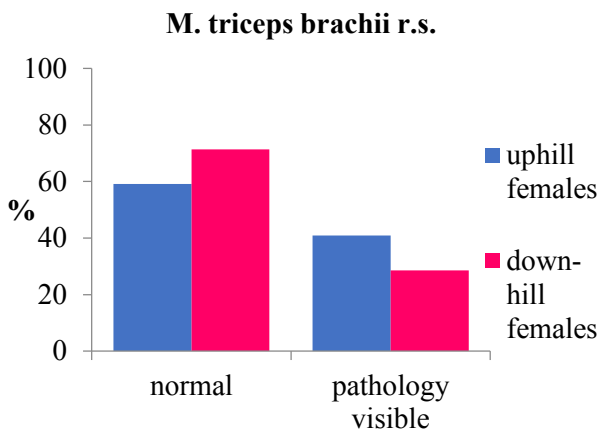
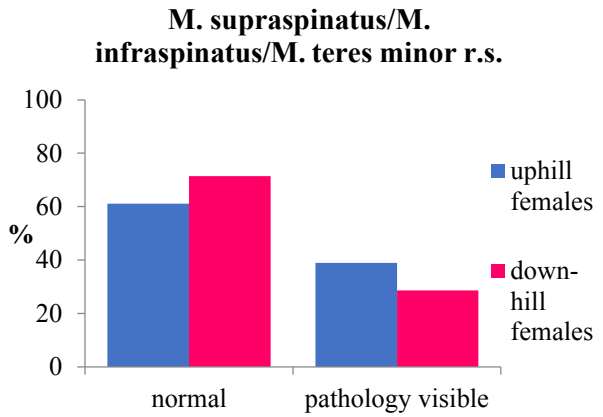
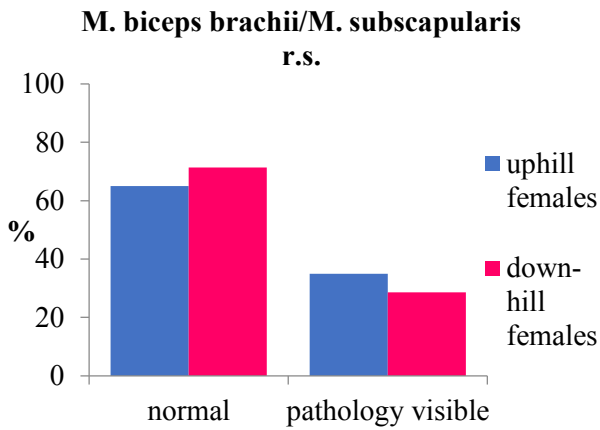
<b>entheses, right side</b>	<b>group of males</b>	<b>% normal</b>	<b>% pathology visible</b>
<b>M. biceps brachii/M. subscapularis</b>	uphill	65.0	35.0
	downhill	71.4	28.6
<b>M. supraspinatus/M. infraspinatus/M. teres minor</b>	uphill	61.1	38.9
	downhill	71.4	28.6
<b>M. triceps brachii</b>	uphill	59.1	40.9
	downhill	71.4	28.6
<b>common extensors</b>	uphill	81.2	18.8
	downhill	66.7	33.3*
<b>common flexors</b>	uphill	70.0	30.0
	downhill	80.0	20.0*
<b>M. biceps brachii/M. brachialis</b>	uphill	63.6	36.4
	downhill	71.5	28.6
<b>M. semimembranosus/M. semitendinosus/M. biceps femoris</b>	uphill	66.7	33.3
	downhill	14.3	85.7
<b>Patella/Lig. patellae (M. quadriceps femoris)</b>	uphill	72.7	27.3
	downhill	83.3	16.7

\*consists only of 3 individuals

**Table 29. b.** Significant result in t-test for *M. semimembranosus/M. semitendinosus/M. biceps femoris*.

entheses	equality of variances	Levene-test		t-test independent samples		
		F	significance	T	df	Sig. (2-tailed)
mean_sme_ste_bif_r	variances are equal	.062	.805	-2.871	26	<b>.008</b>
	variances are not equal			-2.859	10.252	.017

Next page: **Figure 91.** Graphs of the entheses groups, right side, comparison of uphill and downhill females.



### 8.1.3 Description of tables and figures for entheses frequencies of the right upper and lower extremities in uphill and downhill females

The bulk of the females (about two thirds) in both groups do not show any enthesal changes at the *M. biceps brachii* and the *M. subscapularis* muscle attachment site at the scapula. A smaller percentage (between 28% (downhill) and 35% (uphill)) display slight pathologies. The rotator cuff muscles display a similar picture as the other shoulder muscles, most of the females have no observable pathologies, and there is slight pathology visible in about 28% (downhill) to 39% (uphill) of the individuals of both groups. The *M. triceps brachii* is normally developed in about 60% of the uphill and about two thirds of the downhill females. About 40% of the uphill and about 30% of the downhill females display slight pathology here. Slightly more than 80% of the hillfort females and over 65% of the females from the valley show no pathology in the common extensor origin at the lateral epicondyle of the distal humerus. Conversely, between ~19% (uphill) and 33% (downhill) of the females display changes in the common extensors. However, the downhill female group consists only of 3 individuals here. A similar picture is displayed in the common flexors at the females, 30% of the uphill and 20% (again, consisting of 3 individuals) of the downhill females display changes here. Most of the females in both groups display no pathologies at the biceps and brachialis muscle attachment sites at the proximal lower arm bones. In between around 29% (downhill) and 36% (uphill), slight pathology is observable here (compare Table 29 and Figure 91).

Concerning the lower extremities, a third of the uphill females display slight pathology in the muscle markings analysed at the *Tuber ischiadicum*. Conversely, nearly all (~86%) of the females from the valley show slight pathology here. This resulted in a significant difference in t-test (compare above, Table 29b). Between ~73% (uphill) and 83% (downhill) of the females show no pathology in the quadriceps femoris muscle/patellar ligament attachment.

## 8.2 Females – joints – frequencies, right side

### 8.2.1 True prevalence rate of joint changes in the females, right side, upper and lower extremities

The mean frequencies of enthesal changes in percent of the single muscle marking groups, right side, comparison of uphill and downhill females, upper and lower extremities, are shown in Table 30 and Figure 92.

**Table 30.** Number of individuals and true prevalence rate of the joint changes of the right side (RS) in the uphill (UPF) and downhill females (DOF) of Thunau/Kamp, for upper and lower extremities.

uphill/downhill females, right side, joints	UPF_RS		DOF_RS	
	n/N	TPR	n/N	TPR
CHU_CGL (shoulder)	22/25	<b>0.9</b>	6/6	<b>1</b>
CAH_TRO (elbow_hu)	20/23	<b>0.9</b>	4/7	<b>0.6</b>
CRA_CIR_INT_INR (elbow-ra/ul)	20/22	<b>0.9</b>	6/6	<b>1</b>
INU_CIU_CAU_PHW_FAC (wrist)	21/25	<b>0.8</b>	6/7	<b>0.9</b>
FOA_CAF_FOC (hip)	30/30	<b>1</b>	8/8	<b>1</b>
FAP_CMF_CLF_UFO (knee/Fe)	27/30	<b>0.9</b>	7/7	<b>1</b>
CMT_CLT_FMP_FLP (knee/Ti)	28/30	<b>0.9</b>	7/7	<b>1</b>
FIT_FST_FPC (ankle)	28/29	<b>1</b>	6/6	<b>1</b>

Legend: **sbb\_scc**: *M. biceps brachii*/*M. subscapularis*; **ssp\_isp\_hmi**: *M. supraspinatus*, *M. infraspinatus*, *M. teres minor*; **stb\_utb**: *M. triceps brachii*; **com\_ext**: common extensors; **com\_flex**: common flexors; **bib\_bra**: *M. biceps brachii*/*M. brachialis*; **sme\_ste\_bif**: *M. semimembranosus*/*M. semitendinosus*/*M. biceps femoris*; **pat\_tlp**: Patella/patellar ligament: *M. quadriceps femoris*;

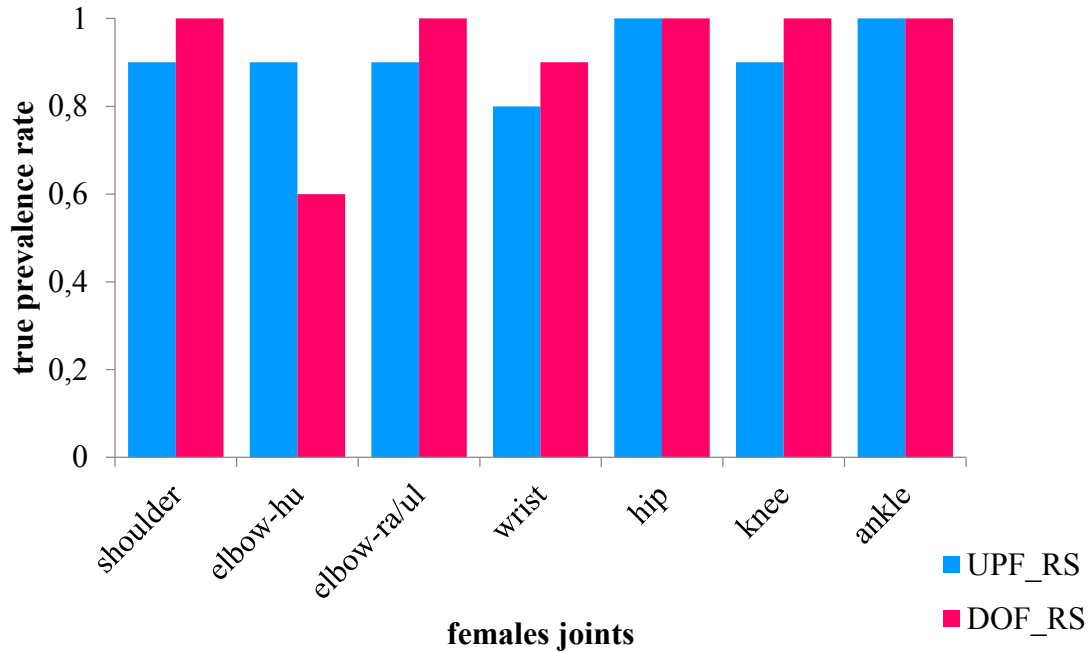


**Figure 92.** True prevalence rate of the joint changes of the right side (RS) in the uphill (UPF) and downhill females (DOF) of Thunau/Kamp, for upper and lower extremities.

Table 30 and Figure 92 show the differences in the true prevalence rates of joint changes of the uphill and downhill females on the right extremities in comparison. The rates are generally similarly high in both groups, with between more than half to all individuals affected by slight joint changes.

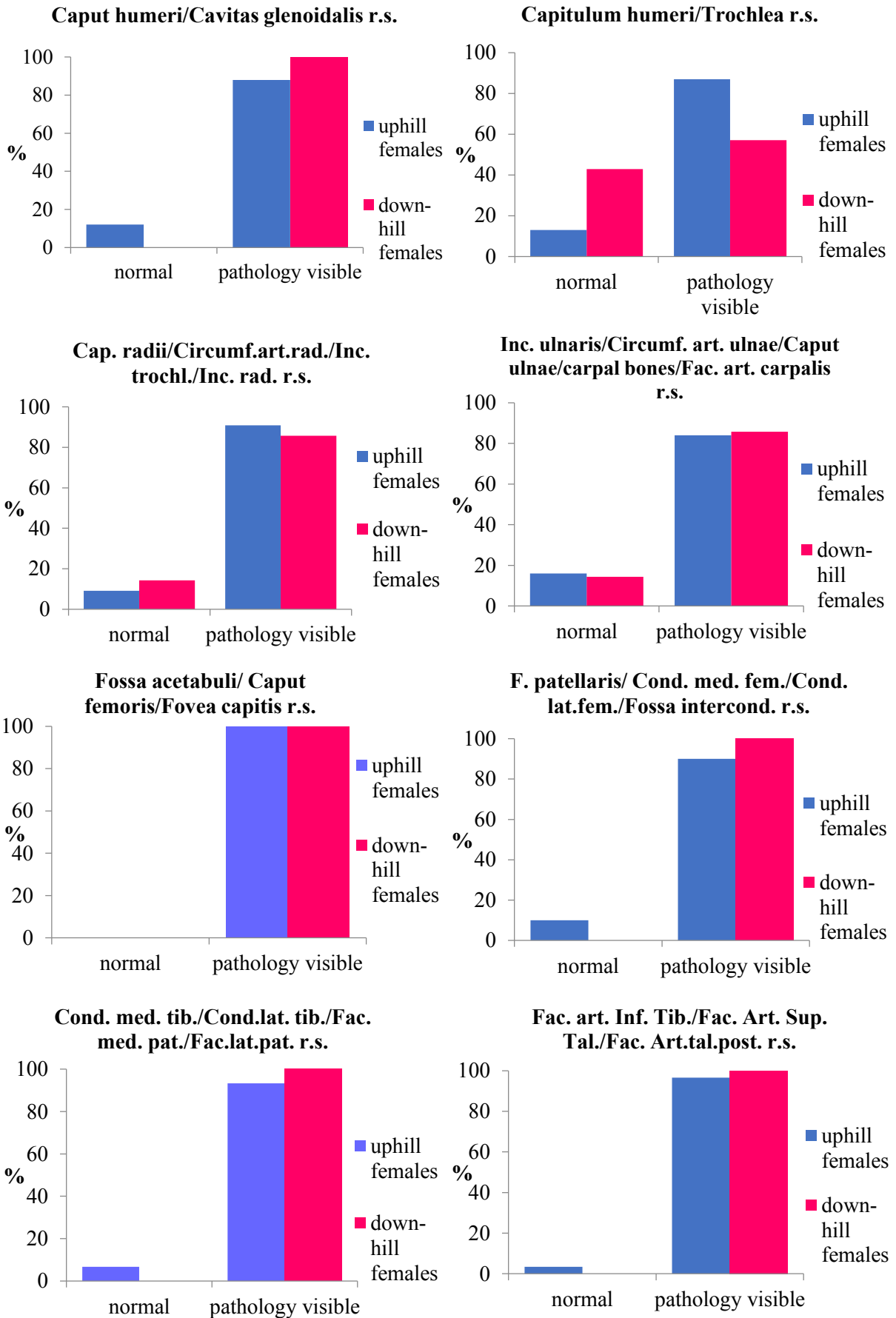
### 8.2.2 Mean frequencies of single joint groups, females right side

The mean frequencies of joint changes in percent of the single muscle groups, right side, comparison of uphill and downhill females, upper and lower extremities, are shown in Table 31 and Figure 93. The females of both sites show high frequencies of slight pathology in the joints here, except for the distal humeral joint facets (*Capitulum humeri/Trochlea*), where the uphill females are not so much affected.

**Table 31 .** Mean frequencies in percent of the single joint groups, right side, comparison of uphill and downhill females, upper and lower extremities.

<b>joints, right side</b>	<b>group of females</b>	<b>% normal</b>	<b>% pathology visible</b>
<b>Caput humeri/Cavitas glenoidalis</b>	uphill	12.0	88.0
	downhill	0.0	100.0
<b>Capitulum humeri/Trochlea</b>	uphill	13.0	87.0
	downhill	42.9	57.1
<b>Caput radii/Circumferentia articularis radii/Incisura trochlearis/Incisura radialis</b>	uphill	9.1	90.9
	downhill	14.3	85.7
<b>Incisura ulnaris/Circumferentia articularis ulnae/Caput ulnae/proximal row of carpal bones/Facies articularis carpalis</b>	uphill	16.0	84.0
	downhill	14.3	85.7
<b>Fossa acetabuli/ Caput femoris/Fovea capitis</b>	uphill	0.0	100.0
	downhill	0.0	100.0
<b>Facies patellaris/ Condylus medialis femoris/Condylus lateralis femoris/Fossa intercondylaris</b>	uphill	10.0	90.0
	downhill	0.0	100.0
<b>Condylus medialis tibiae/Condylus lateralis tibiae/Facies medialis patellae/Facies lateralis patellae</b>	uphill	6.7	93.3
	downhill	0.0	100.0
<b>Facies articularis inferior tibiae/Facies articularis superior tali/Facies articularis talaris posterior calcanei</b>	uphill	3.4	96.6
	downhill	0.0	100.0

Next page: **Figure 93.** Graphs of the joint groups, right side, comparison of uphill and downhill females, upper and lower extremities.



### 8.2.3 Description of tables and figures for joint frequencies of the right upper and lower extremities in uphill and downhill females

Nearly all females from both groups (100% in the valley females) display slight pathology in the right shoulder joint (pooled *Caput humeri/Cavitas glenoidalis*). In the elbow region, pathologies are observable in both groups. Close to 90% of the uphill, and about 60% of the downhill females show slight changes in the distal humeral pooled joints (*Capitulum humeri/Trochlea*). The proximal radius and ulna joints (*Caput radii/Circumferentia articularis radii/Incisura trochlearis/Incisura radialis*) display changes in most of the females of both groups (around 90%). Over 80% of the females in both groups display slight pathological changes in the pooled wrist bone joints (*Incisura ulnaris/Circumferentia articularis ulnae/Caput ulnae/proximal row of carpal bones/Facies articularis carpalis*) (compare Table 31 and Figure 93).

Concerning the lower extremities, all of the females of both groups display slight pathological changes in the hip joint (*Fossa acetabuli/ Caput femoris/Fovea capitis*). Almost all females of in both groups (90-100%) exhibit enthesal changes in the distal femur part of the knee joint (*Facies patellaris/ Condylus med. femoris/Condylus lat. femoris/Fossa intercondylaris*). A very similar picture can be observed in the proximal part of the right tibial joint and the patella; almost all females of in both groups display slight pathologies here (*Condylus medialis tibiae/Condylus lateralis tibiae/Facies medialis patellae/Facies lateralis patellae*). Slight pathologies are further visible in the right ankle joints in almost all females of the hillfort and the valley series females (*Facies articularis inferior tibiae/Facies articularis superior (Talus)/Facies articularis talaris posterior (Calcaneus)*).

The Table on the next page (Table 32) recapitulates details on individual numbers and percentage rates of the pooled entheses and joint frequencies of the left extremities of the uphill/downhill males in comparison.

**Table 32.** Pooled entheses and joint frequencies of the right extremities of the females in comparison.\*insufficient number of individuals

<b>pooled entheses frequencies, uphill females, right side</b>	<b>uphill females n</b>				<b>n path. visible</b>	
	total	recordable	normal	%	visible	%
M. biceps bra./subscap.	23	20	13	65.0	7	35.0
M. suprasp./infrasp./teres min.	23	18	11	61.1	7	38.9
M. triceps brachii	23	22	13	59.1	9	40.9
Common extensors	23	16	13	81.3	3	18.8
Common flexors	23	20	14	70.0	6	30.0
M. biceps brachii/brachialis	23	22	14	63.6	8	36.4
M. semim./semit./biceps fem.	23	21	14	66.7	7	33.3
Patella/pat. lig. (M. quadr. fem.)	23	22	16	72.7	5	22.7
<b>pooled entheses frequencies, downhill females, right side</b>	<b>downhill females n</b>				<b>n path. visible</b>	
	total	recordable	normal	%	visible	%
M. biceps bra./subscap.	7	7	5	71.4	2	28.6
M. suprasp./infrasp./teres min.	7	7	5	71.4	2	28.6
M. triceps brachii	7	7	5	71.4	2	28.6
Common extensors*	7	3	3	100.0	0	0.0
Common flexors*	7	5	0	0.0	0	0.0
M. biceps brachii/brachialis	7	7	5	71.4	2	28.6
M. semim./semit./biceps fem.	7	7	1	14.3	6	85.7
Patella/pat. lig. (M. quadr. fem.)	7	6	5	83.3	1	16.7
<b>pooled joints frequencies, uphill females, right side</b>	<b>uphill females n</b>				<b>n path. visible</b>	
	total	recordable	normal	%	visible	%
Cap. hum./cav. glen.	30	25	3	12.0	22	88.0
Capit. humeri/Trochlea	30	23	3	13.0	20	87.0
Cap. rad./Circ. art. rad./I. trochl./I. rad.	30	22	2	9.1	20	90.9
Inc. ul./Circumf. art. Ul./Cap. ul./prox. row carp. bones/F. art. carp.	30	25	4	16.0	21	84.0
Fossa acetabuli/Caput femoris/Fovea capitis	30	30	0	0.0	30	100.0
F. pat./Cond. medialis fem./Cond. lateralis fem./F. incercondylaris	30	30	3	10.0	27	90.0
Cond. medialis tib./Cond. lateralis tib./Fac. med. Pat./F. lat. Pat.	30	30	2	6.7	28	93.3
Fac. Art. inf. tib./Fac. Art. Sup. Tal./Fac. art. talaris post. Calcan.	30	29	1	3.4	28	96.6
<b>pooled joints frequencies, downhill females, right side</b>	<b>downhill females n</b>				<b>n path. visible</b>	
	total	recordable	normal	%	visible	%
Cap. hum./cav. glen.	8	6	0	0.0	6	100.0
Capit. humeri/Trochlea	8	7	3	42.9	4	57.1
Cap. rad./Circ. art. rad./I. trochl./I. rad.	8	7	1	14.3	6	85.7
Inc. Ul./Circumferentia art. Ulna/Caput ulnae/prox. row of carpal bones/Fac. Art. Carp.	8	7	1	14.3	6	85.7
Fossa acetabuli/Caput femoris/Fovea capitis	8	8	0	0.0	8	100.0
Facies patellaris/Cond. medialis femoris/Cond. lateralis femoris/F. incercondylaris	8	7	0	0.0	7	100.0
Condylus medialis tibiae/Condylus lateralis tibiae/Facies med. Patella/Facies lat. Patella	8	7	0	0.0	7	100.0
Fac. Art. inf. tib./Fac. Art. Sup. Tal./Fac. art. talaris post. Calcan.	8	6	0	0.0	6	100.0

## 8.3 Females – entheses – frequencies, left side

### 8.3.1 True prevalence rate of enthesal changes in the females, left side, upper and lower extremities

The mean frequencies of enthesal changes in percent of the single muscle marking groups, right side, comparison of uphill and downhill females, upper and lower extremities, are shown in Table 33 and Figure 94.

**Table 33.** Number of individuals and true prevalence rate of the enthesal changes of the left side (LS) in the uphill (UPF) and downhill females (DOF) of Thunau/Kamp, for upper and lower extremities.

uphill/downhill females, left side, entheses	UPF_LS		DOF_LS	
	n/N	TPR	n/N	TPR
SBB_SCC (shoulder)	2/16	0.1	3/7	0.4
SSP_ISP_HMI (shoulder)	2/16	0.1	2/6	0.3
STB_UTB (M. triceps br.)	7/19	0.4	3/7	0.4
COM_EXT	4/15	0.3	0/3	0
COM_FLEX	1/16	0.1	2/6	0.3
BIB_BRA (elbow-ra/ul)	6/19	0.3	1/6	0.2
SME_STE_BIF (hip)	9/20	0.5	3/6	0.5
PAT_TLP (knee)	6/22	0.3	1/6	0.2

Legend: **sbb\_scc**: *M. biceps brachii*/*M. subscapularis*; **ssp\_isp\_hmi**: *M. supraspinatus*, *M. infraspinatus*, *M. teres minor*; **stb\_utb**: *M. triceps brachii*; **com\_ext**: common extensors; **com flex**: common flexors; **bib\_bra**: *M. biceps brachii*/*M. brachialis*; **sme\_ste\_bif**: *M. semimembranosus*/*M. semitendinosus*/*M. biceps femoris*; **pat\_tlp**: Patella/patellar ligament: *M. quadriceps femoris*;

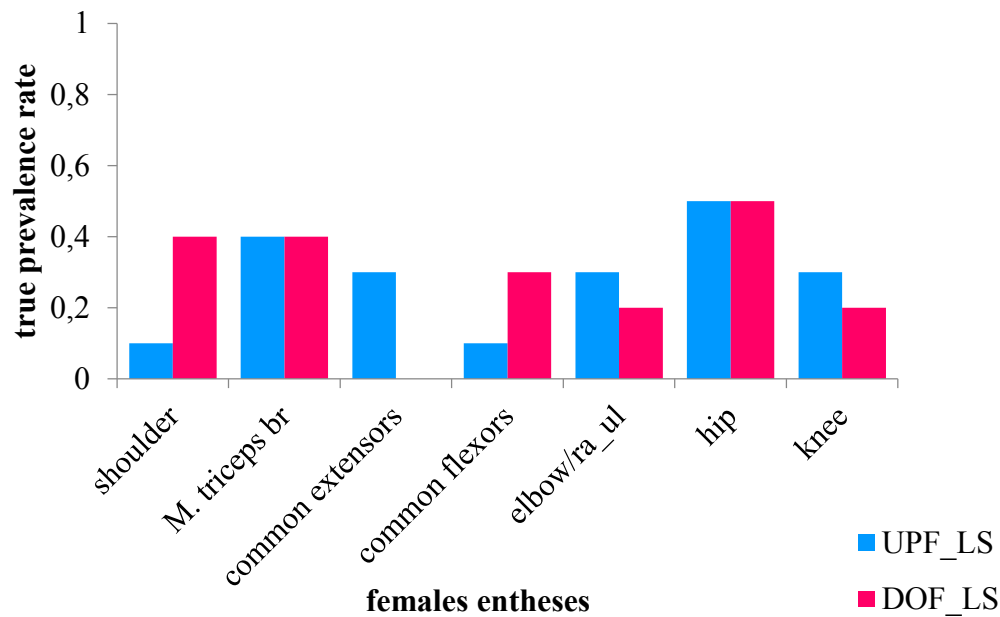


**Figure 94.** True prevalence rate of the enthesal changes of the left side (LS) in the uphill (UPF) and downhill females (DOF) of Thunau/Kamp, for upper and lower extremities.

Table 33 and Figure 94 show the differences in the true prevalence rates of enthesal changes of the uphill and downhill females on the left extremities in comparison. The rates are generally low in both groups (less than half of the individuals are affected).

### 8.3.2 Mean frequencies of single muscle groups, females left side

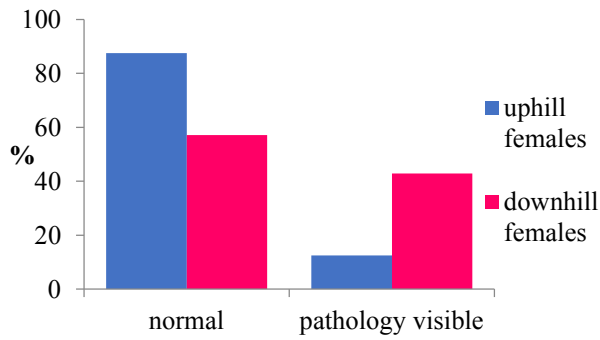
The mean frequencies of joint changes in percent of the single muscle marking groups, right side, comparison of uphill and downhill females, upper and lower extremities, are shown in Table 34 and Figure 95. As on the right side, the percentage of females affected by enthesal changes is rather low, although the downhill females tend to be more affected.

**Table 34.** Mean frequencies in percent of the single muscle groups, left side, comparison of uphill and downhill females, upper and lower extremities.

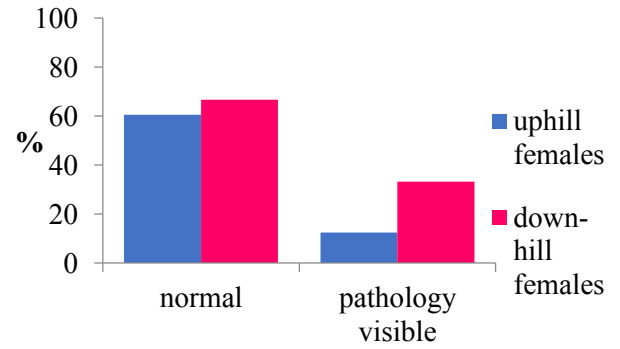
<b>entheses, left side</b>	<b>group of females</b>	<b>% normal</b>	<b>% pathology visible</b>
<b>M. biceps brachii/M. subscapularis</b>	uphill	87.5	12.5
	downhill	57.1	42.9
<b>M. supraspinatus/M. infraspinatus/M. teres minor</b>	uphill	60.6	12.5
	downhill	66.7	33.3
<b>M. triceps brachii</b>	uphill	63.2	36.8
	downhill	57.1	42.9
<b>common extensors</b>	uphill	73.3	26.7
	downhill	100.0	0.0
<b>common flexors</b>	uphill	93.8	6.3
	downhill	66.7	33.3
<b>M. biceps brachii/M. brachialis</b>	uphill	68.4	31.6
	downhill	83.3	16.7
<b>M. semimembran./M. semitend./M. biceps femoris</b>	uphill	55.0	45.0
	downhill	50.0	50.0
<b>Patella/Lig. patellae (M. quadriceps femoris)</b>	uphill	72.7	27.3
	downhill	83.3	16.7

Next page: **Figure 95.** Graphs of the muscle groups, left side, comparison of uphill and downhill females, upper and lower extremities.

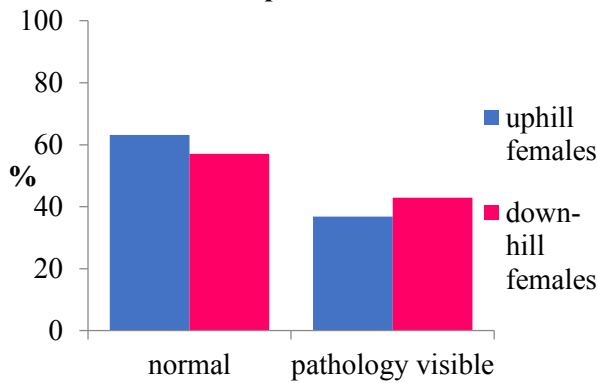
**M. biceps brachii/M. subscapularis l.s.**



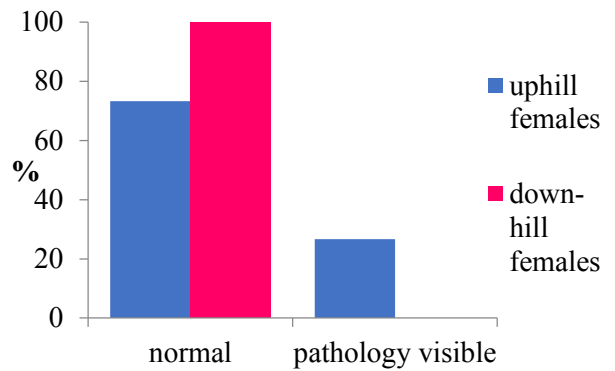
**M. supraspinatus/ infraspinatus/teres minor l.s.**



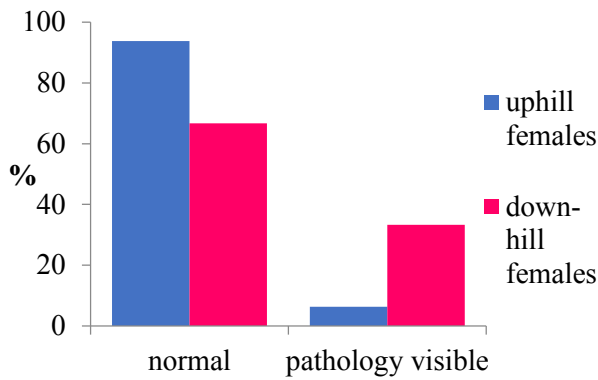
**M. triceps brachii l.s.**



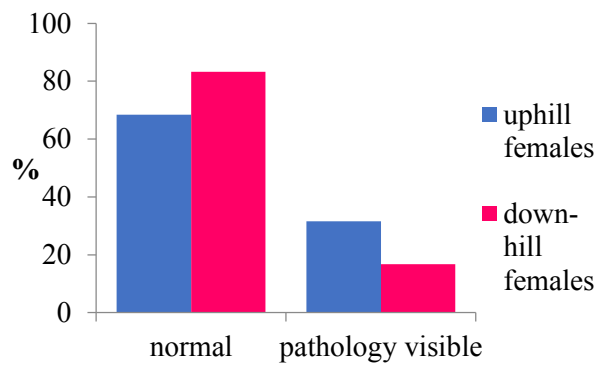
**Common extensors l.s.**



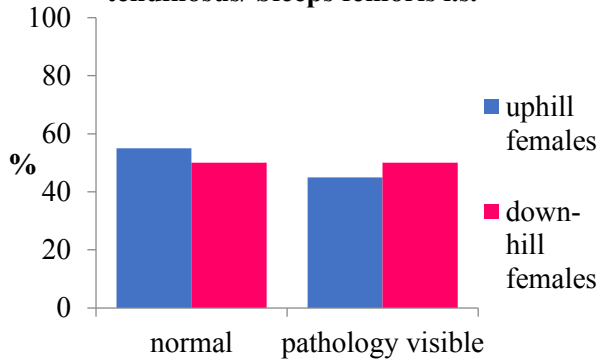
**Common flexors l.s.**



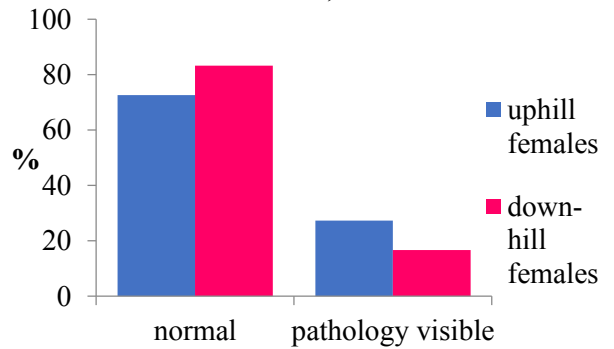
**M. biceps brachii/M. brachialis l.s.**



**M. semimembranosus/semi-tendinosus/ biceps femoris l.s.**



**Patella/Lig. patellae (M. quadriceps femoris) l.s.**



### 8.3.3 Description of tables and figures for entheses frequencies of the left upper and lower extremities in uphill and downhill females

Only a small percentage of the hillfort females (~12%) show enthesal changes in the shoulder muscle markings group (*M. biceps brachii*/*M. subscapularis*). The females from the valley, in comparison, display enthesal changes here in a little more than 40%. A similar picture is visible in the rotator cuff muscles, *Musculus supraspinatus*, *Musculus infraspinatus* and *Musculus teres minor*. Exactly a third of the percentage of the downhill females shows slight pathologies, whereas the uphill females display changes only in about 12%. Between ~37% (uphill) and ~43% (downhill) of the females display slight enthesal changes in the triceps brachii muscle attachment site. More than a third of the uphill females, and 100% of the downhill females display a normal development at the common extensors. A third of the females from the valley site display slight pathologies in the common flexors, compared to a very low number in the uphill females (~6%). Most of the females of both groups are in the normal category according to the proximal lower arm muscles, *Musculus biceps brachii* and *Musculus brachialis*. Around 30% of the uphill females and under 20% of the downhill females display slight pathologies here (compare Table 34 and Figure 95).

Regarding the lower left extremity, the percentage of normal development and enthesal changes is quite similar for the *M. semimembranosus*/*M. semitendinosus*/*M. biceps femoris* at the *tuber ischiadicum* attachment site in both groups (between 45 to 55%). Between ~17% (downhill) and 27% (uphill) of the females show slight pathology at the attachment site of the only extensor at the knee joint (*M. quadriceps femoris*).

## 8.4 Females – joints – frequencies, left side

### 8.4.1 True prevalence rate of joint changes in the females, left side, upper and lower extremities

The mean frequencies of enthesal changes in percent of the single muscle marking groups, left side, comparison of uphill and downhill females, upper and lower extremities, are shown in Table 35 and Figure 96.

**Table 35.** Number of individuals and true prevalence rate of the joint changes of the left side (LS) in the uphill (UPF) and downhill females (DOF) of Thunau/Kamp, for upper and lower extremities.

uphill/downhill males, left side, entheses	UPF_LS		DOF_LS	
	n/N	TPR	n/N	TPR
SBB_SCC (shoulder)	2/16	0.1	3/7	0.4
SSP_ISP_HMI (shoulder)	2/16	0.1	2/6	0.3
STB_UTB (M. triceps br.)	7/19	0.4	3/7	0.4
COM_EXT	4/15	0.3	0/3	0.0
COM_FLEX	1/16	0.1	2/6	0.3
BIB_BRA (elbow-ra/ul)	6/19	0.3	1/6	0.2
SME_STE_BIF (hip)	9/20	0.5	3/6	0.5
PAT_TLP (knee)	6/22	0.3	1/6	0.2

Legend: **sbb\_scc**: *M. biceps brachii*/*M. subscapularis*; **ssp\_isp\_hmi**: *M. supraspinatus*, *M. infraspinatus*, *M. teres minor*; **stb\_utb**: *M. triceps brachii*; **com\_ext**: common extensors; **com flex**: common flexors; **bib\_bra**: *M. biceps brachii*/*M. brachialis*; **sme\_ste\_bif**: *M. semimembranosus*/*M. semitendinosus*/*M. biceps femoris*; **pat\_tlp**: Patella/patellar ligament: *M. quadriceps femoris*;

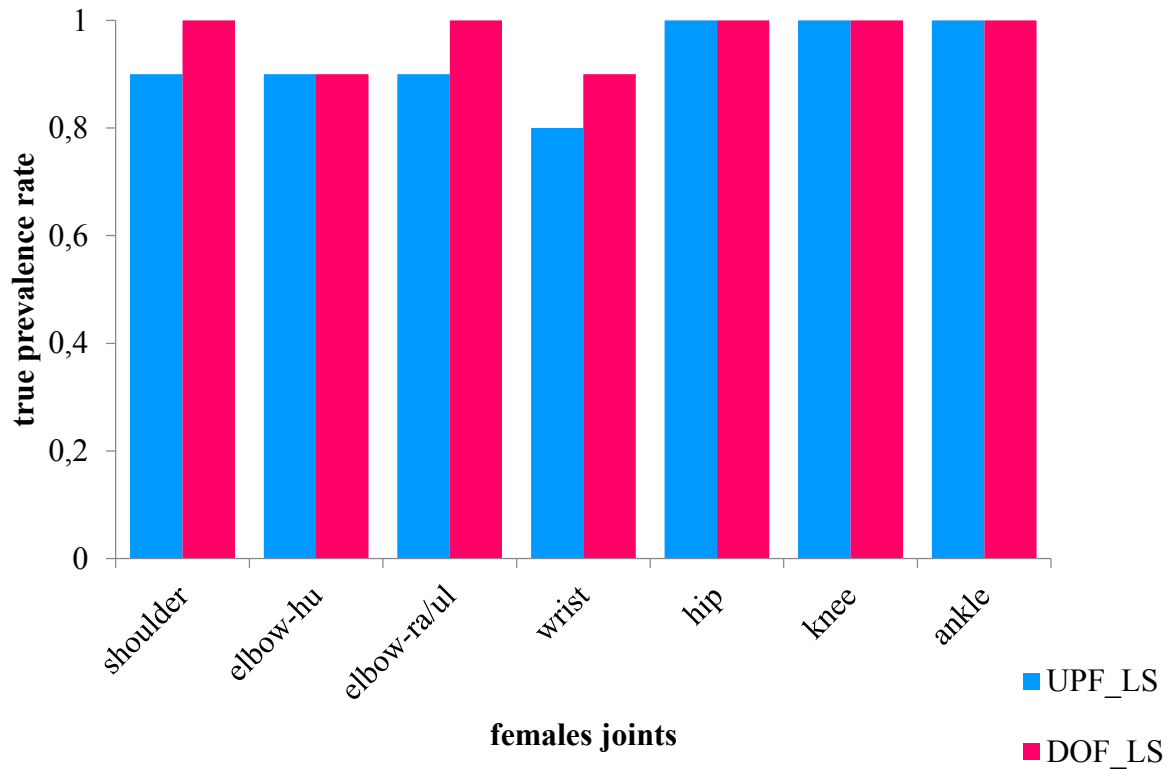


**Figure 96.** True prevalence rate of the joint changes of the left side (LS) in the uphill (UPF) and downhill females (DOF) of Thunau/Kamp, for upper and lower extremities.

Table 35 and Figure 96 show the differences in the true prevalence rates of joint changes of the uphill and downhill females on the left extremities in comparison. The rates are generally very high in both groups (close to 100%).

#### 8.4.2 Mean frequencies of single joint groups, females left side

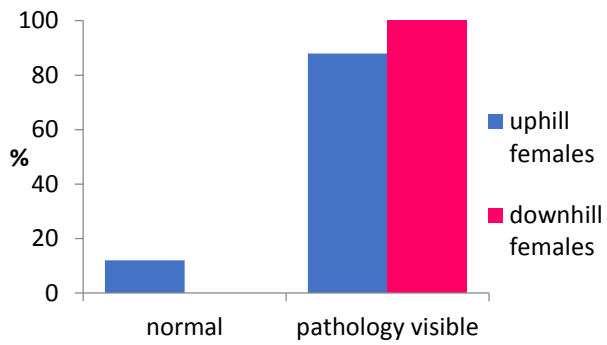
The mean frequencies of joint changes in percent of the single joint groups, left side, comparison of uphill and downhill females, upper and lower extremities, are shown in Table 36 and Figure 97. The picture of the joint facet changes on the left side is similar to the right side; most females of both groups show high frequencies of change. Especially in the downhill females, the frequencies mostly reach 100%.

**Table 36.** Mean frequencies in percent of the single joint groups, left side, comparison of uphill and downhill females, upper and lower extremities.

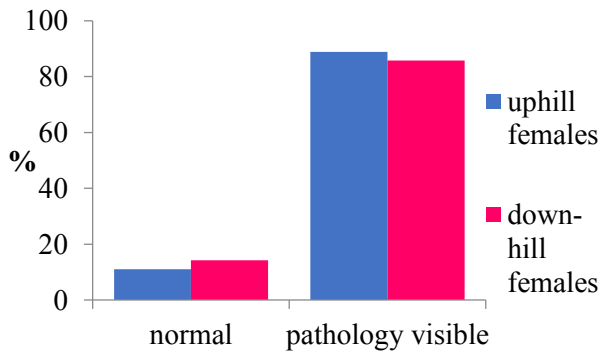
<b>joints, left side</b>	<b>group of females</b>	<b>% normal</b>	<b>% pathology visible</b>
<b>Caput humeri/Cavitas glenoidalis</b>	uphill	12.0	88.0
	downhill	0.0	100.0
<b>Capitulum humeri/Trochlea</b>	uphill	11.1	88.9
	downhill	14.3	85.7
<b>Caput radii/Circumferentia articularis radii/Incisura trochlearis/Incisura radialis</b>	uphill	9.1	9.09
	downhill	14.3	85.7
<b>Incisura ulnaris/Circumferentia articularis ulnae/Caput ulnae/proximal row of carpal bones/Facies articularis carpalis</b>	uphill	19.2	80.8
	downhill	14.3	85.7
<b>Fossa acetabuli/ Caput femoris/Fovea capitis</b>	uphill	3.4	96.6
	downhill	0.0	100.0
<b>Facies patellaris/ Cond. medialis fem./Cond. lateralis fem./F. intercondylaris</b>	uphill	13.8	86.2
	downhill	0.0	100.0
<b>Condylus medialis tibiae/Condylus lateralis tibiae/Fac. medialis pat./Fac. lateralis pat.</b>	uphill	0.0	100.0
	downhill	0.0	100.0
<b>Facies articularis inferior tibiae/Facies articularis superior tali/Facies articularis talaris posterior calcanei</b>	uphill	3.6	96.4
	downhill	0.0	100.0

Next page: **Figure 97.** Graphs of the muscle groups, left side, comparison of uphill and downhill females, upper and lower extremities.

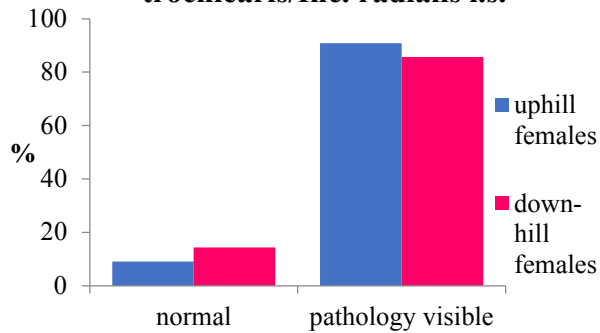
**Caput humeri/Cavitas glenoidalis l.s.**



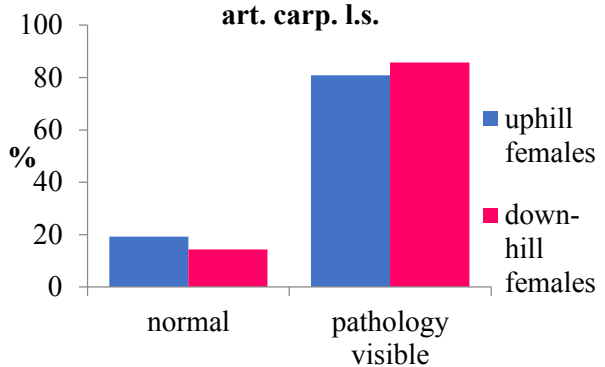
**Capitulum humeri/Trochlea l.s.**



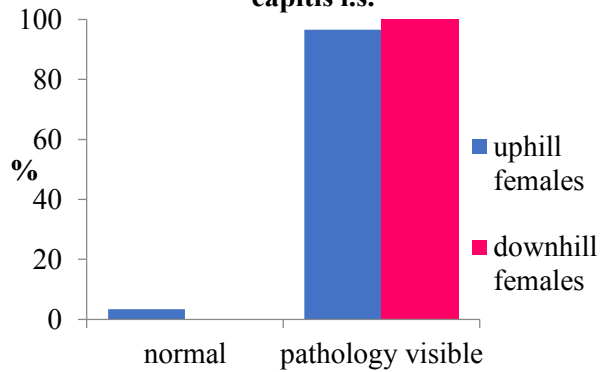
**Cap. radii/Circumf. art. rad./Inc. trochlearis/Inc. radialis l.s.**



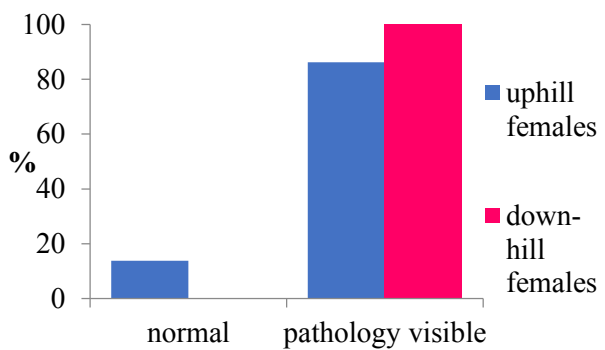
**Inc. ulnae/Circumf. art. ulnae/Caput ulnae/prox. wrist/Fac. art. carp. l.s.**



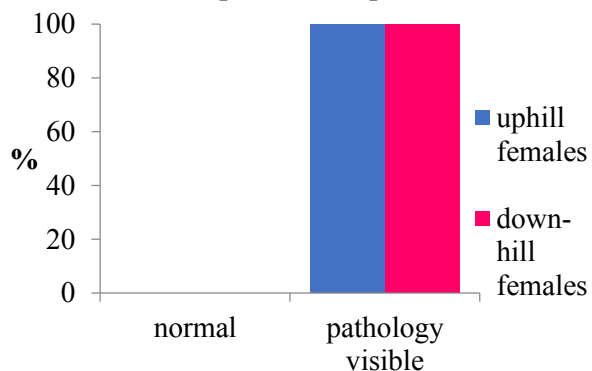
**F. acetabuli/ Caput femoris/Fovea capitis l.s.**



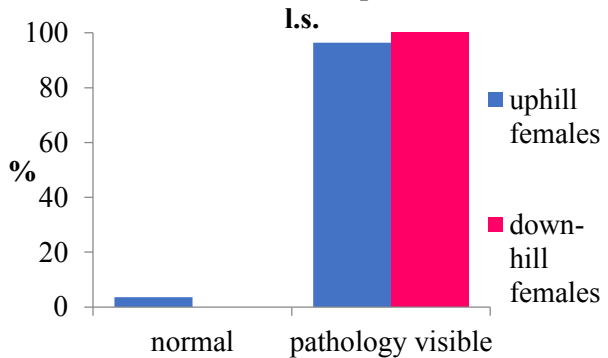
**F. patellaris/ Cond. med. fem./Cond. lat.fem./Fossa intercond. l.s.**



**Cond. med. tib./Cond.lat. tib./Fac. med. pat./Fac.lat.pat. l.s.**



**Fac. art. inf. tibiae/Fac. art. inf. Talus/Fac. art. talaris post. Calc. l.s.**



### 8.4.3 Description of tables and figures for joint frequencies of the left upper and lower extremities in uphill and downhill females

The bulk of uphill females and 100% of the females from the valley site display slight pathologies in the shoulder joint (*Caput humeri/Cavitas glenoidalis*). Close to 90% in both female groups display pathologies in the distal humeral joint (*Capitulum humeri/Trochlea*). In the pooled joints of the proximal lower arm (*Caput radii/Circumferentia articularis radii/Incisura trochlearis/Incisura radialis*), the picture is quite the same as in the distal humeral joint: a percentage of nearly 90% of the females are in the slight pathology category. Most of the females (~81% (uphill) – 86% (downhill)) of both groups show slight pathology in the wrist bone joints (*Incisura ulnaris/Circumferentia articularis ulnae/Caput ulna/carpal bones/Facies articularis carpalis*).

Concerning the joint changes in the lower left extremity, nearly 100% of the uphill females and 100% of the downhill females display slight pathologies in the pooled hip joints (*Fossa acetabuli/Caput femoris/Fovea capitis*). Almost all of the females of the uphill group show pathologies at the distal femur (*Facies patellaris/Condylus medialis femoris/Condylus lateralis femoris/Fossa intercondylaris*), and all of the downhill females are affected by enthesal changes here. In the proximal tibia (*Condylus medialis tibiae/Condylus lateralis tibiae/Facies medialis patellae/Facies lateralis patellae*), the picture is the same as in the distal femur, here, all analysed female skeletons of both groups display slight pathology. In the ankle joint, again, nearly all females of the hillfort group and all females from the valley site in both groups show slight pathology (*Facies articularis inferior tibiae/Facies articularis superior (Talus)/Facies articularis talaris posterior (Calcaneus)*).

Table 37 on the next page recapitulates details on individual numbers and percentage rates of the pooled entheses and joint frequencies of the left extremities of the uphill/downhill females in comparison.

**Table 37.** Pooled entheses and joint frequencies of the left extremities of the females in comparison.

pooled entheses frequencies, uphill females, left side	uphill females n				n path.	
	total	recordable	normal	%	visible	%
M. biceps bra./subscap.	23	16	14	87.5	2	12.5
M. suprasp./infrasap./teres min.	23	16	14	87.5	2	12.5
M. triceps brachii	23	15	11	73.3	4	26.7
Common extensors	23	19	12	63.2	7	36.8
Common flexors	23	16	15	93.8	1	6.3
M. biceps brachii/brachialis	23	19	13	68.4	6	31.6
M. semim./semit./biceps fem.	23	20	11	55.0	9	45.0
Patella/pat. lig. (M. quadr. fem.)	23	22	16	72.7	6	27.3
pooled entheses frequencies, downhill females, left side	downhill females n				n path.	
	total	recordable	normal	%	visible	%
M. biceps bra./subscap.	7	7	4	57.1	3	42.9
M. suprasp./infrasap./teres min.	7	6	4	66.7	2	33.3
M. triceps brachii	7	3	3	100.0	0	0.0
Common extensors	7	6	4	66.7	2	33.3
Common flexors	7	7	4	57.1	3	42.9
M. biceps brachii/brachialis	7	6	5	83.3	1	16.7
M. semim./semit./biceps fem.	7	6	3	50.0	3	50.0
Patella/pat. lig. (M. quadr. fem.)	7	6	5	83.3	1	16.7
pooled joints frequencies, uphill females, left side	uphill females n				n path.	
	total	recordable	normal	%	visible	%
Cap. hum./cav. glen.	30	25	3	12.0	22	88.0
Capit. humeri/Trochlea	30	27	3	11.1	24	88.9
Cap. rad./Circ. art. rad./I. trochl./I. rad.	30	22	2	9.1	20	90.9
Inc. Ul./Circumferentia art. Ulna/Caput ulnae/prox. row of carpal bones/Fac. Art. Carp.	30	26	5	19.2	21	80.8
Fossa acetabuli/Caput femoris/Fovea capitis	30	29	1	3.4	28	96.6
Fac. patellaris/Cond. medialis femoris/Cond. lateralis femoris/F. incercondylaris	30	29	4	13.8	25	86.2
Condylus medialis tibiae/Condylus lateralis tibiae/Facies med. Patella/Facies lat. Patella	30	29	0	0.0	29	100.0
Fac. art.inf. tib./Fac. Art. Sup. Tal./Fac. Art.tal. post. Calcan.	30	28	1	3.6	27	96.4
pooled joints frequencies, downhill females, left side	downhill females n				n path.	
	total	recordable	normal	%	visible	%
Cap. hum./cav. glen.	8	6	0	0.0	6	100.0
Capit. humeri/Trochlea	8	7	1	14.3	6	85.7
Cap. rad./Circ. art. rad./I. trochl./I. rad.	8	7	1	14.3	6	85.7
Inc. Ul./Circumferentia art. Ulna/Caput ulnae/prox. row of carpal bones/Fac. Art. Carp.	8	7	1	14.3	6	85.7
Fossa acetabuli/Caput femoris/Fovea capitis	8	8	0	0.0	8	100.0
Fac. patellaris/Cond. medialis femoris/Cond. lateralis femoris/F. incercondylaris	8	7	0	0.0	7	100.0
Condylus medialis tibiae/Condylus lateralis tibiae/Facies med. Patella/Facies lat. Patella	8	8	0	0.0	8	100.0
Fac. art.inf. tib./Fac. Art. sup. tal./Fac. Art.tal. post. Calcan.	8	6	0	0.0	6	100.0

## 9 THUNAU FEMALES – RESULTS II – VISUAL ANALYSES: ASYMMETRY

### 9.1 Females – entheses – asymmetry, upper and lower extremities

Asymmetries were calculated from scores of enthesal changes following the recommendations of Auerbach & Ruff (2006, compare chapter 5.3., statistical analysis). Concerning asymmetric enthesal changes, they seem to be somewhat more distinct in the downhill females. The females display particularly in the common extensors on the right side and the common flexors on the left side, as well as in the biceps/brachialis muscles on the right side a strong asymmetry. Nevertheless, it has to be kept in mind that these results come from a very little number of individuals in the downhill females in these cases. The uphill females display changes mainly in the common flexors on the right side (compare Table 38 and Figure 98). Univariate analysis did not reveal any significant results.

**Table 38.** Comparison of asymmetry calculated from scores in enthesal changes between right and left extremities for uphill and downhill females.

females	uphill, right side	uphill, left side	% asymmetry	downhill, right side	downhill, left side	% asymmetry
sbb_ssc (shoulder)	0.90	0.81	10.22	0.86	1.02	-17.72
ssp_isp_hmi (shoulder)	1.00	0.96	4.03	0.99	1.13	-13.48
M. triceps brachii	0.89	0.82	7.99	0.98	0.91	7.60
common extensors	0.79	0.83	-5.13	0.67	0.44	40.00
common flexors	0.97	0,85	14.03	1,00	0,81	21.54
bib_bra (elbow/ra_ul)	1.03	0.75	31.78	0.67	1.11	-50.00
sme_ste_bif (hip)	1.02	1.09	-7.19	1.43	1.20	17.39
pat_tlp (knee)	0.90	0.97	-7.62	1.00	0.94	5.71

Legend: **sbb\_scc**: *M. biceps brachii*/*M. subscapularis*; **ssp\_isp\_hmi**: *M. supraspinatus*, *M. infraspinatus*, *M. teres minor*; **stb\_utb**: *M. triceps brachii*; **com\_ext**: common extensors; **com flex**: common flexors; **bib\_bra**: *M.*

*biceps brachii/M. brachialis*; **sme\_ste\_bif**: *M. semimembranosus/M. semitendinosus/M. biceps femoris*; **pat\_tlp**: Patella/patellar ligament; *M. quadriceps femoris*;

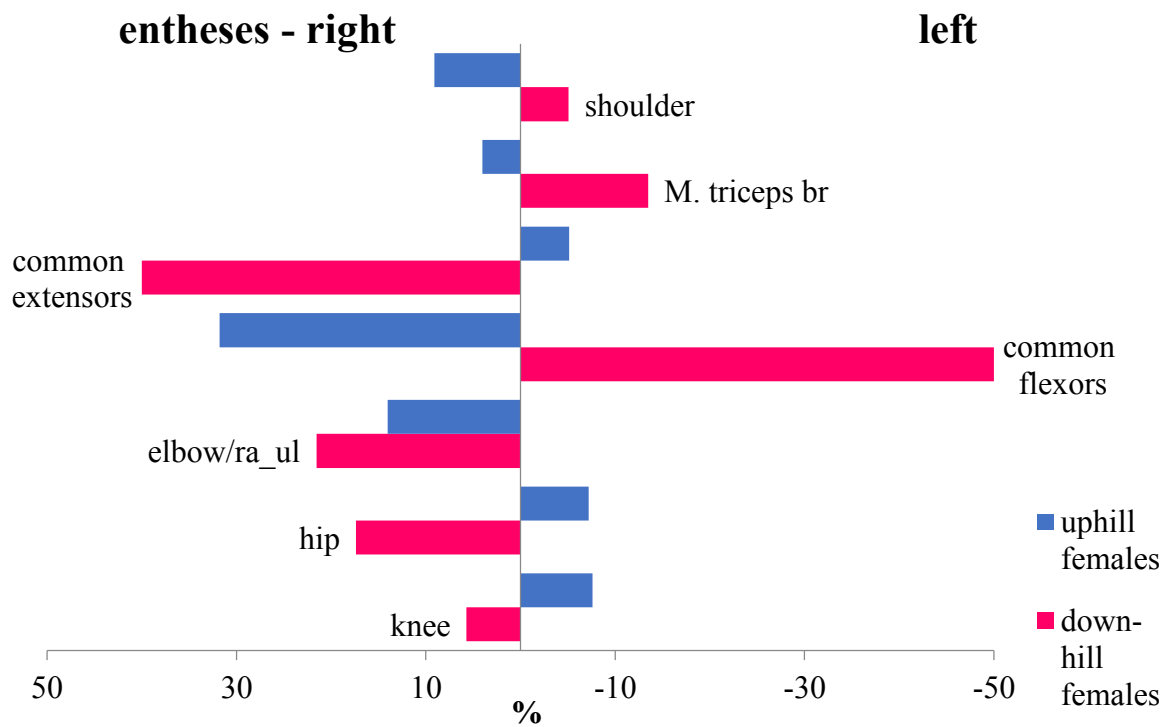


**Figure 98.** Asymmetries in enthesal changes calculated from scores in the right and left upper and lower extremities of the uphill and downhill females.

No significant results were obtained for asymmetries in enthesal changes for the females.

## 9.2 Females – joints – asymmetry, upper and lower extremities

Generally, the displayed asymmetries are quite similar in the joints of the two female subgroups from Thunau. The percentage of asymmetrical joint changes is higher in the distal humeral joint of the left side (elbow-hu) for the downhill females, and to a lesser extent in the pooled wrist joint facets (*Incisura ulnaris/Circumferentia articularis ulna/Caput ulnae/proximal row of carpal bones/Facies articularis carpalis*; Table 39 & Figure 99). No significant results became apparent.

**Table 39.** Comparison of asymmetry in joint changes between right and left extremities for uphill and downhill females.

females	uphill, right side	uphill, left side	% asymmetry	downhill, right side	downhill, left side	% asymmetry
chu_cgl (shoulder)	1.55	1.36	13.20	1.56	1.32	16.10
cah_tro (elbow_hu)	1.43	1.59	-11.17	1.12	1.51	-29.62
cra_cir_int_inr (elbow-ra/ul)	1.43	1.40	1.95	1.22	1.24	-1.65
inu_ciu_cau_phw_fac (wrist)	1.39	1.40	-1.21	1.30	1.41	-8.71
foa_caf_foc (hip)	1.66	1.68	-1.14	1.78	1.79	-0.67
fap_cmf_clf_ufo (knee/Fe)	1.54	1.51	2.01	1.61	1.62	-0.62
cmt_clt_fmp_flp (knee/Ti)	1.53	1.54	-0.13	1.61	1.61	0.07
fit_fst_fpc (ankle)	1.55	1.52	1.66	1.49	1.46	2.42

Legend: **chu\_cgl**: *Caput humeri/Cavitas glenoidalis*; **cah\_tro**: *Capitulum humeri/Trochlea*; **cra\_cir\_int\_inr**: *Caput radii/Circumferentia articularis radii/Incisura trochlearis/Incisura radialis*; **inu\_ciu\_cau\_phw\_fac**: *Incisura ulnaris/Circumferentia articularis ulna/Caput ulnae/proximal row of carpal bones/Facies articularis carpalis*; **foa\_caf\_foc**: *Fossa acetabuli/Caput femoris/Fovea capitis*; **fap\_cmf\_clf\_ufo**: *Facies patellaris/Condylus medialis femoris/Condylus lateralis femoris/distal margin of Fossa intercondylaris*; **cmt\_clt\_fmp\_flp**: *Condylus medialis tibiae/Condylus lateralis tibiae/Facies medialis patellae/Facies lateralis patellae*; **fit\_fst\_fpc**: *Facies articularis inferior tibiae/Facies articularis superior (Talus)/Facies articularis talaris posterior (Calcaneus)*;

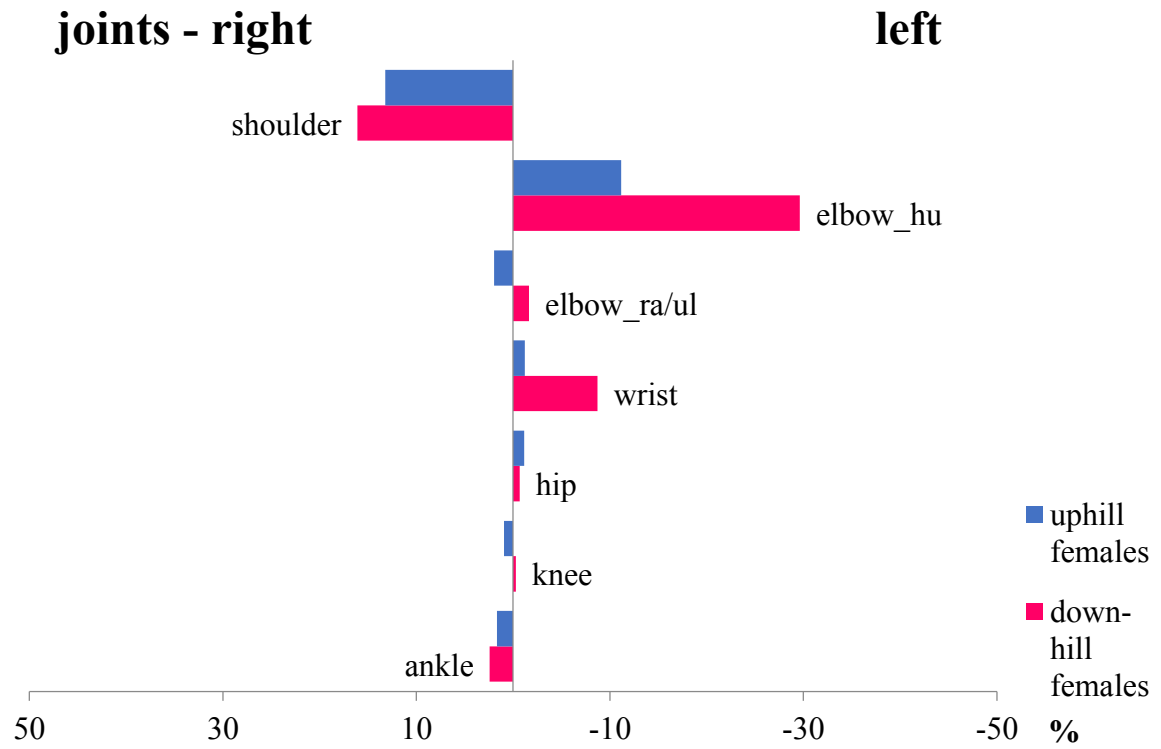


**Figure 99.** Asymmetries calculated from scores in the right and left upper and lower extremities of the uphill and downhill females.

No significant results were apparent for asymmetries in joint changes for the females.

# 10 THUNAU FEMALES – RESULTS III – ASSOCIATION BETWEEN ENTHESES AND MEAN AGE/BODY HEIGHT

## 10.1 Scatterplots entheses – mean age – females

### 10.1.1 Scatterplots entheses – mean age, comparison females uphill-downhill – right side

Differences between the two archaeological sub-sites from Thunau (series 1 = uphill site, series 2 = downhill site), according to mean scores and mean age are shown here in the scatterplots (Figures 100– 111) between the uphill females and the downhill females, respectively. The scores of the muscle markings of the females are plotted against increasing age of both groups, along with the least squares regression line and the 95% confidence regions. Univariate analyses were added if the difference between the groups was significant; graphs are added in cases of clear average differences between the sub-sites.

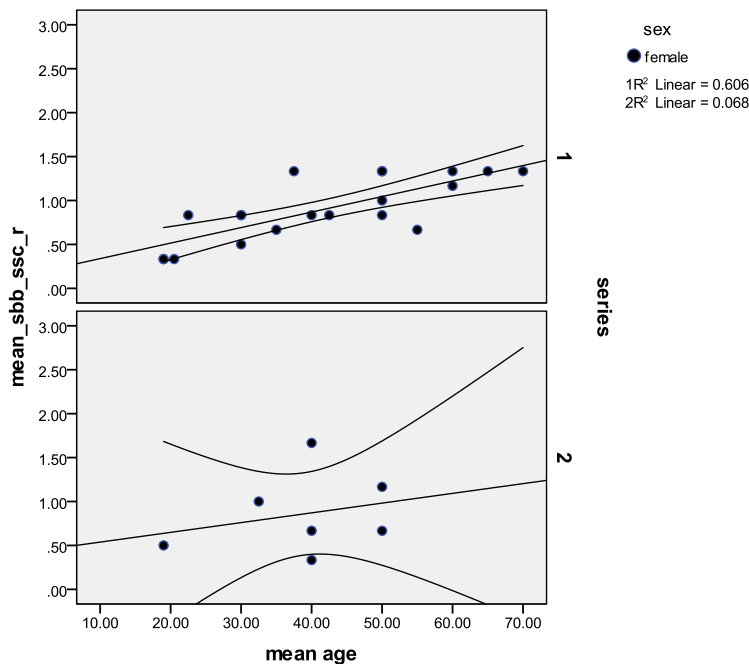


**Figure 100.a.** Pooled muscle group *M. biceps brachii* – *M. subscapularis* (humerus, scapula), females of the uphill (1) and downhill site (2), right side. There is a significant increase of entheses scores with higher age, but not between the sub-sites (compare Figure 100b).

**Figure 100.b.** Results of univariate analysis for the pooled muscle markings group *M. biceps brachii*/*M. subscapularis*.

		N
series	1	20
	2	7

dependent variable: mean\_sbb\_ssc\_r

Quelle	Quadratsumme vom Typ III	Df	Mittel der Quadrate	F	Sig.
Korrigiertes Modell	1.562 <sup>a</sup>	2	.781	8.676	.001
Konstanter Term	.116	1	.116	1.293	.267
mean_age	1.552	1	1.552	17.247	.000
series	.000	1	.000	.004	.953
Fehler	2.160	24	.090		
Gesamt	25.056	27			
Korrigierte Gesamtvariation	3.722	26			

a. R-Quadrat = .420 (korrigiertes R-Quadrat = .371)

The pooled muscle markings group *M. biceps brachii*/*M. subscapularis* at the shoulder is significantly affected by age in the females, but not between the sub-sites.

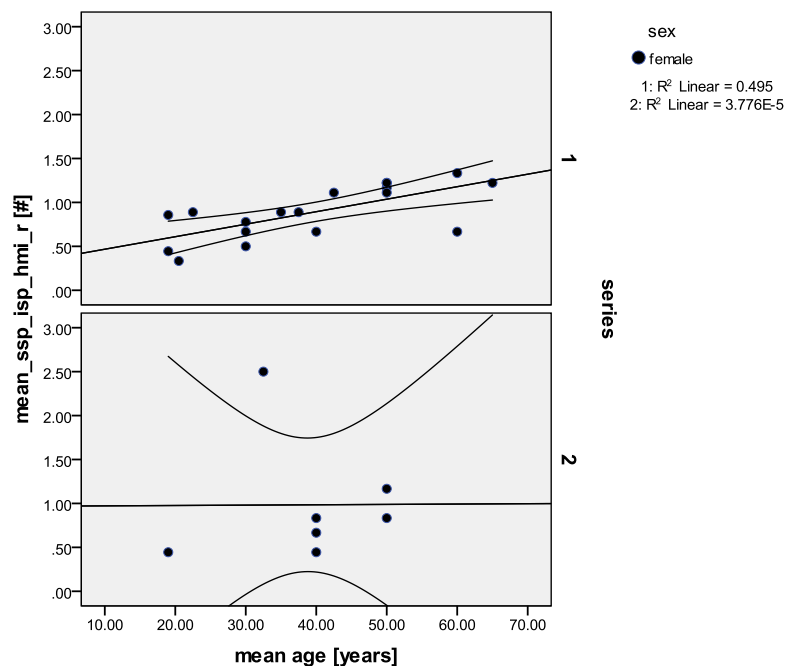


**Figure 101.** Pooled muscle group *M. supraspinatus* - *M. infraspinatus* - *M. teres minor* (prox. humerus), females of the uphill (1) and downhill site (2), right side. There is a slight increase of entheses scores with higher age in the females of the uphill site, but not in the downhill group.

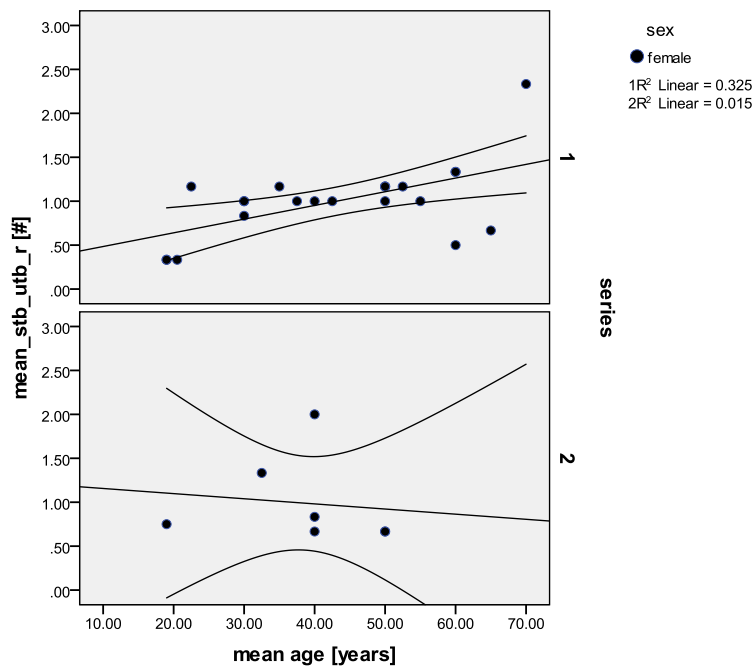


**Figure 102.a.** Pooled *M. triceps brachii* (scapula–proximal ulna), females of the uphill (1) and downhill site (2), right side. There is a slight increase of entheses scores with increasing age in the females of the uphill site, which is not apparent in the downhill group. This feature is significantly affected by age (see Figure 102b).

**Figure 102. b.** Result of the univariate analysis of the pooled *M. triceps brachii*.

		N
series	1	22
	2	7

dependent variable: mean stb utb r

Quelle	Quadratsumme vom Typ III	Df	Mittel der Quadrate	F	Sig.
Korrigiertes Modell	1.008 <sup>a</sup>	2	.504	2.966	.069
Konstanter Term	.633	1	.633	3.728	.064
mean_age	1.007	1	1.007	5.928	<b>.022</b>
series	.010	1	.010	.061	.806
Fehler	4.416	26	.170		
Gesamt	34.257	29			
Korrigierte Gesamtvariation	5.423	28			

a. R-Quadrat = .186 (korrigiertes R-Quadrat = .123)

The females show statistically significant results in this feature according to mean age in the right *M. triceps brachii*, but not between sub-sites.

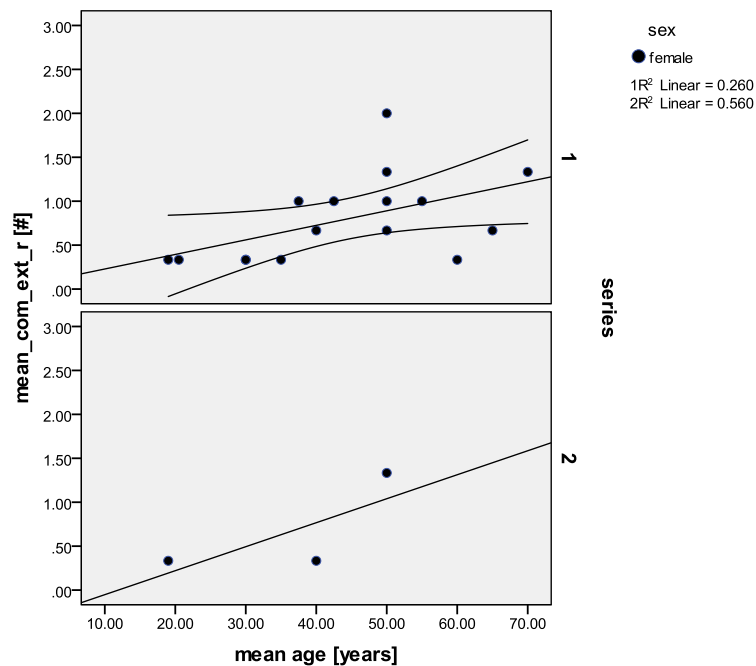


**Figure 103.a.** Scatterplot of the pooled **common extensors** muscle group (distal lateral humerus), females of the uphill (1) and downhill site (2), right side. There is an increase of entheses scores with higher age in the females of both sites. The significant result (Figure 103b) may be biased by the small number of individuals in group 2.

**Figure 103.b.** Results of the univariate analysis for the right common extensors.

		N
series	1	16
	2	3

dependent variable: mean\_com\_ext\_r

Quelle	Quadratsumme vom		Mittel der Quadrate	F	Sig.
	Typ III	Df			
Korrigiertes Modell	1.280 <sup>a</sup>	2	.640	3.467	.056
Konstanter Term	.000	1	.000	.001	.980
mean_age	1.241	1	1.241	6.720	<b>.020</b>
Series	.000	1	.000	.002	.962
Fehler	2.954	16	.185		
Gesamt	15.556	19			
Korrigierte Gesamtvariation	4.234	18			

a. R-Quadrat = .302 (korrigiertes R-Quadrat = .215)

The females show statistically significant results in the common extensor enthesal features according to mean age on the right side, but not between the sub-sites.

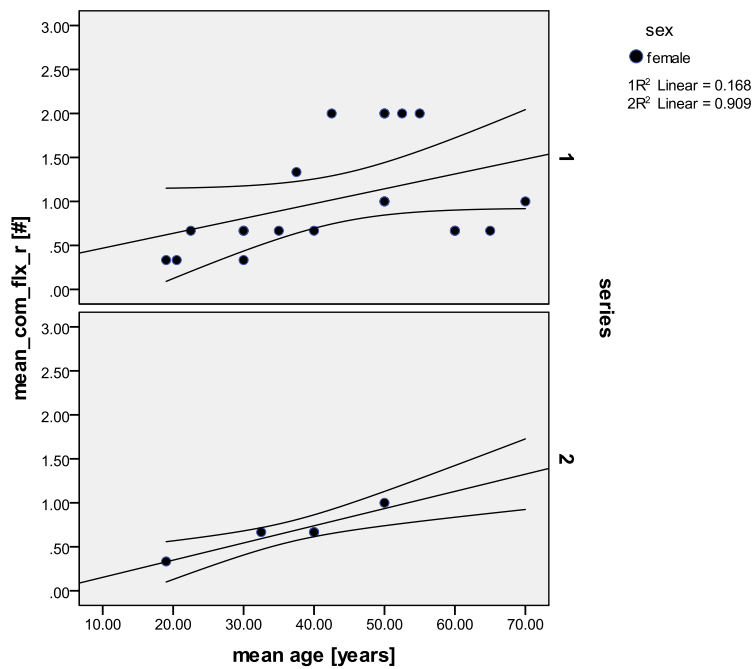


**Figure 104.a.** Scatterplot of the pooled **common flexors muscle group** (distal medial humerus), females of the uphill (1) and downhill site (2), right side. There is an increase of entheses scores with increasing age in the females of both sites. The significant result may be biased by the small number of individuals in group 2 (Figure 104b).

**Figure 104.b.** Results of the univariate analysis for the right common flexors.

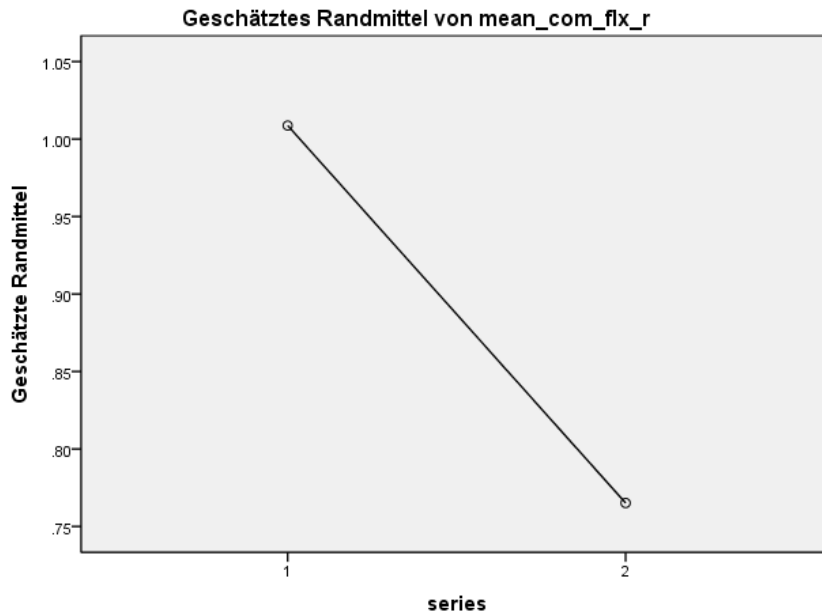
	N
series 1	20
series 2	5

dependent variable: mean\_com\_flex\_r

Quelle	Quadratsumme vom Typ III	Df	Mittel der Quadrate	F	Sig.
Korrigiertes Modell	1.968 <sup>a</sup>	2	.984	3.546	.046
Konstanter Term	.070	1	.070	.254	.619
mean_age	1.430	1	1.430	5.154	<b>.033</b>
Series	.228	1	.228	.821	.375
Fehler	6.103	22	.277		
Gesamt	31.111	25			
Korrigierte Gesamtvariation	8.071	24			

a. R-Quadrat = .244 (korrigiertes R-Quadrat = .175)

The common flexors enthesal features are significantly affected by age in the females on the right side, but not between the sub-sites.



Die Kovariaten im Modell werden anhand der folgenden Werte berechnet: mean age = 42.0400

In the common flexors, the uphill females show slightly higher scores, although they are not very high generally in both series here.

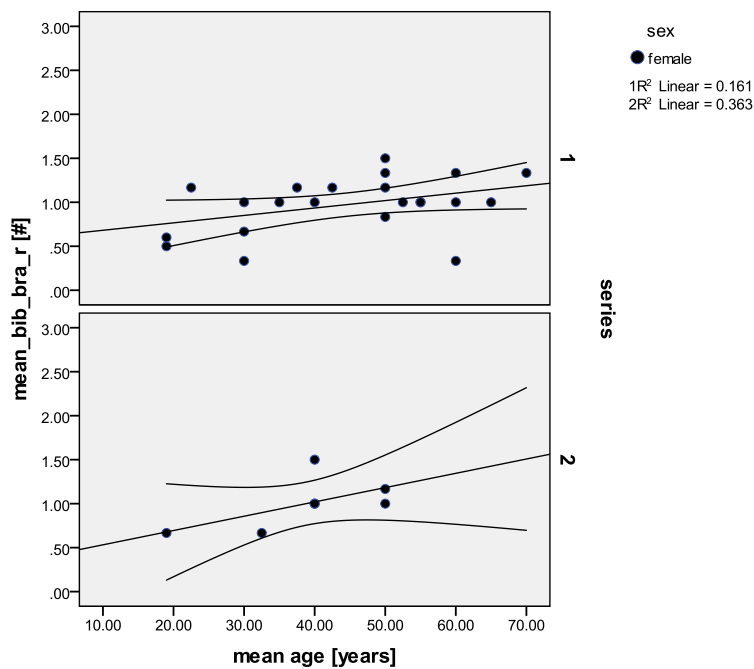


**Figure 105.a.** Scatterplot of the pooled muscle group *M. biceps brachii* – *M. brachialis* (proximal radius - ulna), females of the uphill (1) and downhill site (2), right side. This feature is significantly affected by age in both groups (Figure 105b).

**Figure 105.b.** Results of the univariate analysis for the right *M. biceps brachii* – *M. brachialis*.

		N
series	1	22
	2	7

dependent variable: mean\_bif\_r

Quelle	Quadratsumme vom Typ III	Df	Mittel der Quadrate	F	Sig.
Korrigiertes Modell	.489 <sup>a</sup>	2	.244	2.978	.068
Konstanter Term	.964	1	.964	11.748	.002
mean_age	.485	1	.485	5.913	<b>.022</b>
Series	.034	1	.034	.414	.526
Fehler	2.133	26	.082		
Gesamt	30.499	29			
Korrigierte Gesamtvariation	2.621	28			

a. R-Quadrat = .186 (korrigiertes R-Quadrat = .124)

A statistically significant result with age is apparent in the females but not between the series for the *M. biceps/M. brachialis* pooled muscles on the right elbow.

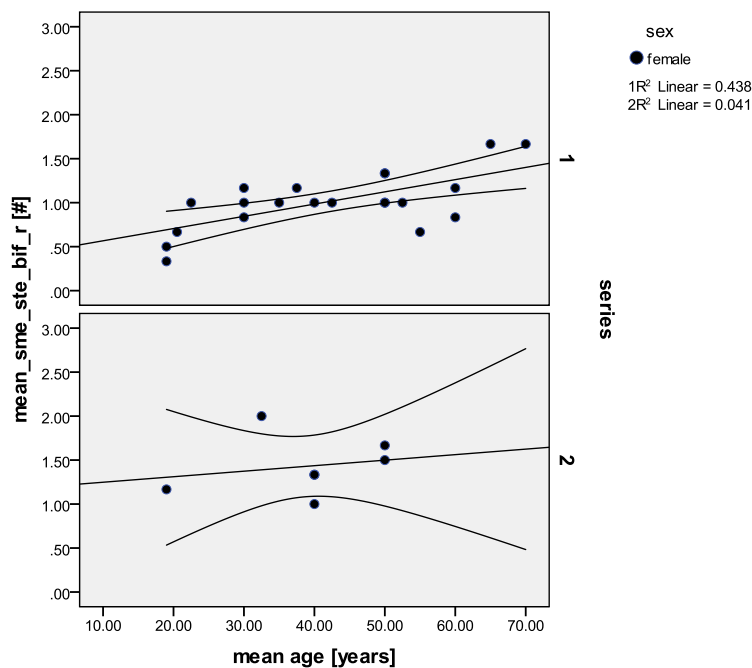


**Figure 106.a.** Scatterplot of the pooled muscle group *M. semimembranosus* – *M. semitendinosus* – *M. biceps femoris* (tuber ischiadicum), females of the uphill (1) and downhill site (2), right side. There is a slight increase of entheses scores with increasing age in both groups, which was significant in univariate analysis (see Figure 106b).

**Figure 106.b.** Results of the univariate analysis for the right *M. semimembranosus* – *M. semitendinosus* – *M. biceps femoris*.

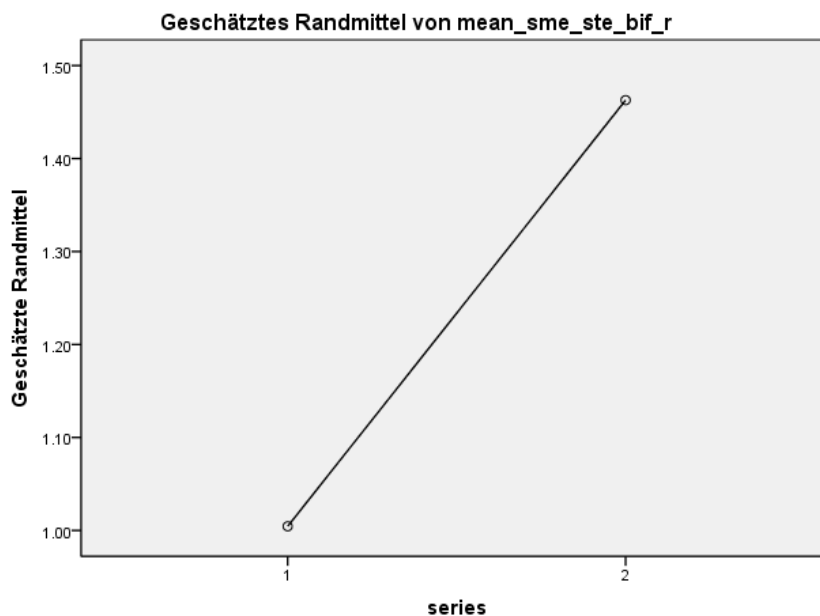
		N
series	1	21
	2	7

dependent variable: mean\_sme\_ste\_bif\_r

Quelle	Quadratsumme vom Typ III	Df	Mittel der Quadrate	F	Sig.
Korrigiertes Modell	1.834 <sup>a</sup>	2	.917	12.190	.000
Konstanter Term	1.418	1	1.418	18.858	.000
mean_age	.940	1	.940	12.492	<b>.002</b>
Series	1.090	1	1.090	14.497	<b>.001</b>
Fehler	1.880	25	.075		
Gesamt	38.778	28			
Korrigierte Gesamtvariation	3.714	27			

a. R-Quadrat = .494 (korrigiertes R-Quadrat = .453)

The pooled hip enthesal features are significantly affected by age, and there is a significant difference between the female series on the right side.



Die Kovariaten im Modell werden anhand der folgenden Werte berechnet: mean age = 41.4286

There is a marked difference in the scores between the females in the hip enthesal changes, whereat the downhill females show distinctly higher mean scores.

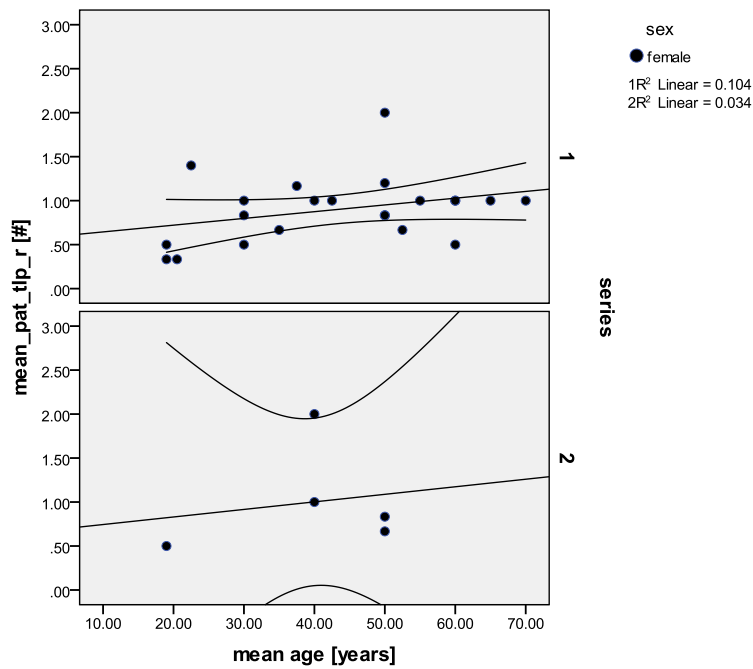


**Figure 107.** Scatterplot of the pooled muscle group *M. quadriceps femoris* (Patella – patellar ligament), females of the uphill (1) and downhill site (2), right side. There is a slight increase of entheses scores with higher age in the females of both sites.

### 10.1.2 Short summary

A statistically significant association in enthesal changes according to age was found in the females on the right side in the shoulder muscle markings *M. biceps brachii/subscapularis*, the *M. triceps brachii* (higher scores at younger age in the downhill females), the common extensors (only three individuals downhills), the common flexors, and the *M. biceps brachii*. Furthermore, in the *M. semimembranosus/ semitendinosus/biceps femoris* a significant result was found according to higher age and between the series. A non-significant age trend is apparent in the pooled muscle markings group *M. quadriceps femoris*.

### 10.1.3 Scatterplots joints – mean age, comparison females uphill-downhill – right side

Differences between the two archaeological sub-sites from Thunau (series 1 = uphill site, series 2 = downhill site), according to mean scores and mean age are shown here in the scatterplots (Figures 108 – 115) between the uphill and the downhill females, respectively. The scores of the joints of the females are plotted against increasing age of both groups, along with the least squares regression line and the 95% confidence regions. Univariate analyses were added if the difference between the groups was significant; graphs are added in cases of clear average differences between the sub-sites.

Legend for the graphs: dot: females: entheses – mean age, rhombus: females: joints – mean age

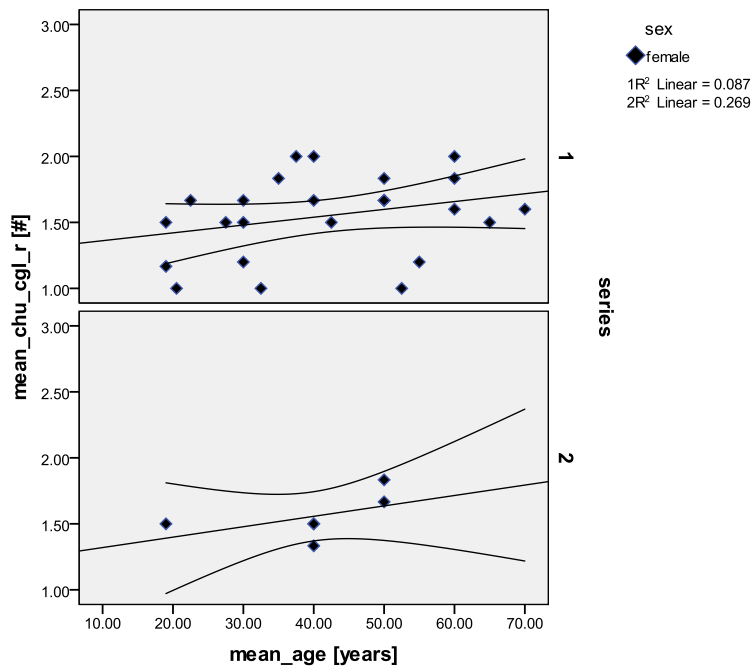


**Figure 108.** Scatterplot of pooled joint group *Caput humeri – Cavitas glenoidalis* (humerus, scapula – shoulder), females of the uphill (1) and downhill site (2), right side. There is a slight increase of joint changes with higher age visible in the females of both sub-sites. The scores are at about the same level in both groups.

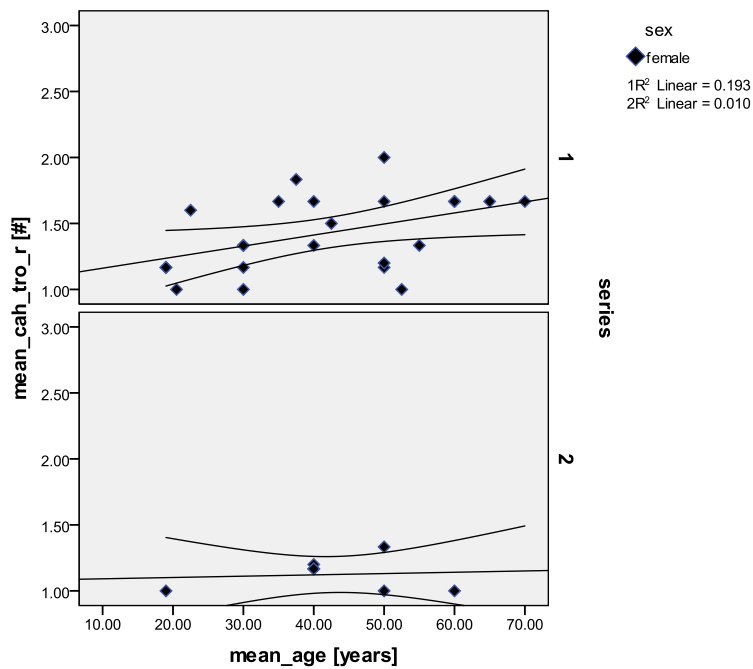


**Figure 109. a.** Scatterplot of the pooled joint group *Capitulum humeri* – *Trochlea* (distal humerus - elbow), right side, females of the uphill (1) and downhill site (2), right side. An increase of joint changes in the elbow with higher age is apparent in the females of sub-site 1, but not in series 2. A significant association was found (see Figure 109b).

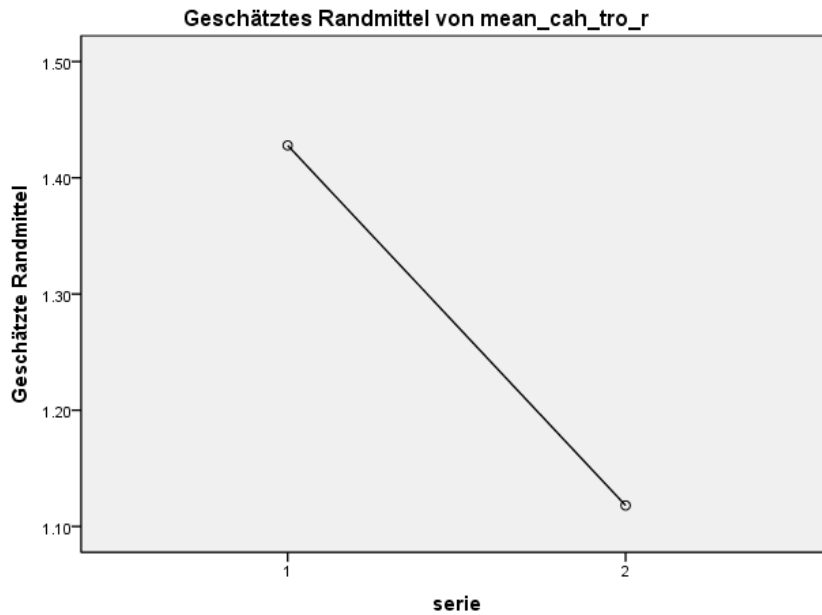
**Figure 109. b.** Results of the univariate analysis for the right *Capitulum humeri* – *Trochlea*.

		N
series	1	23
	2	7

dependent variable: mean\_cah\_tro\_r

Quelle	Quadratsumme vom Typ III	df	Mittel der Quadrate	F	Sig.
Korrigiertes Modell	.800 <sup>a</sup>	2	.400	6.647	.004
Konstanter Term	2.771	1	2.771	46.037	.000
mean_age	.310	1	.310	5.146	<b>.032</b>
series	.514	1	.514	8.546	<b>.007</b>
Fehler	1.625	27	.060		
Gesamt	57.551	30			
Korrigierte Gesamtvariation	2.425	29			

The pooled joint group *Capitulum humeri*/*Trochlea* is significantly affected by age and by sub-sites ( $p=.007$ ) in the females on the right side.



Die Kovariaten im Modell werden anhand der folgenden Werte berechnet: mean\_age = 41.9167

There is a marked difference apparent between the scores of the two female sub-sites, whereat the uphill females display the higher mean scores in the distal humeral joint facets.

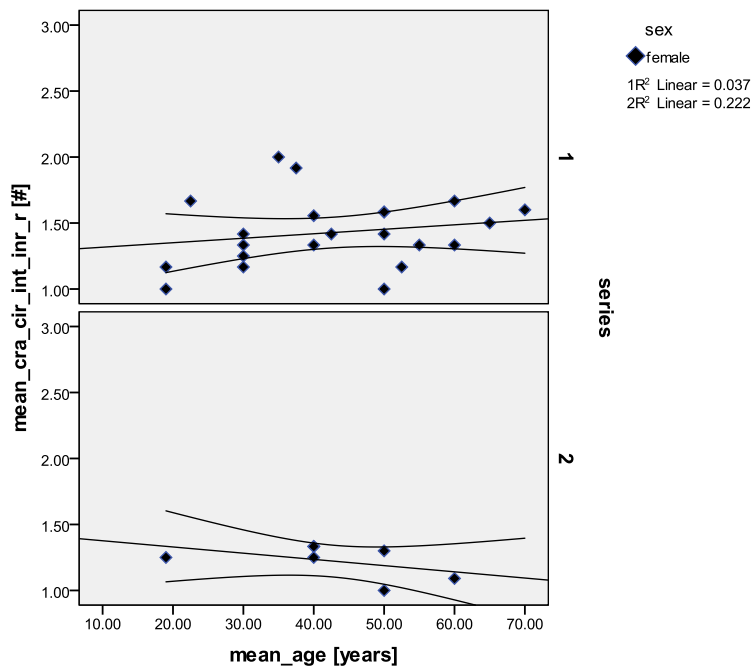


**Figure 110.** Scatterplot of the pooled joint group *Caput radii, Circumferentia articularis radii, Incisura trochlearis, Incisura radialis* (distal humerus - elbow), females of the uphill (1) and downhill (2) site, right side. There is a slight increase of joint changes at the elbow with increasing age in the females of sub-site 1, but not in series 2.

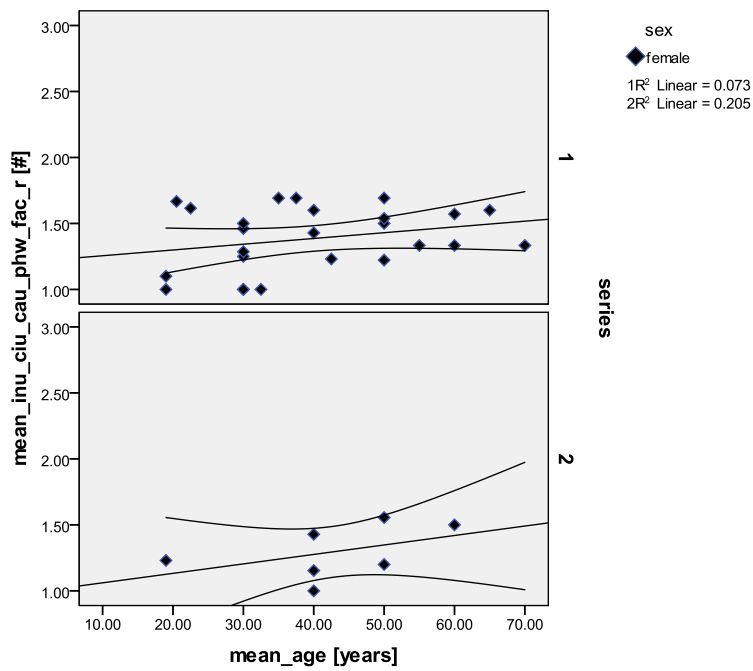


**Figure 111.** Pooled joints *Incisura ulnaris*, *Circumferentia articularis ulnae*, *Caput ulnae*, proximal wrist bones, *Facies articularis carpalis* (distal radius and ulna, proximal row of wrist bones - wrist), females of the uphill (1) and downhill site (2), right side. There is a slight increase of joint changes with higher age in the wrist bones of the female sub-sites.

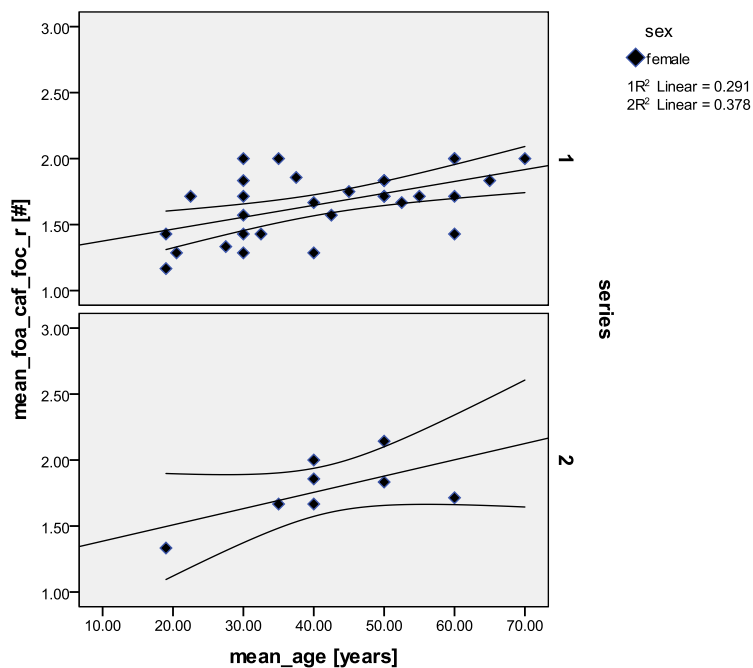


**Figure 112.a.** Scatterplot of the pooled joint group *Fossa acetabuli*, *Caput femoris*, *Fovea capitis (Os ilium acetabulum)*, femoral head - hip joint), females of the uphill (1) and downhill site (2), right side. This feature is significantly affected by age in the females of both groups (see Figure 112b).

**Figure 112.b.** Results of the univariate analysis for the right *Fossa acetabuli*, *Caput femoris*, *Fovea capitis*.

		N
series	1	30
	2	8

dependent variable: mean\_foa\_caf\_foc\_r

Quelle	Quadratsumme vom Typ III	df	Mittel der Quadrate	F	Sig.
Korrigiertes Modell	.749 <sup>a</sup>	2	.374	8.617	.001
Konstanter Term	6.346	1	6.346	146.099	.000
mean_age	.661	1	.661	15.222	<b>.000</b>
series	.083	1	.083	1.916	.175
Fehler	1.520	35	.043		
Gesamt	110.018	38			
Korrigierte Gesamtvariation	2.269	37			

a. R-Quadrat = .330 (korrigiertes R-Quadrat = .292)

The pooled hip joint features are statistically significantly affected by age ( $p=.000$ ) in the two female sub-sites.

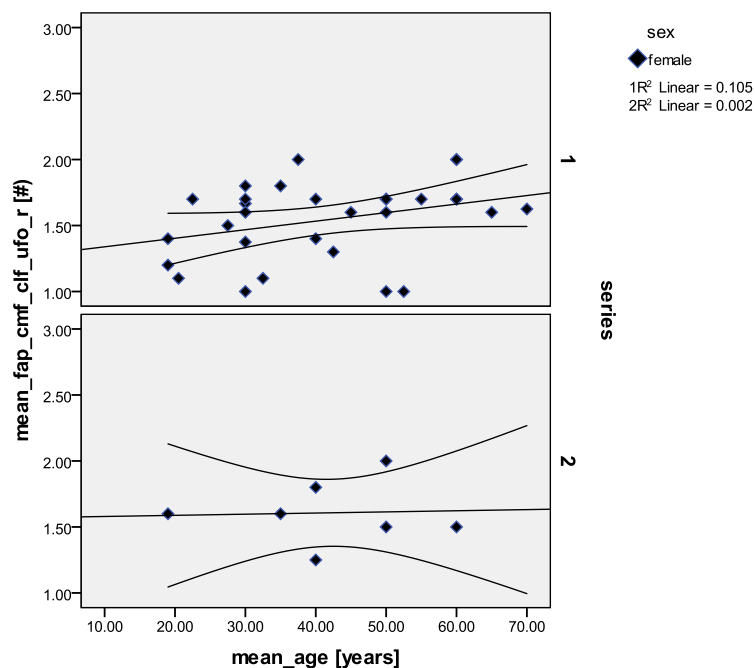


**Figure 113.** Pooled joint group *Facies patellaris*, *Condylus medialis femoris*, *Condylus lateralis femoris*, distal margin of *Fossa intercondylaris* (distal femur - knee), females of the uphill (1) and downhill (2) site, right side. There is a slight increase of scores in the knee joint with increasing age in the females of series 1, but not in series 2.

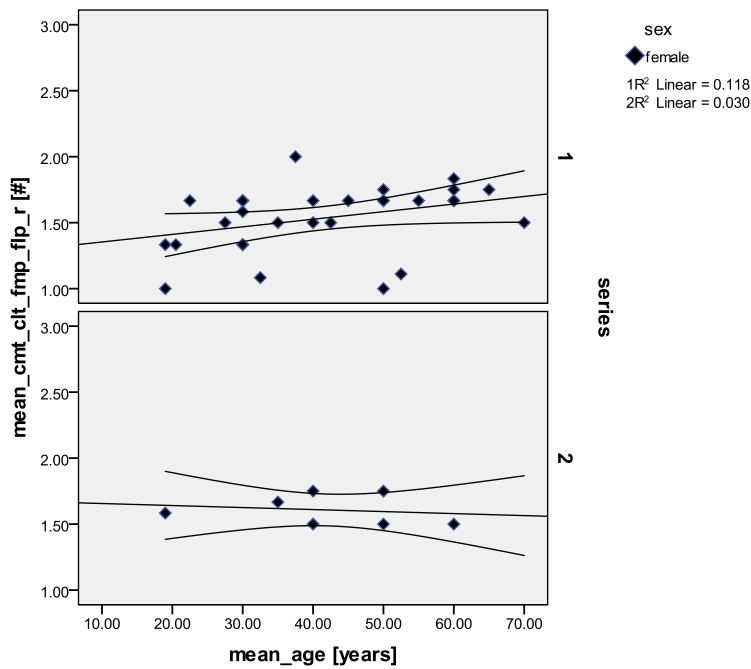


**Figure 114.** Scatterplot of the pooled joint group *Condylus medialis tibiae*, *Condylus lateralis tibiae*, *Facies medialispatellae*, *Facies lateralis patellae* (proximal tibia, patella - knee joint), females of the uphill (1) and downhill site (2), right side. There is a slight increase of joint changes with increasing age in the females of sub-site 1, but not in group 2.

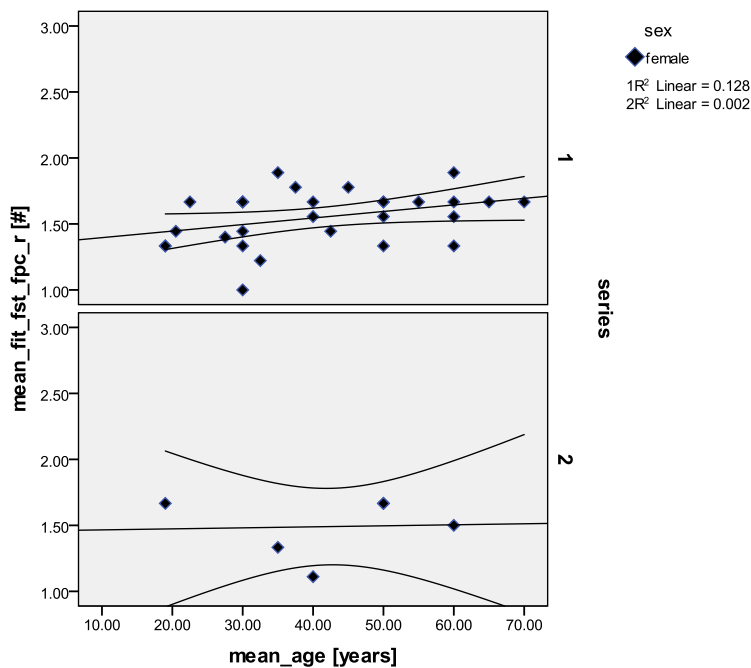


**Figure 115.** Scatterplot of the pooled joint group *Facies articularis inferior tibiae*, *Facies articularis superior talus*, *Facies aricularis talaris posterior calcanei* (distal tibia - ankle), females of the uphill (1) and downhill site (2), right side. A slight increase of joint changes with higher age is apparent in the females of the uphill site, but not in the downhill site.

#### 10.1.4 Short summary

A statistically significant association with both age and between the series was found in the females on the right side for the pooled joints *Capitulum humeri/Trochlea*. Further significant results with higher age became apparent in the right pooled joint features *Fossa acetabuli/Caput femoris*, *Fovea capitis* of the hip.

### 10.1.5 Scatterplots entheses – mean age, comparison females

#### uphill-downhill – left side

According to mean scores and mean age, differences between the two archaeological sub-sites from Thunau (series 1 = uphill site, series 2 = downhill site), are shown in the scatterplots (Figures 116 – 127) between the uphill and the downhill females, respectively. The scores of the enthesal changes of the females are plotted against increasing age of both groups, along with the least squares regression line and the 95% confidence regions. Univariate analyses were added if the difference between the groups was significant; graphs are added in cases of clear average differences between the sub-sites.

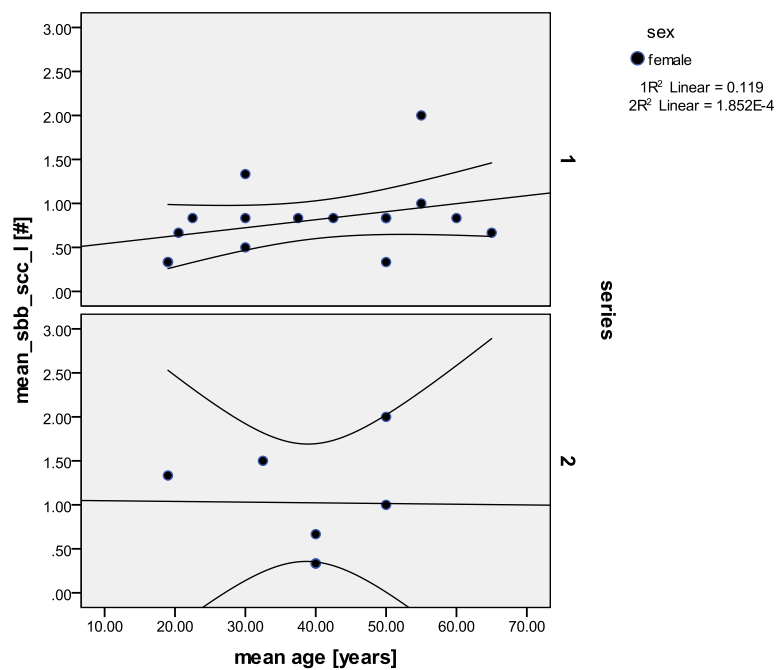


**Figure 116.** Scatterplot of the pooled muscle group *M. biceps brachii* – *M. subscapularis* (scapula and proximal humerus - shoulder), females of the uphill (1) and downhill site (2), left side. There is a slight increase of enthesal changes with higher age in the females of sub-site 1, but not in sub-site 2.

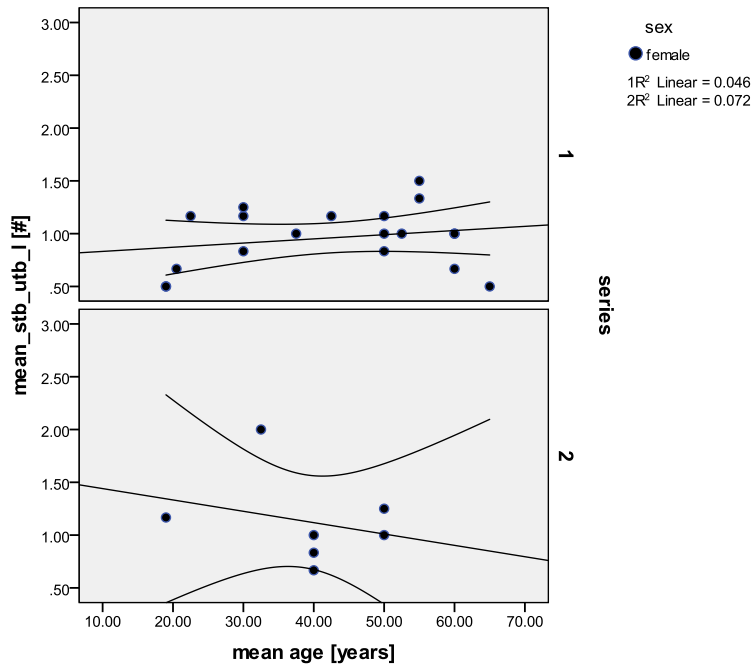


**Figure 116.** Scatterplot of the pooled muscle group *M. triceps brachii* (scapula – proximal ulna), females of the uphill (1) and downhill site (2), left side. There is no noticeable association of scores with higher age in the females of both sub-sites.

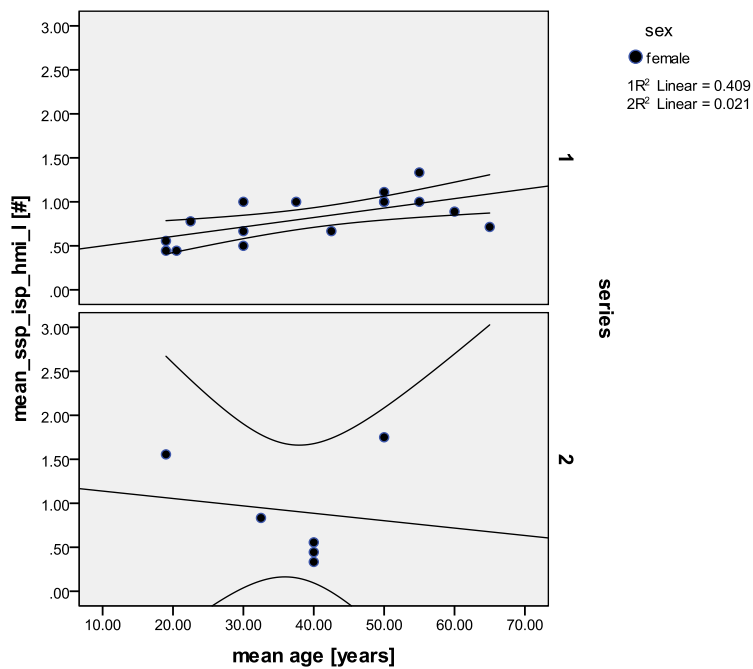


**Figure 117.** Scatterplot of the pooled muscle group *M. supraspinatus - M. infraspinatus - M. teres minor* (prox. humerus), females of the uphill (1) and downhill site (2), left side. There is a slight increase of the scores with higher age in the females of sub-site 1, but not in group 2.

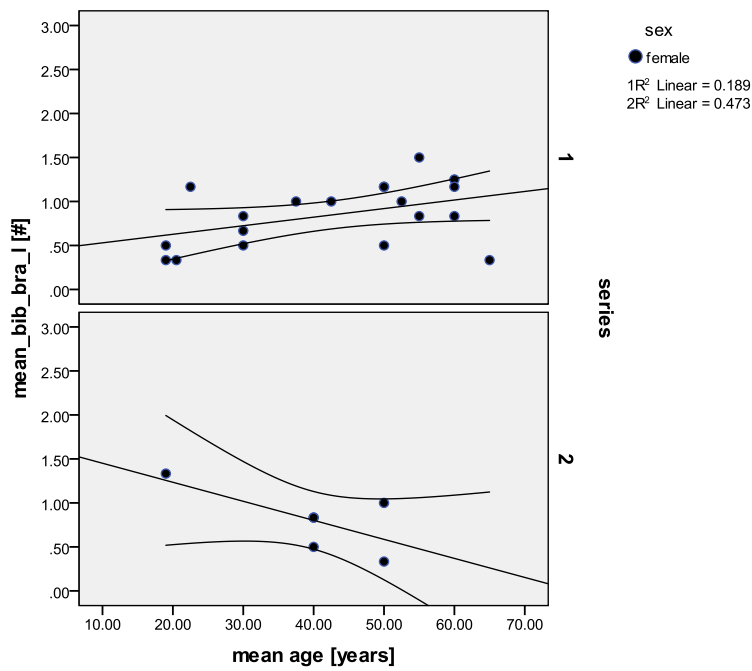


**Figure 118.** Scatterplot of the pooled muscle group *M. biceps brachii* – *M. brachialis* (prox. radius and proximal ulna - elbow), females of the uphill (1) and downhill site (2), left side. There is a slight increase of scores with higher age in the females of sub-site 1, contrary to group 2.

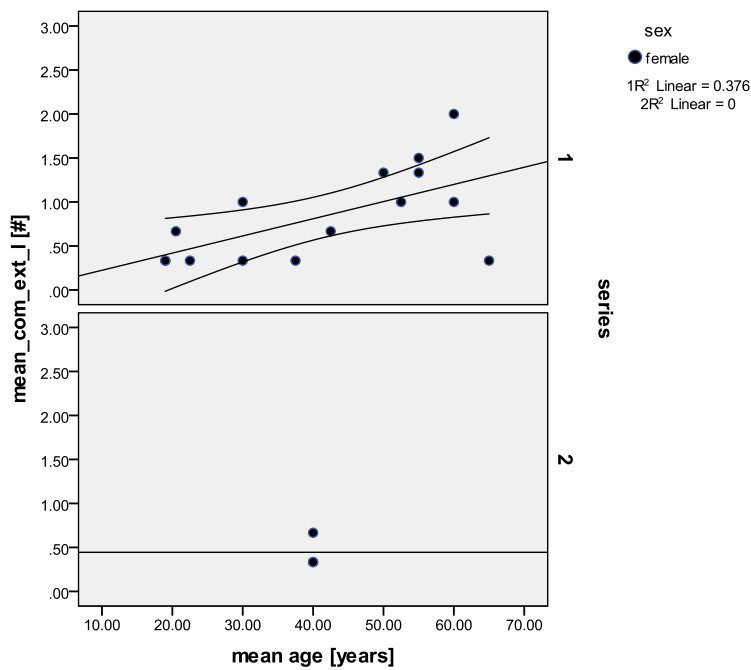


**Figure 119.a.** Scatterplot of the pooled **common extensors** muscle group (distal lateral humerus), females of the uphill (1) and downhill site (2), left side. There is an increase of scores with higher age in the females of sub-site 1, contrary to group 2. The significant result may be biased by the small number of individuals in group 2 (see Figure 119b).

**Figure 119. b.** Results of the univariate analysis for the left common extensors.

		N
series	1	15
	2	3

dependent variable: mean\_com\_ext\_1

Quelle	Quadratsumme vom Typ III	df	Mittel der Quadrate	F	Sig.
Korrigiertes Modell	1.860 <sup>a</sup>	2	.930	5.499	.016
Konstanter Term	.045	1	.045	.267	.613
mean_age	1.482	1	1.482	8.762	<b>.010</b>
series	.332	1	.332	1.966	.181
Fehler	2.537	15	.169		
Gesamt	15.028	18			
Korrigierte Gesamtvariation	4.397	17			

a. R-Quadrat = .423 (korrigiertes R-Quadrat = .346)

The common extensor muscle markings in the females on the left side are significantly affected by age ( $p=.010$ ), but not between the sub-sites.

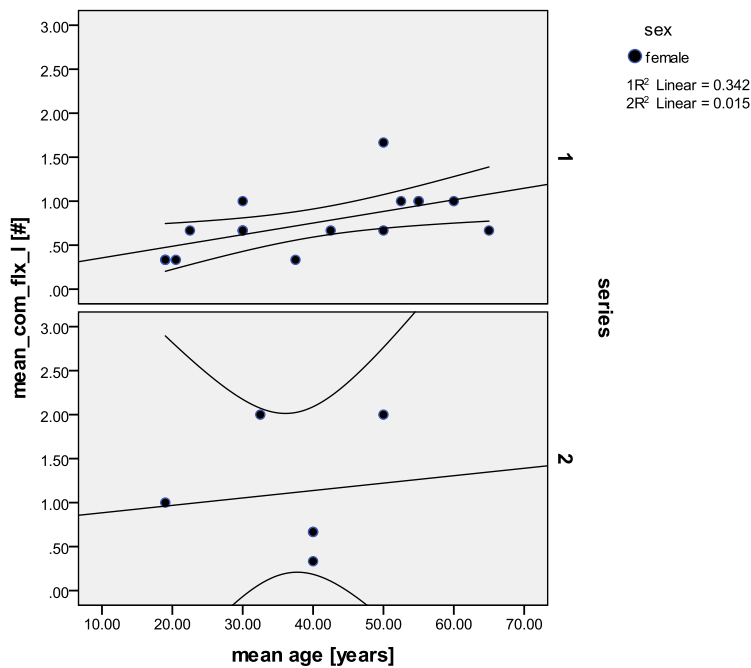


**Figure 120.** Scatterplot of the pooled **common flexors muscle group** (distal medial humerus), females of the uphill (1) and downhill site (2), left side. There is a slight increase of scores with higher age in both female groups.

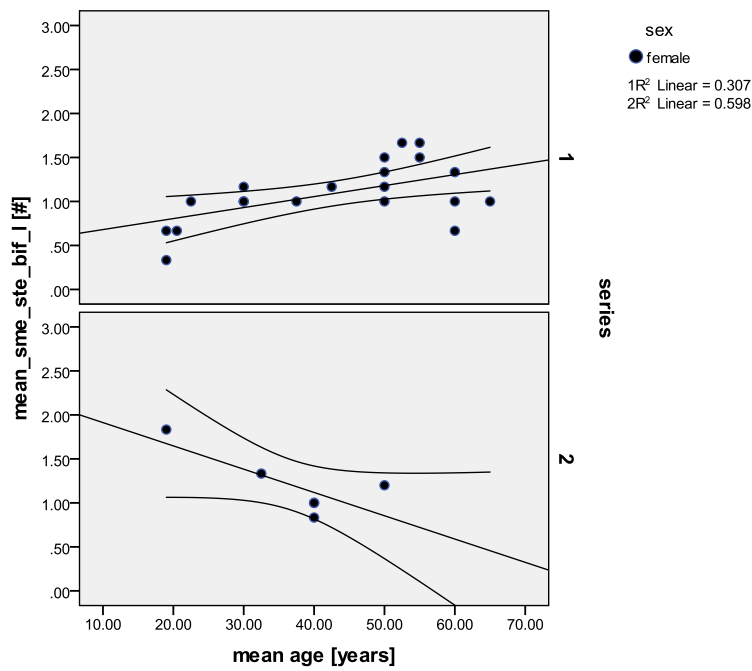


**Figure 121.** Scatterplot of the pooled muscle group *M. semimembranosus* – *M. semitendinosus* – *M. biceps femoris* (tuber ischiadicum), females of the uphill (1) and downhill site (2), left side. There is an increase of scores with higher age in the females of sub-site 1, contrary to group 2.

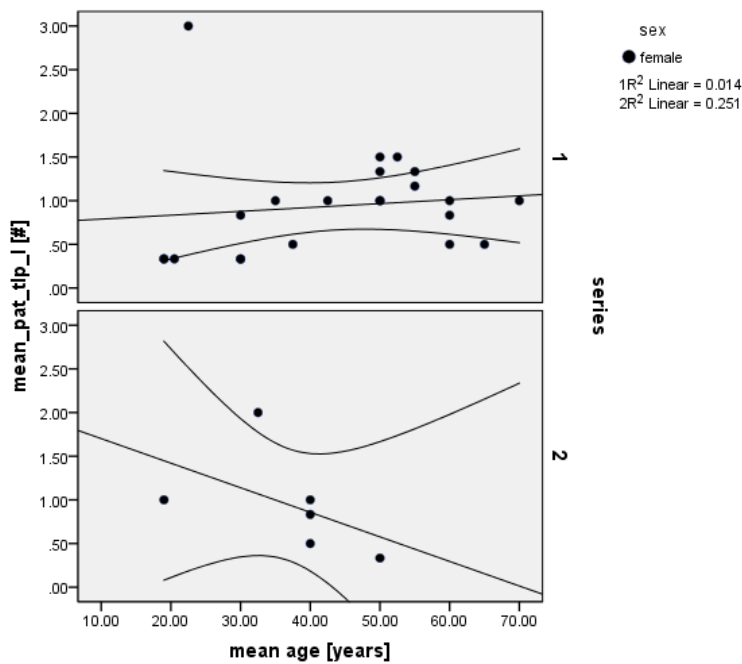


**Figure 122.** Scatterplot of the pooled muscle group *M. quadriceps femoris* (Patella – patellar ligament), females of the uphill (1) and downhill site (2), left side. There is a very slight rise of scores with increasing age in the females of sub-site 1, contrary to group 2.

### 10.1.6 Short summary

A statistically significant association with higher age was found in the females in the left extremity for the common extensors (this result may be biased by the small number of individuals (2) in the downhill females). A non-significant age trend is visible in the common flexors. The downhill females show partially markedly higher scores at younger age than the uphill females (*M. triceps brachii*, *M. supraspinatus/infraspinatus/teres minor*, *M. biceps/brachialis*, especially *M. semimembranosus/semitendinosus/biceps femoris* and *M. quadriceps femoris*; however, the results may be biased by the low number of individuals in the downhill series).

### 10.1.7 Scatterplots joints – mean age, comparison females uphill-downhill – left side

Differences between the two archaeological sub-sites from Thunau (series 1 = uphill site, series 2 = downhill site), according to mean scores and mean age are shown here in the scatterplots (Figures 123 – 131) between the uphill and the downhill females, respectively. The scores of the left side joint features of the females are plotted against increasing age of both groups, along with the least squares regression line and the 95% confidence regions. Univariate analyses were added if the difference between the groups was significant; graphs are added in cases of clear average differences between the sub-sites.

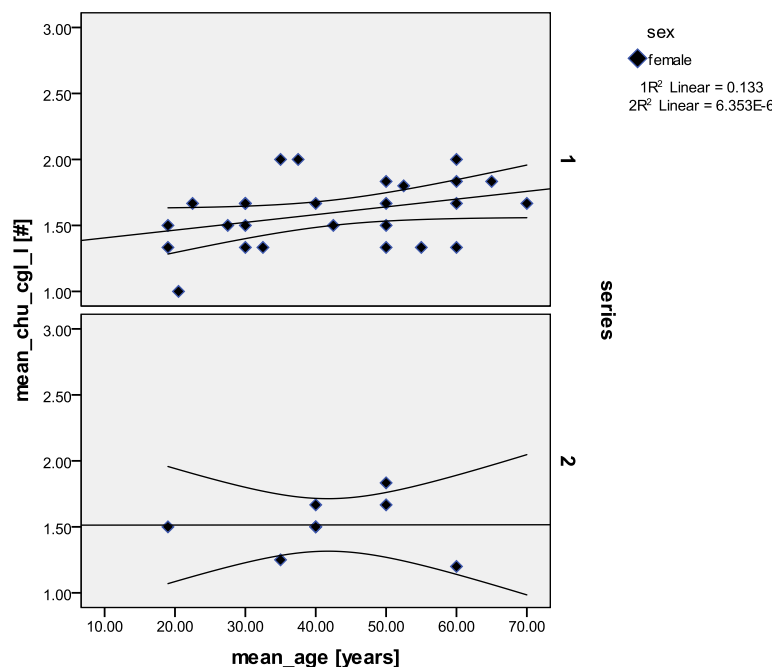


**Figure 123.** Scatterplot of the pooled joint group *Caput humeri – Cavitas glenoidalis* (shoulder - humerus, scapula), females of the uphill (1) and downhill site (2), left side. There is a slight increase of joint feature scores with higher age in the females of sub-site 1, but not in group 2.

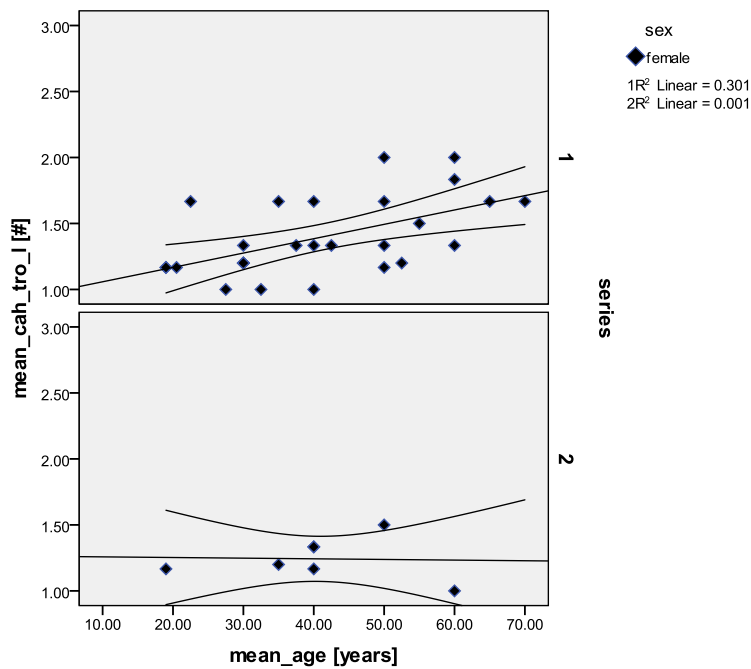


**Figure 124. a.** Scatterplot of the pooled joint group *Capitulum humeri – Trochlea* (dist. humerus - elbow), females of the uphill (1) and downhill site (2), left side. There is an increase of scores with higher age in the females of sub-site 1, but not in sub-site 2. However, this feature was found to be significant with age (see Figure 124b).

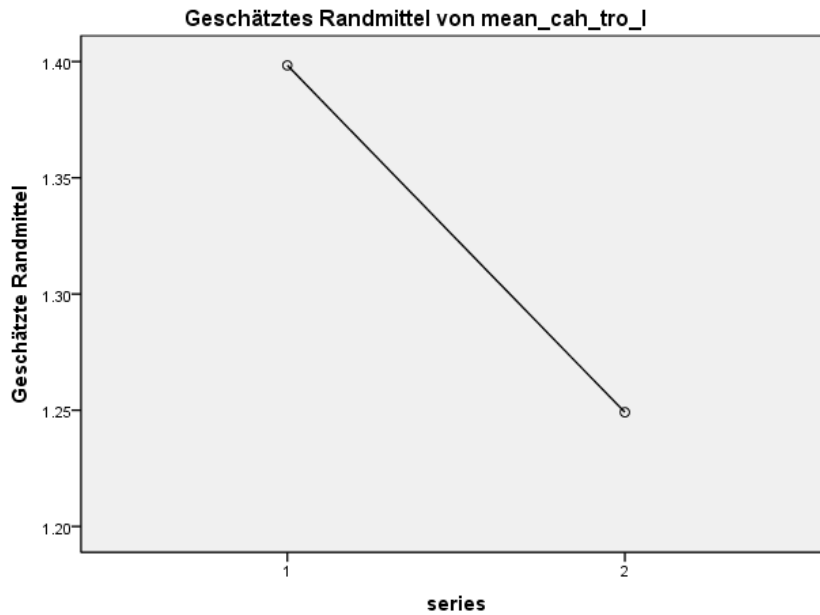
**Figure 124. b.** Results of the univariate analysis of the left side for the pooled joint group *Capitulum humeri/Trochlea*.

	N
series 1	27
2	7

dependent variable: mean\_cah\_tro\_l

Quelle	Quadratsumme vom				
	Typ III	df	Mittel der Quadrate	F	Sig.
Korrigiertes Modell	.702 <sup>a</sup>	2	.351	5.983	.006
Konstanter Term	2.981	1	2.981	50.806	.000
mean_age	.565	1	.565	9.626	<b>.004</b>
series	.124	1	.124	2.109	.156
Fehler	1.819	31	.059		
Gesamt	66.117	34			
Korrigierte Gesamtvariation	2.521	33			

A statistically significant result ( $p=.004$ ) was found for the left distal humeral features with higher age in the females.



Die Kovariaten im Modell werden anhand der folgenden Werte berechnet: mean\_age = 41.2500

The uphill females display somewhat higher mean scores in the *Capitulum humeri/Trochlea* joint features on the left side.

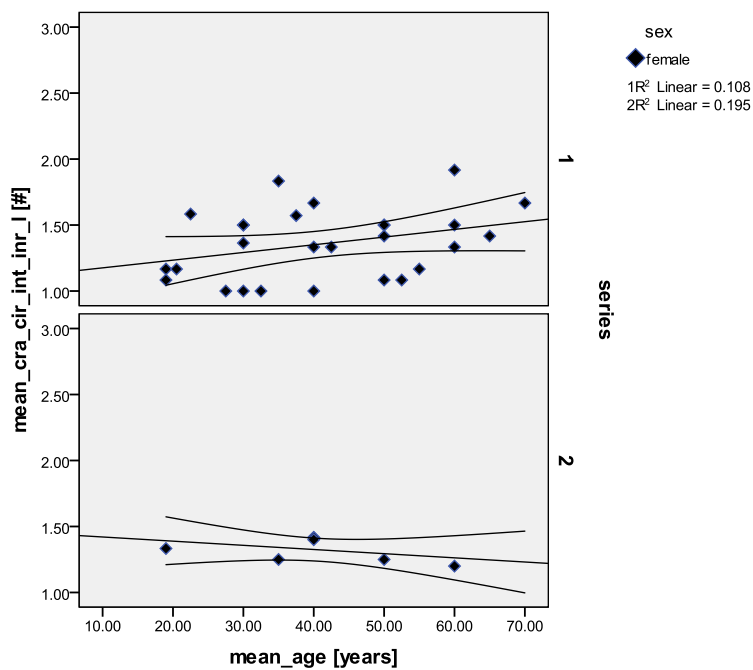


**Figure 125.** Pooled joint group *Caput radii*, *Circumferentia articularis radii*, *Incisura trochlearis*, *Incisura radialis* (proximal radius and ulna - elbow), females of the uphill (1) and downhill site (2), left side. An increase of scores with higher age is visible in the females of sub-site 1, but not in series 2.

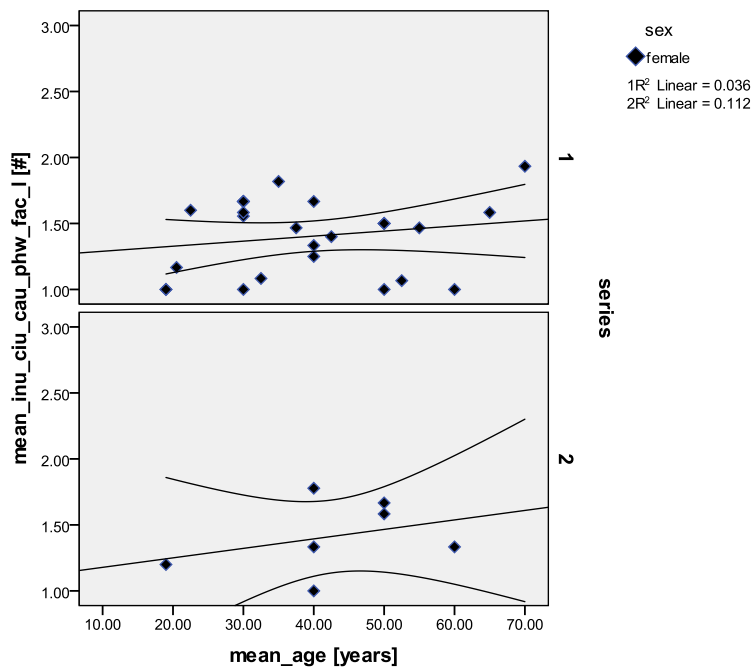


**Figure 126.** Pooled joint group *Incisura ulnaris*, *Circumferentia articularis ulnae*, *Caput ulnae*, proximal wrist bones, *Facies articularis carpalis* (distal radius and ulna, proximal row of wrist bones - wrist), females of the uphill (1) and downhill site (2), left side. There is a slight increase of scores with higher age in the females of both sub-sites.

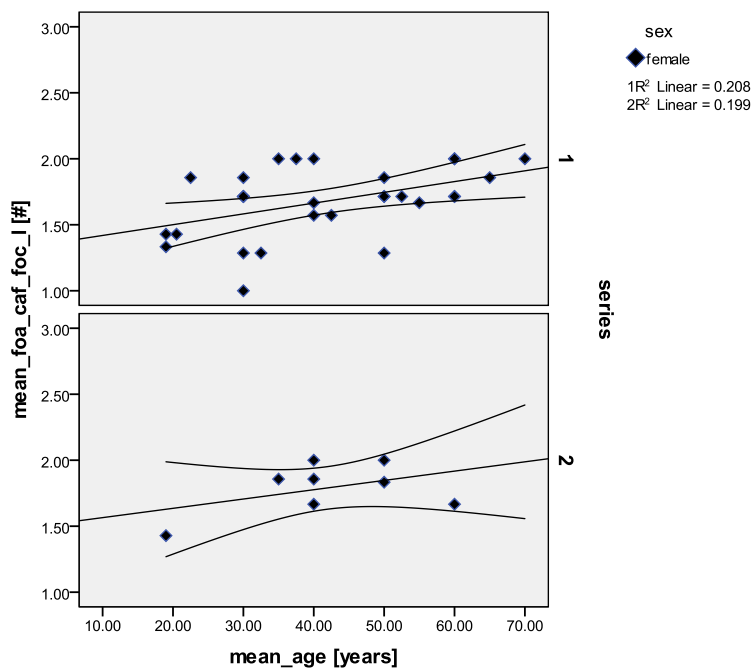


**Figure 127.a.** Scatterplot of the pooled joint group *Fossa acetabuli*, *Caput femoris*, *Fovea capitis* (*Os ilium acetabulum*), femoral head - hip joint), females of the uphill (1) and downhill site (2), left side. There is an increase of scores with higher age in the females of both sub-sites, with higher scores at young age in both groups. A significant result was found with age (see Figure 127b).

**Figure 127.b.** Results of the univariate analysis for the pooled joint facets *Fossa acetabuli*, *Caput femoris*, *Fovea capitis*.

	N
series 1	29
2	8

dependent variable: mean\_foa\_caf\_foc\_1

Quelle	Quadratsumme vom Typ III	df	Mittel der Quadrate	F	Sig.
Korrigiertes Modell	.532 <sup>a</sup>	2	.266	5.163	.011
Konstanter Term	6.878	1	6.878	133.401	.000
mean_age	.456	1	.456	8.840	<b>.005</b>
series	.077	1	.077	1.488	.231
Fehler	1.753	34	.052		
Gesamt	109.474	37			
Korrigierte Gesamtvariation	2.285	36			

a. R-Quadrat = .233 (korrigiertes R-Quadrat = .188)

In the left pooled hip joint features, a significant result ( $p=.005$ ) was apparent with higher age in the females of Thunau.

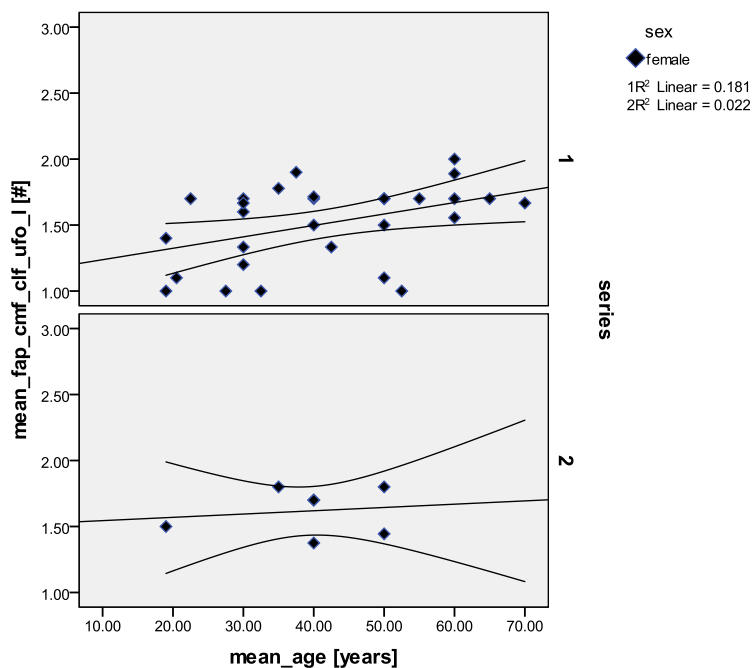


**Figure 128.a.** Scatterplot of the pooled joint group *Facies patellaris*, *Condylus medialis femoris*, *Condylus lateralis femoris*, distal margin of *Fossa intercondylaris* (distal femur - knee), females of the uphill (1) and downhill site (2), left side. This feature is significantly affected by age in both female sub-sites (see Figure 128b).

**Figure 128.b.** Results of the univariate analysis for the pooled joint facets *Facies patellaris*, *Condylus medialis femoris*, *Condylus lateralis femoris*.

		N
series	1	29
	2	7

dependent variable: mean\_fap\_cmf\_clf\_ufo\_1\_new

Quelle	Quadratsumme vom				
	Typ III	Df	Mittel der Quadrate	F	Sig.
Korrigiertes Modell	.504 <sup>a</sup>	2	.252	3.641	.037
Konstanter Term	5.398	1	5.398	77.934	.000
mean_age	.442	1	.442	6.376	<b>.017</b>
series	.089	1	.089	1.282	.266
Fehler	2.286	33	.069		
Gesamt	87.295	36			
Korrigierte Gesamtvariation	2.790	35			

a. R-Quadrat = .181 (korrigiertes R-Quadrat = .131)

A statistically significant result in the left distal femoral joint features was found for the females.

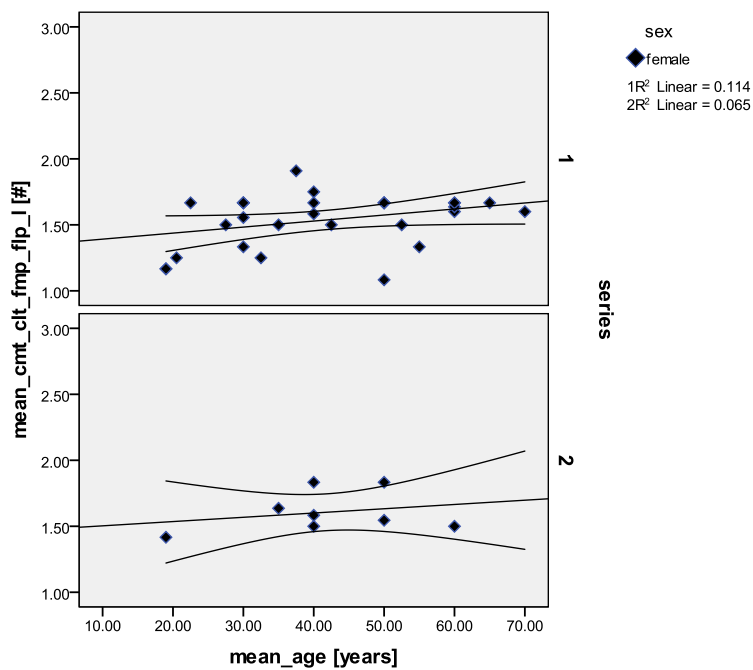


**Figure 129.** Scatterplot of the pooled joint group *Condylus medialis tibiae*, *Condylus lateralis tibiae*, *Facies medialis patellae*, *Facies lateralis patellae* (proximal tibia, patella - knee joint), females of the uphill (1) and downhill site (2), left side. A very slight increase of scores with higher age is apparent in the females of both sub-sites.

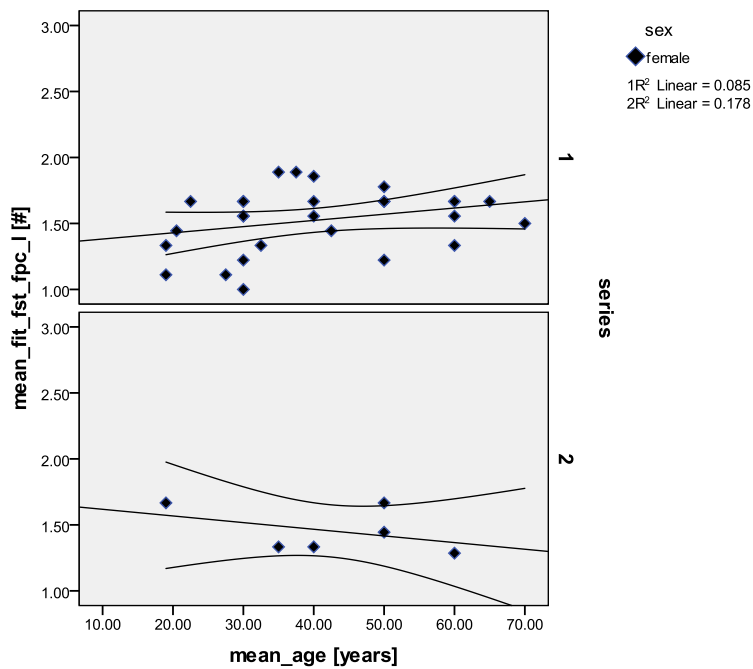


**Figure 130.** Scatterplot of the pooled joint group *Facies articularis inferior tibiae*, *Facies articularis superior talus*, *Facies articularis talaris posterior calcanei* (distal tibia - ankle), females of the uphill (1) and downhill (2) site, left side. A slight increase of scores with higher age was found in the females of sub-site 1, but not in group 2.

### 10.1.8 Short summary

A statistically significant result with age in the left extremity joint features of the females was found for the *Capitulum humeri/Trochlea* and the *Fossa acetabuli/Caput femoris/Fovea capitis* as well as for the *Facies patellaris*, *Condylus medialis femoris*, *Condylus lateralis femoris*, and the distal margin of the *Fossa intercondylaris*. A non-significant age trend is apparent in the *Condylus medialis tibiae/Condylus lateralis tibiae/Facies medialis patellae/Facies lateralis patellae*.

## 10.2 Scatterplots entheses – body height – females

### 10.2.1 Scatterplots entheses – body height, comparison females uphill-downhill – right side

Differences between the female groups of the two archaeological sub-sites of Thunau (series 1 = uphill site, series 2 = downhill site), according to mean scores of entheses and body height, are shown in scatterplots (Figures 131 – 138, right side, and section 10.2.3., Figures 139 – 146, left side). The scores of the muscle markings of the females of the two groups are plotted against increasing body height, along with the least squares regression line and the 95% confidence regions. Univariate analyses were added if the difference between the groups was significant; in cases of clear average differences between the sub-sites, graphs are added accessorially.

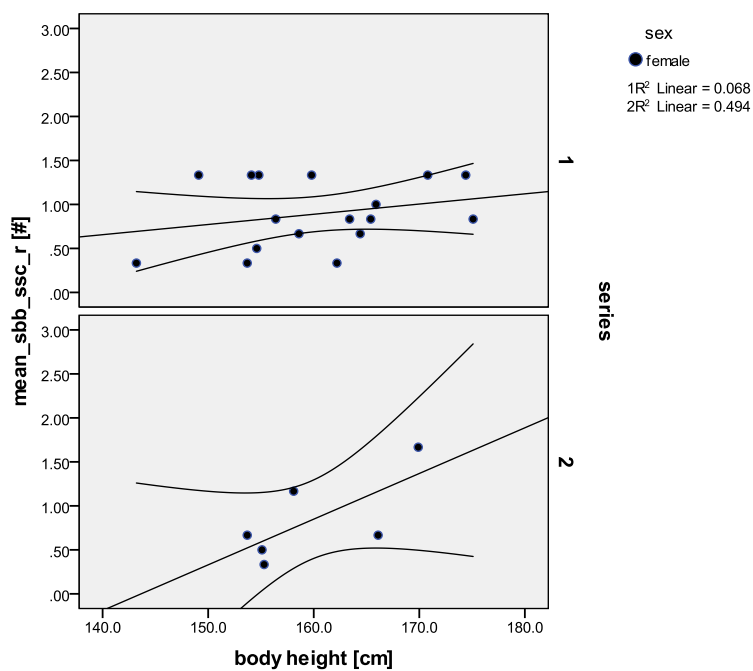


**Figure 131.** Scatterplot of the pooled muscle group *M. biceps brachii* – *M. subscapularis* (scapula – proximal humerus), females of the uphill (1) and downhill site (2), right side. There is a marked increase of scores with higher body size in the females of sub-site 2, and a rather slight one in the females of series 1.

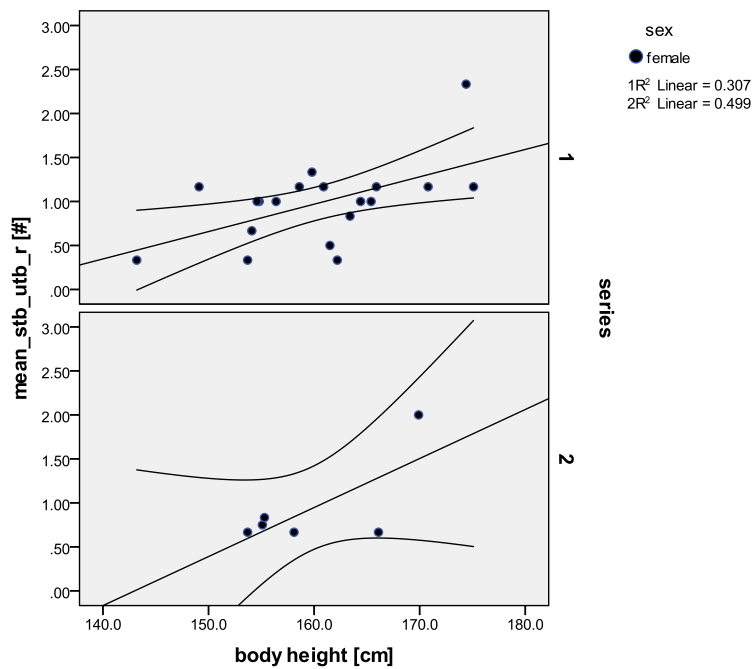


**Figure 132.a.** Scatterplot of the pooled muscle group *M. triceps brachii* (scapula – proximal ulna), females of the uphill (1) and downhill site (2), right side. There is a strong increase of scores with body height in the females of both sub-sites. A significant result was found (see Figure 132b).

**Figure 132. b.** Results of the univariate analysis for the pooled *M. triceps brachii*.

	N
series 1	19
series 2	6

dependent variable: mean\_stb\_utb\_r

Quelle	Quadratsumme vom Typ III	df	Mittel der Quadrate	F	Sig.
Korrigiertes Modell	1.753 <sup>a</sup>	2	.876	5.627	.011
Konstanter Term	1.193	1	1.193	7.660	.011
body height	1.740	1	1.740	11.174	<b>.003</b>
series	.003	1	.003	.020	.889
Fehler	3.426	22	.156		
Gesamt	28.701	25			
Korrigierte Gesamtvariation	5.179	24			

a. R-Quadrat = .338 (korrigiertes R-Quadrat = .278)

The pooled joint group of the *M. triceps brachii* is significantly affected by body height ( $p=.003$ ) in the females, but not by sub-site.

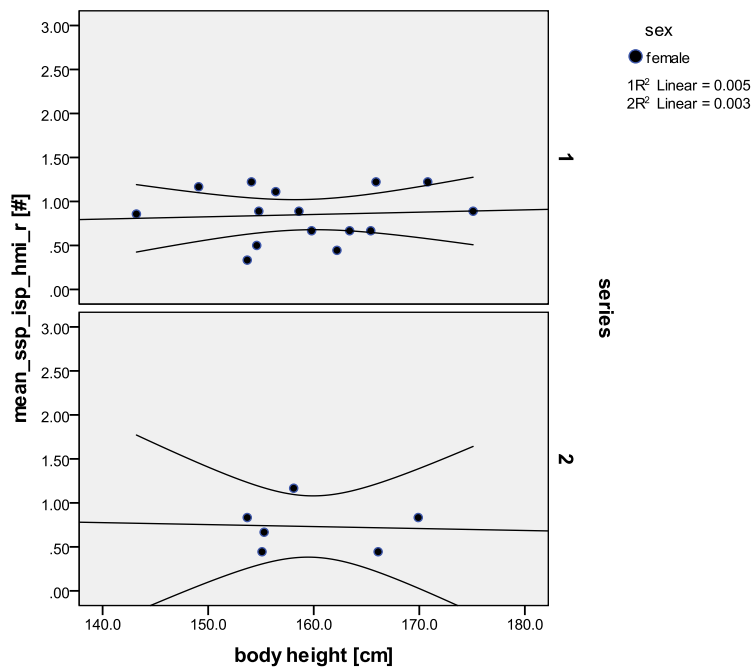


**Figure 133.** Scatterplot of the pooled muscle group *M. supraspinatus - M. infraspinatus - M. teres minor* (prox. humerus), females of the uphill (1) and downhill site (2), right side. There is no clear relationship between scores and body size in this feature.

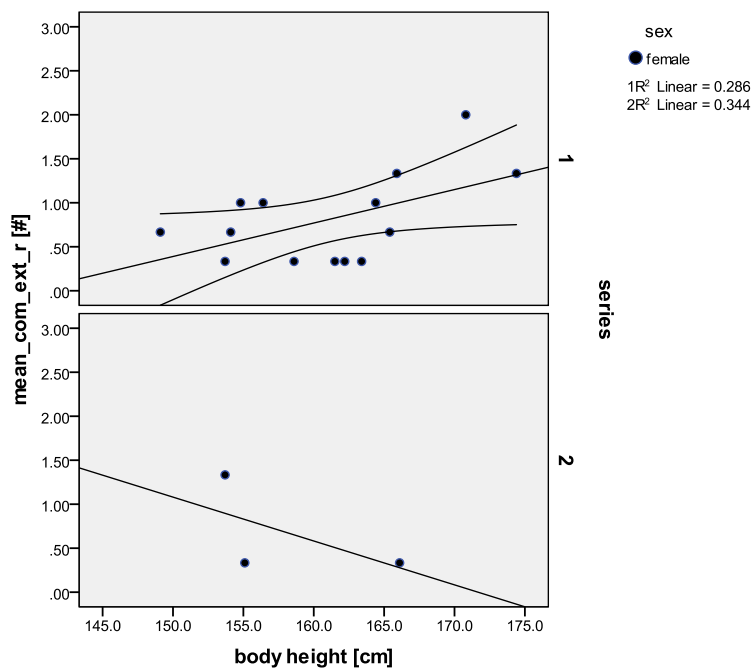


**Figure 134.** Scatterplot of the pooled **common extensors** muscle group (distal lateral humerus), females of the uphill (1) and downhill (2) site, right side. An increase of scores with higher body size is apparent in the females of sub-site 1, contrary to group 2. This result may be biased by the small number of individuals in sub-site 2.

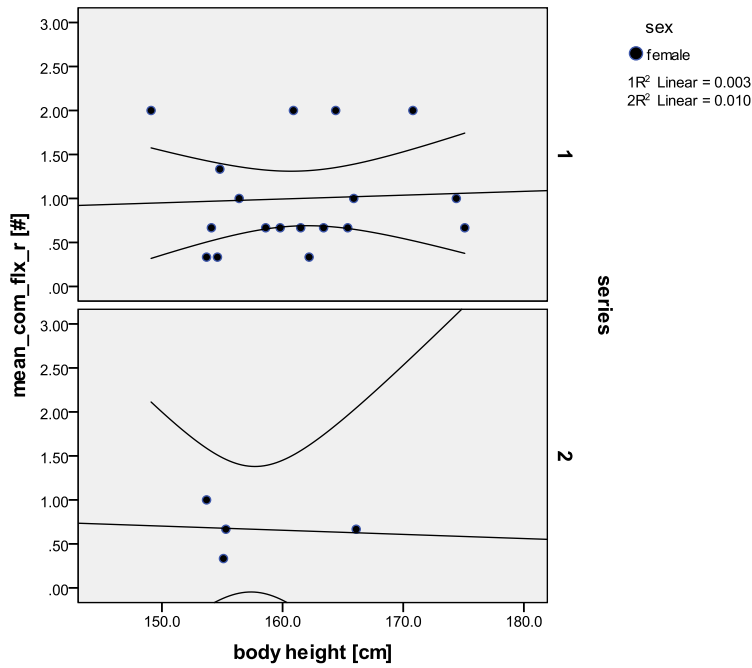


**Figure 135.** Scatterplot of the pooled **common flexors muscle group** (distal medial humerus), females of the uphill (1) and downhill (2) site, right side. There is no clear association between scores and body height in this feature.

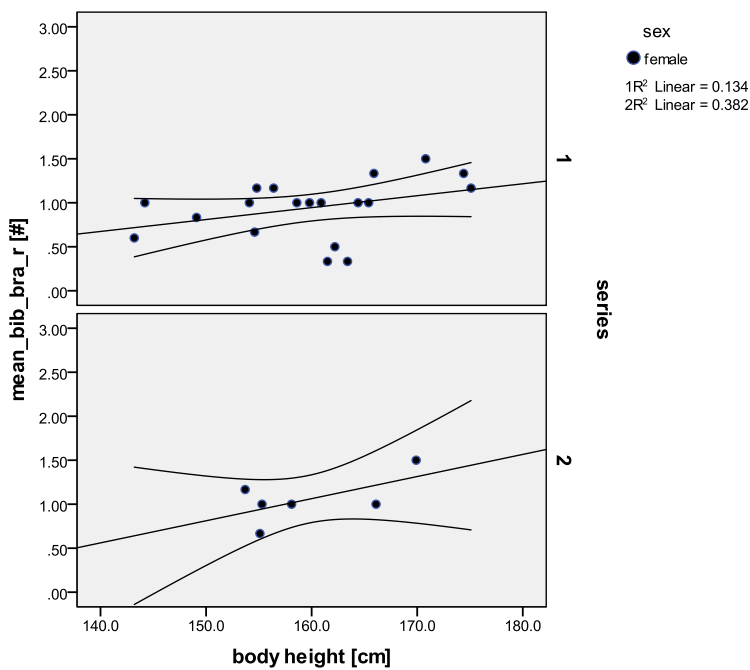


**Figure 136. a.** Scatterplot of the pooled muscle group *M. brachialis* (prox. radius - ulna), females of the uphill (1) and downhill site (2), right side. There is a slight increase of scores with increasing body height in the females of both sub-sites. This result was found to be significant (see Figure 136b).

**Figure 136. b.** Results of the univariate analysis for the pooled entheses attachment sites *M. biceps brachii* – *M. brachialis*.

		N
series	1	19
	2	6

dependent variable: mean\_bif\_bra\_r

Quelle	Quadratsumme vom Typ III	df	Mittel der Quadrate	F	Sig.
Korrigiertes Modell	.432 <sup>a</sup>	2	.216	2.460	.109
Konstanter Term	.129	1	.129	1.465	.239
body height	.375	1	.375	4.272	<b>.051</b>
series	.061	1	.061	.691	.415
Fehler	1.929	22	.088		
Gesamt	25.916	25			
Korrigierte Gesamtvariation	2.361	24			

a. R-Quadrat = .183 (korrigiertes R-Quadrat = .109)

A marginally significant result of higher scores with increasing body height was found in the right *M. biceps brachii*/*M. brachialis* in the females, but not between the series.

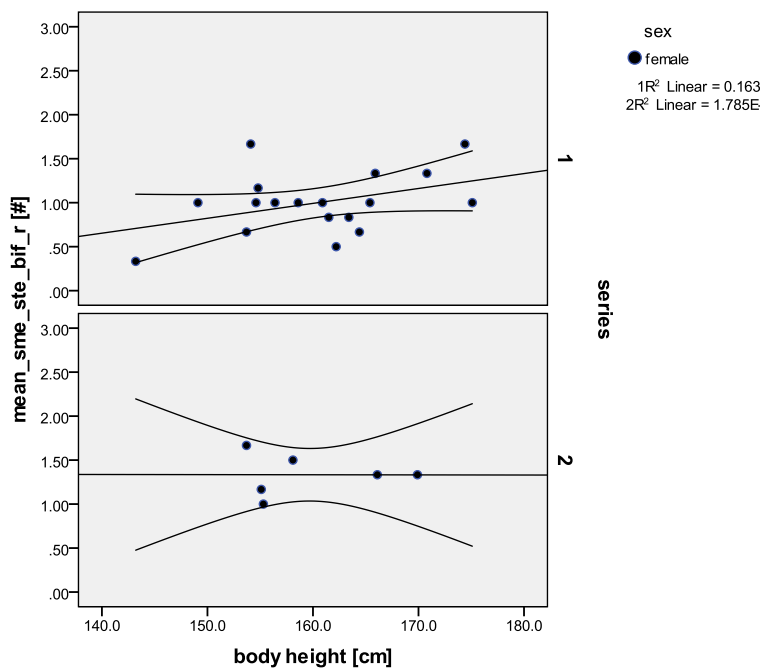


**Figure 137. a.** Scatterplot of the pooled muscle group *M. semimembranosus* – *M. semitendinosus* – *M. biceps femoris* (tuber ischiadicum), females of the uphill (1) and downhill site (2), right side. There is a slight increase of scores with higher body size in the females of sub-site 1, but not in series 2. This result was found to be significant (see Figure 137b).

**Figure 137. b.** Results of the univariate analysis for the pooled entheses attachment sites *M. semimembranosus* – *M. semitendinosus* – *M. biceps femoris*.

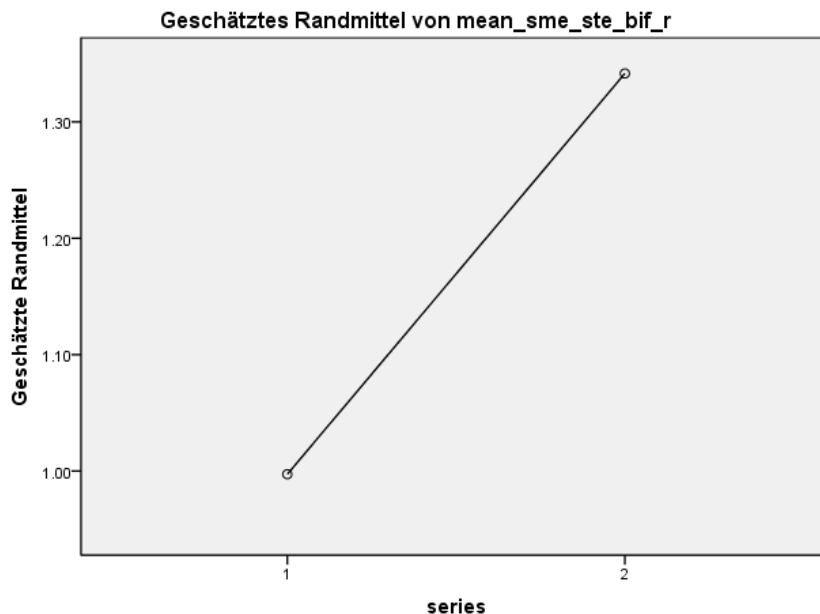
		N
series	1	18
	2	6

dependent variable: mean\_sme\_ste\_bif\_r

Quelle	Quadratsumme vom Typ III	df	Mittel der Quadrate	F	Sig.
Korrigiertes Modell	.788 <sup>a</sup>	2	.394	3.942	.035
Konstanter Term	.069	1	.069	.686	.417
body height	.288	1	.288	2.884	.104
series	.533	1	.533	5.324	<b>.031</b>
Fehler	2.100	21	.100		
Gesamt	31.056	24			
Korrigierte Gesamtvariation	2.889	23			

a. R-Quadrat = .273 (korrigiertes R-Quadrat = .204)

Univariate analysis revealed a statistically significant difference with body height between the two female sub-sites in the enthesal changes at the right hip.



Die Kovariaten im Modell werden anhand der folgenden Werte berechnet: body height = 160.279

The downhill females show somewhat higher scores in the right hip entheses.

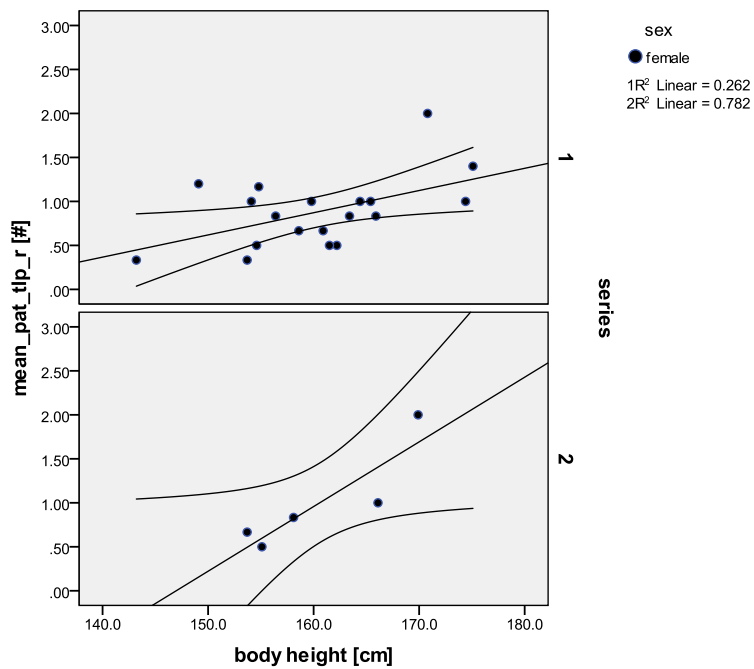


**Figure 138.** Scatterplot of the pooled muscle group *M. quadriceps femoris* (Patella – patellar ligament), females of the uphill (1) and downhill (2) site, right side. There is an increase of scores apparent in both series.

### 10.2.2 Short summary

A significant result with higher body size was found in the right *M. triceps brachii* and the pooled *M. biceps brachii*/*M. brachialis*. A significant difference between the series was found in the pooled right *M. semimembranosus*/*M. semitendinosus*/*M. biceps femoris* with body height. The downhill females show somewhat higher scores here in the right hip entheses.

### 10.2.3 Scatterplots entheses – body height, comparison females uphill-downhill – left side

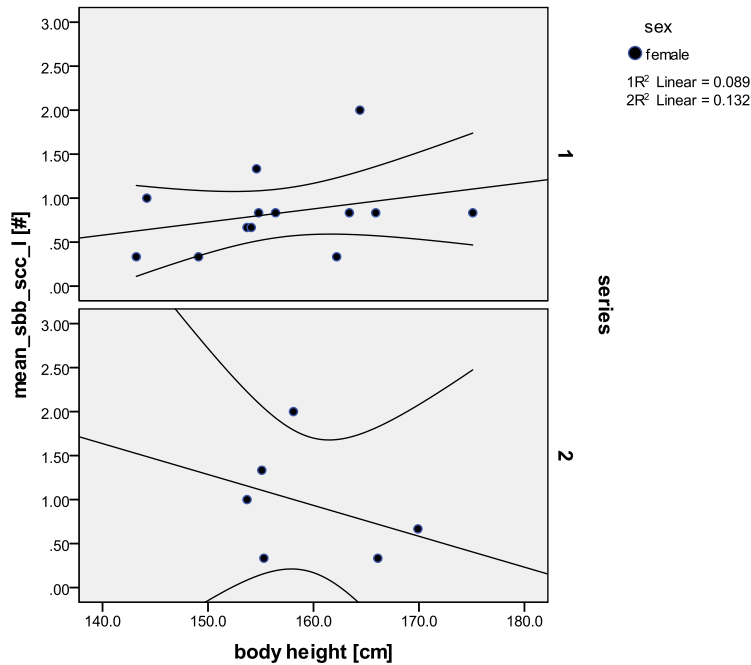


**Figure 139.** Scatterplot of the pooled muscle group *M. biceps brachii* – *M. subscapularis* (scapula – proximal humerus), females of the uphill (1) and downhill site (2), left side. There is a slight increase of scores with higher body size in the females of sub-site 1, contrary to group 2.

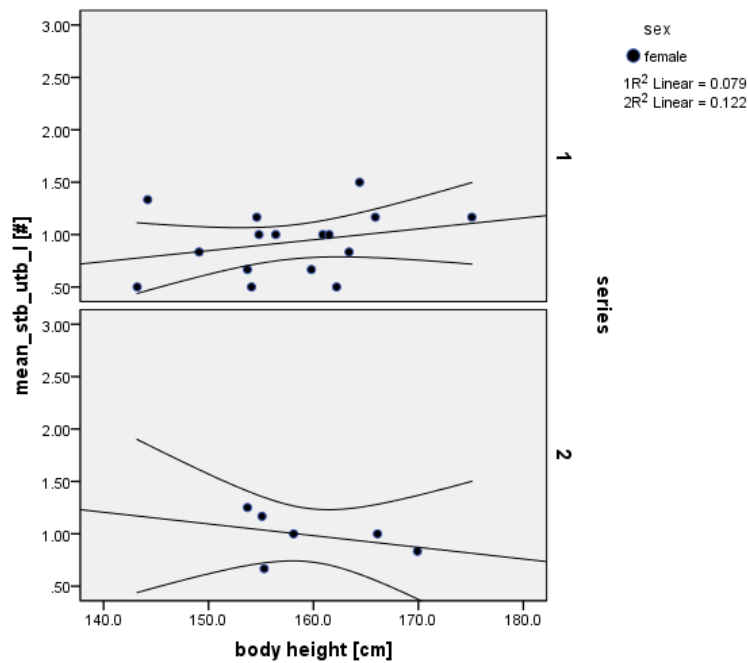


**Figure 140.** Scatterplot of the pooled muscle group *M. triceps brachii* (scapula – proximal ulna), females of the uphill (1) and downhill site (2), left side. There is a slight increase of scores with body height in the uphill females, but not in the downhill females.

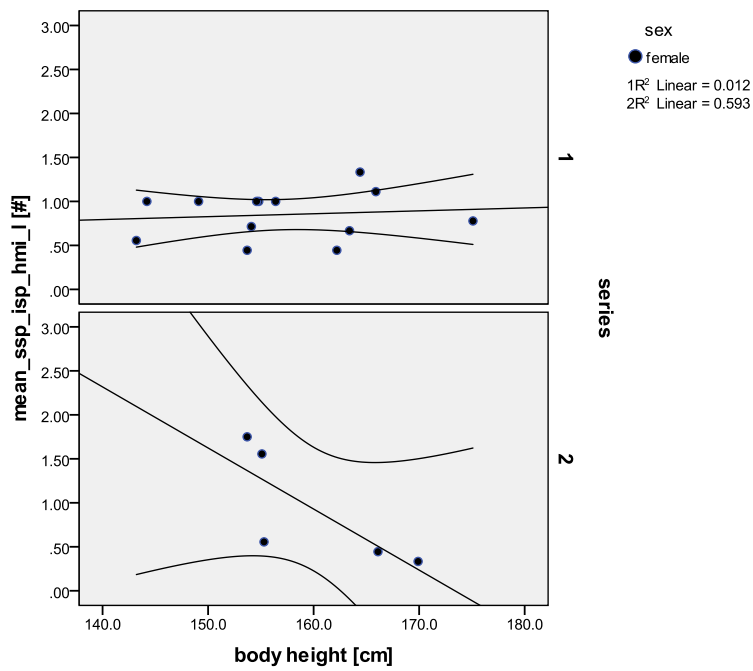


**Figure 141.** Scatterplot of the pooled muscle group *M. supraspinatus - M. infraspinatus - M. teres minor* (prox. humerus), females of the uphill (1) and downhill site (2), left side. There is no clear association between scores and body height in this feature in neither group.

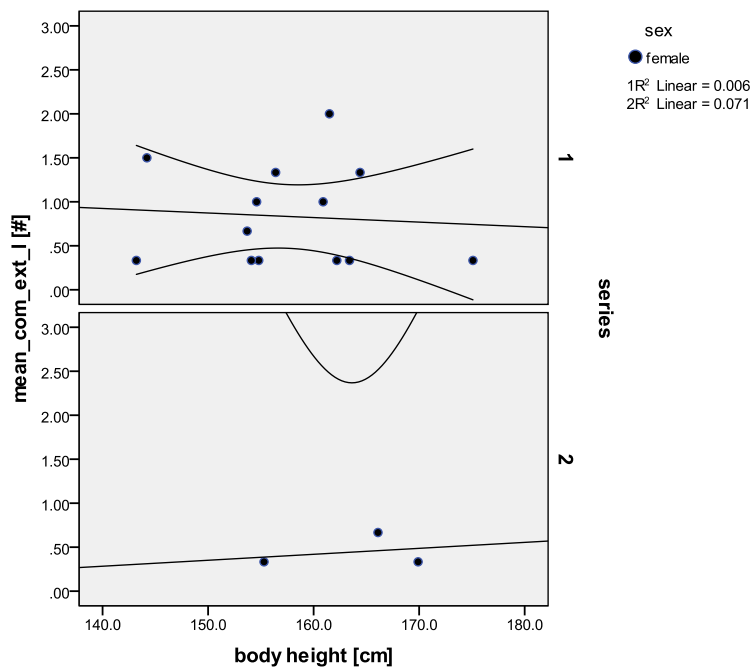


**Figure 142.** Scatterplot of the pooled **common extensors** muscle group (distal lateral humerus), females of the uphill (1) and downhill (2) site, left side. There is no clear relationship between scores and body height in this feature in neither group. This result may be biased by the small number of individuals in group 2.

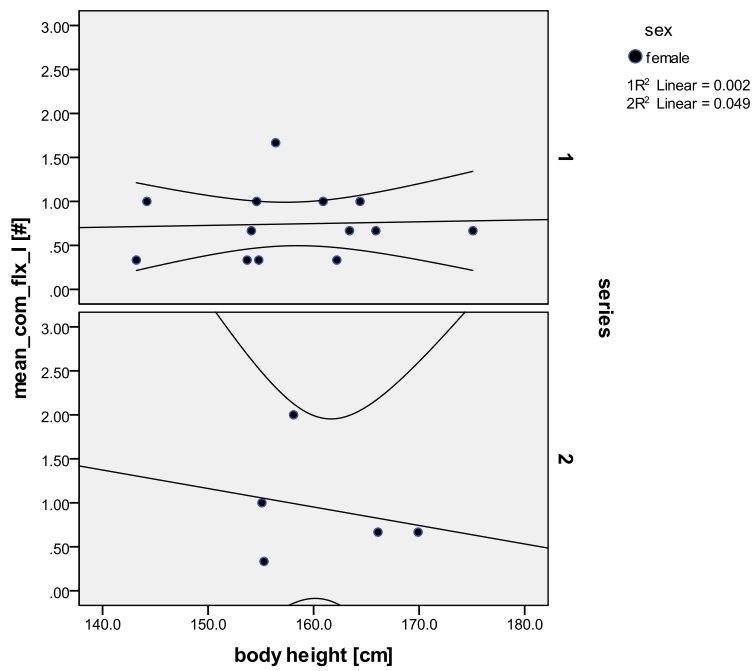


**Figure 143.** Scatterplot of the pooled **common flexors muscle markings group** (distal medial humerus), females of the uphill (1) and downhill (2) site, left side. There is no clear relationship between scores and body height in this feature in neither of the two groups.

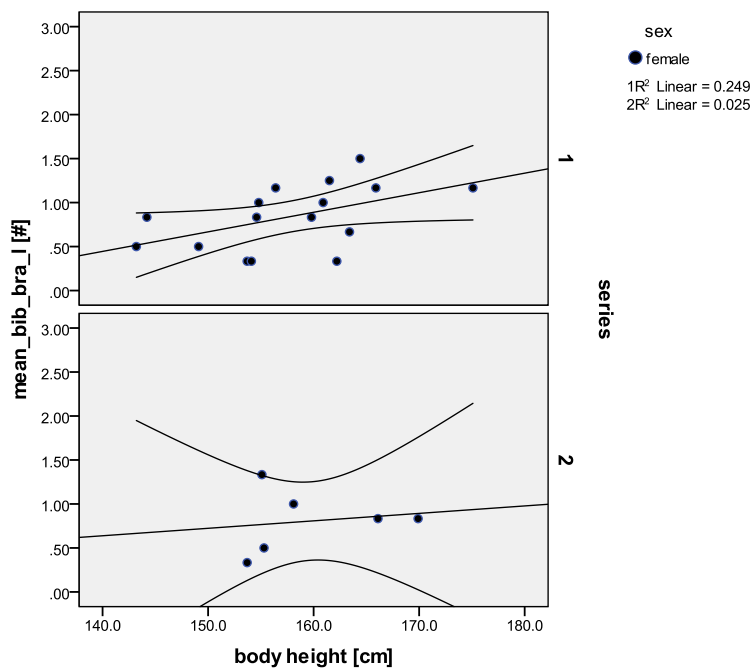


**Figure 144.a.** Scatterplot of the pooled muscle group *M. biceps brachii* – *M. brachialis* (prox. radius - ulna), females of the uphill (1) and downhill site (2), left side. There is an increase of scores with higher body size in the females of series 1, and also a slight one in group 2. This result was found to be marginally significant (see Figure 144b).

**Figure 144. b.** Results of the univariate analysis for the pooled entheses attachment sites *M. biceps brachii* – *M. brachialis*.

		N
series	1	16
	2	6

dependent variable: mean\_bib\_bra\_1

Quelle	Quadratsumme vom Typ III	df	Mittel der Quadrate	F	Sig.
Korrigiertes Modell	.486 <sup>a</sup>	2	.243	2.140	.145
Konstanter Term	.261	1	.261	2.300	.146
body height	.482	1	.482	4.239	<b>.053</b>
series	.023	1	.023	.198	.661
Fehler	2.159	19	.114		
Gesamt	17.785	22			
Korrigierte Gesamtvariation	2.646	21			

a. R-Quadrat = .184 (korrigiertes R-Quadrat = .098)

A statistically marginally significant result was found in the proximal radius/ulna entheses with higher body height in the females on the right side.

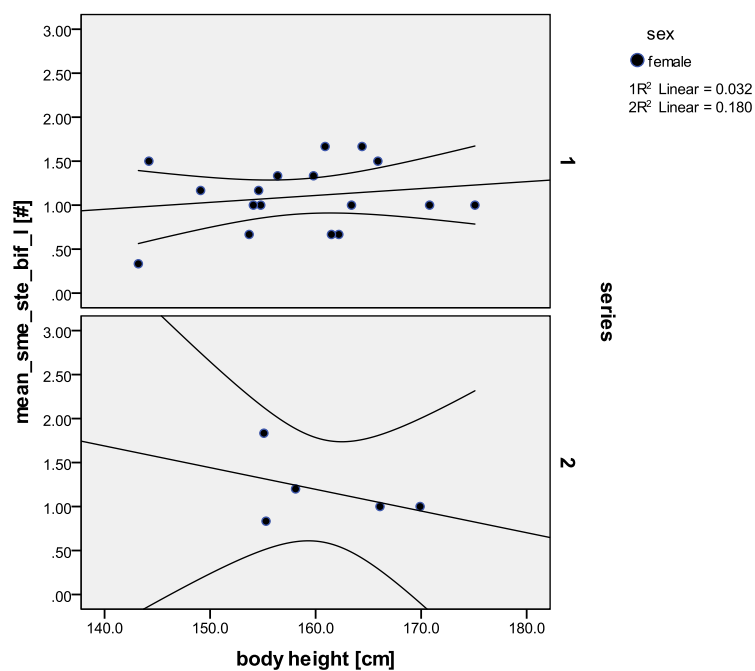


**Figure 145.** Scatterplot of the pooled muscle group *M. semimembranosus* – *M. semitendinosus* – *M. biceps femoris* (tuber ischiadicum), females of the uphill (1) and downhill site (2), left side. There is no clear relationship between scores and body height in this feature in neither group.

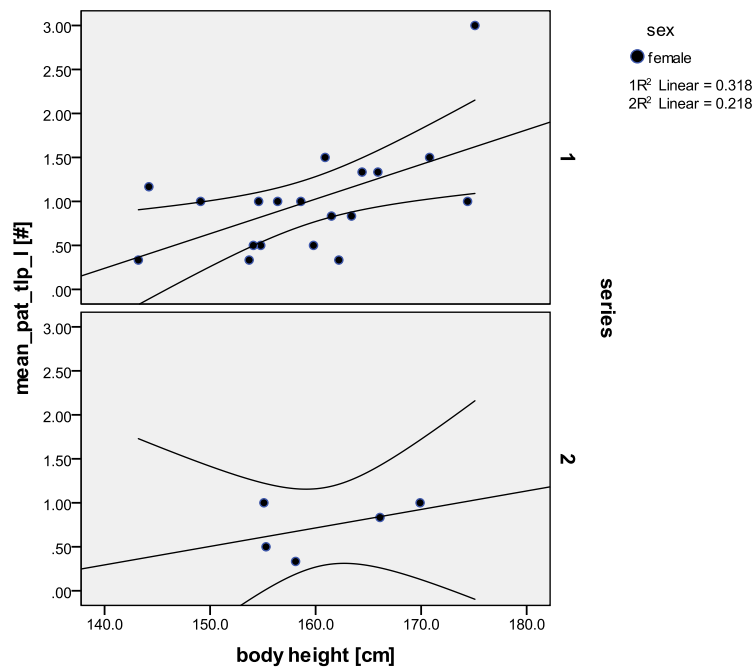


**Figure 146. a.** Scatterplot of the pooled muscle markings group *M. quadriceps femoris* (Patella – patellar ligament), females of the uphill (1) and downhill (2) site, left side. There is an increase of scores apparent in both series, and a significant result was found (see Figure 148b).

**Figure 146. b.** Results of the univariate analysis of the right, pooled entheses group *M. quadriceps femoris* in the females.

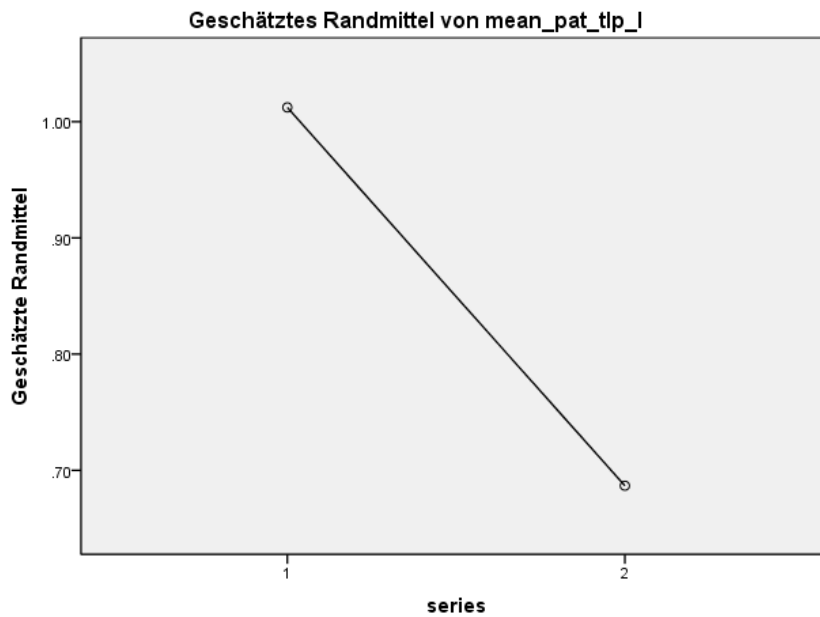
		N
series	1	19
	2	5

dependent variable: mean\_pat\_tlp\_l

Quelle	Quadratsumme vom Typ III	Df	Mittel der Quadrate	F	Sig.
Korrigiertes Modell	2.496 <sup>a</sup>	2	1.248	5.199	.015
Konstanter Term	1.612	1	1.612	6.714	.017
body height	2.215	1	2.215	9.226	<b>.006</b>
series	.417	1	.417	1.737	.202
Fehler	5.041	21	.240		
Gesamt	28.944	24			
Korrigierte Gesamtvariation	7.537	23			

a. R-Quadrat = .331 (korrigiertes R-Quadrat = .267)

The pooled Patella/patellar ligament entheses attachment sites on the left side are significantly affected ( $p=.006$ ) by increasing body height in the females.



Die Kovariaten im Modell werden anhand der folgenden Werte berechnet: body height = 159.650

The uphill females display somewhat higher scores in the left Patella/patellar ligament entheses attachment site, but the scores are generally rather low.

#### 10.2.4 Short summary

A statistically marginally significant result was apparent in the left *M. biceps brachii*/*M. brachialis* entheses attachment sites with higher body size in the females on the left side. Further, the left tibial knee muscle markings of the *M. quadriceps femoris* are significantly affected by higher body size in the females.

### 10.2.5 Comments on the body height sections for males and females

The relationship between higher scores in enthesal changes and body height has been questioned and is frequently discussed and analysed (e.g. Foster *et al.* 2014, Henderson & Alves Cardoso 2013, Milella *et al.* 2012, Molnar *et al.* 2011, Niinimäki 2011, Niinimäki & Baiges Sotos 2012, Nolte & Wilczak 2013, Villotte *et al.* 2010, Weiss 2003, 2004, Weiss *et al.* 2012, Wilczak 1998a). A possible association was tested here because of a considerable and significant difference in sexual dimorphism in body height between males and females of the two Thunau groups. Summing up the results of the tests for a possible association between higher entheses scores and body size, no specific pattern was found in the Thunau skeletons. However, significant results for higher entheses scores with larger body size were found in the right common flexors muscle marking group and the left *M. quadriceps femoris* attachment sites of the males. The latter significance is probably resulting from the distinct increase of scores in group 1, due to 2 individuals being over 180 cm tall and showing high scores. Concerning the females, a significant result with higher body size was obtained in the right *M. triceps brachii*, probably due to one female in each group being taller than the others and displaying higher scores. Further significant results were found for the pooled right *M. biceps brachii*/*M. brachialis* attachment sites. In the left extremity of the females, a statistically marginally significant result was obtained in the left *M. biceps brachii*/*M. brachialis* entheses attachments with higher body height in the females. Further, a statistically significant result was obtained for the left tibial knee muscle markings with higher scores of the *M. quadriceps femoris* and higher body size in the females. The uphill females display somewhat higher scores here. The only significant difference between the series was found in the pooled right *M. semimembranosus*/*M. semitendinosus*/*M. biceps femoris* with body height in the females, whereat the downhill females show somewhat higher scores here in the right hip entheses. One noticeable thing is that the *M. biceps brachii*/*M. brachialis* and the *M. quadriceps femoris* show a significant result with higher scores and higher body size two times (the former in the females, the latter in males and females). Further, a difference between the female series became apparent in the right hip entheses attachment sites (compare Figure 144a, b, pages 177-178). The fact that the *M. quadriceps femoris* entheses attachment sites show significant results in males and females could be related with the structure of this enthesis (although it is a fibrocartilaginous one, the structures (outlines) are not always clearly demarcated and may therefore lead to errors in scoring). This may apply to other entheses, too. What is further interesting is that body height shows a high standard deviation in both

groups and both sexes, which might be evidence for heterogeneity in the group. However, Villotte *et al.* (2010, 7) notes that body height is not relevant in fibrocartilaginous entheses. Henderson & Alves Cardoso (2013, 130) found no relationship between enthesal changes and body size. Niinimäki and Baiges Sotos (2012, 226) found low effects of size on EC testing on single muscle groups, contrary to the results by Weiss (2003, 2004). The latter tested with aggregate muscle markings, and states that there are correlations between upper limb size and musculoskeletal stress markers. This correlation proved insignificant when it was controlled for age and sex. Weiss' theory applies to diaphyseal attachments (=fibrous entheses), and she admits that the relation found in her study may be weak because it is based on human upper limbs, which are freed from weight-bearing (Weiss 2003, 238). However, Nolte & Wilczak (2013, 170) found high correlations of body size proxies and enthesis size based on 3D area of the *M. biceps brachii* and distal articular breadth of the humerus in a 20<sup>th</sup> century American sample. As is visible from these results taken from the literature, there is no consensus between the results of different researchers in this area according to body size and entheses scores. However, for the Thunau samples, no specific pattern was obvious, although significant results were found in the upper as well as in the lower limb for males and females for single fibrocartilaginous muscle groups. Therefore, the decision not to compare males with females here due to a significant difference in body size is justifiable.

## 11 DISCUSSION

### 11.1 General comments

The mostly well preserved skeletal remains from Thunau/Kamp provided a very convenient base for this kind of statistical group analysis on enthesal and joint changes. However, the downhill group is considerably smaller than the uphill group, limiting the validity of some results. The aim of this work was to find activity-related patterns on the skeletons of Thunau/Kamp by comparing changes at entheses attachment sites and osteoarthritic changes at joints in relation to archaeological data between the uphill (hillfort) and the downhill (valley site) series. Although my thesis concentrates on scoring morphological features at skeletons, an initial test was performed according to a quantitative scoring method in using a surface scanner for a 3D analysis on one enthesal feature (compare chapter 3.6.). Yet, supposed activity related patterns on skeletal remains based on a population level (not upon specific activities of single individuals, Stirland 1997, Robb 1998, Pearson & Buikstra 2006) were in the focus of attention here. These results are put into context to supposedly performed activities by the Thunau people reconstructed from archaeological data (settlement structures, grave goods) in the two groups. Studies of workload and activity in historic skeletal populations solely based on one selected group of skeletal features, e.g. alterations at entheses or joint changes have often been criticised and are still frequently discussed (e.g. Alves Cardoso & Henderson 2010, Bridges 1997, Jurmain *et al.* 2012, Knüsel 2000, Pearson & Buikstra 2006, Villotte *et al.* 2010, Weiss 2006, Weiss & Jurmain 2007). Thus, enthesal and joint data were combined in this thesis. Havelková *et al.* (2011, 2013) performed a study on enthesal changes where a direct link between grave goods and the incidence of enthesal changes in individuals from Great Moravia (Mikulčice castle, Klášterisko) was suspected and in large part confirmed. The archaeological complex of Mikulčice is, except in terms of size, well comparable to Thunau with regard to time period (9<sup>th</sup> century) and type of the site. The combination of enthesal and joint changes, as performed in the present study, may provide a broader and more reliable insight into workload and habitual activities of past people, and, in combination with the archaeological data, even give a tentative insight into the social organization and “everyday life” of an Early Medieval society.

As this study is part of a comprehensive analysis focusing on the bioarchaeological aspects of Thunau, several other analyses were performed. One study is already finished and is according to pathologies in the vertebral column (Nittmann 2012, Nittmann & Teschler-

Nicola 2014). In a selected number of adult uphill individuals from Thunau the authors found that the males were more often affected by Spondylosis deformans at the cervical and thoracic spine, women more often at the lower part of the lumbar spine. In the higher age classes, they found that males not only showed a higher frequency, but also more pronounced joint changes than women. Further, Schmorl's nodes occurred frequently and more often in males and a significant sexual dimorphism was found according to spondylolysis, which was found only in females, and in a total of 25%. Overall, the spinal changes are interpreted as work related (military context, riding, daily tasks, and field work) (Nittmann 2012, Nittmann & Teschler-Nicola 2014). As archaeological indications of craftwork in the uphill series are rare (only marginal finds at the Schanze and the Lower Holzweise, Szameit 1995), no further implications can be made. Other parts of the comprehensive study are still in preparation for publication, e.g. demography, frequencies of pathologies or traumatic injuries (Novotny, Spannagl-Steiner, Teschler-Nicola, Wiltschke-Schrotta in preparation).

## **11.2 Association between enthesal and joint changes in the Thunau samples**

The first hypothesis in this study is that there is an association **between the degree of changes of selected entheses and the degree of the osteoarthritis at the joints** in the Thunau samples. This is one of the main research questions addressed in this study.

Generally, there was a rather weak association between frequencies of enthesal and joint changes in the Thunau series. However, differences in **frequencies** between the male and the female uphill and downhill samples were found. Interestingly, they are more pronounced in enthesal changes than in degenerative joint alterations. In this regard, the uphill and downhill sample are very similar (compare chapters 4 for the males and chapter 8 for the females).

The **frequencies of enthesal** changes of **males** in both groups are overall moderate to high and relatively similar in the upper right extremity (compare chapter 4). However, in the right elbow, the downhill males display the highest frequency of changes in a muscle involved in extension of the elbow, and especially in stroke movements (*M. triceps brachii*) and the pooled *M. biceps/M. brachialis* muscles (true prevalence rate (TPR) = 0.9 each), working in flexion and supination of the forearm and flexion of the elbow. From archaeological data, a large blacksmith's shop area and lots of millstones are known in the downhill settlement

(which is interpreted as craft-production oriented, Obenaus 2011). This kind of work would require work sequences that would go along with increased activity in the mentioned muscle groups. On the left body side, the frequencies of enthesal changes in both groups are rather low in the common extensors and the common flexors of the elbow (as on the right side), and comparably high in the other entheses of the upper extremity of the right side.

Especially in the lower extremities, the frequencies on the right and left side in both male groups do not differ much between the series. These results confirm the statement of Nolte & Wilczak (2013) that in the lower limb, activity patterns are not likely to differ as much between individuals as in the upper limb due to bilateral asymmetry and a larger range of movement possible in the upper limb (Nolte & Wilczak 2013, 171).

In Mikulčice-Klášteřísko, Havelková *et al.* (2013, 248) found main correlations between skeletal loading and special kinds of grave goods for males. An association between enthesal changes at the insertion of the *M. triceps brachii* and the presence of “warrior equipment” (which may include swords, spurs, axes, spear heads or arrowheads) in graves deeper than 90 cm, which are probably representative of a social elite, was detected. Axes are the most frequent type of warrior equipment there, but of course these could also have served as work tools. In shallower graves with objects of daily use, the individuals showed more incidences of changes at the entheses of the common flexors and the common extensors in Klášteřísko. **High frequencies of joint alterations** (TPR mostly > 0.8) in the **male** individuals of the two sub-sites are seen on both body sides in the upper and lower extremities. Somewhat lower frequencies are seen in the distal humeral elbow joint facets (*Capitulum humeri/Trochlea*) on the right and left side, and the elbow joint facets at the proximal radius and ulna in the downhill males on the left side. In a study on Neolithic skeletal remains Crubézy *et al.* (2002, 582) also found the elbow as least often affected with osteoarthritis in the upper limb. Overall, in the males from Thunau, the frequencies of the enthesal changes show that they have a distinctly higher prevalence rate of pathological changes than the females. This picture is different in the joints, where the slight osteoarthritic changes are distributed all over the skeleton of males and females in a relatively equal pattern (especially in the lower extremities).

Concerning the **females**, the **frequency of enthesal changes** is rather low (overall  $< 0.5$  in the true prevalence rate) in upper and lower extremities on the right side. An exception is apparent in the downhill females, where the frequency of changes at the muscle markings at the right ischial tuberosity (*M. semimembranosus*, *M. semitendinosus* and *M. biceps femoris*, responsible for retroversion of the hip, flexion and internal rotation of the knee) reaches more than 80%. On the left side, the frequencies are also generally low, but about half of the females of the upper and lower sub-site are affected by slight pathological changes at the ischial tuberosity. This is an interesting hint to mobility habits of the females. The **frequencies of joint OA** display a very similar picture in the females and in the males, especially in the lower extremities. Nearly all individuals of both groups are affected by slight joint changes over the entire skeleton, indicating a high base activity level in both groups. It is difficult to assess whether repetitive or continuous stress is the more important predisposing factor for OA (Burt *et al.* 2013). Crubézy *et al.* (2002: 583) found in a study on Neolithic skeletal remains that the hip was the joint most often affected by osteoarthritis, whereas its occurrence in the knee and the ankle was uncommon. In the Thunau groups, the given, but rather weak association (which is even more apparent in the females with the low frequencies of enthesal changes) of joint and enthesal changes, is in accordance with the results of e.g. Molnar *et al.* (2011), although the time periods differ. She analysed bilateral asymmetry of entheses scores and eburnation frequency in two Middle Neolithic samples from Gotland and found a vague pattern. However, in the Thunau sample, eburnation was only rarely found.

## 11.3 Differences between the Thunau sub-sites

### 11.3.1 Sex differences

The second hypothesis in this thesis is that there is **a specific pattern of enthesal and joint changes visible in male and female individuals**, which is different in the two groups. Long bone length and body height differed significantly between males and females in both sub-sites, but was very similar in males and females, respectively. Due to this fact, and an unknown hormonal contribution on enthesal changes in females (Mariotti *et al.* 2007, Villotte *et al.* 2009, 8, Villotte & Knüsel 2013, 140) and body mass variation between the sexes probably influencing osteoarthritic changes (Weiss 2006), only males with males and females with females were compared for the final analysis between the groups. Apart from this, an overall visible aspect in the females was that they show lower prevalence rates in enthesal changes than the males, but the frequencies of joint changes are relatively similar in

the two sexes. This result points to only a weak relationship between enthesal and joint changes at the skeleton. However, the downhill females show the strongest asymmetries in the joints but even more in the enthesal changes (flexors/extensors) of the upper extremities, also compared to the males (compare asymmetry section). This result strongly suggests a high activity level in the upper limb for the females from the valley site (compare below).

### 11.3.2 Population differences

Due to the reasons discussed in the foregoing section, these results were compared for male and female individuals separately. In male individuals, the downhill **males** show generally slightly higher frequencies of **enthesal** changes than the uphill males, and a distinctly stronger **asymmetry**, especially in the upper extremities. In two entheses (*M. triceps brachii*, and *M. quadriceps femoris*, both right side) significant results according to asymmetries were found. Further, non-significant differences are visible in the common flexors and the *M. biceps/M. brachialis* (right side), and the common extensors (left side) show strong asymmetry in the downhill males. The latter result goes along with an asymmetry in the distal humeral (elbow) joint on the left side. Other studies found bilateral symmetry for almost all entheses (e.g. Alves Cardoso & Henderson 2010). Obviously, intrinsic and mechanical factors play a role in the appearance of enthesal changes (Henderson *et al.* 2013: 159). When upper and lower extremities are considered separately, asymmetries in the upper limb are more frequent and more common on the right side, especially for bone production at the margin and the surface (Henderson *et al.* 2013).

Assuming that osteoarthritis is caused by physical strain, joint load should be asymmetric, and in particular with greater involvement of the right side in right handed individuals (Weiss & Jurmain 2007). Asymmetries especially in the upper limbs have been verified in different populations using different methods. Particularly interesting in comparison to the Thunau samples are the results of Kujanová *et al.* (2008), who found very high percentages especially of male, but also of female “right handers” in two Great Moravian populations (Mikulčice-Kostelisko and Prušánsky) based on maximum humeral length (Kujanová *et al.*, 2008). Kanz *et al.* (2013) observed radiographically detected bone mineral density differences to be significant for the right (preferred) hand. Sládek *et al.* (2007) tested asymmetry by means of humeral external measurements and cross-sectional parameters, finding right handed asymmetry mainly in male individuals. Milella *et al.* (2012, 380, 382) found a right side

dominance in the mean robusticity score for both sexes in the upper limb, especially in the shoulder. Villotte *et al.* (2009, 2010) state that if asymmetry is found, then more frequently in the upper extremities and on the right side for osteophyte growth (Villotte *et al.* 2009, 2010). Weiss (2012) found fibrocartilaginous entheses to be more useful in reconstructing activity patterns because they display more asymmetry in upper limbs and are less affected by body size than are fibrous entheses (Weiss 2012). In the Thunau sample, a stronger asymmetry in the upper extremities could be observed in the enthesal changes of the downhill males compared to the uphill males, obviously preferring the right arm. This could be a hint for the downhill males being more frequently and/or continuously involved in strenuous activities.

In the **females**, the downhill individuals display considerable **asymmetry** in the right common extensors (extension of wrist and fingers, supination) and the left common flexors (flexion of wrist, pronation), and the uphill females in the right common flexors. There is also a higher asymmetry visible in the left distal elbow joint facets of the downhill females, fitting with the changes in the left common flexors. However, no statistically significant changes between the local female groups were observed in the females. There are no indications of special activities from archaeology for the uphill females, contrary to the downhill settlement area, where a high number of loom weights and findings of baking ovens are reported (compare chapter 2.1.2). Weaving at a loom is a highly physically demanding activity placing particularly high strain on the shoulder (bilaterally), and on the elbow joints, but is rather mechanical in nature. Following Knüsel (2000, 112), physically active individuals like weavers do not display osteoarthritis even in old age. However, the frequency of joint changes in the shoulder and the elbow in the Thunau sample is high for the females in both groups, but the enthesal changes are rather low. Asymmetries are not very high in the shoulder joints and entheses of the females, but high in the elbow entheses of the downhill females. No more specific pattern could be detected here for the females. However, the stronger asymmetries in the upper limbs in the downhill females compared to the uphill females indicate them to having been more involved in strenuous activities during their lives.

Summarized, the downhill males and females show stronger asymmetric changes in entheses and joints than the uphill group, especially in the upper limb. This could point to a higher frequency of strenuous working activities performed by the valley sub-site individuals through their lifetime.

## 11.4 Age differences in the Thunau sub-sites

The third hypothesis is that the **degree of enthesal changes and joint alterations increases with age**. A strong dependence of enthesal changes and osteoarthritic joint changes on age was supposed and demonstrated frequently (for entheses, in identified and archaeological skeletal collections) (e.g. Alves Cardoso 2008, Alves Cardoso & Henderson 2010, Carter & Beaupré 2001, 223, Cunha & Umbelino 1995, Henderson *et al* 2012, Henderson *et al* 2013, Herrmann *et al.* 1989, Jurmain 1991 & 1999, Jurmain *et al.* 2012, Mariotti *et al.* 2004, 153, 2007, 556; Merbs 1983, Milella *et al.* 2012, Niinimäki 2011, 2012, Pearson & Buikstra 2006, Robb 1998, Villotte 2006, Villotte *et al.* 2010, Weiss & Jurmain 2007). According to enthesal changes, on the basis of a new method (Coimbra method), Henderson *et al.* (2012, 2013) recently showed that the effect of age is different for feature, enthesis and even side. The strength of the age effect varies by enthesis. Further, Milella *et al.* (2012) found the mean robusticity score in entheses to be positively correlated with age, higher in males, and in both sexes, young adult subjects (20-40 years) were characterised by the highest increase in mean robusticity scores. The age effect on robusticity and osteophyte growth is tentatively linked to an accumulation of microtraumatic stress on enthesal surfaces due to daily, normal biomechanical loading patterns (Milella *et al.* 2012, 381, 383). Further, changes in tissue properties of tendons by increasing tendon stiffness and thus mechanical loading of entheses play a role (Jurmain *et al.* 2012). Villotte *et al.* (2010) also found main differences of enthesopathy prevalence between occupation groups before the age of 50 years.

### 11.4.1 Population differences

For the Thunau sub-sites, a one-way-ANOVA was calculated for the series (uphill-downhill group comparison, in order to get a group overview) and revealed an association **between the expression of higher scores with increasing age** in about half of the features in joints and entheses, mainly in the uphill series. A post-hoc test (Bonferroni) displayed several inter-age group associations: in the **hillfort individuals** (right side), the shoulder muscles (*M. biceps brachii*/*M. subscapularis*), the forearm muscles (*M. biceps*/*M. brachialis*), the common flexors and the hip muscles show statistically significant differences in the Bonferroni test between the young (18-29 years) and the middle age group (30-49 years). In the distal humeral and the hip joint facets, this is also the case. Further, statistically significant results (right side) are seen between the youngest and the oldest (50-70 years) age groups in all

shoulder muscles, in the distal humeral joint and the hip joint. Statistically significant results in Bonferroni test in the entheses (left side) are found between the young and the old age group in the common extensors. Concerning the joints of the uphill individuals (left side), statistically significant differences in the Bonferroni test between the young and the middle age group are obvious in the distal humeral joint facets, the hip joint facets, the distal femoral joint facets and the ankle joint facets. Between the young and the old age group, the shoulder and elbow joint facets, the hip and the distal femoral joint facets showed significant results. Regarding the **downhill individuals**, statistically significant results in the Bonferroni test are found in the shoulder joint facets (marginally significant between young and old and between middle and old), and on the left side between the middle and the old age group in the rotator cuff muscles (*M. supraspinatus*, *M. infraspinatus* and *M. teres minor*). The high number of statistically significant results in the Bonferroni tests in the uphill sample (right extremity) between the young and the middle age groups from Thunau is especially interesting, because main differences of enthesopathy prevalence between occupation groups is mainly seen before the age of 50 years (Milella *et al.* 2012, 379, Havelková *et al.* 2013, 502, Villotte *et al.* 2010). Milella *et al.* (2012, 379) state that several studies stress the importance of age related change, as enthesal differences between professions tend to vanish with age. Relevant factors are a decrease in muscle mass and a change in locomotor patterns which occur with advanced age (Milella *et al.* 2012, 384), as well as a change in tissue properties (Jurmain *et al.* 2012). For the Thunau samples, some scatterplots show that there are generally also already higher scores in entheses and joints present in younger individuals, especially in the valley site group. For the latter this could be an evidence for a physically more demanding life from young age on (compare below).

**Concerning the expression of higher scores with increasing age**, an exemplary test where osteophyte growth was omitted from significance calculations (one-way ANOVA), was performed, again, like before, for males and females of the two groups together (compare chapter 7). Osteophyte growth is the main feature affected by age changes in entheses and joints, and distinctly more age related than e.g. porosity (Henderson *et al.* 2012, Henderson *et al.* 2013, 158, Jurmain 1991, Knüsel 2000, 114, Milella *et al.* 2012). Further, there is a strong positive relation between the growth of enthesophytes and osteophytes (Rogers *et al.* 1997). In the uphill group (right extremity) of Thunau, statistically significant results (Bonferroni test) between the young and the middle age group remained in the right common flexors

(marginally significant) and in the hip muscles after omitting osteophyte growth. The two shoulder muscle pools showed further statistically significant changes between the young and the old age groups. In the joints of the right side, the hip joint facets still show a statistical significance between the first and the third age group when osteophyte growth is omitted. On the left side, no statistically significant results remained after omitting osteophyte growth. It is conspicuous here that the statistically significant results remain in the hip entheses and joints in the uphill group, pointing to high physical activity. Further, these results are really interesting because according to the enthesal changes in the uphill group, the significant changes are mainly visible between the young and the middle age group. In the uphill group, left side, no significant results omitting osteophyte growth were found in the entheses and in the joints. Taken together, this could be an argument for mostly right-handed individuals in the uphill Thunau sample. Therefore, these results could be tentatively interpreted as work related. However, in the downhill sample, no statistically significant results remained in either entheses or joints after omitting osteophyte growth, maybe due to a small sample size. Enthesophytes show increased prevalence with age but also result from trauma to a joint in younger individuals (Jurmain 1999, Knüsel 2000, 113). Henderson *et al.* (2013, 157) state that there is also a difference in the effect of age depending on feature, enthesis site or even side. Bone formation (enthesophyte growth at entheses and osteophyte growth at synovial joints) has been associated with a higher sensitivity to mechanical stress in entheses and joints (Benjamin *et al.* 2006, Robb 1998, Milella *et al.* 2012). Osteoarthritis is known to appear only from regular, uniform and heavy labour sequences performed over a long period, but there are also other causes like age and weight as well as genetic predisposition (Jurmain 1999, 74, Waldron 1994, 94). Molnar *et al.* (2011, 289) found a high number of eburnation lesions in two Neolithic samples from Gotland, which were statistically significant with higher age. However, she states that not all old individuals are affected by osteoarthritic changes (Molnar *et al.* 2011, 286). The possibility that some entheses or joints are more sensitive to stress and strain is partially reflected in the scatterplots of the Thunau people.

#### 11.4.2 Sex differences and age

For the **males**, the **scatterplots** and univariate analysis for **joint changes with age** displayed significant results between the two series on both sides in the hip joint, whereas the downhill males show higher scores, respectively (also at a younger age). The pooled joint group *Capitulum humeri/Trochlea* at the elbow and the distal femoral joint is significantly affected

by age in the males on both sides. Furthermore, a significant result ( $p=.005$ ) was found in the males with increasing age and between the series in the pooled *Caput radii*, *Circumferentia articularis radii*, *Incisura trochlearis*, *Incisura radialis* at the right elbow (proximal radius and ulna) joint and for the hip joint facets (*Fossa acetabuli*, *Caput femoris* and *Fovea capitis*). The significant result in the hip joint was found on both body sides between the series, and the downhill males showed higher scores, respectively. This is especially interesting because “...the hip (and spine) appear to be more at risk as the result of heavy lifting” (Jurmain 1999, 105). Further significant results with age in the males were detected in the right pooled joints *Facies patellaris*, *Condylus medialis femoris*, *Condylus lateralis femoris* and distal margin of *Fossa intercondylaris*, right side. There are some non-significant age trends with higher age in the entheses scatterplots of the males in both groups (common extensors, *M. biceps/M. brachialis*, hip muscles) on the right side. In the right wrist and ankle, a trend of higher scores with higher age is visible in both groups but no significant results were found. On the left side, a non-significant age trend was apparent in the *M. quadriceps femoris* at the knee.

According to the **females** of the two groups, a statistically significant result was observed in univariate analysis according to **entheses scores** and **increasing age** in the right pooled muscle markings group *M. biceps brachii/M. subscapularis*. Further, significant results for the females with increased age were found in the right pooled *M. triceps brachii*. Other statistically significant results were detected in the right and left pooled common extensors muscle group (downhill  $n = 2$ ), and in the common flexors muscle group (downhill  $n = 4$ ). In this case the uphill females show slightly higher scores, although they are not very high generally in both series for the common flexors. However, these results are limited by the small number of individuals in the downhill females. Significantly higher scores with increased age were found in the right muscle group *M. biceps brachii/M. brachialis*. In the pooled *M. semimembranosus/ M. semitendinosus/M. biceps femoris*, right side, statistically significant results are visible with higher age and also between the series. The downhill females show distinctly higher scores here (compare 10.1.1). Additionally, in many cases the downhill females show high scores at a younger age than the uphill females (e.g. *M. triceps brachii*, *M. supraspinatus – M. infraspinatus – M. teres minor*, *M. biceps brachii*, especially the hip muscles, and the *M. quadriceps femoris*. These results could point to an earlier entry into a working environment and a higher mobility in the downhill females compared to the uphill females.

Concerning the **joints**, the scatterplots for higher scores with higher age for the **females** in the pooled joint group *Capitulum humeri – Trochlea* (right side), and the univariate analysis showed significant results in this feature according to mean age. A significant result was obtained comparing the two series ( $p=.007$ ). The uphill females display (exceptionally) the higher mean scores here in the distal humeral joint facets. Further, a significant result with higher age ( $p=.000$  right side,  $p=.005$  left side) was obtained for the females in the scatterplots and univariate analysis in the right and left pooled hip joint group *Fossa acetabuli*, *Caput femoris* and *Fovea capitis*. In this case, the scores are already relatively high at young age in both groups, but were not very different between the series. These results are pointing to a high mobility of the females. Moreover, a significant result ( $p=.004$ ) was apparent for the females in the left *Capitulum humeri – Trochlea*. The uphill females display somewhat higher scores here. Significant results with higher age were found in the pooled joint group *Facies patellaris*, *Condylus medialis femoris*, *Condylus lateralis femoris*, distal margin of the *Fossa intercondylaris* (distal femur - knee), left side.

## 11.5 Social differences in the Thunau sub-sites

The fourth and main hypothesis to be tested here is that there is a **social difference** visible between the two groups: **warriors versus working men?** We assumed that the differences in the “functions” of the settlements, as deduced from the archaeological record, are visible in the populations; e.g. political functions like the (militant) protection of the fortified hilltop settlement (Friesinger & Friesinger 1991, Teschler-Nicola *et al.* 2015), or a professional involvement in craft production (in the downhill settlement, distinct evidence for textile production, a smithery and a stone masonry is present, Obenaus 2011, Szameit & Obenaus 2007) and that this would be more visible in the males. From the entheses and joint results, due to stronger asymmetry and partially higher frequencies, a tendency is apparent that especially the downhill males were involved in more specialized (and therefore more power demanding in certain muscle groups) activities. This is also reflected by the results of the scatterplots, where the downhill males frequently display higher scores already at a younger age (e.g. shoulder, *M. triceps brachii*, common flexors and extensors). This result is consistent with the archaeological evidence strongly pointing to the downhill males working as professional craftsmen (large industrial area in the downhill settlement, Obenaus 2011). Compared to the uphill females, the downhill females display higher scores at a younger age

(visible in the scatterplots), mainly in the enthesal changes. Whereas for the uphill males and females no specific pattern of the features pointing to a distinct profession could be found, as was shown before (hypotheses 1 – 3), the results for the downhill individuals (stronger asymmetry, higher scores at younger age, hints for higher mobility in the downhill females) point to a stronger involvement in physically demanding tasks in their life from young age.

According to the archaeologists, the north-western area of the cemetery at the hillfort site seems to have been the burial place of socially higher standing families, whereas in the south-eastern area socially lower status individuals have been interred (Friesinger & Friesinger 1991, Nowotny 2011). Graves found outside of this area might be associated with individuals of socially lower or lowest status, or they were generated at the end of the occupancy period of the cemetery (end of the 9<sup>th</sup> century) when also the custom of grave goods disappeared (Nowotny 2011, 180-181). Therefore, it can be assumed from the archaeological record that we have the span of all social status groups represented in the graves. A social elite in the uphill group was located by the archaeologists in some male graves; these are the rich graves including swords, axe and spurs (Friesinger & Friesinger 1991, Szameit 1995, Nowotny 2011). In total, the warrior- and rider equipment (swords, axes, spurs) in the uphill Thunau sample is rather marginal compared to other cemeteries of Great Moravian centres e.g. the 6<sup>th</sup> church of Mikulčice, except in the number of the swords (Nowotny 2011, 92). In the hillfort series of Thunau, some males, mainly in well equipped graves, were found to have a knife longer than 15cm, which is generally interpreted as fighting knife (especially when it appears in “warrior graves”) and as a replacement for a weapon (Nowotny 2011, 95). However, a social interpretation from grave goods is difficult, and whilst a social elite is recognisable (mainly grave group 129/130) in the male uphill sample, an interpretation of this grave group as “gentry” remains difficult (Nowotny 2011). Teschler-Nicola *et al.* (2015) found a higher mortality rate of young males in the fortified hilltop. Nevertheless, for professional warriors, a high frequency of strong asymmetrical changes, especially of the shoulder and elbow muscles and joints of the preferred arm, with which the sword would have been operated, would have been expected and has been reported in other publications (e.g. Belcastro *et al.* 2001, Wentz & de Grummond 2009, 113), but was not observed in the Thunau sample. Further, more (healed) traumatic injuries due to sword cuts, for example in the head, would be expectable for professional warriors (Novak 2000, 100). There are some hints in the individuals from the uphill site from Thunau for traumatic injuries, though, there are males, and also a few females

with healed and unhealed fractures in the upper extremity (involving the skull), and to a lesser extent, in the lower extremity (Teschler-Nicola, personal communication). One of the sword (and spurs) carriers was decapitated (grave 129 uphill site). In the Slavonic population of Břeclav-Pohansko (Czech Republic), which is comparable to Thunau in regards of time period and structure of the Herrenhof sites (Herold 2008, Macháček 2011, Přichystalová 2011), the total number of fractures is low and rather related to accidents than to interpersonal violence (Konášová *et al.* 2009). However, concerning the downhill sample of Thunau, the systematic analysis of fractures is still ongoing. These results with regard to social status and the stratigraphic context will allow further conclusions here (Teschler-Nicola *et al.* in preparation). Interestingly, although about 400 years later, Thordeman (2001) reports on the victims of the battle of Wisby (Gotland) 1361, where by far the most numerous injuries were generated by cutting weapons like swords and axes, that the highest frequency of cuts was found in the tibia. Generally, the lower extremities were more intensely affected by cuts, because they were not so well protected as the upper body (Thordeman 2001, 167, 171). Further, inflammatory changes in the elbow joints and wrists of warriors in the battle of Wisby in 1361 are reported and linked to the hard work those individuals had to perform with their hands and arms (Thordeman 2001, 194).

Havelková *et al.* (2012) reports the presence of axes as closely associated with the loading of the elbow extensor in the Mikulčice sample. Enthesal changes in the common flexor/extensor muscles are rare in the Thunau sample (but it is known that especially osteolytic changes are generally rarely found in these entheses, Villotte *et al.* 2010). However, according to the prevalence of enthesal changes at the common flexors/extensors muscle attachments in the Thunau samples, there are some “outliers” visible in the scatterplots, mainly based on robusticity (compare chapter 6.1.1.). Asymmetry and occupation studies provide some positive evidence for an association between enthesal robusticity and habitual activities (Foster *et al.* 2014, 527). In the Thunau males, the “outliers” observation concerns the highest possible scores in these entheses, mainly based on enthesal robusticity (in the common flexors, right side, three middle aged uphill males (from graves 92, 129 and 188), and one young (2004/18) and one old downhill male (2004/6) show highest scores; in the common flexors, left side, one uphill male (grave 188) and two downhill males (graves 2004/6 and 2004/18) display highest scores; in the common extensors, right side, six uphill males aged between 30 – 45 years showed higher scores (from graves 12, 26, 79, 81/1, 129

and 146). In the common extensors, right side, one downhill male (grave 2004/18) showed the highest possible score. In the common extensors, left side, one uphill male from grave 175 (mean age 50 years), and one male from the downhill site (grave 2004/18) displayed the highest possible scores. Interestingly, frequently the same individuals are involved here, among them the tall (181cm), decapitated male buried with the sword and spurs from the social “elite” grave 129, as well as the decapitated male buried with the spurs from the valley site (2004/18). Furthermore, these “outliers” are not visible in the joint changes and also not in the female samples, indicating that these males might have been involved in more specialised activities. The possibility that only a small number of high status individuals (equalized with warriors) were buried here, as reflected by grave customs in the uphill site, would mean that the bulk of individuals mainly performed daily activities rather related to subsistence and maybe trading activities, which would not produce special signs at the skeletons. Given the assumption that professional warriors would be detectable with this kind of statistical analysis over a group, maybe too few of these specialists (if existent like this) were buried in the uphill site graveyard, and therefore a “warrior pattern” did not emerge. Velemínský *et al.* (2005) come to a similar conclusion for the cemetery of Mikulčice/Kostelisko in Greater Moravia, where the hypothesis that it is a necropolis of the princely military entourage could not be confirmed from anthropological results. Rather, they assume that it was a “general” necropolis, where the warriors have also been buried (Velemínský *et al.* 2005, 620). Further, concerning the females, in Mikulčice-Klášteřisko, Havelková *et al.* (2013) found that the relationship between the occurrence of grave goods and the occurrence of enthesal changes as found in the males could not be proven in the females.

Concerning the downhill group, there is stronger evidence from the anthropological results, especially in the males that they were involved in more specialised tasks, demanding certain muscle groups. The significant result in the hip joint e.g. was found for both body sides between the series, and the downhill males showed higher scores, respectively. This is especially interesting because “...the hip (and spine) appear to be more at risk as the result of heavy lifting” (Jurmain 1999, 105). This finding could go along with the work in a smithery or stone masonry, as indicated from the archaeological data at the valley site (Szameit & Obenaus 2009, Obenaus 2013). However, the downhill females show distinct differences as well compared to the uphill females, for example a stronger asymmetry in the upper limbs,

and an obvious earlier entry into worklife as apparent from the scatterplots. It is not possible to deduce more specific tasks performed by the females here, but the group difference is existent in the entheses and joint data.

## 12 CONCLUSION

Within the frame of the research issues addressed here, an attempt was made to answer questions relating to associations between enthesal and joint changes as well as trying to find differences and/or commonalities between two archaeologically – from settlement structures and grave goods – and therefore socially differently classified groups of skeletal remains from Thunau/Kamp. Though the methods used, i.e. morphological analysis of enthesal and joint changes, bear an element of uncertainty concerning the deduction of changes to specific activities, group-level inferences are possible and have contrasted groups with different lifeways in the past (Pearson & Buikstra 2006, 289). Especially the combination of the two methods, as performed in this study, should aid in interpreting the results of this group comparison.

Concerning the people settling in the valley of Thunau close to the river Kamp, there is archaeological evidence that the settlement was a production-oriented outer bailey, a “suburb”, with an associated graveyard. Big storage holes, pottery kilns, baking ovens, and a blacksmith’s shop, millstones and several hundreds of loom weights and spindle whorls have been recovered in the settlement area, the latter two strongly pointing to a textile-production oriented settlement part, probably producing for trading. Agricultural commodities were very probably purchased from outside the community due to spatial restrictions (Obenaus *et al.* 2006, Obenaus 2011).

In some graves at the uphill site of Thunau, the archaeologists located a social elite, especially in the male graves with rich assemblages including swords, an axe and spurs in the north-western part of the graveyard. However, the generally small number of added weapons in Great Moravian cemeteries (and in Thunau) is an argument against the assumption that weapons in the grave would mark warriors. Rather, weapons as grave goods probably stand in a relationship to a higher social status of the individuals. Furthermore, a small group of elite females buried with silver and gilded earrings was identified (Friesinger & Friesinger 1991, Nowotny 2013, Obenaus 2013). The most common grave goods of females are jewellery, rings for headdresses, ear- and finger rings. No evidence for any special activity of the females was obvious from findings in the settlement or in the graves (Nowotny 2011). The interpretation of individuals belonging to a higher standing social group concerns only a special part of the cemetery. Apart from that, there is generally only little archaeological

evidence from the uphill settlement area concerning activities, except for minor signs of a metal- and a bone workshop, the production of jewellery and textile, and for trading (at the Schanze and Untere Holzweise, e.g. a balance was found, Herold 2008, 296, Szameit 1995, 279). Only in a small number of graves (10) in the hillfort series of Thunau were tools found, including a needle, an awl, a grindstone, a spindle whorl and a piercer. These were probably tools of daily life and do not point to any specific occupation. However, it seems to be a general trend in early medieval graves to reduce grave goods (Nowotny 2011).

Generally, there was a rather weak association between frequencies of enthesal and joint changes in the Thunau series. However, in total the predicted population differences between the uphill and the downhill settlement groups can be confirmed. This can be deduced from the frequencies, asymmetry and statistically significant patterns in the younger (less than 50 years) age groups for the enthesal and joint changes. The slight osteoarthritic changes are found to be more or less equally distributed in the uphill and the downhill group all over the skeleton. Conversely, the enthesal changes reveal more details due to their relation to more specialised, power demanding work sequences, which is mainly apparent in the downhill males. The males of the hillfort group seem to represent, however, a rather inhomogeneous, diverse group, as they show general signs of activity at their skeletons (e.g. significant enthesal changes are mainly visible between the young and the middle age groups, which can tentatively be interpreted as work related), but do not show a special pattern in their enthesal and joint changes. The general diversity of the samples is also reflected by the considerable variation in the long bones (resulting in significant differences in body height). Additionally, the results of other analyses performed on the Thunau group, for example strontium isotope ratios to identify the provenience of the inhabitants of the hilltop area show that actually 83-89% of the people buried in the uphill graveyard are non-locals (about a third of the individuals has been analysed). This supports the hypothesis that the 'central settlement' character of the site may be related to a particular military and trading centre function, with frequently changing occupation forces on the periphery of the Frankish Empire (Teschler-Nicola *et al.* 2015). Further, high mobility, limited space and a very high frequency of infectious diseases such as tuberculosis, probably related to poor hygienic conditions in the population supported this hypothesis (Teschler-Nicola *et al.* 2015). In addition, an analysis of  $\delta^{13}\text{C}$  and  $\delta^{15}\text{N}$  values in the two populations, which was expected to reveal differences in social status, neither reflected differences in diet between the sites, nor between males and

females (Rumpelmayer 2011, 2015, 19). The high probability that the site has served as a market place implying a high passage of people, could also be added to explain the situation found at the Thunau hillfort site.

The weak association between EC and OA is somewhat more accentuated in the males. Both sexes in all groups (hillfort and valley) show high frequencies in OA, but high EC frequencies were only found in the males and the increase of changes with higher age can be confirmed in both groups for most entheses and joints. The downhill females show the most distinct asymmetries in the joints but even more in the enthesal changes (flexors/extensors) of the upper extremities, also compared to the males. Further, the data of the downhill females indicate a younger age when the changes first appear compared to the uphill females as apparent from the scatterplots, and possibly a higher mobility (statistically significant results in enthesal changes of the right hip). Overall, these results indicate that the downhill females reflect an earlier entry into worklife as well as a stronger involvement in physically demanding tasks in their life (more marked asymmetry in the upper limb) and being more mobile. Concerning the uphill males, significant enthesal changes are mainly visible between the young and the middle age group, which could indicate work related changes. Further, significant results in the hip joints on both body sides between the series were found, where the downhill males showed higher scores, respectively, pointing to an even higher mobility of the latter. Moreover, the downhill males display the highest frequencies of enthesal changes in the *M. triceps brachii* and the pooled *M. biceps/M. brachialis* (extension in the elbow, stroke movements; flexion of the elbow and supination of the forearm), and a distinctly stronger asymmetry, especially in the upper extremities. In two entheses (*M. triceps brachii*, and *M. quadriceps femoris*, both right body side) significant results according to asymmetries were found in the males from the valley compared to the hillfort males. These results point to a physically demanding lifestyle of the males of both series, whereas the details visible in the downhill males indicate a higher mobility and a higher specialisation in their tasks (probably craft-production related, as e.g. smithing and stone masonry is proven in the downhill settlement). The social elite in the uphill males depicted by the “warriors” does not seem to be reflected in the group statistics, but group differences between the uphill and the downhill males and females are obvious. Apart from that, the uphill males also show signs of physically demanding activities, partly, as in the downhill site, from young age on, but obviously in a more generalized manner; they do not seem to have performed very specialised tasks in

defensive functions. The possibility that only a small number of high status individuals (equalised with warriors) were buried here, as reflected by grave customs in the hillfort necropolis, would mean that the bulk of individuals were rather generalists performing daily activities related to subsistence and probably trading activities, which would not produce a special pattern at their entheses and joints.

In summary, the differences and similarities in the results according to the prevalence of enthesal and joint changes in the Thunau groups generally indicate a physically demanding lifeway for the individuals inhabiting the two sub-sites. However, from the present data, there is more evidence for specialised work sequences for the males and the females of the valley sub-site, beyond beginning at a younger age. This analysis, in combination with the archaeological findings, allowed an insight into the daily life, the social- and working environment of these two populations from Thunau am Kamp.

## 13 REFERENCES

- Alves Cardoso F. 2008. A Portrait of Gender in Two 19th and 20th Century Portuguese Populations: A Palaeopathological Perspective. [Ph.D. Thesis, Department of Archaeology, Durham University].
- Alves Cardoso F., and Henderson CY. 2010. Enthesopathy formation in the humerus: Data from known age-at-death and known occupation skeletal collections. *American Journal of Physical Anthropology* 141(4):550-560.
- ArcGIS 9.2. 2007. ESRI Inc. In: Redlands C, editor.
- Auerbach B., and Ruff C. 2006. Limb bone bilateral asymmetry: variability and commonality among modern humans. *Journal of Human Evolution* 50:203-218.
- Belcastro MG., Facchini F., Neri R., and Mariotti V. 2001. Skeletal markers of activity in the Early Middle Ages necropolis of Vicenne-Campochiaro (Molise, Italy). *Journal of Pathology* 13(3):9-20.
- Benjamin M., Evans EJ., and Copp L. 1986. The histology of tendon attachments to bone in man. *Journal of Anatomy* 149:89-100.
- Benjamin M., and Ralphs JR. 1998. Fibrocartilage in tendons and ligaments - an adaptation to compressive load. *Journal of Anatomy* 193:481-494.
- Benjamin M., Kumai T., Milz S., Boszczyk BM., Boszczyk AA., and Ralphs JR. 2002. The skeletal attachment of tendons - tendon 'entheses'. *Comparative Biochemistry and Physiology* 133(Part A):931-945.
- Benjamin M., Toumi H., Ralphs J., Bydder G., Best T., and Milz S. 2006. Where tendons and ligaments meet bone: attachment sites ("entheses") in relation to exercise and/or mechanical load. *Journal of Anatomy* 208 471-490.
- Biermann H. 1957. Die Knochenbildung im Bereich periostaler-diaphysärer Sehnen- und Bandansätze. *Zeitschrift für Zellforschung* 46:635-671.
- Breibert W., and Wiltschke-Schrotta K. 2010. Frühmittelalterliche Hügelgräber auf der Schanze von Thunau am Kamp, Niederösterreich. *Archaeologica Austriaca* 94(127-149).
- Bridges PS. 1997. The relationship between muscle markings and diaphyseal strength in prehistoric remains from West-Central Illinois. *American Journal of Physical Anthropology* 104: S24, 82.

- Burt NM., Semple D., Waterhouse K., and Lovell N. 2013. Identification and Interpretation of Joint Disease in Paleopathology and Forensic Anthropology: Charles C. Thomas, Springfield, Illinois, USA.
- Campanacho V., and Santos AL. 2013. Comparison of the Entheseal Changes of the os coxae of Portuguese Males (19th–20thcenturies) with Known Occupation. *International Journal of Osteoarchaeology* 23 (229-236).
- Carter DR., and Beaupré GS. 2001. Skeletal function and form: Cambridge University Press.
- Crubézy E., Goulet J., Bruzek J., Jelinek J., Rougé D., and Ludes B. 2002. Epidemiology of osteoarthritis and enthesopathies in a European population dating back 7700 years. *Joint Bone Spine* 69:580-588.
- Cunha E., and Umbelino C. 1995. What can bones tell about labour and occupation: the analysis of skeletal markers of occupational stress in the Identified Skeletal Collection of the Anthropological Museum of the University of Coimbra (preliminary results). *Antropologia Portuguesa* 13:49 - 68.
- Dolgo-Saburoff B. 1929/30. Über Ursprung und Insertion der Skelettmuskeln. *Anatomischer Anzeiger* 68:80-87.
- Doying A. 2010. Differentiation of Labor-Related Activity by Means of Musculoskeletal Markers. [Master thesis, University of Florida].
- Dutour O. 1986. Enthesopathies (lesions of muscular insertions) as indicators of the activities of neolithic Saharan populations. *American Journal of Physical Anthropology* 71:221-224.
- Foster A., Buckley H., and Tayles N. 2014. Using Enthesis Robusticity to Infer Activity in the Past: A Review. *Journal of Archaeological Method and Theory* 21:511-533.
- Friesinger H., and Friesinger I. 1991/1. Ein Vierteljahrhundert Grabungen in Thunau/Gars am Kamp. *Archäologie Österreichs*, Mitteilungen der österreichischen Gesellschaft für Ur- und Frühgeschichte 2:6- 22.
- Gray H. 1995. Gray's Anatomy of the Human Body: Churchill Livingstone, New York.
- Havelková P., Villotte S., Velemínský P., Poláček L., and Dobisíková M. 2011. Enthesopathies and Activity Patterns in the Early Medieval Great Moravian Population: Evidence of Division of Labour. *International Journal of Osteoarchaeology* 21: 487-504.
- Havelková P., Hladík M., and Velemínský P. 2012. Entheseal changes: Do they reflect socioeconomic status in the Early Medieval Great Moravian Population? (Mikulčice,

- 9th - 10th century, Czech Republic). Poster at the Meeting of the American Association of Physical Anthropology, Portland, OR.
- Havelková P., Hladik M., and Velemínský P. 2013. Enteseal Changes: Do They Reflect Socioeconomic Status in the Early Medieval Central European Population? (Mikulčice - Klášteřisko, Great Moravian Empire, 9th - 10th century). *International Journal of Osteoarchaeology* 23:237-251.
- Hawkey D., and Merbs CF. 1995. Activity-induced musculoskeletal stress markers (MSM) and subsistence strategy changes among ancient Hudson Bay Eskimo. *International Journal of Osteoarchaeology* 5: 324-338.
- Henderson CY. 2003. Rethinking Musculoskeletal Stress Markers. British Association of Biological Anthropology and Osteoarchaeology (BABAO). Poster at the 5<sup>th</sup> Annual Conference.
- Henderson CY. 2009. Musculo-skeletal stress markers in bioarchaeology: indicators of activity levels of human variation? A re-analysis and interpretation. [PhD thesis, University of Durham, UK].
- Henderson CY., and Gallant A. 2006. Quantitative Recording of Enteses. Paper presented at the 16th European Meeting of the Paleopathology Association. Santorini, Greece.
- Henderson CY, Gallant, A. J. 2007. Quantitative recording of enteses. *Paleopathology Newsletter* 137:7-12.
- Henderson, CY., Mariotti, V., Pany-Kucera, D., Perréard-Lopreno G., Villotte, S., Wilczak, C. 2010. Scoring enteseal changes: proposal of a new standardised method for fibrocartilaginous enteses. Abstract & Poster. 18<sup>th</sup> meeting of the Paleopathology Association, Vienna, Austria.
- Henderson CY., Mariotti, V., Pany-Kucera, D., Perréard-Lopreno, G., Villotte, S., Wilczak, C. 2012. The effect of age on enteseal changes at some fibrocartilaginous enteses. *American Journal of Physical Anthropology* 147 (S54):163 (abstract).
- Henderson CY., and Alves Cardoso, F. 2013. Special Issue Enteseal Changes and Occupation: Technical and Theoretical Advances and Their Applications. *International Journal of Osteoarchaeology* 23: 127-134.
- Henderson CY., Mariotti V., Pany-Kucera D., Villotte S., and Wilczak C. 2013. Recording specific enteseal changes of fibrocartilaginous enteses: Initial tests using the Coimbra method. *International Journal of Osteoarchaeology* 23 (2):152-162.

- Henderson CY., Mariotti V., Pany-Kucera D., Villotte S., and Wilczak C. 2015 (forthcoming). The new "Coimbra method": a biologically appropriate method for recording specific features of fibrocartilagenous enthesal changes. Submitted to *International Journal of Osteoarchaeology*.
- Herold H. 2008. Der Schanzberg von Gars-Thunau in Niederösterreich. Sonderdruck aus *Archäologisches Korrespondenzblatt* 38(2): 283-299.
- Herrmann B. 1990. *Prähistorische Anthropologie*. Springer Berlin Heidelberg.
- Jurmain RD. 1991. Degenerative changes in peripheral joints as indicators of mechanical stress: opportunities and limitations. *International Journal of Osteoarchaeology* 1: 247-252.
- Jurmain R. 1999. *Stories from the Skeleton. Behavioral Reconstruction in Human Osteology*. Australia, Gordon and Breach: Amsterdam.
- Jurmain R., and Villotte S. 2010. Terminology – entheses in medical literature: a brief review. In *Workshop in Musculoskeletal Stress markers (MSM): Limitations and Achievements in the Reconstruction of Past Activity Patterns*. URL:[http://www.uc.pt/en/cia/msm/MSM\\_terminology3.pdf](http://www.uc.pt/en/cia/msm/MSM_terminology3.pdf)
- Jurmain R., Cardoso FA., Henderson C., and Villotte S. 2012. Bioarchaeology's Holy Grail: The Reconstruction of Activity. In: *A Companion to Paleopathology*. Grauer, A. (editor): Wiley-Blackwell, Chichester, UK. 531-552.
- Kanz F., Grossschmidt K., Risy R., and Risser D. 2013. X-ray study on the laterality of the humeral bone mineral density for determination of handedness. *American Journal of Physical Anthropology* 150:162.
- Kennedy KAR. 1998. Markers of occupational stress: Conspectus and prognosis of research. *International Journal of Osteoarchaeology* 8:305-310.
- Knese K-H., and Biermann H. 1958. Die Knochenbildung an Sehnen und Bandansätzen im Bereich ursprünglich chondraler Apophysen. *Zeitschrift für Zellforschung* 49:142-187.
- Knüsel CJ. 2000. Bone adaptation and its relationship to physical activity in the past. In: Cox M, and Mays S, editors. *Human Osteology in Archaeology and Forensic Science* London, Greenwich: Medical Media. p 381-402.
- Konášová K., Drozdová E., and Smrčka V. 2009. Fracture trauma in Slavonic population from Pohansko u Břeclavi (Czech Republic). *Anthropologie* 47: 3, 243-252.
- Kujanová M., Bigoni L., Velemínská J., and Velemínský P. 2008. Skeletal Asymmetry of Locomotor Apparatus at Great Moravian Population. In: Velemínský P, and Poláček

- L, editors. Studien zum Burgwall von Mikulčice VIII. Brno: Archäologisches Institut der Akademie der Wissenschaften der tschechischen Republik. 235-263.
- Macháček J. 2011. Fünfzig Jahre archäologische Ausgrabungen in Pohansko bei Břeclav. In: Macháček J, and Ungermanš., editors. Frühgeschichtliche Zentralorte in Mitteleuropa, Studien zur Archäologie Europas, 15-33.
- Mariotti V. 1998. Ricerche sugli indicatori scheletrici morfologici di attività. [Tesi di Dottorato in Scienze Antropologiche, Università degli Studi di Bologna].
- Mariotti V., Facchini F., and Belcastro MG. 2004. Enthesopathies - Proposal of a standardized scoring method and applications. *Collegium Anthropologicum* 28: 145-159.
- Mariotti V., Facchini F., and Belcastro MG. 2007. The study of entheses: Proposal of a Standardized Scoring Method for Twenty-Three Entheses of the Postcranial Skeleton. *Collegium Anthropologicum* 31: 291-313.
- Merbs CF. 1983. Patterns of Activity-induced Pathology in a Canadian Inuit Population. Ottawa National Museums of Canada.
- Milella M., Belcastro M., Zollikofer P., and Mariotti V. 2012. The Effect of Age, Sex, and Physical Activity on Enthesal Morphology in a Contemporary Italian Skeletal Collection. *American Journal of Physical Anthropology* 148: 379-388.
- Meyer C., Niklisch N., Held P., Fritsch B., and Alt KW. 2011. Tracing patterns of activity in the human skeleton: An overview of methods, problems, and limits of interpretation. *HOMO - Journal of Comparative Human Biology* 62:202-217.
- Niinimäki S. 2011. What do Muscle Marker Ruggedness Scores Actually Tell us? *International Journal of Osteoarchaeology* 21: 292-299.
- Niinimäki S. 2012. Reconstructing Physical Activity from Human Skeletal Remains. [PhD thesis: University of Oulu].
- Niinimäki S., and Baiges Sotos L. 2013. The Relationship Between Intensity of Physical Activity and Enthesal Changes on the Lower Limb. *International Journal of Osteoarchaeology* 23:221-228.
- Nittmann J. 2012. Degenerative Veränderungen an der Wirbelsäule der frühmittelalterlichen Population von Gars/Thunau, Niederösterreich. [Diploma thesis, University of Vienna].
- Nittmann J., Teschler-Nicola, M. 2014. Veränderungen der Wirbelsäule als Indikatoren physischer Belastung am Beispiel der frühmittelalterlichen Bevölkerung von

- Gars/Thunau, Niederösterreich. *Mitteilungen der Anthropologischen Gesellschaft in Wien* (MAGW) 144, 201-220.
- Nolte M., and Wilczak C. 2013. Three-dimensional Surface Area of the Distal Biceps Enthesis, Relationship to Body Size, Sex, Age and Secular Changes in a 20th Century American Sample. *International Journal of Osteoarchaeology* 23: 163-174.
- Novak S. 2000. Battle-related trauma. In: Fiorato V, Boylston A, and Knüsel CJ, editors. *Blood red roses*. Oxford, Great Britain: Oxbow books, 90-102.
- Nowotny E. 2011. Das frühmittelalterliche Gräberfeld von Thunau, Obere Holzweise. Untersuchungen zur Archäologie eines Grenzraumes in der späten Karolingerzeit [PhD thesis: University of Vienna].
- Nowotny E. 2013. Repräsentation zwischen Karolingerreich und Großmähren. Das Beispiel des Gräberfeldes von Thunau am Kamp, Obere Holzweise. In: Hardt M, and Heinrich-Tamáška O, editors. *Macht des Goldes Gold der Macht*: Verlag Bernhard Albert Greiner. 439-459.
- Obenaus M., Breibert W., and Szameit E. 2006. Frühmittelalterliche Bestattungen und Siedlungsbefunde aus Thunau am Kamp, Niederösterreich - ein Vorbericht. *Sonderdruck aus Fundberichte aus Österreich*, Band 44, 2005.
- Obenaus M. 2008. Ostösterreich - Ein Grenzraum im 9. und 10. Jahrhundert aus archäologischer Sicht. *NÖLA, Mitteilungen aus dem Niederösterreichischen Landesarchiv* 13:194-218.
- Obenaus M. 2011. Die neuen Forschungen in der frühmittelalterlichen Talsiedlung von Thunau am Kamp (Ein Zwischenbericht). In: Macháček J, and Ungerman Š., editors. *Frühgeschichtliche Zentralorte in Mitteleuropa, Studien zur Archäologie Europas*. p 529-549.
- Obenaus M. 2013. Das turbulente 9. Jahrhundert. Geschichte aus dem Boden. In Pieler, F. (Hrsg.): *Geschichte aus dem Boden. Archäologie im Waldviertel*: 316-333. Waldviertler Heimatbund.
- OptoCAT 4.0.1. 2005. Meersburg (D): Breuckmann GmbH.
- Pany D. 2003. Mining for the miners? An analysis of occupationally- induced stress markers on the skeletal remains from the ancient Hallstatt cemetery. [Master thesis: University of Vienna].

- Pany D., Viola TB., and Teschler-Nicola M. 2007. An attempt in using a 3D surface scanner for recording musculoskeletal stress markers (MSM). 2<sup>nd</sup> Paleopathology Association Meeting in South America (PAMinSA). Santiago, Chile.
- Pany D., Viola TB., and Teschler-Nicola M. 2008. Analysis of musculoskeletal stress markers and joint disease on the early medieval skeletons from Thunau (Austria) and the evaluation of a new methodological approach. 77<sup>th</sup> Annual Meeting of the American Association of Physical Anthropologists. Columbus, Ohio.
- Pany D., Viola TB., and Teschler-Nicola M. 2009. The scientific value of using a 3D surface scanner to quantify entheses. Abstract & talk at the “Workshop in Musculoskeletal stress markers (MSM): limitations and achievements in the reconstruction of past activity patterns”. University of Coimbra, Portugal.
- Pearson OM., and Buikstra JE. 2006. Behavior and the Bones. In: Buikstra, JE. and Beck, LA. (eds.): *Bioarchaeology The Contextual Analysis of Human Remains* Amsterdam, Academic Press. 207-226.
- Platzer, W. 1991: *Bewegungsapparat. Band 1*. Georg Thieme Verlag Stuttgart, New York. Deutscher Taschenbuch Verlag.
- Přichystalová, R. 2011. Die Bestattungen in Břeclav-Pohansko. Alte und neue Ausgrabungen. In: Macháček J, and Ungerman Š., editors. *Frühgeschichtliche Zentralorte in Mitteleuropa, Studien zur Archäologie Europas*, 35-61.
- Rapidform 2006. Inus Technology Inc. Seoul (Korea).
- Robb JE. 1998. The Interpretation of Skeletal Muscle Sites: A Statistical Approach. *International Journal of Osteoarchaeology* 8:363–377.
- Rogers J., Shepstone L., and Dieppe P. 1997. Bone formers: osteophyte and enthesophyte formation are positively associated. *Annals of the Rheumatic Diseases* 56: 85-90.
- Rogers J., and Waldron T. 1995. *A Field Guide to Joint Diseases in Archaeology*. John Wiley & Sons.
- Rumpelmayer K. 2012. Reconstructing diet by stable isotope analysis (d13C and d15N): Two case studies from Bronze Age and Early Medieval Lower Austria. [Ph.D. Thesis, Vienna University].
- Rumpelmayer K., Wild E-M., Teschler-Nicola M., and Pavlik A. 2015 [in press]. Paläodiät-Rekonstruktion mittels Stabil-Isotopenuntersuchungen ( $\delta^{13}\text{C}$  und  $\delta^{15}\text{N}$ ) an den frühmittelalterlichen Skelettresten von Thunau/Gars am Kamp. *Archäologie Österreichs*.

- Santos AL., Alves Cardoso F., Assis S., and Villotte S. 2011. The Coimbra Workshop in Musculoskeletal Stress Markers (MSM): an annotated review. *Anthropologia Portuguesa* 28: 135-161.
- Schlecht SH. 2012. Understanding Entheses: Bridging the Gap Between Clinical and Anthropological Perspectives. *The anatomical record* 295: 1239-1251.
- Schultz M. 1988. Paläopathologische Diagnostik. In: Knußmann R., editor. Anthropologie. Handbuch der vergleichenden Biologie des Menschen. Band I: Wesen und Methoden der Anthropologie, Bd.1. 4. Stuttgart, New York: Gustav Fischer Verlag, 480–496.
- Sjøvold T. 1990. Estimation of stature from long bones utilizing the line of organic correlation. *Human Evolution* 5(5): 431-447.
- Sládek V., Berner M., Sosna D., and Sailer R. 2007. Human manipulative behavior in the Central European Late Eneolithic and Early Bronze Age: Humeral bilateral asymmetry. *American Journal of Physical Anthropology* 133: 669-681.
- Steckel RH., Larsen CS., Sciulli PW., Walker PL. 2005. Data Collection Codebook. The Global History of Health Project. [global.sbs.ohio-state.edu/docs/Codebook-12-12-05.pdf](http://global.sbs.ohio-state.edu/docs/Codebook-12-12-05.pdf)
- Stirland AJ. 1998. Musculoskeletal evidence for activity problems of evaluation. *International Journal of Osteoarchaeology* 8:354-362.
- Szameit E. 1995. Gars–Thunau – frühmittelalterliche fürstliche Residenz und vorstädtisches Handelszentrum. In: Brachmann H. (Hrsg.), Burg-Burgstadt-Stadt. Zur Genese mittelalterlicher nichtagrarischer Zentren in Ostmitteleuropa, Berlin. 274-282.
- Szameit E., and Obenaus M. 2007. KG Thunau am Kamp, MG Gars am Kamp, VB Horn. *Fundberichte aus Österreich* 46:726-727.
- Szameit E., and Obenaus M. 2009. KG Thunau am Kamp, MG Gars am Kamp, VB Horn. *Fundberichte aus Österreich* 46: 462-464.
- Teschler-Nicola M., Wiltschke-Schrotta K., Prossinger H., Berner M. 1994. The epidemiology of an early medieval population from Gars/Thunau, lower Austria. *Homo* 1994, S45, 131.
- Teschler-Nicola M., Novotny F., Spannagl-Steiner M., Stadler P., Prohaska T., Irrgeher J., Zitek A., Däubel B., Haring E., Rumpelmayr K., and Wild E-M. 2015. The Early Medieval Manorial Estate of Gars/Thunau, Lower Austria: An Enclave of Endemic Tuberculosis? *Tuberculosis* 2, 1-9.

- Velemínský P., Likovský J., Trefný P., Dobisíková M., Velemínská J., Poláček L., and Hanáková H. 2005. Anthropologische Analyse des großmährischen Gräberfeldes Kostelisko im Suburbium des Burgwalls von Mikulčice. In: Poláček L., editor. Studien zum Burgwall von Mikulčice VI. Brno: Archäologisches Institut der Akademie der Wissenschaften der tschechischen Republik. 539-633.
- Villotte S. 2006. Connaissance médicales actuelles, cotation des enthésopathies. *Bulletin et Mémoires de la Société d'Anthropologie de Paris* : 18 (1-2):65-85.
- Villotte S., Castex D., Couallier V., Dutour O., Knüsel CJ., Henry-Gambier D. 2009. Enthesopathies as occupational stress markers: evidence from the upper limb. *American Journal of Physical Anthropology* 42: 224-234.
- Villotte S., Churchill SE., Dutour OJ., Henry-Gambier D. 2010. Subsistence Activities and the sexual division of labor in the European Upper Paleolithic and Mesolithic: Evidence from upper limb enthesopathies. *Journal of Human Evolution* 59: 35-43.
- Villotte S., Knüsel, C. 2013. Understanding Enteseal Changes: Definition and Life Course Changes. *International Journal of Osteoarchaeology* 23:135-146.
- Waldron T. 1994. *Counting the Dead: The Epidemiology of Skeletal Populations*. Chichester, Wiley.
- Weiss E. 2003. Understanding muscle markers: aggregation and construct validity. *American Journal of Physical Anthropology* 21: 230-240.
- Weiss E. 2004. Understanding muscle markers: lower limb. *American Journal of Physical Anthropology* 25: 232-238.
- Weiss E. 2006. Osteoarthritis and body mass. *International Journal of Osteoarchaeology* 33: 690-695.
- Weiss E., and Jurmain R. 2007. Osteoarthritis Revisited: A Contemporary Review of Aetiology. *International Journal of Osteoarchaeology* 17: 437-450.
- Weiss E., Corona L., and Schultz B. 2012. Sex Differences in Musculoskeletal Stress Markers: Problems with Activity Pattern Reconstructions. *International Journal of Osteoarchaeology* 22: 70-80.
- Wentz RK., and de Grummond NT. 2009. Life on Horseback: Palaeopathology of Two Scythian Skeletons from Alexandropol, Ukraine. *International Journal of Osteoarchaeology* 19: 107-115.

- Wilczak CA. 1998a. Consideration of sexual dimorphism, age, and asymmetry in quantitative measurements of muscle insertion sites. *International Journal of Osteoarchaeology* 8: 311-325.
- Wilczak CA. 1998b. A new method for quantifying musculoskeletal stress markers (MSMs): A test of the relationship between enthesis size and habitual activity in archaeological populations. [PhD thesis, Cornell University].
- Wilczak CA., Henderson CY., Mariotti V., Pany-Kucera D., Villotte S. 2014. Meet me in Coimbra: An international saga of interobserver error rates. 83<sup>rd</sup> Annual Meeting of the American Association of Physical Anthropologists, Calgary, Canada.

## **ADDENDUM**

### **13.1 Scoring sheet entheses**

Enthesopathiebefund	Objekt:	Grab-Nr.
Signatur:	Datum:	Alter:
Arch. Bemerk.:		Geschlecht:
Cranium: nicht erodiert	tlw. erod.	stark erod.
Postcranium: nicht erodiert	tlw. erod.	stark erod.

### Enthesopathiebefund:

Muskel/Ligament	rechts			links			Anmerkung
	R	S	OS	R	S	OS	
Scapula							
1 M. TRICEPS BRACHII U							
2 M. TERES MINOR U							
3 M. TERES MAJOR.....U							
4 M. INFRASPINATUS.....U							
5 M. TRAPEZIUS A							
6 M. BICEPS BRACHII (long head)...U							
7 M. PECTORALIS MINOR U							
Clavicula							
5 LIG. COSTOCLAVIC. A							
6 M. PECTORALIS MAJOR U							
7 LIG. CONOIDEUM A (Coracocl.)							
8 LIG. TRAPEZOIDEUM A (Coracocl.)							
7 M. DELTOIDEUS							
9 1. Rippe LIG. COSTOCLAVIC. ..U							
Humerus							
9 M. PECTORALIS MAJOR A							
10 M. LATISSIMUS DORSI A							
11 M. TERES MAJOR A							
12 M. DELTOIDEUS A							
13 M. CORACOBRACHIALIS A							
14 M. SUBSCAPULARIS							
15 M. SUPRASPINATUS A							
16 M. INFRASPINATUS A							
17 M. TERES MINOR A							
18 COMMON EXTENSORS U							
19 COMMON FLEXORS U							

Legende:

M= Muskelmarker, A= Muskelansatz U= Muskelursprung, Lig.=Ligament, G=Gelenk, R= Robustizität, S= Stressläsion, O=Osteophyten (Ossification), T = Tendo.

f. Muskeln: 0=R nicht ausgeprägt, 1=R schwache Ausprägung. Cortex leicht gerundet, Erhebung bei Angreifen spürbar, keine Kämme/Leisten.

2=R mittlere Ausprägung. Corticalis ist uneben u. leicht erkennbare hügelartige Erhebung. Keine scharfen Kämme oder Leisten.

3=R starke Ausprägung. Scharfe Kämme und Leisten sind deutlich ausgebildet. Zwischen zwei Kämmen oder Leisten leichte Depressionen, die sich aber nicht in den Cortex fortsetzen (z.B. zwischen pectoralis major und teres major Insertions sichtbar).

f. Ligamente: 0=R nicht ausgeprägt, 1=R schwache Ausprägung. Leichte Vertiefung oder Ausbuchtung, nicht scharf abgegrenzt.

2=R mittlere Ausprägung. Rauigkeit a. d. Ansatzstelle, meistens mit klar definierter Umgrenzung.

3=R starke Ausprägung. Starke Eintiefung mit klar definiertem Knochenrand. Scharfe Kämme auf dem Areal.

4-8 schwache Ausprägung. Eine schmale „Furche“, eine Art Aushöhlung im Cortex mit lytischem Erscheinungsbild. Weniger als 1mm tief.

5-8 mittlere Ausprägung. Die Aushöhlung ist tiefer und größer als 1mm, aber weniger als 3mm tief. Ev. verschieden lang, nicht länger als 5mm.

6-8 starke Ausprägung. Ausgeprägte Aushöhlung, mehr als 3mm tief und länger als 5mm.

7-0S schwache Ausprägung. Leichte Exostose erkennbar, meistens leicht abgerundet und nicht größer als 2mm.

8-0S mittlere Ausprägung. Deutliche Exostose, unterschiedlich in der Form, größer als 2mm, kleiner als 5mm.

9-0S starke Ausprägung. Die Exostose erhebt sich mehr als 5mm über die Knochenoberfl. oder bedeckt gr. Teil der corticalen Oberfläche.

1

Enthesopathiebefund	Objekt:	Grab-Nr.
Signatur:	Datum:	Alter:
Arch. Bemerk.:		Geschlecht:
Cranium: nicht erodiert	tlw. erod.	stark erod.
Postcranium: nicht erodiert	tlw. erod.	stark erod.

Radius							
20 M. BICEPS BRACHII A							
21 M. PRONATOR TERES A							
22 M. SUPINATOR A							
23 M. PRON. QUADRATUS A							
<b>Muskel/Ligament</b>	<b>rechts</b>			<b>links</b>			<b>Anmerkung</b>
	R	S	OS	R	S	OS	
Ulna							
24 M. BRACHIALIS A							
25 M. TRICEPS BRACHII A							
26 M. ANCONAEUS A							
27 M. FLEXOR DIG. SUPERF. U							
Os coxae							
28 M. SEMIMEMBRANOSUS U							
29 M. SEMITENDINOSUS U							
Femur							
30 M. GLUTEUS MAXIMUS A							
31 LINEA ASPERA A							
32 Patella							
Tibia							
33 LIG. PATELLAE A							
34 M. SOLEUS U							

Legende:

M- Muskelmarker, A- Muskelansatz U- Muskelursprung, Lig.-Ligament, G-Gelenk, R- Robustizität, S- Stressläsion, O-Osteophyten (Ossification), T - Tendo.

- f. Muskeln: 0=R nicht ausgeprägt, 1=R schwache Ausprägung. Cortex leicht gerundet, Erhebung bei Angreifen spürbar, keine Kämme/Leisten.  
 2=R mittlere Ausprägung. Corticalis ist uneben u. leicht erkennbare hügelartige Erhebung. Keine scharfen Kämme oder Leisten.  
 3=R starke Ausprägung. Scharfe Kämme und Leisten sind deutlich ausgebildet. Zwischen zwei Kämmen oder Leisten leichte Depressionen, die sich aber nicht in den Cortex fortsetzen (z.B. zwischen pectoralis major und teres major Insertions sichtbar).  
 f. Ligamente: 0=R nicht ausgeprägt, 1=R schwache Ausprägung. Leichte Vertiefung oder Ausbuchtung, nicht scharf abgegrenzt.  
 2=R mittlere Ausprägung. Rauigkeit a. d. Ansatzstelle, meistens mit klar definierter Umgrenzung.  
 3=R starke Ausprägung. Starke Eintiefung mit klar definiertem Knochenrand. Scharfe Kämme auf dem Areal.  
 4-8 schwache Ausprägung. Eine schmale „Furche“, eine Art Aushöhlung im Cortex mit lytischem Erscheinungsbild. Weniger als 1mm tief.  
 5-8 mittlere Ausprägung. Die Aushöhlung ist tiefer und größer als 1mm, aber weniger als 3mm tief. Ev. verschieden lang, nicht länger als 5mm.  
 6-8 starke Ausprägung. Ausgeprägte Aushöhlung, mehr als 3mm tief und länger als 5mm.  
 7-0S schwache Ausprägung. Leichte Exostose erkennbar, meistens leicht abgerundet und nicht größer als 2mm.  
 8-0S mittlere Ausprägung. Deutliche Exostose, unterschiedlich in der Form, größer als 2mm, kleiner als 5mm.  
 9-0S starke Ausprägung. Die Exostose erhebt sich mehr als 5mm über die Knochenoberfl. oder bedeckt gr. Teil der corticalen Oberfläche.

## 13.2 Scoring sheet joints

Fundkomplex	Grabnr.
Bemerkung	

Gelenke		rechts			links				
		Rand-OP	Fläche KN	P	Bewertung	Rand-OP	Fläche KN	P	Bewertung
Schultergelenk	Caput humeri								
	Cavitas glenoidalis								
Ellenbogengelenk	Capitulum humeri								
	Caput radii								
	Trochlea								
	Incisura trochlearis								
Radio-Ulnar-Gelenk	Circumferentia art. (Radius)								
	Incisura radialis (Ulna)								
	Incisura ulnaris (Radius)								
	Circumferentia art. (Ulna)								
Proximales Handgelenk	Prox. Reihe Handwurzelkn.								
	Fac. art. carpalis (Radius)								
	Caput ulnae								
Interphalang.gel.	Pollux proximal								
Hüftgelenk	Acetabulum								
	Caput femoris								
	Fovea capitis femoris		X				X		
Kniegelenk	Facies patellaris (Femur)								
	Condylus med. femoris								
	Condylus lat. femoris								
	Unterrand d. Foss. intercond.		X				X		
	Condylus med. tibiae								
	Condylus lat. Tibiae								
	Facies med. (Patella)								
Facies lat. (Patella)									
Proximales Sprunggelenk	Facies art. inf. (Tibia)								
	Facies art. sup. (Talus)								
Dist. Sprungg.	Facies art. tal. post. (Calcan.)								
Interphalang.gel.	Hallux proximal								

OP = Osteophytenwachstum, KN = Knochenneubildung an der Gelenksfläche, P = Porositäten an der Gelenksfläche; / = nicht vorhanden, 0 = nicht beurteilbar, 1 = normal, 2 = Pathologie erkennbar (OP < 3mm, = II.-III. nach Schultz 1988), 3 = starke Pathologie erkennbar (> Hälfte des Gelenkes betroffen, = IV.-VI. nach Schultz 1988); E = Eburnisation, a = < als d. Hälfte des Gelenkes vorhanden

### 13.3 List of analysed individuals from Thunau for enthesal changes, right extremities

In this list, the individuals analysed for the entheses investigation of the right extremities can be found. The skeletons are currently housed at the Natural History Museum in Vienna.

Legend: series 1 = uphill/hillfort site, series 2 = downhill/valley site; sex: 1 = male, 2 = female

graveyard	series	specific location	gravenumber	inventory number	sex
Thunau/Kamp	1	Herrenhof, Obere Holzweise	1	24953	1
Thunau/Kamp	1	Herrenhof, Obere Holzweise	2	25193	1
Thunau/Kamp	1	Herrenhof, Obere Holzweise	9	24960	2
Thunau/Kamp	1	Herrenhof, Obere Holzweise	10	24961	1
Thunau/Kamp	1	Herrenhof, Obere Holzweise	11	24962	2
Thunau/Kamp	1	Herrenhof, Obere Holzweise	12	24963	1
Thunau/Kamp	1	Herrenhof, Obere Holzweise	18	24970	1
Thunau/Kamp	1	Herrenhof, Obere Holzweise	20	24972	2
Thunau/Kamp	1	Herrenhof, Obere Holzweise	21	24973	2
Thunau/Kamp	1	Herrenhof, Obere Holzweise	22	24974	1
Thunau/Kamp	1	Herrenhof, Obere Holzweise	24	24977	1
Thunau/Kamp	1	Herrenhof, Obere Holzweise	26	24979	1
Thunau/Kamp	1	Herrenhof, Obere Holzweise	30	24984	1
Thunau/Kamp	1	Herrenhof, Obere Holzweise	41	24995	2
Thunau/Kamp	1	Herrenhof, Obere Holzweise	51	25007	1
Thunau/Kamp	1	Herrenhof, Obere Holzweise	56	25012	1
Thunau/Kamp	1	Herrenhof, Obere Holzweise	69	25024	2
Thunau/Kamp	1	Herrenhof, Obere Holzweise	79	25034	1
Thunau/Kamp	1	Herrenhof, Obere Holzweise	82	25038	1
Thunau/Kamp	1	Herrenhof, Obere Holzweise	90	25050	2
Thunau/Kamp	1	Herrenhof, Obere Holzweise	91	25051	1
Thunau/Kamp	1	Herrenhof, Obere Holzweise	92	25052	1
Thunau/Kamp	1	Herrenhof, Obere Holzweise	100	25063	2
Thunau/Kamp	1	Herrenhof, Obere Holzweise	101	25064	2
Thunau/Kamp	1	Herrenhof, Obere Holzweise	104	25070	1
Thunau/Kamp	1	Herrenhof, Obere Holzweise	118	37283	2
Thunau/Kamp	1	Herrenhof, Obere Holzweise	126	25096	2
Thunau/Kamp	1	Herrenhof, Obere Holzweise	128	25098	1
Thunau/Kamp	1	Herrenhof, Obere Holzweise	129	25099	1
Thunau/Kamp	1	Herrenhof, Obere Holzweise	132	25103	2
Thunau/Kamp	1	Herrenhof, Obere Holzweise	133	25104	2
Thunau/Kamp	1	Herrenhof, Obere Holzweise	139	25116	2
Thunau/Kamp	1	Herrenhof, Obere Holzweise	146	25123	1
Thunau/Kamp	1	Herrenhof, Obere Holzweise	156	25135	2
Thunau/Kamp	1	Herrenhof, Obere Holzweise	169	25148	2

Thunau/Kamp	1	Herrenhof, Obere Holzwiese	175	25154	1
Thunau/Kamp	1	Herrenhof, Obere Holzwiese	179	25158	1
Thunau/Kamp	1	Herrenhof, Obere Holzwiese	188	25167	1
Thunau/Kamp	1	Saugrube	191	25170	1
Thunau/Kamp	1	Herrenhof, Obere Holzwiese	198	25177	2
Thunau/Kamp	1	Herrenhof, Obere Holzwiese	205	25187	2
Thunau/Kamp	1	Herrenhof, Siedlung	218	25359	1
Thunau/Kamp	1	Herrenhof, Obere Holzwiese	102_1	25065	2
Thunau/Kamp	1	Herrenhof, Obere Holzwiese	135_1	25109	1
Thunau/Kamp	1	Herrenhof, Obere Holzwiese	136_1	25111	1
Thunau/Kamp	1	Herrenhof, Obere Holzwiese	138_1	25114	2
Thunau/Kamp	1	Schanze	1966/1	25206	1
Thunau/Kamp	1	Holzweise, auerhalb SW-Wall	1972/1	25222	2
Thunau/Kamp	1	Obere Holzweise, Terrasse/Kirche	1974/3A	25227	2
Thunau/Kamp	1	Saugrube	1985/6	25260	1
Thunau/Kamp	1	Schanze/Nordtor	1999/3	25365	2
Thunau/Kamp	1	Herrenhof, Obere Holzwiese	45_1	24999	1
Thunau/Kamp	1	Herrenhof, Obere Holzwiese	81_1	25036	1
Thunau/Kamp	1	Herrenhof, Obere Holzwiese	96_1	25057	1
<b>graveyard</b>	<b>series</b>	<b>specific location</b>	<b>gravenumber</b>	<b>inventory number</b>	<b>sex</b>
Thunau/Kamp	2	Goldberggasse	1983/2	25384	1
Thunau/Kamp	2	Goldberggasse	1983/4	25386	2
Thunau/Kamp	2	Goldberggasse	1983/6	25388	1
Thunau/Kamp	2	Goldberggasse	1983/8	25390	2
Thunau/Kamp	2	Goldberggasse	1986/5	25407	2
Thunau/Kamp	2	Schimmelsprungg.	2004/18	25427	1
Thunau/Kamp	2	Schimmelsprungg.	2004/19	24428	1
Thunau/Kamp	2	Schimmelsprungg.	2004/27	25438	2
Thunau/Kamp	2	Schimmelsprungg.	2004/34	25443	1
Thunau/Kamp	2	Schimmelsprungg.	2004/6	25415	1
Thunau/Kamp	2	Schimmelsprungg.	2004_11_1	25420	2
Thunau/Kamp	2	Schimmelsprungg.	2004_23_1	25432	2
Thunau/Kamp	2	Goldberggasse	2006/1	25453	1
Thunau/Kamp	2	Goldberggasse	2006/2	25453	2
Thunau/Kamp	2	Goldberggasse	Fn. 145/2006	25458	1

## 13.4 List of analysed individuals from Thunau for joint changes, right extremity

In this list, the individuals analysed for the joint investigation of the right extremity can be found. The skeletons are currently housed at the Natural History Museum in Vienna.

Legend: series 1 = uphill/hillfort site, series 2 = downhill/valley site; sex: 1 = male, 2 = female

graveyard	series	specific location	gravenumber	inventory number	sex
Thunau	1	Herrenhof, Obere Holzweise	1	24953	1
Thunau	1	Herrenhof, Obere Holzweise	2	25193	1
Thunau	1	Herrenhof, Obere Holzweise	9	24960	2
Thunau	1	Herrenhof, Obere Holzweise	10	24961	1
Thunau	1	Herrenhof, Obere Holzweise	11	24962	2
Thunau	1	Herrenhof, Obere Holzweise	12	24963	1
Thunau	1	Herrenhof, Obere Holzweise	18	24970	1
Thunau	1	Herrenhof, Obere Holzweise	20	24972	2
Thunau	1	Herrenhof, Obere Holzweise	21	24973	2
Thunau	1	Herrenhof, Obere Holzweise	22	24974	1
Thunau	1	Herrenhof, Obere Holzweise	23	24976	1
Thunau	1	Herrenhof, Obere Holzweise	24	24977	1
Thunau	1	Herrenhof, Obere Holzweise	26	24979	1
Thunau	1	Herrenhof, Obere Holzweise	29	24982, 24983	1
Thunau	1	Herrenhof, Obere Holzweise	30	24984	1
Thunau	1	Herrenhof, Obere Holzweise	40	24994	1
Thunau	1	Herrenhof, Obere Holzweise	41	24995	2
Thunau	1	Herrenhof, Obere Holzweise	43	24997	2
Thunau	1	Herrenhof, Obere Holzweise	51	25007	1
Thunau	1	Herrenhof, Obere Holzweise	53	25009	2
Thunau	1	Herrenhof, Obere Holzweise	56	25012	1
Thunau	1	Herrenhof, Obere Holzweise	67	25022	1
Thunau	1	Herrenhof, Obere Holzweise	69	25024	2
Thunau	1	Herrenhof, Obere Holzweise	78	25033	1
Thunau	1	Herrenhof, Obere Holzweise	79	25034	1
Thunau	1	Herrenhof, Obere Holzweise	82	25038	1
Thunau	1	Herrenhof, Obere Holzweise	90	25050	2
Thunau	1	Herrenhof, Obere Holzweise	91	25051	1
Thunau	1	Herrenhof, Obere Holzweise	92	25052	1
Thunau	1	Herrenhof, Obere Holzweise	100	25063	2
Thunau	1	Herrenhof, Obere Holzweise	101	25064	2
Thunau	1	Herrenhof, Obere Holzweise	104	25070	1
Thunau	1	Herrenhof, Obere Holzweise	118	37283	2
Thunau	1	Herrenhof, Obere Holzweise	126	25096	2
Thunau	1	Herrenhof, Obere Holzweise	128	25098	1

Thunau	1	Herrenhof, Obere Holzweise	129	25099	1
Thunau	1	Herrenhof, Obere Holzweise	133	25104	2
Thunau	1	Herrenhof, Obere Holzweise	139	25116	2
Thunau	1	Herrenhof, Obere Holzweise	146	25123	1
Thunau	1	Herrenhof, Obere Holzweise	156	25135	2
Thunau	1	Herrenhof, Obere Holzweise	167	25146	1
Thunau	1	Herrenhof, Obere Holzweise	169	25148	2
Thunau	1	Herrenhof, Obere Holzweise	175	25154	1
Thunau	1	Herrenhof, Obere Holzweise	179	25158	1
Thunau	1	Herrenhof, Obere Holzweise	188	25167	1
Thunau	1	Saugrube	191	25170	1
Thunau	1	Herrenhof, Obere Holzweise	198	25177	2
Thunau	1	Herrenhof, Obere Holzweise	205	25187	2
Thunau	1	Herrenhof, Siedlung	218	25359	1
Thunau	1	Herrenhof, Obere Holzweise	102_1	25065	2
Thunau	1	Herrenhof, Obere Holzweise	124_1	25093	2
Thunau	1	Herrenhof, Obere Holzweise	130_1	25100	1
Thunau	1	Herrenhof, Obere Holzweise	135_1	25109	1
Thunau	1	Herrenhof, Obere Holzweise	136_1	25111	1
Thunau	1	Herrenhof, Obere Holzweise	138_1	25114	2
Thunau	1	Schanze	1966/1	25206	1
Thunau	1	Schanze	1966/2	25207	1
Thunau	1	Schanze	1968/1	25215	2
Thunau	1	Holzweise, außerhalb SW-Wall	1972/1	25222	2
Thunau	1	Obere Holzweise, Terrasse/Kirche	1974/3A	25227	2
Thunau	1	Saugrube	1976/1	25232	2
Thunau	1	Saugrube	1985/6	25260	1
Thunau	1	Saugrube	1985/8	25262	1
Thunau	1	Schanze/Nordtor	1999/3	25365	2
Thunau	1	nahe der Kirche	2000/1	25367	2
Thunau	1	Herrenhof, Obere Holzweise	204_1	25185	2
Thunau	1	Herrenhof, Obere Holzweise	216 (93/8)	25200	1
Thunau	1	Herrenhof, Obere Holzweise	81_1	25036	1
Thunau	1	Herrenhof, Obere Holzweise	88_1	25047	2
Thunau	1	Herrenhof, Obere Holzweise	96_1	25057	1
<b>graveyard</b>	<b>series</b>	<b>specific location</b>	<b>gravenumber</b>	<b>inventory number</b>	<b>sex</b>
Thunau	2	Schimmelsprungg.	2004/18	25427	1
Thunau	2	Schimmelsprungg.	2004/19	24428	1
Thunau	2	Goldberggasse	1983/3	25385	1
Thunau	2	Goldberggasse	1983/6	25388	1
Thunau	2	Goldberggasse	2006/3	25455	1
Thunau	2	Schimmelsprungg.	2004/34	25443	1
Thunau	2	Goldberggasse	2006/1	25453	1
Thunau	2	Goldberggasse	Fn. 145/2006	25458	1

Thunau	2	Schimmelsprungg.	2004/27	25438	2
Thunau	2	Schimmelsprungg.	2004_11_1	25420	2
Thunau	2	Schimmelsprungg.	2004_23_1	25432	2
Thunau	2	Goldberggasse	1983/8	25390	2
Thunau	2	Goldberggasse	1987/6	25408	2
Thunau	2	Goldberggasse	1983/4	25386	2
Thunau	2	Goldberggasse	1986/3	25404	2
Thunau	2	Goldberggasse	1986/5	25407	2

## 13.5 List of analysed individuals from Thunau for enthesal changes, left extremities

In this list, the individuals analysed for the joint investigation of the left extremities can be found. The skeletons are currently housed at the Natural History Museum in Vienna.

Legend: series 1 = uphill/hillfort site, series 2 = downhill/valley site; sex: 1 = male, 2 = female

graveyard	series	specific location	gravenumber	inventory number	sex
Thunau	1	Herrenhof, Obere Holzweise	1	24953	1
Thunau	1	Herrenhof, Obere Holzweise	2	25193	1
Thunau	1	Herrenhof, Obere Holzweise	7	24958	1
Thunau	1	Herrenhof, Obere Holzweise	9	24960	2
Thunau	1	Herrenhof, Obere Holzweise	12	24963	1
Thunau	1	Herrenhof, Obere Holzweise	18	24970	1
Thunau	1	Herrenhof, Obere Holzweise	20	24972	2
Thunau	1	Herrenhof, Obere Holzweise	21	24973	2
Thunau	1	Herrenhof, Obere Holzweise	22	24974	1
Thunau	1	Herrenhof, Obere Holzweise	23	24976	1
Thunau	1	Herrenhof, Obere Holzweise	24	24977	1
Thunau	1	Herrenhof, Obere Holzweise	26	24979	1
Thunau	1	Herrenhof, Obere Holzweise	30	24984	1
Thunau	1	Herrenhof, Obere Holzweise	41	24995	2
Thunau	1	Herrenhof, Obere Holzweise	43	24997	2
Thunau	1	Herrenhof, Obere Holzweise	67	25022	1
Thunau	1	Herrenhof, Obere Holzweise	82	25038	1
Thunau	1	Herrenhof, Obere Holzweise	90	25050	2
Thunau	1	Herrenhof, Obere Holzweise	91	25051	1
Thunau	1	Herrenhof, Obere Holzweise	92	25052	1
Thunau	1	Herrenhof, Obere Holzweise	100	25063	2
Thunau	1	Herrenhof, Obere Holzweise	101	25064	2
Thunau	1	Herrenhof, Obere Holzweise	104	25070	1
Thunau	1	Herrenhof, Obere Holzweise	114	25082	1
Thunau	1	Herrenhof, Obere Holzweise	118	37283	2
Thunau	1	Herrenhof, Obere Holzweise	126	25096	2
Thunau	1	Herrenhof, Obere Holzweise	128	25098	1
Thunau	1	Herrenhof, Obere Holzweise	133	25104	2
Thunau	1	Herrenhof, Obere Holzweise	139	25116	2
Thunau	1	Herrenhof, Obere Holzweise	148	25125	2
Thunau	1	Herrenhof, Obere Holzweise	156	25135	2
Thunau	1	Herrenhof, Obere Holzweise	169	25148	2
Thunau	1	Herrenhof, Obere Holzweise	175	25154	1
Thunau	1	Herrenhof, Obere Holzweise	179	25158	1
Thunau	1	Herrenhof, Obere Holzweise	188	25167	1

Thunau	1	Saugrube	191	25170	1
Thunau	1	Herrenhof, Obere Holzweise	198	25177	2
Thunau	1	Herrenhof, Obere Holzweise	205	25187	2
Thunau	1	Herrenhof, Obere Holzweise	208	25190	2
Thunau	1	Herrenhof, Siedlung	218	25359	1
Thunau	1	Herrenhof, Obere Holzweise	102_1	25065	2
Thunau	1	Herrenhof, Obere Holzweise	130_1	25100	1
Thunau	1	Herrenhof, Obere Holzweise	135_1	25109	1
Thunau	1	Herrenhof, Obere Holzweise	138_1	25114	2
Thunau	1	Schanze	1966/1	25206	1
Thunau	1	Schanze	1966/2	25207	1
Thunau	1	Schanze	1968/1	25215	2
Thunau	1	Holzweise, außerhalb SW-Wall	1972/1	25222	2
Thunau	1	Obere Holzweise, Terrasse/Kirche	1974/3A	25227	2
Thunau	1	Saugrube	1976/1	25232	2
Thunau	1	Saugrube	1985/6	25260	1
Thunau	1	Saugrube	1985/8	25262	1
Thunau	1	nahe der Kirche	2000/1	25367	2
Thunau	1	Herrenhof, Obere Holzweise	216 (93/8)	25200	1
Thunau	1	Herrenhof, Obere Holzweise	81_1	25036	1
Thunau	1	Herrenhof, Obere Holzweise	96_1	25057	1
<b>graveyard</b>	<b>series</b>	<b>specific location</b>	<b>gravenumber</b>	<b>inventory number</b>	<b>sex</b>
Thunau	2	Goldberggasse	1983/6	25388	1
Thunau	2	Goldberggasse	1983/8	25390	2
Thunau	2	Goldberggasse	1985_2_1	25396	2
Thunau	2	Goldberggasse	1986/5	25407	2
Thunau	2	Goldberggasse	1987/6	25408	2
Thunau	2	Schimmelsprungg.	2004/18	25427	1
Thunau	2	Schimmelsprungg.	2004/19	24428	1
Thunau	2	Schimmelsprungg.	2004/27	25438	2
Thunau	2	Schimmelsprungg.	2004/34	25443	1
Thunau	2	Schimmelsprungg.	2004/6	25415	1
Thunau	2	Schimmelsprungg.	2004_11_1	25420	2
Thunau	2	Schimmelsprungg.	2004_23_1	25432	2
Thunau	2	Goldberggasse	2006/1	25453	1
Thunau	2	Goldberggasse	Fn. 145/2006	25458	1

## 13.6 List of analysed individuals from Thunau for joint changes, left extremities

In this list, the individuals analysed for the joint investigation of the left extremities can be found. The skeletons are currently housed at the Natural History Museum in Vienna.

Legend: series 1 = uphill/hillfort site, series 2 = downhill/valley site; sex: 1 = male, 2 = female

graveyard	series	specific location	gravenumber	inventory number	sex
Thunau	1	Herrenhof, Obere Holzweise	1	24953	1
Thunau	1	Herrenhof, Obere Holzweise	2	25193	1
Thunau	1	Herrenhof, Obere Holzweise	9	24960	2
Thunau	1	Herrenhof, Obere Holzweise	10	24961	1
Thunau	1	Herrenhof, Obere Holzweise	11	24962	2
Thunau	1	Herrenhof, Obere Holzweise	12	24963	1
Thunau	1	Herrenhof, Obere Holzweise	18	24970	1
Thunau	1	Herrenhof, Obere Holzweise	20	24972	2
Thunau	1	Herrenhof, Obere Holzweise	21	24973	2
Thunau	1	Herrenhof, Obere Holzweise	22	24974	1
Thunau	1	Herrenhof, Obere Holzweise	23	24976	1
Thunau	1	Herrenhof, Obere Holzweise	24	24977	1
Thunau	1	Herrenhof, Obere Holzweise	26	24979	1
Thunau	1	Herrenhof, Obere Holzweise	29	24982, 24983	1
Thunau	1	Herrenhof, Obere Holzweise	30	24984	1
Thunau	1	Herrenhof, Obere Holzweise	40	24994	1
Thunau	1	Herrenhof, Obere Holzweise	41	24995	2
Thunau	1	Herrenhof, Obere Holzweise	43	24997	2
Thunau	1	Herrenhof, Obere Holzweise	51	25007	1
Thunau	1	Herrenhof, Obere Holzweise	53	25009	2
Thunau	1	Herrenhof, Obere Holzweise	56	25012	1
Thunau	1	Herrenhof, Obere Holzweise	67	25022	1
Thunau	1	Herrenhof, Obere Holzweise	69	25024	2
Thunau	1	Herrenhof, Obere Holzweise	78	25033	1
Thunau	1	Herrenhof, Obere Holzweise	79	25034	1
Thunau	1	Herrenhof, Obere Holzweise	82	25038	1
Thunau	1	Herrenhof, Obere Holzweise	90	25050	2
Thunau	1	Herrenhof, Obere Holzweise	91	25051	1
Thunau	1	Herrenhof, Obere Holzweise	92	25052	1
Thunau	1	Herrenhof, Obere Holzweise	100	25063	2
Thunau	1	Herrenhof, Obere Holzweise	101	25064	2
Thunau	1	Herrenhof, Obere Holzweise	104	25070	1
Thunau	1	Herrenhof, Obere Holzweise	118	37283	2
Thunau	1	Herrenhof, Obere Holzweise	126	25096	2
Thunau	1	Herrenhof, Obere Holzweise	128	25098	1

Thunau	1	Herrenhof, Obere Holzwiese	129	25099	1
Thunau	1	Herrenhof, Obere Holzwiese	133	25104	2
Thunau	1	Herrenhof, Obere Holzwiese	139	25116	2
Thunau	1	Herrenhof, Obere Holzwiese	146	25123	1
Thunau	1	Herrenhof, Obere Holzwiese	156	25135	2
Thunau	1	Herrenhof, Obere Holzwiese	167	25146	1
Thunau	1	Herrenhof, Obere Holzwiese	169	25148	2
Thunau	1	Herrenhof, Obere Holzwiese	175	25154	1
Thunau	1	Herrenhof, Obere Holzwiese	179	25158	1
Thunau	1	Herrenhof, Obere Holzwiese	188	25167	1
Thunau	1	Saugrube	191	25170	1
Thunau	1	Herrenhof, Obere Holzwiese	198	25177	2
Thunau	1	Herrenhof, Obere Holzwiese	205	25187	2
Thunau	1	Herrenhof, Siedlung	218	25359	1
Thunau	1	Herrenhof, Obere Holzwiese	102_1	25065	2
Thunau	1	Herrenhof, Obere Holzwiese	124_1	25093	2
Thunau	1	Herrenhof, Obere Holzwiese	130_1	25100	1
Thunau	1	Herrenhof, Obere Holzwiese	135_1	25109	1
Thunau	1	Herrenhof, Obere Holzwiese	136_1	25111	1
Thunau	1	Herrenhof, Obere Holzwiese	138_1	25114	2
Thunau	1	Schanze	1966/1	25206	1
Thunau	1	Schanze	1966/2	25207	1
Thunau	1	Schanze	1968/1	25215	2
Thunau	1	Holzweise, außerhalb SW-Wall	1972/1	25222	2
Thunau	1	Obere Holzweise, Terrasse/Kirche	1974/3A	25227	2
Thunau	1	Saugrube	1976/1	25232	2
Thunau	1	Saugrube	1985/6	25260	1
Thunau	1	Saugrube	1985/8	25262	1
Thunau	1	Schanze/Nordtor	1999/3	25365	2
Thunau	1	nahe der Kirche	2000/1	25367	2
Thunau	1	Herrenhof, Obere Holzwiese	204_1	25185	2
Thunau	1	Herrenhof, Obere Holzwiese	216 (93/8)	25200	1
Thunau	1	Herrenhof, Obere Holzwiese	81_1	25036	1
Thunau	1	Herrenhof, Obere Holzwiese	88_1	25047	2
Thunau	1	Herrenhof, Obere Holzwiese	96_1	25057	1
<b>graveyard</b>	<b>series</b>	<b>specific location</b>	<b>gravenumber</b>	<b>inventory number</b>	<b>sex</b>
Thunau	2	Goldberggasse	1983/3	25385	1
Thunau	2	Goldberggasse	1983/4	25386	2
Thunau	2	Goldberggasse	1983/6	25388	1
Thunau	2	Goldberggasse	1983/8	25390	2
Thunau	2	Goldberggasse	1986/3	25404	2
Thunau	2	Goldberggasse	1986/5	25407	2
Thunau	2	Goldberggasse	1987/6	25408	2

Thunau	2	Schimmelsprungg.	2004/18	25427	1
Thunau	2	Schimmelsprungg.	2004/19	24428	1
Thunau	2	Schimmelsprungg.	2004/27	25438	2
Thunau	2	Schimmelsprungg.	2004/34	25443	1
Thunau	2	Schimmelsprungg.	2004_11_1	25420	2
Thunau	2	Schimmelsprungg.	2004_23_1	25432	2
Thunau	2	Goldberggasse	2006/1	25453	1
Thunau	2	Goldberggasse	2006/3	25455	1
Thunau	2	Goldberggasse	Fn. 145/2006	25458	1

## 13.7 ZUSAMMENFASSUNG

### **„Krieger und Handwerker?“ – Eine Untersuchung von Muskelmarken- und Gelenksveränderungen an den frühmittelalterlichen Skelettresten von Thunau/Kamp**

Die Skelettreste von zwei Fundstellen in Thunau/Kamp – Schanzberg und Goldberggasse/Schimmelsprunggasse im Tal, beide 9-10. Jahrhundert A.D. – wurden einer systematisch-anthropologischen Analyse bezüglich ausgewählter Muskelmarken- und Gelenkveränderungen unterzogen. Als Muskelmarken bezeichnet man die Stellen am Knochen, an denen Muskeln, Sehnen und Bänder befestigt sind. Es wird angenommen, dass die Frequenz und das Ausmaß der Veränderung an den Muskelansatzstellen und Gelenken etwas über Arbeitsbelastung und damit soziale Organisation einer Bevölkerung aussagen können. Die beiden Fundstellen in Thunau unterscheiden sich in der Siedlungsstruktur und in den materiellen Hinterlassenschaften, was auch auf Unterschiede in der Sozialstruktur der beiden Gruppen hinweisen könnte. Die Fundstelle Schanzberg liegt auf einem Höhenrücken und umfaßt eine mehrphasige Befestigungsanlage, einen Herrenhof, ein mit Holzpalisaden umgrenztes Siedlungsareal, sowie ein Gräberfeld (Nowotny 2011). Diese Anlage stellte vermutlich ein Handelszentrum in der Peripherie des Frankenreiches dar (Szameit 1995, Teschler-Nicola *et al.* 2015), wobei einige der Bestatteten aufgrund ihrer besonderen Grabbeigaben bzw. spezieller Bestattungslagen einer sozialen, vermutlich militärischen „Elite“ zugerechnet werden können. Die zweite Fundstelle liegt im Tal am Fuß des Hügels, und kann als „Suburbium“ (Obenaus *et al.* 2006, Obenaus 2011) angesprochen werden, hier wurden ein Siedlungsareal mit deutlichem Fokus auf handwerklichen Erzeugnissen sowie Gräber entdeckt. Die Altersstruktur in den beiden Gruppen ist sehr ähnlich. Ausgewählte faserknorpelige Muskelansatzstellen (diese sind, nach neuesten medizinischen Erkenntnissen in ihrer Aussagekraft bezüglich Arbeitsspuren am Skelett zuverlässiger) und Gelenke der oberen und unteren Extremität wurden visuell makroskopisch befundet. Für die statistische Auswertung wurden die einzeln befundeten Muskelansatzstellen und Gelenke funktionell in Muskel- und Gelenkgruppen unterteilt, ferner jeweils die Männer und Frauen der beiden Gruppen separat verglichen. Eine Kovarianz zwischen den Veränderungen an den Muskelmarken und den Gelenken wurde angenommen. Weiters wurden Hypothesen bezüglich Geschlechts- und Populationsunterschieden, einem Anstieg der Muskelmarken- und Gelenkveränderungen mit höherem Alter, einem Unterschied in der „Funktion“ der beiden archäologischen Fundstellen sowie eine soziale Diskrepanz (Krieger und Handwerker?)

anhand von Gruppenanalysen statistisch getestet. Die Auswertungen ergaben eine schwache Assoziation zwischen Muskelmarken- und Gelenkveränderungen, wobei diese bei den Männern etwas ausgeprägter war. Zwischen den Populationen konnten Unterschiede festgestellt, sowie ein Zunehmen der Veränderungen mit steigendem Alter der Individuen für beide Gruppen bestätigt werden. Männer und Frauen beider Gruppen zeigen hohe Frequenzen bei den Gelenkveränderungen, anders als bei den Muskelmarken, wo nur die Männer hohe Frequenzen aufweisen. Die Männer und Frauen der Talsiedlung zeigen deutlichere Asymmetrien bei den Muskel- und Gelenkveränderungen als die der oberen Gruppe, besonders in der oberen Extremität, was auf ein körperlich anspruchsvolleres (Arbeits-)Leben hinweist. Des Weiteren zeigen die Ergebnisse bei den Frauen der unteren Gruppe einen signifikant höheren Ausprägungsgrad bei den Hüftmuskelmarken und das bereits im jüngeren Altersbereichs die Frauen der Höhengiedlung. Im Unterschied zu den Frauen der oberen Gruppe weisen diese Ergebnisse darauf hin, dass die Frauen der unteren Gruppe mobiler und bereits in jüngerem Alter in physisch anspruchsvollere Arbeit involviert waren. Was die Männer der oberen Gruppe betrifft, waren signifikante Veränderungen an den Muskelmarken nur zwischen den jungen und den mittleren Altersgruppen sichtbar. Signifikante Ergebnisse zwischen den Serien wurden bei den Hüftgelenken gefunden, wobei die Männer der unteren Gruppe höhere Werte aufwiesen. Letzere zeigten weiters die höchsten Frequenzen bei Veränderungen einiger Muskelmarken der Schulter und des Ellbogens und eine deutlich stärkere Asymmetrie, besonders in der oberen Extremität. Diese Ergebnisse deuten auf einen körperlich fordernden Lebensstil der Männer beider Gruppen, wobei die Details darauf hinweisen, dass die Männer der Talsiedlung mobiler waren und spezialisiertere Arbeiten (Handwerk) ausgeführt haben dürften. Die "Krieger" der oberen Gruppe scheinen sich in der Gruppenstatistik nicht widerzuspiegeln, die geschlechtsspezifischen Gruppenunterschiede zwischen dem Schanzberg und der Talsiedlung wurden in dieser Untersuchung jedoch sichtbar. Die Ergebnisse zeigen das Potential methodischer Kombinationen für Gruppenanalysen auf, und vermitteln uns einen Eindruck von der arbeitsteilig organisierten Tätigkeit dieser frühmittelalterlichen Gesellschaft.

## 13.8 CURRICULUM VITAE

**MAG. DORIS PANY-KUCERA**

### **MAIN AREAS OF RESEARCH**

- Hallstatt skeletons
- Muscle marks and joint diseases
- Paleopathology
- Experimental cremations

My main research interest focuses on osteology, paleopathology and the investigation of physical stress visible as muscle markings (enthese) in archaeological human remains. I have been following the development of this relatively new special field since the first systematic paper according to it was published in 1998 and I am a member of the international working group on enthesal changes since its foundation in 2009 (MSM working group on methods). Already in my diploma thesis I investigated entheses on the Hallstatt skeletons which was completed in 2003 (see below). Analysis and interpretation of musculo-skeletal stress markers and osteoarthritis of prehistoric skeletons is also the topic of my Ph.D. thesis (see below).

Since 1999 I have been working with the Hallstatt skeletons, participated in excavations and recorded paleodemographic and paleopathological characters. Parts of these investigations and their results were published and presented at congresses and in national and international exhibitions.

I am further interested in the theory of cremation and between 2005 and 2012 I annually performed cremation experiments and the experimental reconstruction of pyres together with colleagues in order to gain a better understanding of the time and effort prehistoric people invested in cremating their dead.

## **ACADEMIC CAREER AND POSITIONS HELD TO DATE**

1.1.2015 Scientific assistant in the project “The social status of motherhood in Bronze Age Europe” (FWF P 26820); <http://www.orea.oeaw.ac.at/mutterschaft.html>

2014 Freelancer in Physical Anthropology (projects for MAMUZ (archaeological complex Haselbach), Lower Austria, and the Upper Austrian State Museum (archaeological complex Leonding))

1.3.2013 – 31.10.2013 Marginal employment for the scientific anthropologic investigation of the Hallstatt skeletons and cremations excavated from 2002 – 2012 (Prehistoric Department, Natural History Museum Vienna)

1.3.2013 – 31.8.2013 educational leave

1.8.2012 – 28.2.2013 Scientific anthropologic investigation of selected Hallstatt skeletons in the HALL-IMPACT - project (project management Mag. Kerstin Kowarik): “Disentangling climate and culture impact on prehistoric alpine cultures” (funded by the Austrian Academy of Sciences)

16.4.2011 – 31.7.2012 Maternity leave (birth of son Gabriel 23.6.2011)

1.6.2010 – 16.4.2011 20h Scientific assistant in the „forMUSE“- project (BMWF)  
„EuphorischerAnfang – dysphorische Gegenwart: Anthropologische Sammlungen im Spannungsfeld von Wissenschaft und Ethik“, Department of Anthropology, Natural History Museum Vienna

Since 2009 Freelancer at the Vienna Institute for Archaeological Science (VIAS): Anthropological investigation of the skeletons from the archaeological complexes Geitzendorf, Herzogbirbaum, Mitterretzbach, Haselbach for the Museum of Prehistory in Asparn/Zaya (Lower Austria)

2008 Lectorship in paleopathology, focus on muscle marks, at the University of Pilsen, Czech Republic

2007 – 2011: Annual lectorship „presentation techniques“ at the Department of Anthropology, Vienna

1.12.2005 – 31.11.2008 20h scientific assistant at the Natural History Museum (BDA Project: The Avar Skeletons of Bruckneudorf, S6, sponsored by the ASFINAG)

2005 – 2007, 2009 – 2011 Annual lectorship „Cremated human remains“ in the lecture series „experimental archaeology“ Institute of Prehistory and Early Medieval Archaeology, Vienna

1.11.2002 – 31.10.2005 20h Scientific assistant at the Natural History Museum (BDA Project: The Avar Skeletons of Vösendorf, S1, sponsored by the ASFINAG)

Since 2003 involved in several exhibition projects eg. on Hallstatt and “The Iceman” in the Natural History Museum Vienna, Leonding (Upper Austria), Bibracte (France), Helsinki (Finland)

Since 2002 involved in several small projects as scientific assistant e.g. Hallstatt, Gars/Thunau, Gnadendorf, Albrechtsberg, Rebešovice (Czech Republic), Carnuntum, Traisental (FWF P18131), Jabuticabeira (Brazil), St. Paul

1998 – 2004 participation in archaeological excavations in e.g. Hallstatt, Thunau/Gars/Kamp, municipal archaeology Vienna, and Baar, Switzerland

1998 – 2008 active in pedagogic programs (guided tours for children and adults in anthropology and archaeology at the Natural History Museum Vienna)

#### **UNIVERSITY EDUCATION**

8. April 2003 MA in Physical Anthropology, Natural History Museum/University of Vienna  
Thesis “Mining for the miners? An analysis of occupationally - induced stress markers on the skeletal remains from the ancient Hallstatt cemetery”

1993 – 2003 Student at the University of Vienna, Department of Anthropology, Faculty of Life Sciences, combined with courses in genetics, microbiology and ethnology

1999 – 2000 ERASMUS stay at the Johannes-Gutenberg Universität Mainz, Germany

#### **ADDITIONAL EDUCATIONS**

2005 Bone Paleopathology in Brazil: A short course. Museu Nacional, Rio de Janeiro, Brazil

2006 Workshop zu spezieller Skelettpathologie, Santorini, Greece

2008 Short Course in Human Skeletal Palaeopathology in Bradford, West Yorkshire, U.K.  
(sponsored by a short-term grant abroad, University of Vienna)

#### **ACADEMIC RECOGNITION**

Invited lectures and workshops

- 21.7. – 28.7.2013 Coimbra University, Portugal, workshop of the “entheses method group.” This research was supported by Wenner-Gren Foundation (grant number Gr. CONF-632, CIAS - Research Centre for Anthropology and Health and CRIA - Centro em Rede de Investigação em Antropologia).
- 30.6. – 04.07.2009 University of Coimbra, Portugal: “The scientific value of using a 3D surface scanner to quantify entheses”
- 23.6. – 27.6.2010 Geneva University, Switzerland, workshop organised by the „entheses method group“ relating to pathologic changes at entheses (pathologic muscle marks)
- 17.2. – 21.2.2006 Leuven University, Belgium: “Working in a salt mine – everyday life for the Hallstatt females?”
- 12.3. – 15.3.2006 Archäologisches Museum Frankfurt: “BergarbeiterInnen im Salzbergwerk Hallstatt – auf der Suche nach Belastungsspuren an den eisenzeitlichen Skeletten”
- 12. – 14.12.2005 Universität Zürich, Switzerland: „Frauenarbeit im Salzbergwerk – Alltag in der Hallstattzeit? “

#### **SCHOLARSHIPS AND AWARDS**

Travel grants (ÖFG, BMWF) for several international scientific meetings 2003 Tempe, Arizona, 2004 Tampa, Florida, 2005 Rio de Janeiro, Brazil, 2007 Philadelphia, Pennsylvania, 2007 Santiago de Chile, Chile, 2008 Kopenhagen, Denmark, 2009 & 2013 Coimbra, Portugal, 2014 Lund, Sweden

#### **PEER REVIEW ACTIVITIES**

HOMO (Journal of Comparative Human Biology)

International Journal of Osteoarchaeology

Journal of Paleopathology

JAS (Journal of Archaeological Science)

MEMBERSHIPS IN ACADEMIC ORGANISATIONS

“MSM working group on methods“ (international working group according to pathologic alterations at muscle marks at bones) [www.uc.pt/en/cia/events/msm/MSM\\_methods](http://www.uc.pt/en/cia/events/msm/MSM_methods)

Paleopathology Association

American Association of Physical Anthropologists

Gesellschaft für Archäozoologie und Prähistorische Anthropologie (GAPA)

Arbeitsgruppe Experimentelle Archäologie